Carlos Alberto da Silva Ribeiro de Melo

# The additive effects in Matrix Dispersed Liquid Crystals

Lisboa
2009

FACULDADE DE CIÊNCIAS E TECNOLOGIA
UNIVERSIDADE NOVA DE LISBOA

Departamento de Química

# The additive effects in Matrix Dispersed Liquid Crystals

By

Carlos Alberto da Silva Ribeiro de Melo

*Dissertation presented at Faculdade de Ciências e Tecnologia from Universidade Nova de Lisboa to obtain the degree of Master in Chemical and Biochemical Engineering*

Supervised by

João Carlos da Silva Barbosa Sotomayor

Lisboa

2009

*“Science without Religion is lame.*

*Religion without Science is blind.”*

Albert Einstein, 1941

# Acknowledgements

*First of all, I would like to thank Prof. João Sotomayor of FCT-UNL, regarding the thesis coordination and support, since the first day that it started.*

*To all the elements associated with this project, in particular to Prof. João Figueirinhas of IST-UTL, for all the help provided with the electro-optical results and his knowledge in the area of the liquid crystals.*

*To Prof. Helena Godinho of FCT-UNL for all the provided equipment for the polarized optical microscopy photos and dedication on the understanding of the diverse structures of the samples, as well as João Canejo and Ana Ferreira.*

*To Prof. Madalena Dionísio, Prof. Natália Correia and Ana Brás of FCT-UNL for the dielectric relaxation spectroscopy analysis and contribution of knowledge and dedication.*

*To Carla Rodrigues of FCT-UNL for the differential scanning calorimetry analysis.*

*To Isabel Nogueira of IST-UTL, for the scanning electron microscopy photos.*

*To all the personnel in Laboratory 415 and to my master thesis partner, Alexandre Maiau, who helped me along the work and made this journey as simple as fun.*

*To Krasimira Petrova, Ana Mouquinho and Mara Saavedra for diverse chemical processes and analysis, as well as their estimated friendship.*

*Finally, to all the persons who contributed in some way to the elaboration of this dissertation and to all of you, who are reading these words,*

*Obrigado!*

This work was partially funded by
Fundação para a Ciência e Tecnologia
through project
PTDC/CTM/69145/2006.

# Abstract

The main objective of this work was to optimize the structure of a matrix that will support a nematic mixture of liquid crystals, known as $E7$ from Merck, in order to produce a matrix dispersed liquid crystal device with good electro-optical responses.

The composites are based on monomers, such as tri(ethylene glycol) dimethacrylate and poly(ethylene glycol) dimethacrylate with typical molecular weight of $875\ g.mol^{-1}$ with two different types of polymerization, a thermal polymerization with initiation by α,α'-azoisobutyronitrile and a photochemical polymerization with initiation by p-xylene N,N-diethyldithiocarbamate.

To do that, some additives have been used as a way to format the shape and the size of the liquid crystal microdroplets and to avoid its coalescence and, therefore, optimizing the performance of the device as being able to electro-optical application. Octanoic acid, ethylene glycol, triton X-100, cetyl trimethyl ammonium bromide and sodium dodecyl sulfate have been used as additives to the systems.

Different aspects were investigated, such as the study of the dynamics of the transition ON/OFF state using a high-frequency alternate voltage and the attempt to minimize and maximize the liquid crystal anchorage breaking to the polymer matrix observed when tension is applied. The polymer morphology and the composites synthesized were analyzed by polarized optical microscopy and scanning electron microscopy and those results were related with the electro-optical response curves of the composites in study.

The best results were obtained with the system containing the triton X-100 as an additive, thus this system was analyzed with additional studies of differential scanning calorimetry, dielectric relaxation spectroscopy and a scanning temperature through polarized optical microscopy.

# Resumo

O objectivo principal deste trabalho foi o de optimizar a estrutura de uma matriz que irá suportar uma mistura nemática de cristais líquidos, conhecida como $E7$ da Merck, de modo a produzir um dispositivo de cristal líquido disperso em matriz com boas respostas electro-ópticas.

Os compósitos são baseados em monómeros, como tri(etilenoglicol) dimetacrilato e poli(etilenoglicol) dimetacrilato com peso molecular típico de $875\ g.mol^{-1}$ com dois tipos de polimerização diferentes, uma polimerização térmica com iniciação por α,α'-azoisobutironitrilo e uma polimerização fotoquímica com iniciação por p-xileno N,N-dietilditiocarbamato.

Para isso, alguns aditivos foram usados como um meio para moldar a forma e o tamanho das microgotas de cristal líquido e evitar a sua coalescência e, assim, optimizar o desempenho do dispositivo como sendo passível de aplicação electro-óptica. Ácido octanóico, etilenoglicol, triton X-100, brometo de cetil trimetil amónio e dodecil sulfato de sódio foram usados como aditivos aos sistemas.

Foram investigados diferentes aspectos, como o estudo da dinâmica de transição do estado ON/OFF usando uma corrente alterna de alta frequência e a tentativa de minimização e maximização da desancoragem do cristal líquido da matriz polimérica quando é aplicada tensão. A morfologia do polímero e dos compósitos sintetizados foi observada por microscopia de luz polarizada e por microscopia electrónica de varrimento e esses resultados foram relacionados com as curvas de resposta electro-óptica dos compósitos em estudo.

Os melhores resultados foram obtidos com o sistema contendo triton X-100 como aditivo, assim este sistema foi analisado com estudos adicionais de calorimetria diferencial de varrimento, espectroscopia de relaxação dieléctrica e varrimento de temperatura através de microscopia de luz polarizada.

# Table of Abbreviations

| Text | Abbreviation |
|---|---|
| α,α'-Azoisobutyronitrile | AIBN |
| Octanoic Acid with different addition order | AO |
| Cetyl Trimethyl Ammonium Bromide | CTAB |
| Dielectric Relaxation Spectroscopy | DRS |
| Differential Scanning Calorimetry | DSC |
| Ethylene Glycol | EG |
| Hexadecanoic Acid | HDA |
| Indium Tin Oxide | ITO |
| Liquid Crystal | LC |
| Nuclear Magnetic Resonance | NMR |
| Octanoic Acid | OA |
| Octanoic Acid in 1% of weight | OA1 |
| Octanoic Acid in 10% of weight | OA10 |
| Polarized Optical Microscopy | POM |
| Poly(ethylene glycol) Dimethacrylate | POLY875 |
| Scanning Electron Microscopy | SEM |
| Sodium Dodecyl Sulfate | SDS |
| Tri(ethylene glycol) Dimethacrylate | TRI |
| Triton X-100 | TX100 |
| p-Xylene N,N-diethyldithiocarbamate | XDT |

# Table of Contents

# Index of Figures

### *Chapter One*



### *Chapter Two*



### *Chapter Three*

### *Chapter Four*

### *Chapter Five*



### *Appendix Section*

# Index of Tables

# *The additive effects in Matrix Dispersed Liquid Crystals*

# *Chapter One*

# 1. Introduction

## 1.1. The Liquid Crystals

The liquid crystals are a state of matter intermediate between the solid and the liquid phases. The difference between crystals and liquids is that the molecules in a crystal are ordered whereas in a liquid they are dispersed randomly (Collings & Hird, 2004).
This intermediate state is known as mesophase which is the phase of a liquid crystalline compound between the crystalline and the isotropic liquid phases.

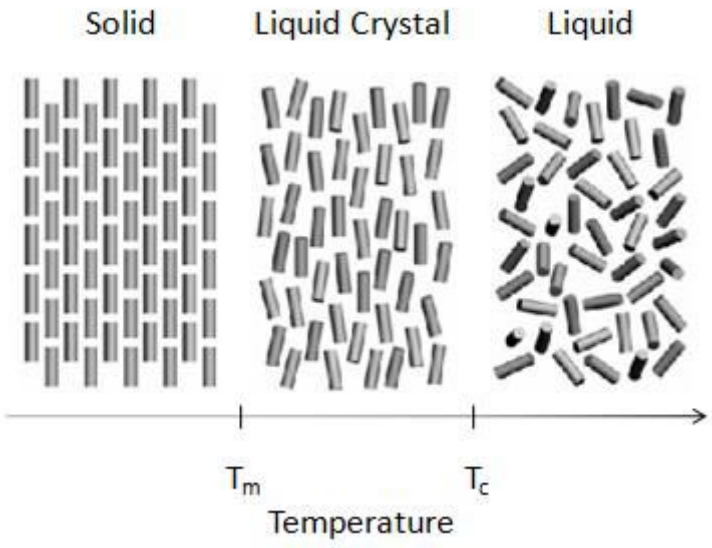


**Figure 1.1 – Schematic illustration of the solid, liquid crystal and liquid phases.**

Figure 1.1, adapted (Senyuk, 2006), illustrates the degree of order present in the solid, liquid crystal and liquid phases and the temperatures, $T_m$ and $T_c$, in which the phase transition occurs.

$T_m$ represents a melting point where the molecules lose their positional degrees of freedom and $T_c$ represents a clearing point where the molecules lose their orientational degrees of freedom.

This phase exhibits simultaneously optical properties and mechanical properties, characteristics of the crystals and the liquids, respectively, such as anisotropy in their optical, electrical and mechanical properties or high fluidity and coalescence of droplets.

Although liquid crystals combine the properties from a solid and an isotropic liquid, they exhibit a very specific electro-optical phenomenon that is not verified in a single crystal or in a single isotropic liquid (Senyuk, 2006).

### 1.1.1. Types of Liquid Crystals

A number of different types of molecules form liquid crystal phases and what they all have in common is that they are anisotropic (Collings & Hird, 2004). Liquid crystal phases can be divided into two classes, the thermotropic and the lyotropic.

The thermotropic liquid crystalline phase occurs among a certain temperature interval (Collings & Hird, 2004), which means that it is the temperature, that by decreasing or increasing, turns the substance into a crystal or into a liquid, respectively (Collings, 2002). These substances do not require the presence of a solvent to form liquid crystalline materials. Figure 1.2 a) (Senyuk, 2006), 4-cyano-4'-n-pentyl-1,1'-byphenyl, represents a molecule whose format is rod shaped, characteristic of the calamitic thermotropic liquid crystals.

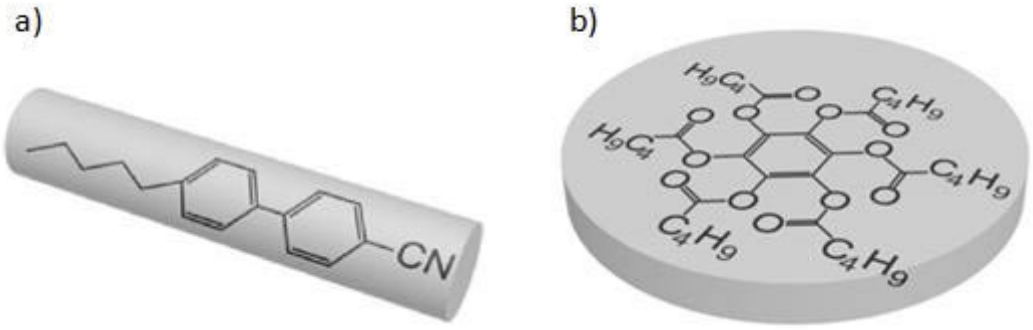


**Figure 1.2 – Examples of thermotropic liquid crystal molecules.**

There is another kind of thermotropic liquid crystals where molecules format is disc shaped, as shown in Figure 1.2 b) (Senyuk, 2006), benzene-hexa-n-pentanoate. Therefore, these are called as discotic liquid crystals. Although calamitic and discotic liquid crystal structures are different, their appearance at the microscope is similar (Collings, 2002).

On the other hand, there are types of molecules that only form a liquid crystal phase when mixed with a solvent of some kind. In these cases, it is the concentration of the solution that determines whether a liquid crystal phase is stable, instead of the temperature (Collings, 2002). These substances are named lyotropic liquid crystals. Examples of this kind of molecules are soaps, illustrated in Figure 1.3 (Senyuk, 2006), sodium dodecyl sulfate, a molecule with a hydrophilic polar head and a hydrophobic non-polar tail.


**Figure 1.3 – Example of a lyotropic liquid crystal molecule.**

### 1.1.2. Liquid Crystal Phases

There are various kinds of liquid crystal structures, but the more common are the nematic, the cholesteric and the smectic phases.

The nematic phase is the liquid crystal phase correspondent to the liquid crystal used in this work. In this phase, the molecules maintain a preferred orientational direction as they diffuse throughout the sample and there is no positional order in the molecules, as shown in Figure 1.4 (Senyuk, 2006).

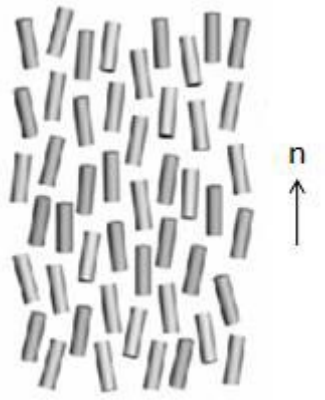


**Figure 1.4 – Schematic illustration of the nematic liquid crystal phase.**

Some deformation can occur in the nematics such as splay, twist and band types, being the twist type the deformation behind the most common liquid crystal displays.

Nematics are similar in their basic structure to other liquid crystal phase, the cholesterics, illustrated in Figure 1.5 (Senyuk, 2006). But the optical properties of the cholesterics are significantly different due to their strong twisting presented in a kind of helical axis where each layer is twisted.

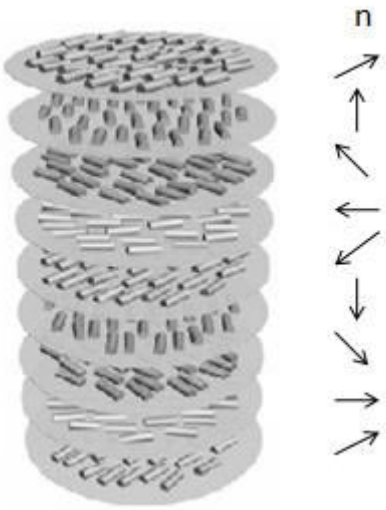


**Figure 1.5 – Schematic illustration of the cholesteric liquid crystal phase.**

If the molecules that form the liquid crystal are chiral, then those chiral molecules are responsible for the helical phase of the cholesteric, causing a twist in the nematic structure as phases are replaced (Collings & Hird, 2004).

One other phase of the liquid crystals is the smectic phase. Contrary to the nematics, the smectics are arranged in layers.

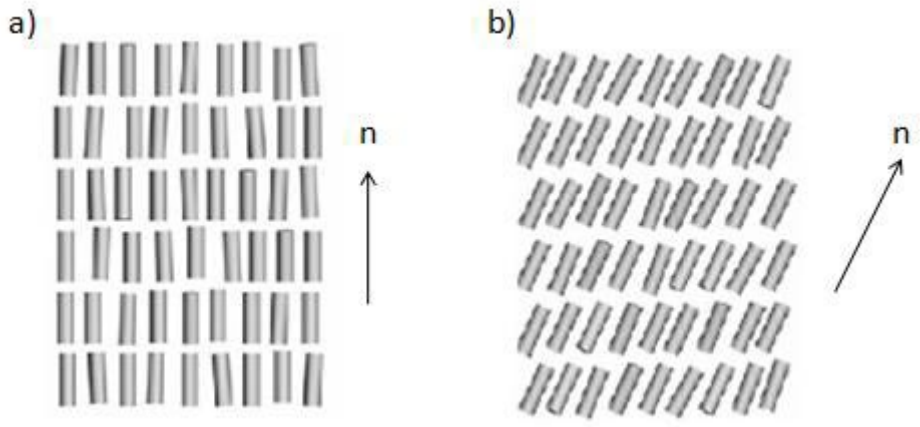


**Figure 1.6 – Schematic illustration of the smectic liquid crystal phase.**

Figure 1.6 a) (Senyuk, 2006) shows the structure of the smectic A phase and Figure 1.6 b) (Senyuk, 2006) shows the structure of the smectic C phase. These two phases are the most common inside the smectic phases and differ one to another by the direction that the molecules are more likely to be aligned, according to the director vector, explained below.

## 1.2. Basics of Liquid Crystals

In general, some terms are common to all kinds of liquid crystals described above and those definitions are important to understand how the liquid crystals work. These basics will be described below, as follow.

### 1.2.1. Director and Degree of Order

The distinguishing characteristic of the liquid crystalline state is the tendency of the molecules to point along a common axis, called the director vector, represented by $n$.
The director gives the direction of the preferred orientation of the liquid crystal molecules, being directions, $+n$ and $-n$, equivalent. The important thing is the direction that the molecules are pointing, except for molecules with permanent dipole moments.
Liquid crystals possess more order than liquids but less than solids and because molecular orientations are not perfect due to fluctuations, this value is quantified by

the degree of order, defined by $S$, $0 < S < 1$. In a perfectly oriented system, $S = 1$, and in an isotropic liquid state, with no orientational order, $S = 0$.

In the mesophase, this value is among the two limits of the degree of order interval, being in the range of $S = 0.3{\sim}0.9$, as temperature decreases (Senyuk, 2006).

Almost all surfaces make the director to orient in a specific direction near that surface. Thus, three types of alignment can be considered, according to different orientations. This way, liquid crystals can have planar, tilted or homeotropic orientations.

### 1.2.2. Anisotropy

The property of liquid crystals that distinguishes them from liquids is the higher degree of order among the molecules.

All liquids and gases are isotropic, that is, any property measured along one direction of space has the same value when measured along any other direction. Obtaining the same result regardless of direction is called isotropy.

The order of the molecules, as they become liquid crystals or solids, destroys the isotropy of liquids and produces anisotropy. This means that any property measured along one direction of space would be different from any other direction, that is, the physical properties vary with the direction (Collings, 2002).

The orientational order of the anisotropic molecules depends on the optical, mechanical, electric and magnetic properties. This orientation of the liquid crystal molecules is, effectively, controlled by electric and magnetic fields. By changing the liquid crystal molecules orientation, it is possible to change the optical and mechanical properties of the system (Senyuk, 2006).

In liquid crystals there are two main types of anisotropies, the optic and the dielectric anisotropies. The optic anisotropy is related to the refractive indices of the compound, which are two different ones, the ordinary and the extraordinary indices, $n_o$ and $n_e$, respectively. The first one is measured perpendicularly to the optic axis while the second is measured parallel to the same axis.

Dielectric anisotropy defines the director alignment and, consequently, the orientation of the liquid crystal molecules in the presence of an electric field. This anisotropy is characterized by the dielectric constants measured parallel and perpendicularly to the

director, designated by $\varepsilon_{\parallel}$ and $\varepsilon_{\perp}$, respectively. For applications based on the variation of an applied electric field it is wise that $\Delta\varepsilon$ is reasonably high to achieve a fast orientation of the director with the applied field for low voltages (Almeida, 2003).

### 1.2.3. Liquid Crystals in Electric Fields

When electric fields are applied to molecules, different kinds of molecules experience different forces. If the molecule is charged, it experiences a force in the direction of the field if it is positively charged and in the direction opposite to the field if it is negatively charged. This force tends to move the molecule along one of these two directions.

Figure 1.7 illustrates a liquid crystal molecule in the presence of an electric field. If the dipole moment of the molecule is parallel to the director, Figure 1.7 a), adapted (Senyuk, 2006), the molecules tend to align according to the direction of the electric field and if the dipole moment of the molecule is normal to the director, Figure 1.7 b), adapted (Senyuk, 2006), the molecules tend to align perpendicularly to the direction of the electric field.

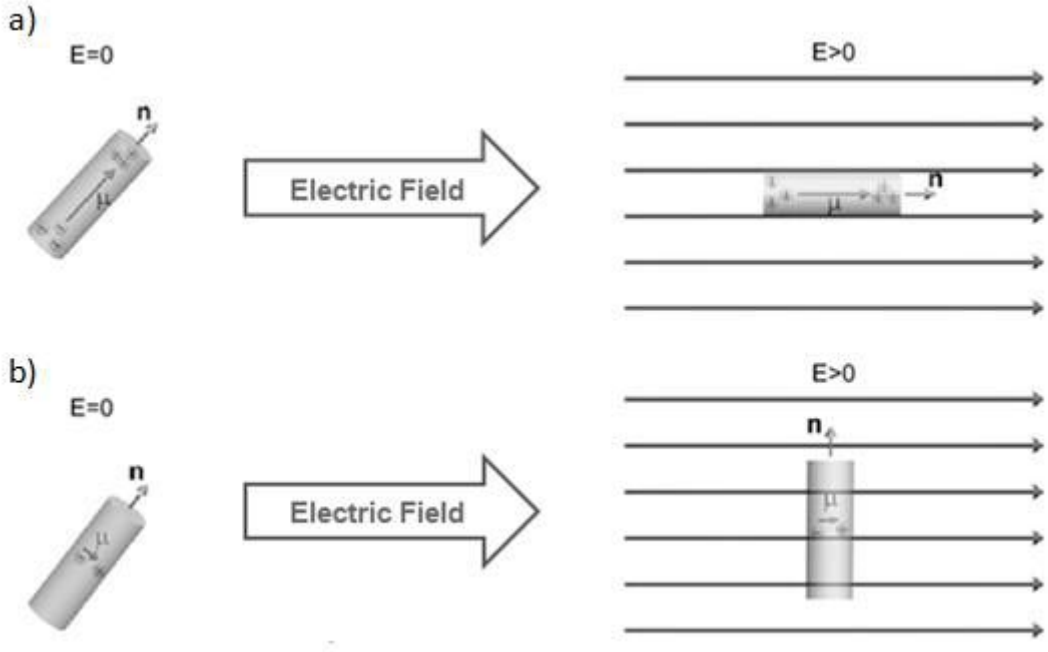


**Figure 1.7 – Effects of an electric field in a liquid crystal molecule.**

The strength of the electric field necessary to orient the director of a liquid crystal is relatively low since the director of a liquid crystal is usually free to orient in any direction.

### 1.2.4. Surface Anchorage and Memory Effect

The surface anchorage is a peculiarity of the liquid crystal molecules when they lose their orientational degrees of freedom. Figure 1.8 (Brás et al., 2008) shows a scheme on how anchorage and anchorage breaking works.

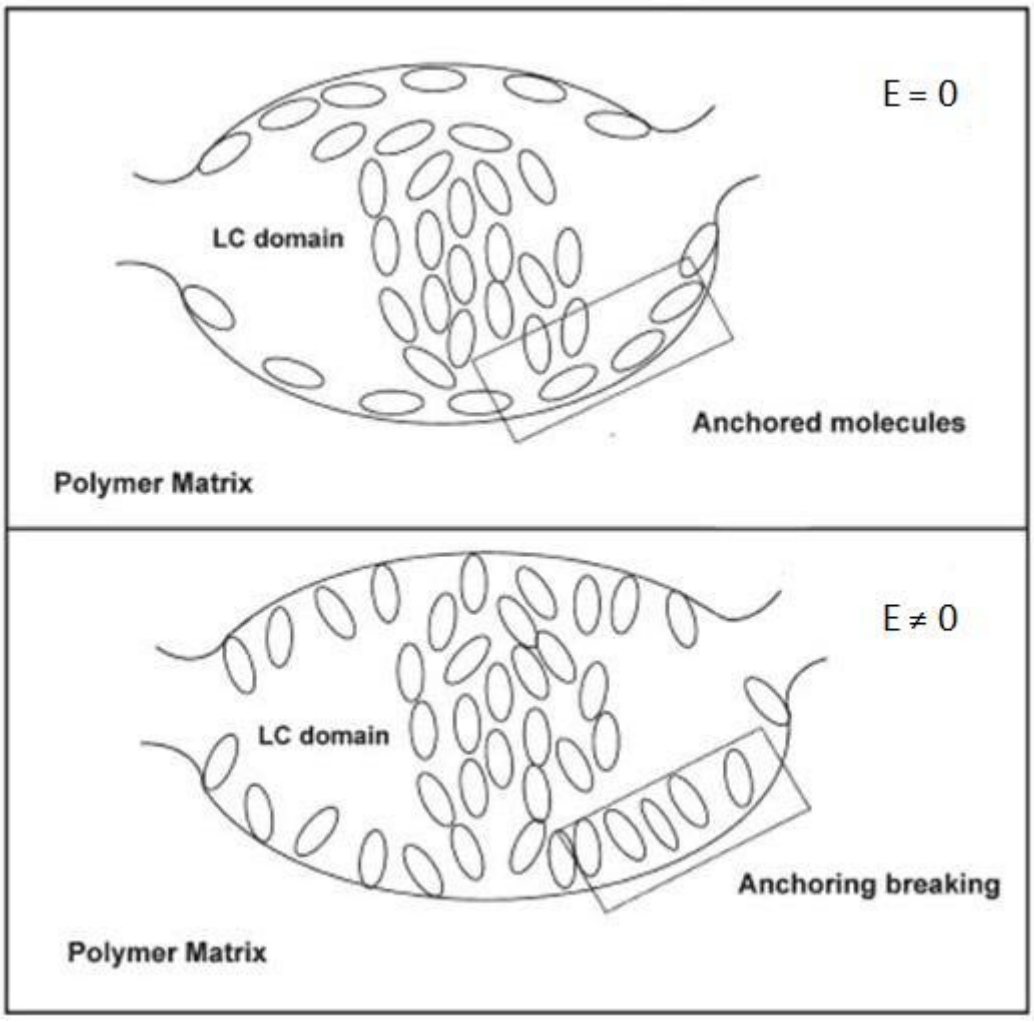


**Figure 1.8 – Surface anchorage when external fields are applied.**

The molecules nearest to the surface remain anchored to the substrate surface, not being reoriented when energy is supplied or taken, while the other molecules suffer the alignment and misalignment that are, normally, exposed. If we understand the liquid crystal domain as consisting of an interfacial shell of immobilized molecules due

to the anchoring interaction with the polymer surface, this interfacial shell holds in its interior anchored molecules that will influence the orientation of the adjacent ones through the elastic restoring forces arising in the deformed nematic. Before applying any field the inclusions are randomly distributed. Under the action of a determined electric field, the molecules in the bulk reorient along the field but the anchored molecules at the interface impair a full homeotropic alignment. Above that determined field, the anchoring of the molecules to the polymeric surface is broken and the molecules at the surface adopt an alignment towards the field direction that tends to persist after field removal. This alignment at the surface determines the orientation of the remaining liquid crystal giving rise to a higher transparency even in the off state, here defined as permanent memory effect. These anchorage links are easily broken by the increase of temperature. Figure 1.9 illustrates the difference between surface anchorage and permanent memory effect. The arrows represent liquid crystal molecules and their respective director.

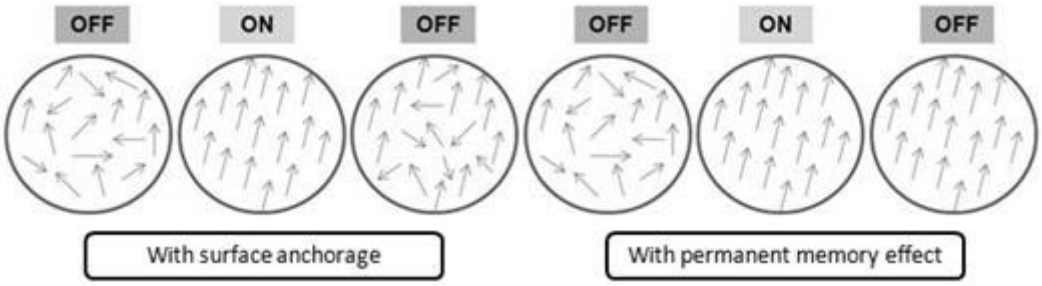


**Figure 1.9 – Surface anchorage and permanent memory effect.**

In literature, the memory effect is understood as a hysteresis, this is, when the applied voltage is taken and the cell returns to the opaque state, it does not return at the exactly same voltage and transmittance coordinates that it took to turn into a transparent state when voltage was applied. The difference between those two paths is understood as the hysteresis of the sample, which is its memory effect.

Another kind of memory effect might occur within the polymer dispersed liquid crystals and will be classified as permanent memory effect. Permanent memory effects occur when the initial transmittance of a sample, supposed to be opaque, differs from the final transmittance after voltage was applied, which is slightly higher. This is a good property for memory devices where we can write, read and erase data.

## 1.3. Polymer Liquid Crystals

If combined with a polymer, thermotropic and lyotropic liquid crystals can originate a new type of liquid crystal, called polymer liquid crystals, and as in a single liquid crystal, in polymer liquid crystals there can be two classes, the thermotropic and the lyotropic. They might occur either by solving a polymer in a solvent or by heating a polymer above its glass or melting transition point.

The first class consists of monomers that are fairly rigid, anisotropic and highly polarizable. These monomers are either rod-shaped or disc-shaped. The second class of monomers causing liquid cristallinity in the polymer is the amphiphilic monomers (Collings, 2002).

### 1.3.1. Types of Polymer Liquid Crystals

The thermotropic polymer liquid crystals are formed when the polymeric material is heated to a point where the solid phase melts and lyotropic polymer liquid crystals consist of large molecules that form phases with orientational order when dissolved in ordinary solvents, becoming the polymer liquid crystal phase more dependent on concentration than on temperature.

The monomers can be attached together to form a polymer in two different ways, main chain polymers if the monomers form a long single chain by attaching to one another and side chain polymers if the monomers end up as branches extending away from the polymer chain. Figure 1.10, adapted (Gordon, 1997), illustrates the types of polymers that can be formed with anisotropic units.

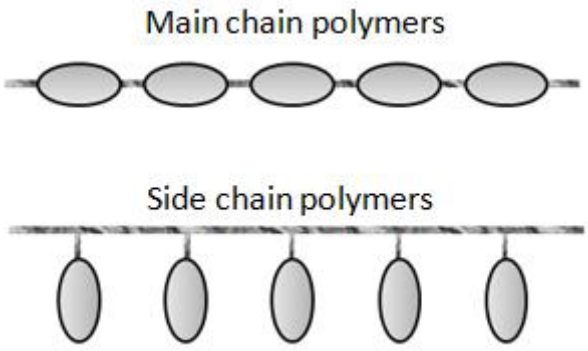


**Figure 1.10 – Types of polymers that can be formed with anisotropic units.**

Each ellipse represents a mesogenic unit, the rigid part of the monomer, and the links represent the spacers, the flexible parts of the monomer. The mesogens are the monomer sections that display orientational order in the liquid crystal phases. The functionality of the liquid crystal is similar to the previous mentioned, without the polymer extensions.

Other factors influencing the mesomorphic behavior of polymers include the presence of long flexible spacers, a low molecular weight, and regular alternation of rigid and flexible units along the main chain (Gordon, 1997).

## 1.4. Liquid Crystal Displays

Nowadays we live in the age of information. Liquid crystal displays have played an important role of development in this era and are meant to keep playing it in the future.

Information displays use the ability to control light in order to operate by controlling what parts of a display are bright and what parts are dark. That way, active and passive displays are considered, light-emitting diode and liquid crystal displays, respectively. Both active and passive displays that are illuminated from behind or beside must use electrical power to generate light. Passive displays that utilize ambient light do not consume electrical power in order to generate light and, therefore, require much less power to operate. This is the largest advantage of liquid crystal displays that rely on ambient light for their operation (Collings, 2002). The amount of power needed to operate these displays is much less than for other displays, making liquid crystal displays ideal for battery-operated equipments.

### 1.4.1. Applied Voltages

With both active and passive displays, the control of light from each area is usually achieved by applying a voltage to a device in that area. How well the device operates as a display depends on how it responds to this applied voltage.

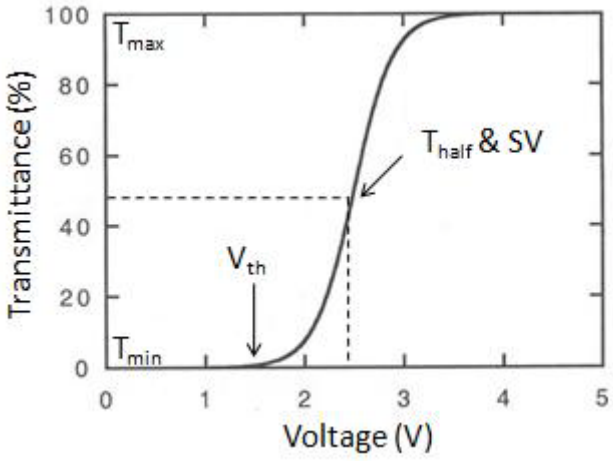


**Figure 1.11 – Electro-optic response curve of a typical display.**

Voltage is important in three characteristics of the response. The change in the brightness, called threshold voltage, $V_{th}$ in Figure 1.11 (Collings, 2002), and the need to increase voltage so the brightness also increases. A third characteristic is related with the quickness of the device response as the voltage is either applied or removed (Collings, 2002).

In most liquid crystal displays, this characteristic differs because the device turns on by responding to the application of a voltage, but simply relaxes back to its initial state when the voltage is removed. This can be seen in Figure 1.12 a) and b) (Collings, 2002), respectively, where $T_{on}$ and $T_{off}$ represent the times between application of the voltage and a $90\%$ change in brightness. $T_{on}$ is also symbolized as $V_{90}$ and $T_{off}$ is also symbolized as $V_{10}$ (Collings, 2002).

The characteristic of the liquid crystal that is most important in determining how quickly it responds is its orientational viscosity, that is, the amount of resistance in the liquid crystal when it is forced to change its director configuration.

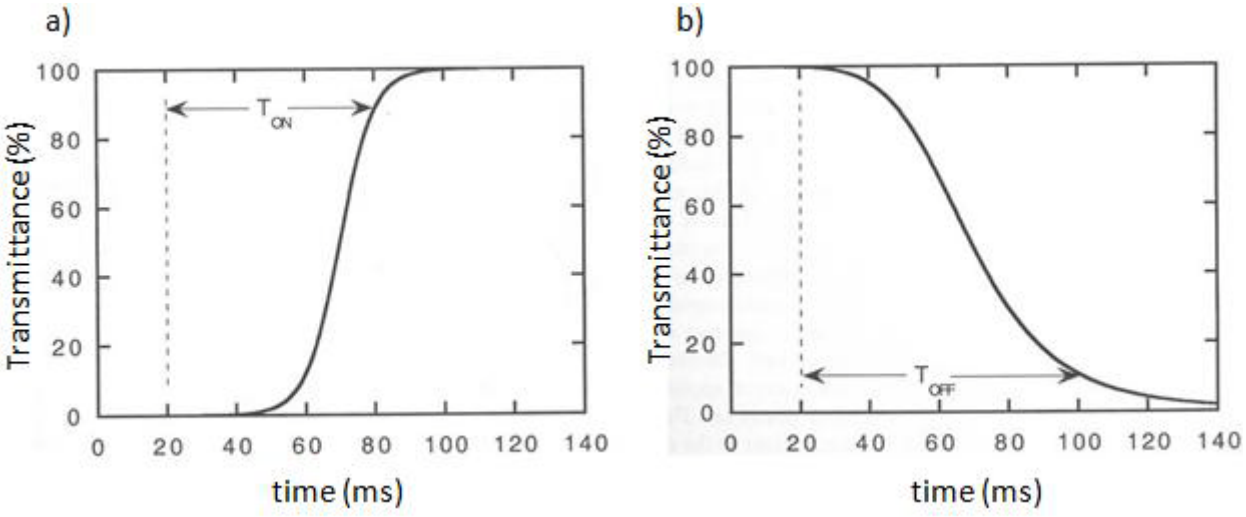


**Figure 1.12 – Turn-on and turn-off responses for a typical liquid crystal display.**

The characterization of the composites in this work is made through the following parameters, like transmittance, contrast and applied voltages. $T_{max}$ represents the maximum transmittance obtained with the respective sample, $T_{min}$ represents the minimum transmittance obtained with the respective sample and $T_{half}$ is calculated by Equation 1 and represents the average transmittance to switch the cell from its opaque to transparent state.

$$T_{half} = \frac{T_{max} - T_{min}}{2} \quad \textbf{(1)}$$

The switching voltage, $SV$, that characterizes the composite is the applied voltage in which transmittance is $T_{half}$.

The contrast ratio is an important factor to the functionality of a polymer dispersed liquid crystal display. A high contrast ratio is the desired aspect of any display, but there are various methods of measuring it. The general formula to calculate the contrast ratio is given by Equation 2. Meanwhile, some of the samples prepared have a minimum transmittance of zero, meaning that mathematically it is impossible to define a contrast ratio number to be comparable with the other samples. Therefore, the values presented for the contrast of the samples were calculated by Equation 3.

$$Contrast\ Ratio = \frac{T_{max}}{T_{min}} \quad \textbf{(2)}$$

$$Contrast = \frac{T_{max} - T_{min}}{100} \quad (3)$$

The $T/V$ Ratio represents the transmission-to-voltage ratio, Equation 4. This is a measure of performance of the device as a whole, with the switching transmittance divided by the switching voltage, to give an idea of the device is need on voltages to state transitions. When this ratio is higher, the better, meaning that the system needs only a few applied voltage to reach its half transmittance point, while low ratios mean that the system require high voltages to reach its half transmittance point or even might the voltages be low, but the transmittance is not good enough.

$$\mathrm{T/V}\ Ratio = \frac{T_{half}}{Switching\ Voltage\ (V)} \quad (4)$$

### 1.4.2. Types of Liquid Crystal Displays

There are many types of liquid crystal displays, such as the dynamic scattering mode that consists in two glass plates involving transparent electrodes and it works with low voltages in a range of approximately $10{\sim}20\ V$, but the liquid crystal must possess some charged impurities, which can be achieved by adding impurities to the liquid crystal. The disadvantage of this display is that the contrast ratio is not very high (Collings, 2002).

Another type is the chiral nematic mode, which uses the same technique of the previous one, except it utilizes cholesteric liquid crystals. That forces the molecules to align parallel to the glass surfaces, adopting a texture with the helical axis perpendicular to the glass surfaces, making the cell appears clear. The disadvantages of this type of display are the contrast ratio and the higher voltages required for it to operate, in a range of $40{\sim}100\ V$ to start and $300\ V$ to shut down (Collings, 2002).

The most common mode of a liquid crystal display is the twisted nematic mode, which is, presently, the predominant type of liquid crystal displays. This device consists of the twisted nematic liquid crystal confined between two glass substrates with homogeneous planar orientation. The cell is then placed between two polarizers that

are crossed on either side of it. In the absence of an electric field, the surface induces a twist of the director, which rotates the polarization axis of the light, thus allowing it to pass through the second polarizer. The presence of an electric field removes this rotation, therefore allowing no light to pass through the second polarizer.

The main advantage of the twisted nematic liquid crystal display is its higher contrast ratio and the threshold voltage being low, on the order of a few volts. But it also has disadvantages such as different areas of the cell would twist in opposite directions when no voltage was applied or the brightness versus voltage curves is not great (Collings, 2002).

Liquid crystal displays can use dyes, which absorb light of a certain wavelength, causing the light reflected from or transmitted through the dye to appear colored.

Other displays use birefringent liquid crystals using the birefringence effect to operate. This effect can be explained when the phase angle between light polarized along one direction and light polarized along a perpendicular direction changes continuously as the light propagates through a liquid crystal.

As nematics and cholesterics can be used to make liquid crystal displays, also the smectics can. The smectic liquid crystal displays usually do not respond to applied electric and magnetic fields as easily as nematics do. For this reason, simple application of an electric field rarely produces enough change in the optical properties of a smectic liquid crystal to be useful for display purposes.

These last three types are still in development but recently, development in liquid crystal displays utilizes polymers either to contain the liquid crystal material or to promote a specific texture. These displays are easily fabricated and offer some significant advantages over other types of liquid crystal displays.

### 1.4.3. Polymer Dispersed Liquid Crystal Displays

Polymer dispersed liquid crystals are a relatively new class of materials that hold promise for many applications ranging from switchable windows to projection displays and consist of liquid crystal droplets that are dispersed in a solid polymer matrix. These materials, which are simply a combined application of polymers and liquid crystals, are the focus of extensive research in the display industry (Collings, 2002).

Three methods of polymer dispersed liquid crystal films preparation are described in the literature. The first one consists in filling the polymer micropores with a liquid crystal, the second one involves the formation of polymer dispersed liquid crystal films from an aqueous emulsion and the third one, and used in this work, is the polymerization induced phase separation (Torgova et al., 2004). Usually, there are two types of morphologies in a polymer dispersed liquid crystal. One is a kind of swiss cheese, Figure 1.13 a), adapted (Han, 2006), and the other is based on polymer balls, Figure 1.13 b), adapted (Han, 2006). The last case is the scenario verified in this work, which promotes the appearance of permanent memory effects.

Although the morphologies are very different, the theory behind its operation is, practically, the same. In the systems studied, the morphology is of polymer balls, this is, instead of droplets, the liquid crystal runs through channels within the polymer formed when phase separation occurs.

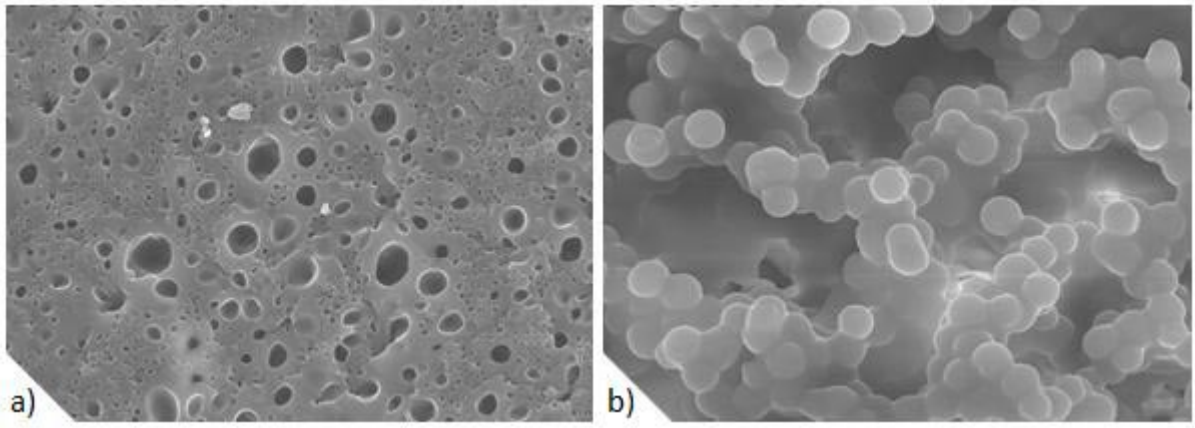


**Figure 1.13 – Polymer dispersed liquid crystal morphology.**

By changing the orientation of the liquid crystal molecules with an electric field, it is possible to vary the intensity of transmitted light. The configuration of the liquid crystal droplets in a polymer matrix is the focus of much current research. Many different configurations have been observed and they depend on factors such as droplet size and shape, surface anchoring and applied fields (Collings & Hird, 2004).

In a polymer dispersed liquid crystal display there are many droplets with different configurations and orientations. Figure 1.14 (Gordon, 1997) shows those orientations. The radial configuration occurs when the liquid crystal molecules are anchored with their long axes perpendicular to the droplet walls. The axial configuration of the liquid crystal droplets also occurs when the molecules are oriented perpendicular to the

droplet wall, but only when there is weak surface anchoring. Finally, the bipolar configuration is obtained by tangential anchoring of the liquid crystal molecules that creates two point defects at the poles of the droplet (Gordon, 1997).

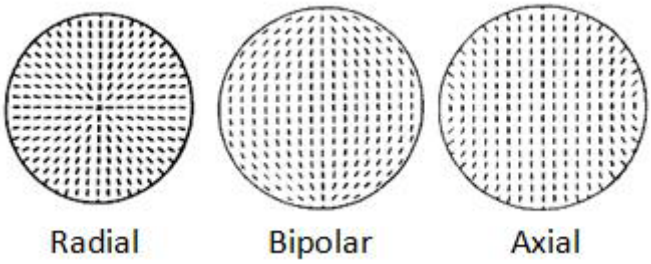


**Figure 1.14 – Possible orientations and configurations of liquid crystal droplets.**

In a typical polymer dispersed liquid crystal sample, there are many droplets with different configurations and orientations. A thin polymer dispersed liquid crystal film is deposited between clear glass covers that are coated with a very thin layer of a conducting material known as indium tin oxide.

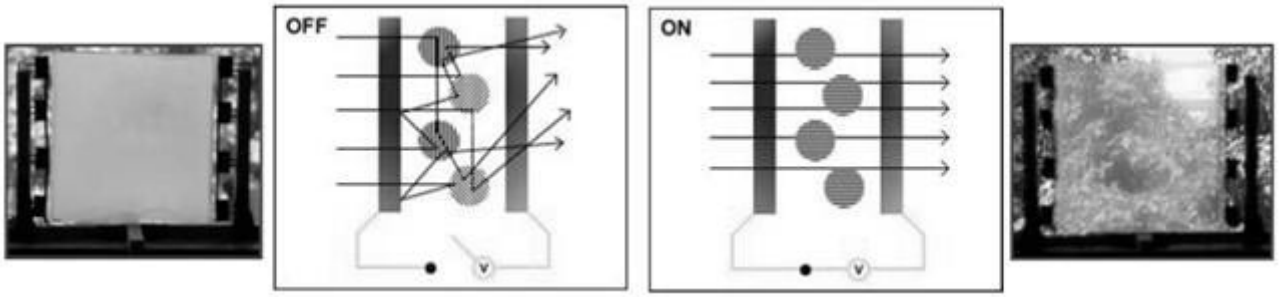


**Figure 1.15 – Working principle of a polymer dispersed liquid crystal display.**

When an electric field is applied, however, the molecules within the droplets align along the field and have corresponding optical properties, as can be seen in Figure 1.15, adapted (Martins, 2004). When voltage is not applied, the light enters the cell and, following the orientation of the liquid crystal molecules, takes different directions, meaning that the cell keeps its opacity and the image is not transmitted. When voltage is applied, the light enters the cell and, once the liquid crystal molecules are completely aligned, follows the orientation of those molecules allowing the image to be transmitted, meaning that the cell is clear.

Besides the presence of an electric field is an important factor to the operation of a display of this kind, there is a crucial detail for the transition from opaque to transparent state, which is related with the refractive indices of the components in

question. In the absence of an external electric field, the director orientation of the liquid crystal varies randomly from droplet to droplet. In this case, the liquid crystal refractive indices are different from the polymer refractive index and produce a strong light scattering that makes the sample opaque. While in the presence of an external electric field of sufficient intensity, the liquid crystal droplets align towards the direction of applied electric field and sample appears transparent, due to the matching of refractive indices of liquid crystal droplets and polymer (Malik & Raina, 2004).

## 1.5. Applications of Liquid Crystals

Liquid crystal technology has had a major effect in many areas of science and engineering, as well as device technology. Applications for this special kind of material are still being discovered and continue to provide effective solutions to many different problems (Collings, 2002).

The most common application of liquid crystal technology is liquid crystal displays, such as digital watches, calculators, thermometers, personal laptops, among others. An application of liquid crystals that is only now being explored is optical imaging and recording. Liquid crystals have a massive amount of other uses. They are used for non destructive mechanical testing of materials under stress or used in medical applications. Low molar mass liquid crystals have applications including erasable optical disks, full color electronic slides for computer-aided drawing and light modulators for color electronic imaging (Collings & Hird, 2004).

In this field, the investigations are far from done and new functional liquid crystals are prepared by self-assembly of a variety of molecules, not only organic, but also inorganic components such as salts and minerals that have been incorporated into liquid-crystalline materials. Such new material designs expand the applicability of liquid crystals in the field of electro-optics, electronics, separation, sensing and nanotechnology (Kato & Mizoshita, 2002).

### 1.5.1. Polymer Liquid Crystals applications

Polymer liquid crystals will most certainly become more important as research into this field progresses. Applications for these materials range from the production of high-strength materials, such as resistant plastics to their use in optical devices.

An application of polymer liquid crystals that has been successfully developed for industry is the area of high strength fibers and applications calling for strong and light weight materials (Collings & Hird, 2004).

At this time, polymer liquid crystals demonstrate relatively slow response times when compared to polymer dispersed liquid crystals, giving rise to displays based on polymer dispersed liquid crystals.

### 1.5.2. Polymer Dispersed Liquid Crystals applications

Polymer dispersed liquid crystals hold potential for a variety of electro-optic applications ranging from displays to light shutters (Doane, 2006). These windows are based on the ability of the nematic director of the liquid crystal droplets to align under an electric field, case of study in this master thesis.

Other possible application is digital paper, due to conducting polymers are better mechanical and interfacial compatible with plastic substrates, integration of driving electrodes based on conducting polymer thin films in display devices can have some advantages for the improvement on the flexibility of the device itself. As rigid alignment structures on the substrates involving the liquid crystal components are not required, these polymer dispersed liquid crystal devices intrinsically can better tolerate mechanical bending than other types of liquid crystal displays (Wang & MacDiarmid, 2007).

# *Chapter Two*

# 2. Literature Review

## 2.1. Before the Discovery

Before the discovery of liquid crystals, a few European investigators observed some new and interesting phenomena but never fully realized exactly what was happening in their experiments.

In a time frame from 1850 to 1888, three different types of studies were carried out. The first one concerned the study of some biological specimens where effects on the polarization microscopy were observed. The second one involved the study of how substances crystallize where the transitions from liquid to solid state were not so direct, but change to an amorphous form of state, which then crystallized. Finally, an experience with stearin, reported that it possesses an unusual melting behavior, appearing as two melting points (Collings, 2002).

These phenomenons were the first notices published of strange materials, known today as liquid crystals.

## 2.2. The Discovery of Liquid Crystals

By 1888 Reinitzer, an Austrian botanist to whom the credit of discovering the liquid crystals have been given, observed the melting behavior of an organic substance related to cholesterol and evidenced that it also has two melting points, meaning the presence of an intermediate state of matter.

However, the labeling liquid crystals is attributed to Lehmann, a German professor of physics that described that substance as a combination of characteristics such as flow properties like a liquid and optical properties like a solid.
From this point, chemists, physicists, biologists, engineers and medical doctors are involved in liquid crystal researches (Collings, 2002).

## 2.3. After the Discovery

After the discovery, scientists reported that many substances known as liquid crystals behaved differently from ones to the others and by the turn of the $20^{th}$ century, Lehmann observed that a solid surface in contact with a liquid crystalline substance causes the liquid crystal to orient in a certain direction. This was of extreme importance when modern scientists began to experiment with liquid crystal displays.
The liquid crystal phases were published by Friedel in $1922$, where themes like the molecular ordering, orientations, structures and the presence of the electric fields were spoken for the first time. The action of the electric and magnetic fields on liquid crystals began to be understood, mainly due to experiments performed in Holland and in the former Soviet Union. The first empirical equation was the degree of order, described by the order parameter, which proved to be the closest to describe the actual order present in liquid crystals. This order parameter is the base of all the recent developments since $1940$ (Collings, 2002).

## 2.4. Recent Developments

In $1957$, Brown, an American chemist, published an article reviewing the liquid crystal phase and in $1962$, Gray, an English chemist, published a full length book describing the molecular structure and properties of liquid crystals. It started to become apparent that liquid crystalline substances had the ability to detect extremely small changes in temperature, mechanical stress, electro-magnetic radiation and chemical environment.

By the year of $1968$, two scientists demonstrated that a thin layer of liquid crystal was capable of switching from cloudy to clear when an electrical voltage was applied. Although this was the first liquid crystal display, it required too high a voltage, consumed too much power and produced a display of poor quality. Within ten years liquid crystal displays that required extremely little power were being used by manufacturers of battery-operated equipments.

During the decade of $1980$, the study of liquid crystals played an important role in understanding how molecules behave cooperatively and how molecular structure influences this behavior.

Since the beginning of the $21^{st}$ century the field of liquid crystals is maturing, for instance, the study of the interactions between liquid crystals and surfaces has revealed a great deal of new information, opening the door to both improved and new applications. What has characterized the last ten years has been the increase in performance and reliability over earlier liquid crystal applications (Collings, 2002).

### 2.4.1. Polymer Dispersed Liquid Crystals

One of those areas that have been maturing since the last two decades is the polymer dispersed liquid crystals. Investigation of very kinds has been developed in the scope of the search for the optimum device.

The role of polymeric materials in the blends is very important. Polymer plays an auxiliary but very important role in achieving required effects related to the presence of a liquid crystal in various devices (Mucha, 2002).

To study the effect of the monomer functionality, Pogue et al. studied uniform illumination and non-uniform illumination using monomers with different number of acrylate groups, while keeping the liquid crystal concentration constant. The tendency is to form anisotropically-shaped domains for higher functional syrups. These domain anisotropy differences are correlated with the number of reactive double bonds per monomer (Pogue et al., 2000).

The morphology of polymer matrix changes with the weight ratio between polymer and liquid crystal and curing temperature, resulting in a large change in the droplet size of liquid crystal domains in the polymer dispersed liquid crystal film. The

hydrophobicity of the liquid crystalline polymer changes the droplet size of the polymer dispersed liquid crystal films and the anchoring energy between the polymer matrix and the liquid crystal droplets. As the hydrophobicity of the matrix increases, the droplet size of liquid crystal domain also increases, on the contrary, anchoring energy decreases, leading to the decrease of driving voltage (Park et al., 2000).

An important parameter to keep in mind is the effect of the temperature on the optical and electro-optical behaviors of these materials, once the liquid crystal used is a thermotropic liquid crystal. This temperature effect has influence in the electro-optical properties because for high liquid crystal concentrations it is observed that at room temperature the transmittance suffers a strong decrease due to the homogeneous distribution of phase-separated liquid crystal droplets that occupy a large part of the polymer matrix (Deshmukh & Malik, 2008).

The effect of lowering the viscosity and that of decreased degree of polymerization with increased temperature, leads to easier coalescence of liquid crystal droplets after phase separation (Ahn & Ha, 1999).

Yet another important aspect is the dependence of the electro-optic activity on the separation of the polymer and liquid crystal phases. Since the phase structure develops in a non-equilibrium system, the morphology of the liquid crystal domains depends on the details of the chemical and physical processes active during domain formation (Justice et al., 2005).

Optical devices based on polymer dispersed liquid crystal thin films derive their functional properties from the electric field induced reorientation of liquid crystal microdroplets. In these materials, the liquid crystal reorientation dynamics are strongly dependent on droplet size and shape, as well as interfacial interactions between polymer and liquid crystal (Higgins et al., 2005).

This takes us to the next level of crucial factors in which a polymer dispersed liquid crystal performance is dependent, as the application of external fields, the surface anchorage and its memory effects, the additive effects on reducing the driving voltages and the electro-optical studies that confirm that scenario.

### 2.4.2. External Fields

The science behind the operation of a polymer dispersed liquid crystal involves the use of external fields, nominated, an electric field. Some studies have been conducted, exclusively, in this area.

The electrical properties of polymer dispersed liquid crystals are an important characteristic in their electro-optical performance. Doping a polymer dispersed liquid crystal with low percentages of a conducting polymer allows a fine adjustment of polymer matrix conductivity. This leads to a large reduction in the reorientational fields and relaxation times, making them optimal for the electro-optical studies (Cupelli et al., 2004).

Huang et al. studied the electrical field in a nematic droplet dispersed in a polymer matrix. The field within the droplet is uniform and its direction is different from that of the applied field (Huang et al.).

Meanwhile, Zhang et al. studied the effects of the electric field, through direct current on the phase separation of polymer dispersed liquid crystals. They verified that this phase separation process accelerates when the electric field is applied. This appliance during the phase separation process yields the polymer dispersed liquid crystal with small liquid crystal domains and fine morphologies (Zhang et al., 2003).

This way, the electric field is a very important step, not only to the operation of the devices, but also to the shapes and morphologies that the polymers will exhibit when submitted to the presence of an external field.

### 2.4.3. Surface Anchorage

The surface anchorage is, directly, connected to the surface tension of the liquid crystal molecules.

In this field, Kim et al. studied the interfacial tension of an interface of a nematic liquid crystal with water, while the surface alignment was homeotropic. In this publication, a surfactant was used, the cetyl trimethyl ammonium bromide, and the adsorption of this component lowers the interfacial tension value and induce a transition in liquid crystal surface alignment from planar to homeotropic. The presence of the surfactant

also changes the shape of the drops from spherical to, approximately, ellipsoidal, due to a reduction in the interfacial tension (Kim et al., 2004).

Anisotropy is a very important characteristic of the liquid crystals and Tsvetkov et al. studied it on the liquid crystal surface tension. The lowest surface tension is observed for homeotropic orientation, the highest for planar orientation and average for the homeoplanar orientation (Tsvetkov et al., 1999).

Related to the surface anchorage are the memory effects. This means that the anchoring strength is dependent on the history of the sample. Once defined, the preferred orientation of the liquid crystals remains stable even under strong applied torque or repetitive nematic to isotropic transitions (Stoenescu et al., 1999). However, this memory effect is not present when the monomer molecules show a low solubility in liquid crystal droplets (Nicoletta et al., 2000). But some composites present a memory state, which means that higher transmittances are preserved without applying voltage. The memory state can be erased and changed to the scattering off-state by heating the film to the clearing temperature of the liquid crystal (Kalkar et al., 1999).

A fine study of the anchoring characteristics and interfacial interactions analyzed that anchoring energies calculated from the interfacial tensions indicated that the liquid crystal and polymer interfaces are strong. On addition of a surfactant, the anchoring energy at the interface of the liquid crystal and the surfactant becomes weaker. This decrease in anchoring strength may be one of the major factors responsible for a reduction in droplet sizes and also a lowering of critical fields for switching. Therefore, the surfactant, at a low concentration, helps reducing the surface tension (Patnaik & Pachter, 1998).

In some polymers this surface anchorage is verified, while in others this effect does not exist. However, the surface anchorage is an important aspect to have in mind, for example, when understanding the morphologies of the composites or the contrast ratios of the displays.

### 2.4.4. Additive Effects

The main theme of this thesis is the additive effects to the polymer dispersed liquid crystals. Other authors have already made some studies based on this theme, studying factors as the influence of surfactants, the surfactant effects on morphologies, the effects of surfactants on electro-optical properties, and so on.

With the addition of a non-reactive surfactant-like molecule, a substantial lowering of the switching field is attributed to a modification of the anchoring properties of the liquid crystal molecules and the polymer host. These molecules act to contaminate the liquid crystal droplets, reducing the clearing temperature (Klosterman et al., 2004).

In agreement with the previous article, other authors studied the effects of octanoic acid on the morphology and electro-optic properties of polymer dispersed liquid crystals and found that droplet sizes decrease with increasing octanoic acid content. An octanoic acid concentration in weight of, approximately, $6\%$ was selected, for which a minimum switching voltage of $5\ V.\mu m^{-1}$ and maximum contrast ratio were obtained (Kim & Woo, 2007).

A very similar study shows that surfactants with greater spreading coefficient give smaller droplets, greater diffraction efficiency, driving voltage, contrast ratio and smaller response times (Shim et al., 2008).

All this thematic is linked with many aspects and yet another study was done on the electro-optical properties of holographic polymer dispersed liquid crystals proving that surfactants can effectively reduce the driving voltage, being the threshold voltage reduced from $13\ V.\mu m^{-1}$ to about $2.3\ V.\mu m^{-1}$ (Liu et al., 2004).

Surfactants can also be used to lower the hysteresis problems in these materials, correlating the hysteresis behavior of the polymer dispersed liquid crystal film with the interaction of the surfactants at the material interface (Chung et al., 1997).

This leads to the basis of our studies, the electro-optics, where many assays have been done within time, sometimes using an additive or some other times experiencing different monomers, among others.

### 2.4.5. Electro-Optical Studies

As described above, many are the studies on electro-optical properties of polymer dispersed liquid crystal films. Usually, they are prepared by the polymerization induced phase separation.

In an experiment, switching can be seen by naked eye. Threshold voltage is measured observing microscopically the polarization texture changes of the liquid crystal as it tends to switch. Transmittance of the film is measured with a visible spectrometer as a function of wavelength (Karapinar, 1998). The transmitted light is usually captured with a collimated beam of polarized $He - Ne$ laser with wavelength at $632.8\,nm$ (Kalkar et al., 1999).

In electro-optic studies, the response curve is slightly different when the elaboration of the films is exposed to electron-beam or ultraviolet radiations. The main difference is that the electro-optical response of the electron-beam cured system shows no evidence of memory effects since the off state transmission remains unchanged, while ultraviolet cured films exhibit a large memory and the voltages $V_{10}$ and $V_{90}$ are relatively high (Maschke et al., 2002).

As every aspect of liquid crystal basics is explicit in every field of investigation in this area, so is the alignment of the liquid crystal droplets connected to the electro-optical responses. For a random distribution, the droplet orientation and the optical phase shift change more gradually with the applied field. These results demonstrate that polymer dispersed liquid crystals may be suitable for a wide range of electro-optic applications (Levy, 2000).

This matrix dispersed liquid crystal is very versatile and even ionic polymer matrix can be used. The electro-optical properties will depend on many parameters of materials, including the liquid crystal properties and the properties of the matrix. The effect of the ionic contents in the polymer matrix is that as the ionic content to liquid crystal ratio increases, more effective are the electro-optic properties of the systems (Choi et al., 1998).

In this field, also monomers affect the electro-optics of these devices. For example, synthesized azobenzene monomers can stabilize the polymer dispersed liquid crystal

and their relative model compounds with various alkyl chain lengths even got better electro-optical effects (Liu & Wu, 2005).

Late improvements in the electro-optical properties of polymer dispersed liquid crystals showed that with the addition of cross-linkers, bonds that attach one polymer chain to another, the droplet size of liquid crystal becomes smaller when more cross-linker is added, affecting the properties of polymer dispersed liquid crystal devices, such as response time and driving voltage (Koo et al., 2008).

With cross-linked films, several trends are observed, for example, the cross-linking agent has strong influence on the cells contrast but not on the cell is maximum transmission or turn on voltages, while the film thickness shows preponderantly its influence on the cell is maximum transmission and turn on voltages (Almeida et al., 2002).

As we might see, there are innumerous experiments that can be made with liquid crystals and how their technology has developed so far, specifically in the area of the polymer dispersed liquid crystals.

## 2.5. Problem Definition and Proposed Solution

In a polymer dispersed liquid crystal, the functionality depends on the applied voltages. To light shutters installed at homes and offices, voltages required for the shutters to operate can be high, using the alternating current available in those buildings, as Figure 2.1 shows (Xinology, 2008).


**Figure 2.1 – Polymer dispersed liquid crystal shutters in an office.**

An interesting application of the polymer dispersed liquid crystals could be in cars windshields and windows where the voltages required must be low, that is, approximately, $12\ V$, the potential supplied by an automotive battery.

For portable displays, such as memos, these voltages must be even lower, so that the device uses an AA battery, $1.5\,V$ or in the maximum, a $9\,V$ battery, considering that these batteries when operated are connected to an inverter, so current is alternate.

### 2.5.1. General Aspects

The major challenge is the reduction of the applied voltages so the polymer dispersed liquid crystal application is a portable device.

To do so, many factors are present like the cell gap, the type of glass used, the monomers in use, among others.

When the spacer length is minimal, the voltages applied are also more reduced than if larger spacers were used. The driving voltage decreases with decreasing thickness, but when the thickness of the cell is below $10\,\mu m$ values start to become similar to the ones observed with the referred thickness, being that sometimes voltages are even superior, because droplets are either smaller or less spherically shaped (Atkins & West). Besides that, when the thickness of the cell becomes smaller, its opacity degree decreases due to the small amounts of liquid crystal present in the sample.

The type of glass used must be conducting glass so that the voltage applied covers the entire sample. This is required for the final application and to test the electro-optical response curves.

Other types of glass, as silica-gel glasses are used by sol-gel processes that trap organic molecules into inorganic oxides. Usually, single molecules are trapped into isolated gel-glass pores, but it is possible to induce larger cavities in the gel-glass. These gel-glass dispersed liquid crystals may provide a lamellar structure and alignment of nematic compounds at the surface (Levy et al., 1997).

The length of the molecular chain and the rigidity and flexibility of molecules influence the structure of the polymer network in the polymer dispersed liquid crystal films, thus affecting the electro-optical properties of the composites accordingly.

The monomers that contain rigid chain segments increase the threshold voltage and can improve the light scattering intensity when the cell is off, while monomers with different molecular structures and the increase of the length of the flexible alkyl molecular chain of polymerizable monomers have the opposite effects, this is, they

decrease the threshold voltage and do not improve the light scattering intensity when the cell is off (Li et al., 2008).

But the most important aspect is the attempt to reduce the high voltages so that they are similar to the ones produced by a low energy battery.

This is almost possible by mixing an additive to the polymer dispersed liquid crystal.

### 2.5.2. Additive Effects

The use of additives in a polymer dispersed liquid crystal is a way to shape the liquid crystal microdroplets and avoid its coalescence, thus, optimizing the performance of the electro-optical system.

The additives modify the interfaces and morphologies of the liquid crystal droplets, involving them, reducing their surface tension, voltages and response times. The scheme below illustrates how the interaction between the surfactant, the liquid crystal and the polymer matrix works.

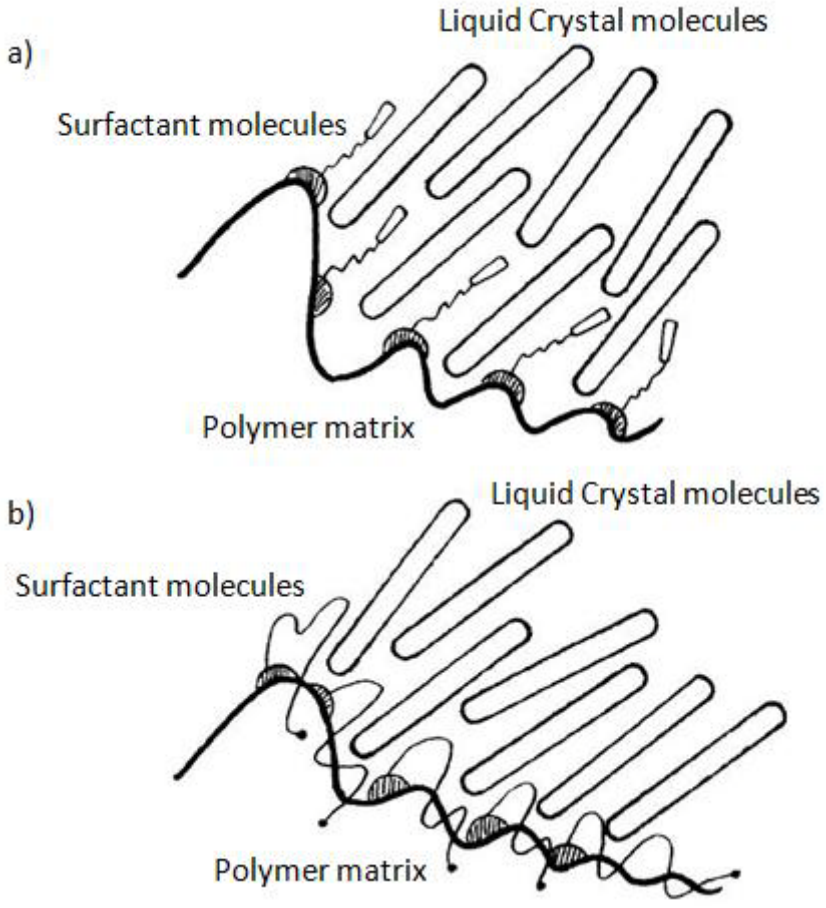


**Figure 2.2 – Interaction and effect of surfactant on a polymer dispersed liquid crystal.**

Figure 2.2 a), adapted (Chung et al., 1997), shows the surfactant molecules behaving as single molecules in grasp with the liquid crystal material for the polymer, which will modify the original anchoring of the liquid crystal molecules to the surface of the polymer. On the other hand, Figure 2.2 b), adapted (Chung et al., 1997), shows the surfactant molecules behaving as a coat over the polymer, thus modifying the anchoring formation and orientation direction of the liquid crystal material with the polymeric surface.

Fundamental control of the polymerization behavior of polymer dispersed liquid crystals is critical to the formation of high performance devices by polymerization induced phase separation.

Additives such as surfactants or reactive diluents can impart significant changes to the electro-optical behavior of a system, especially in acrylate based materials, Figure 2.3.

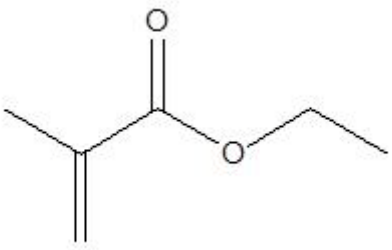


**Figure 2.3 – Chemical structure of methacrylate.**

Some additives improve monomer mobility through plasticizing the polymer to enable faster polymerization rates (White et al., 2007). Although additives can affect the polymerization rate by either increase it or decrease it in some cases, the aim of the study is to get the applied voltage as minimal as it can gets. Nevertheless, aspects as the monomers functionality, surfaces and system responses are also implicated with that aim.

The solution in hand is the addition of surfactants, either anionic or cationic and even non-ionic, as well as comparing molecules with the same functional groups but with larger or shorter chains, and even the effect of the order in which the components of the mixture are added to form the composite.

# *Chapter Three*

# 3. Materials and Methods

## 3.1. Materials

This section is dedicated to the materials used along the work. The main emphasis is attributed to the most important materials, including chemical products, such as monomers, polymerization initiators, the liquid crystal used and, obviously, the additives in study.

### 3.1.1. Monomers

The two monomers used in this work are commercial monomers, tri(ethylene glycol) dimethacrylate and poly(ethylene glycol) dimethacrylate from Fluka and Aldrich, respectively.

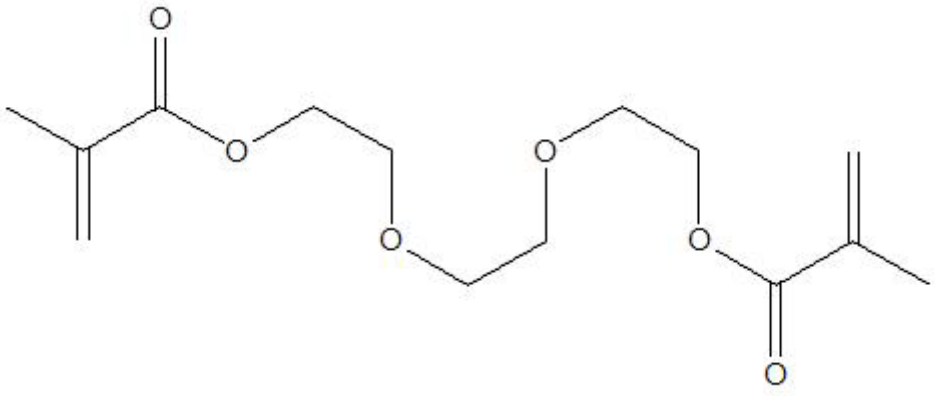

$C_{14}H_{22}O_6$

**Figure 3.1 – Chemical structure and molecular formula of tri(ethylene glycol) dimethacrylate.**

The monomer tri(ethylene glycol) dimethacrylate, Figure 3.1, from Fluka has a molecular weight of $286.33\ g.mol^{-1}$ and a density of $d_4^{20} = 1.075$. Product detailed information can be found under CAS number $109 - 16 - 0$.

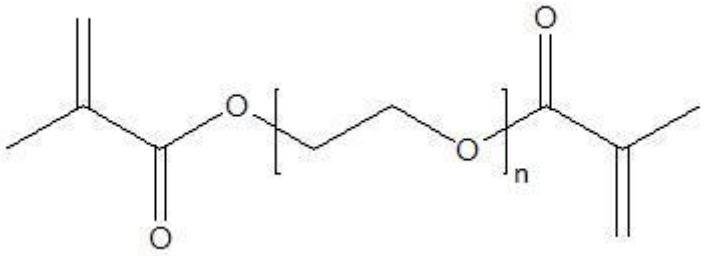


$C_8H_{10}O_3(C_2H_4O)_n \quad n = 16.5$

**Figure 3.2 – Chemical structure and molecular formula of poly(ethylene glycol) dimethacrylate.**

The monomer poly(ethylene glycol) dimethacrylate, Figure 3.2, from Aldrich has a typical molecular weight of $875\ g.mol^{-1}$ and a density of $d_4^{20} = 1.099$. Product detailed information can be found under CAS number $25852 - 47 - 5$.

### 3.1.2. Polymerization Initiators

Two types of polymerization initiators were used in this work. The thermal initiator is a commercial one, α,α'-azoisobutyronitrile from Merck, and the photochemical initiator was synthesized in the laboratory, p-xylene N,N-diethyldithiocarbamate (Cook et al., 2003).

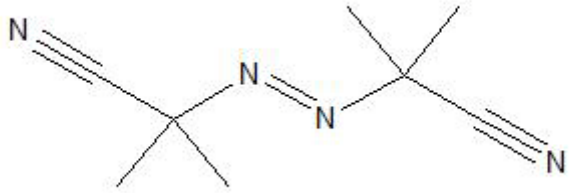


$C_8H_{12}N_4$

**Figure 3.3 – Chemical structure and molecular formula of AIBN.**

The thermal polymerization initiator, Figure 3.3, from Merck has a molecular weight of $164.21\ g.mol^{-1}$ and a melting point of 103~105 ℃. Product detailed information can be found under CAS number $78 - 67 - 1$.

In Figure 3.4 is illustrated the reaction scheme for the preparation of p-Xylene N,N-diethyldithiocarbamate, the photochemical initiator (Otsu & Kuriyama, 1984).

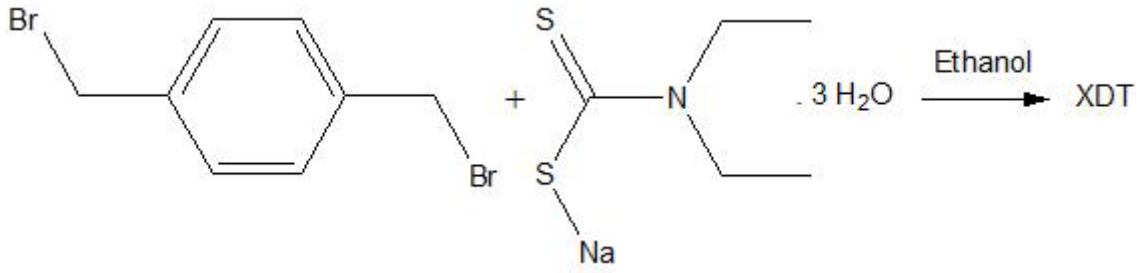


**Figure 3.4 – Reaction scheme for the preparation of XDT.**

This reaction is a $A + B \xrightarrow{Ethanol} XDT$ reaction type where $A$ is dibromo-p-xylene and $B$ is sodium diethyldithiocarbamate trihydrate. Dibromo-p-xylene is a commercial product from Fluka and it has a molecular weight of $263.97\ g.mol^{-1}$ and a melting point of $143{\sim}145$ ℃. The other reagent, diethyldithiocarbamate trihydrate, is also a commercial product from Fluka and it has a molecular weight of $225.31\ g.mol^{-1}$ and a melting point of $96{\sim}98$ ℃. More detailed information on these reagents can be found under CAS numbers $623-24-5$ and $20624-25-3$, respectively.

The preparation of the solution consists in the dissolution of sodium diethyldithiocarbamate trihydrate in ethanol. To that solution is added later dibromo-p-xylene with additional ethanol. This mixture is left in a magnetic stirrer at room temperature for approximately $20$ hours. After this, the solution appears with a relative amount of white powder under the shape of a precipitate along with a colorless liquid. This white powder is filtered in a Büchner funnel and recrystalized in ethanol. The compound is left in a desiccator for approximately $24$ hours to guarantee that the powder is completely dried.

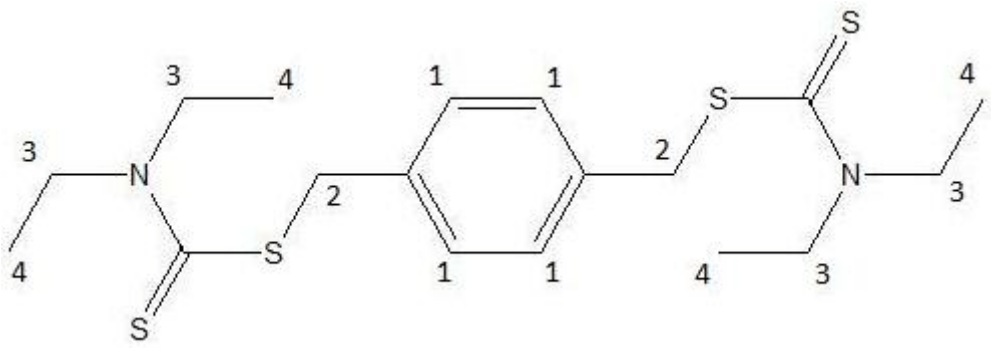


$C_{18}H_{28}N_2S_4$

**Figure 3.5 – Chemical structure and molecular formula of XDT.**

The photochemical initiator, Figure 3.5, has a molecular weight of $400.69\ g.mol^{-1}$ and a melting point of $74{\sim}76$ ℃. This melting point was measured in a melting point apparatus from Electrothermal, which can reach temperatures from $60$ ℃ up to $370$ ℃.

A nuclear magnetic resonance spectrum was made, Figure 3.6, done with deuterated chloroform.

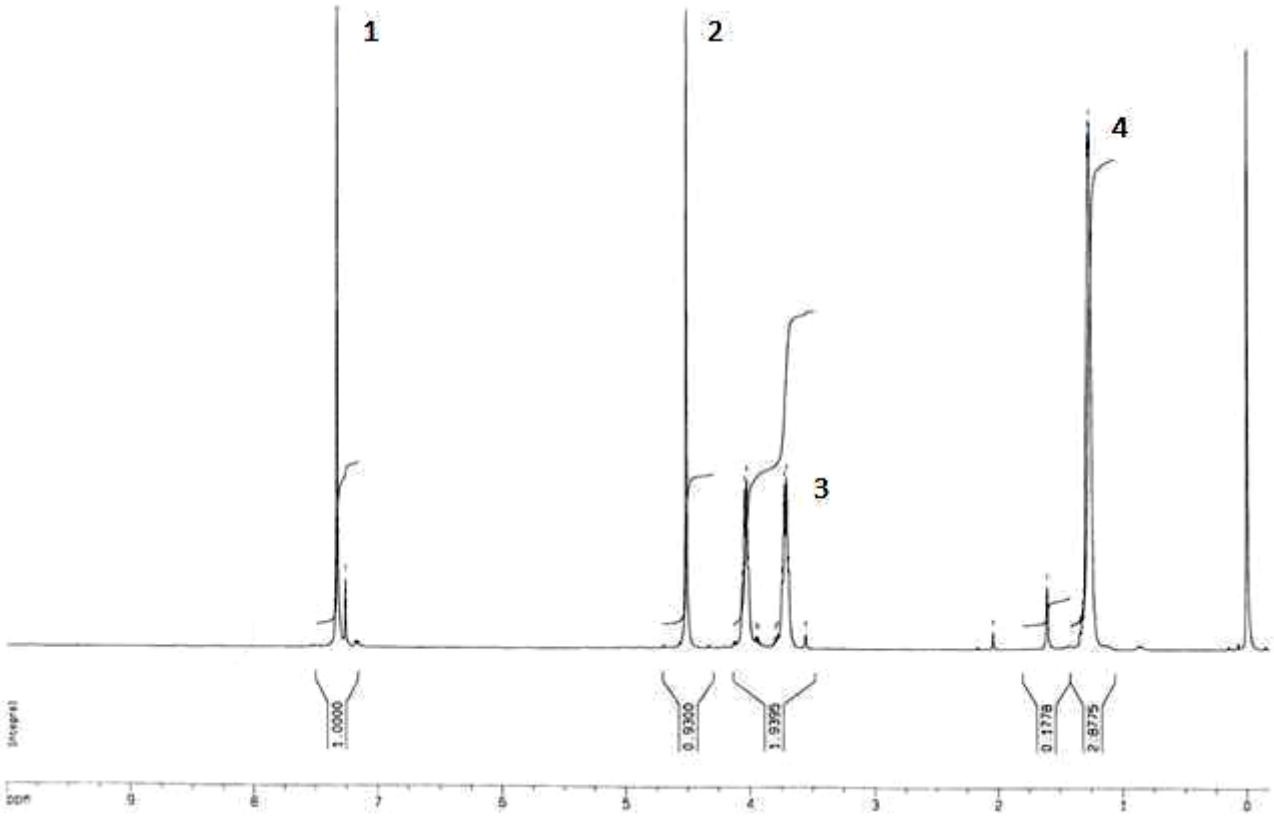


**Figure 3.6 – NMR spectrum of XDT.**

In Table 3.1 is the respective analysis of the peaks presented in the nuclear magnetic resonance spectrum of the synthesized p-xylene N,N-diethyldithiocarbamate.

With the analysis of the spectrum and with the assistance of the prediction given by the software $ChemDraw^{®}\ Ultra\ 8.0$, from CambridgeSoft, it is confirmed that the synthesized product is the referred initiator.

The first singlet is correspondent to the hydrogen protons that are placed between the benzene ring and the sulfurs and the second one corresponds to the protons in the benzene ring, once this peak value is characteristic of the presence of an aromatic group. The first multiplet corresponds to the hydrogen protons in the methyl groups,

while the second and third multiplets correspond to the hydrogen protons that are near the nitrogen atoms.

**Table 3.1 – 1H NMR analysis of XDT.**

| Peak δ (ppm) | Spin Multiplicity | Number of Protons |
|---|---|---|
| 1.30 | Multiplet | 12 |
| 3.72 | Multiplet | 4 |
| 4.04 | Multiplet | 4 |
| 4.52 | Singlet | 4 |
| 7.33 | Singlet | 4 |

### 3.1.3. Liquid Crystal

The liquid crystal used is a blend of various compounds forming a nematic liquid crystal, cyanobiphenyl mixture, known as $E7$, manufactured and commercially available from Merck, division of Licristal.

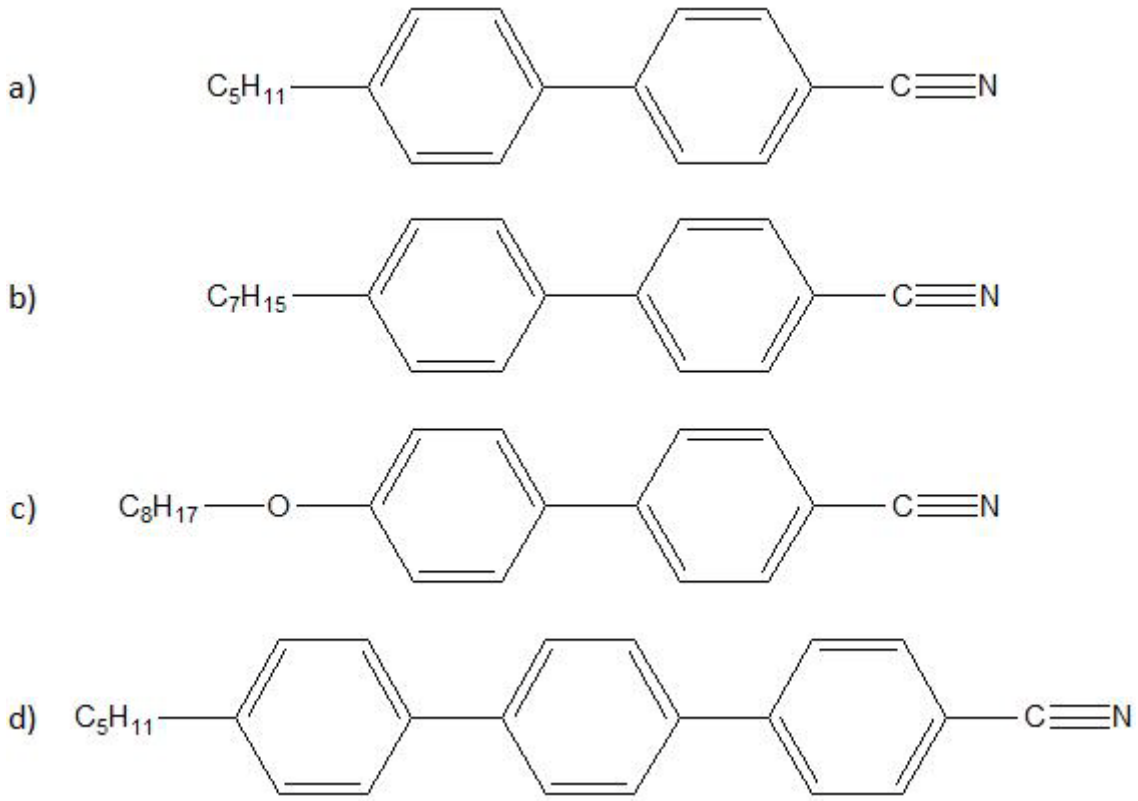


**Figure 3.7 – Chemical structure of the nematic mixture known as E7.**

In Figure 3.7 is illustrated the chemical structures of $E7$ components with all its constituents and Table 3.2, (Brás et al., 2005), presents, from the top to the bottom, the designation of each component according to that illustration, as well as the respective component percentage in the mixture, calculated by high pressure liquid chromatography.

**Table 3.2 – Composition of E7.**

| Designation | Molecular Formula | IUPAC Name | Composition |
|---|---|---|---|
| a) 5CB | $C_{18}H_{19}N$ | 4-cyano-4'-n-pentyl-1,1'-byphenyl | 51 % |
| b) 7CB | $C_{20}H_{23}N$ | 4-cyano-4'-n-heptyl-1,1'-byphenyl | 25 % |
| c) 8OCB | $C_{21}H_{25}NO$ | 4-cyano-4'-n-octyloxy-1,1'-byphenyl | 16 % |
| d) 5CT | $C_{24}H_{23}N$ | 4-cyano-4''-n-pentyl-1,1',1''-terphenyl | 8 % |

The physical properties of this nematic mixture are presented in Table 3.3 and were kindly provided from Merck KGaA, Darmstadt, Germany – Liquid Crystals Division (Merck KGaA, 2008). All the values of the anisotropies are measured at a temperature of $20$ ℃, a wavelength of $589.3\ nm$ and a frequency of $1.0\ kHz$.

**Table 3.3 – Technical data sheet of E7.**

| Physical Properties | | |
|---|---|---|
| Clearing Point (℃) | | 58 |
| Optical Anisotropy | $\Delta n$ | 0.2255 |
| | $n_e$ | 1.7472 |
| | $n_o$ | 1.5217 |
| Dielectric Anisotropy | $\Delta\varepsilon$ | 14.1 |
| | $\varepsilon_{\parallel}$ | 19.3 |
| | $\varepsilon_{\perp}$ | 5.2 |

In spite of its multicomponent nature, $E7$ exhibits a single nematic-isotropic transition temperature, $T_{N\rightarrow I} = 61$ ℃, and a glass transition temperature at $T_g = -62$ ℃ (Bedjaoui et al., 2004). Various authors measured the clearing point of the liquid

crystal, but in a general way it is around the $58$ ℃, as presented by Merck and several other authors.

### 3.1.4. Additives

To test the additive effects in polymer dispersed liquid crystals, several additives were used. A scheme of the solution proposed is presented in Table 3.4.

**Table 3.4 – Monomers and respective additives.**

| Monomers | Additives |
|---|---|
| Tri(ethylene glycol) Dimethacrylate | Ethylene Glycol<br>Octanoic Acid<br>Hexadecanoic Acid |
| Poly(ethylene glycol) Dimethacrylate $Mw = 875\ g.mol^{-1}$ | Triton X-100<br>Cetyl Trimethyl Ammonium Bromide<br>Sodium Dodecyl Sulfate |

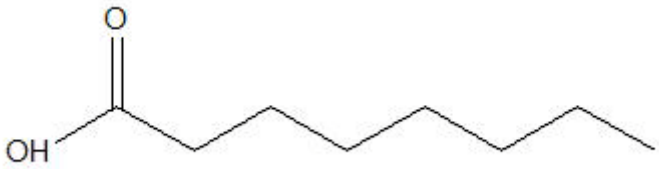


$C_8H_{16}O_2$

**Figure 3.8 – Chemical structure and molecular formula of octanoic acid.**

The octanoic acid, Figure 3.8, from Aldrich has a molecular weight of $144.21\ g.mol^{-1}$ and a density of $d_4^{20} = 0.910$. Product detailed information can be found under CAS number $124 - 07 - 2$.

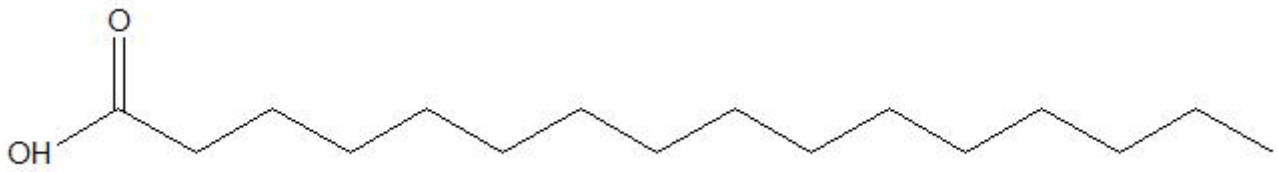


$$C_{16}H_{32}O_2$$

**Figure 3.9 – Chemical structure and molecular formula of hexadecanoic acid.**

The hexadecanoic acid, Figure 3.9, from Merck has a molecular weight of $256.43\ g.mol^{-1}$ and a melting point of $60{\sim}62$ ℃. Product detailed information can be found under CAS number $57-10-3$.


$$C_2H_6O_2$$

**Figure 3.10 – Chemical structure and molecular formula of ethylene glycol.**

The ethylene glycol, Figure 3.10, from Merck has a molecular weight of $62.07\ g.mol^{-1}$ and a density of $d_4^{20} = 1.115$. Product detailed information can be found under CAS number $107-21-1$.

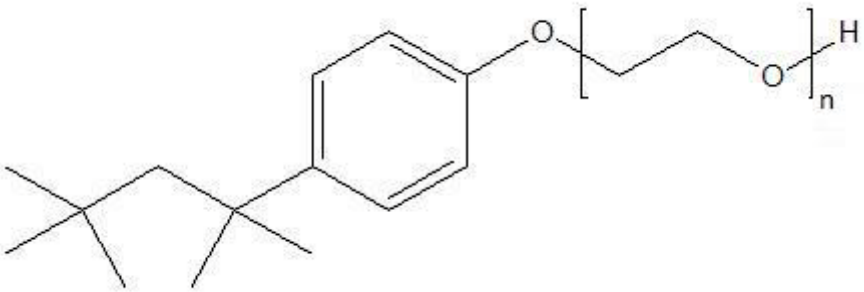


$$C_{14}H_{22}O(C_2H_4O)_n \quad n = 10$$

**Figure 3.11 – Chemical structure and molecular formula of triton X-100.**

The triton X-100, Figure 3.11, from Merck has a typical molecular weight of $647\ g.mol^{-1}$ and a density of $d_4^{20} = 1.065$. Product detailed information can be found under CAS number $9002-93-1$.

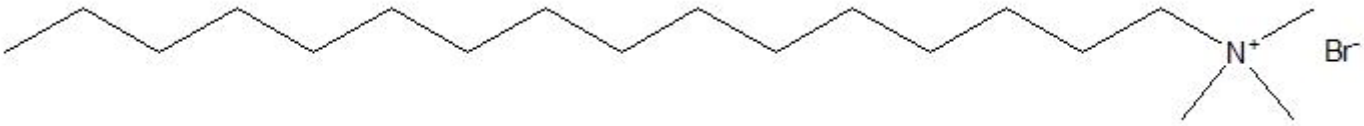


$$C_{19}H_{42}NBr$$

**Figure 3.12 – Chemical structure and molecular formula of cetyl trimethyl ammonium bromide.**

The cetyl trimethyl ammonium bromide, Figure 3.12, from Fluka has a molecular weight of $364.46\ g.mol^{-1}$ and a melting point of $248{\sim}250$ ℃. Product detailed information can be found under CAS number $57-09-0$.

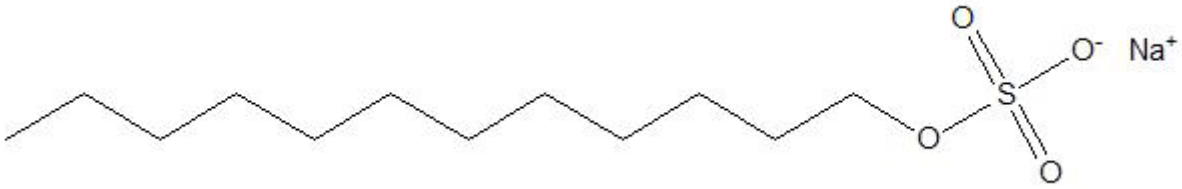


$$C_{12}H_{25}SO_4Na$$

**Figure 3.13 – Chemical structure and molecular formula of sodium dodecyl sulfate.**

The sodium dodecyl sulfate, Figure 3.13, from Panreac has a molecular weight of $288.38\ g.mol^{-1}$ and a melting point of $204{\sim}206$ ℃. Product detailed information can be found under CAS number $151-21-3$.

### 3.1.5. Indium Tin Oxide Cells

The cells for the electro-optic studies are made by conducting glass coated by a thin layer of indium tin oxide. A schematic illustration of an indium tin oxide cell is illustrated in Figure 3.14 (Instec, 2008).

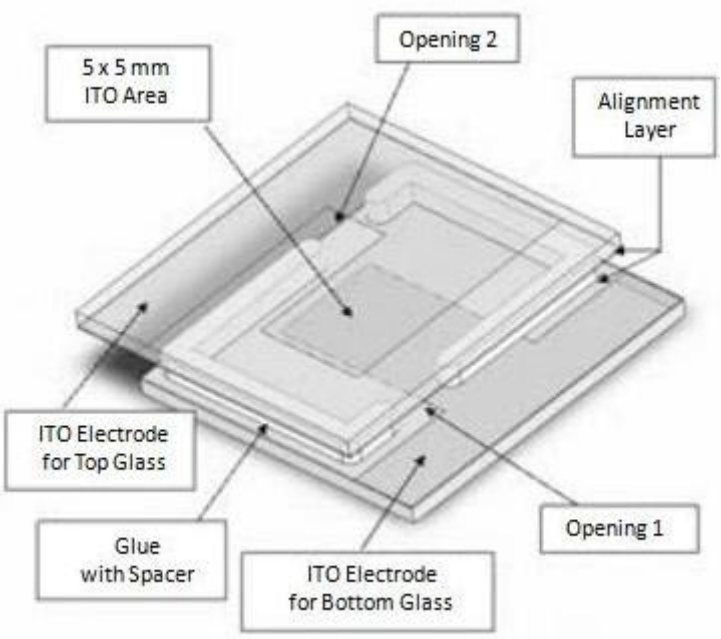


**Figure 3.14 – Schematic illustration of an ITO cell.**

The indium tin oxide area occupies $25\ mm^2$ of the cell and this is the only area where voltage is applied with a resistance up to $100\ \Omega/\square$. This type of cell has a homogeneous anti-parallel alignment layer with $1°$ to $3°$ pre-tilted angle.

Cell spacing is $20.0 \pm 0.2\ \mu m$ and cell thickness is $1.5\ mm$, being that the cell outer dimensions are $15.25 \times 17\ \times 1.5\ mm$. In Figure 3.15 is represented one of these cells.

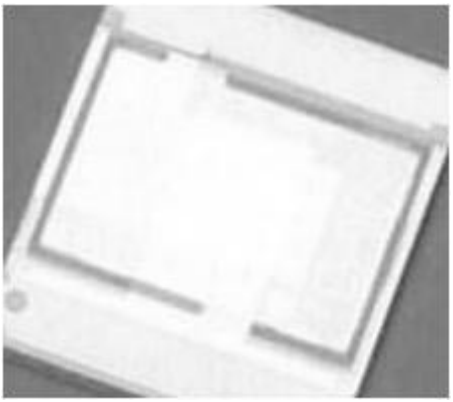

**Figure 3.15 – ITO cell.**

These cells are supplied by Instec, which makes available calibrated cells whose spacing has been individually measured both optically and electronically.

## 3.2. Methods

This section includes all the methods since the first step of the experimental protocol until the last one, which is the electro-optical study. Every step is described with detailed information on procedures, such as the treatment of the monomers, the polymerization, the microscopies used and the electro-optical apparatus.

### 3.2.1. Preparation of Solutions

The monomers commercially available from Fluka and Aldrich are purchased with an inhibitor, so the monomers do not polymerize on storage. In order to remove that inhibitor, hydroquinone and monomethyl ether hydroquinone, specific columns for each of the monomers were used. It consists in a filling column with a capacity of approximately $3\,L$ at $100\,ppm$, being the filling resin of polystyrene divinylbenzene, and its dimensions are $229 \times 20.3\,mm$. These columns are supplied by Aldrich. Further information on the product can be found under CAS number $9003 - 70 - 7$ (Aldrich, 1999).

Procedure is very simple, it just needs to add the monomer to an addition funnel which is secured above the column and let it dropwise to the column, monitoring the rate of addition to prevent overflow of the column and collecting the monomer, now without the inhibitor, in an appropriate container.

Once the monomers do not contain the inhibitor, polymerization initiators are added in an approximately $1\%$ weight relative to the monomer.

The next phase is the addition of the liquid crystal. The amount of liquid crystal to add to the solution containing monomer with polymerization initiator is calculated in order to have a ratio of monomer to liquid crystal of $30/70$.

The final step is the preparation of the composite with an additive. The quantities of additive to be used are made in about $1\%$ and $10\%$ weight relative to the composite containing monomer, polymerization initiator and liquid crystal.

All solutions are made in eppendorf tubes, which mean that low quantities of material are used, so the solutions are always new and fresh to initiate new assays. An electronic balance was used to make these solutions, model $AY120$ from Shimadzu

whose maximum load is $120\ g$ and has a readability of $0.1\ mg$, which means that it takes up to four decimal places. Before transferring the composites into an indium tin oxide cell, the polymerization was tested between two glass substrates, handmade with a $50\ \mu m$ cell spacer, to verify if the composites did or did not polymerize.

### 3.2.2. Octanoic Acid Studies

Some studies were carried with octanoic acid as a basis for some parameters of the additive effects. Factors such as the addition order, the quantity of additive used and the length of the molecular chain were studied.

Figure 3.16 illustrates a scheme of the addition order, according to method I and method II, being that method I stands for a preparation that consists in the addition of the additive to the mixture of monomer and liquid crystal, and method II stands for a different preparation of the mixture, adding the additive to the liquid crystal in first place and then, the respective mixture is added do the monomer.

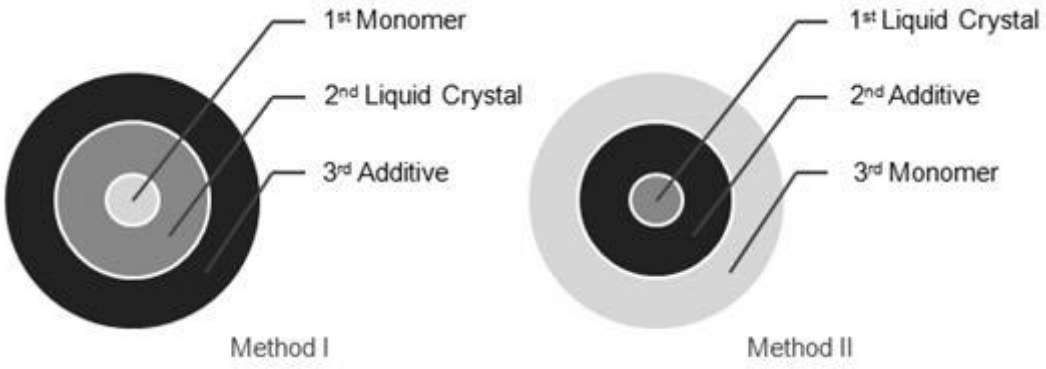


**Figure 3.16 – Schematic illustration of method I and method II for the addition order.**

Other test made was the quantity of additive used and Figure 3.17 illustrates both methods for the quantities of additive used in each method. The preparation made in method I uses $10\%$ of additive and method II only adds $1\%$ of additive to the mixture.

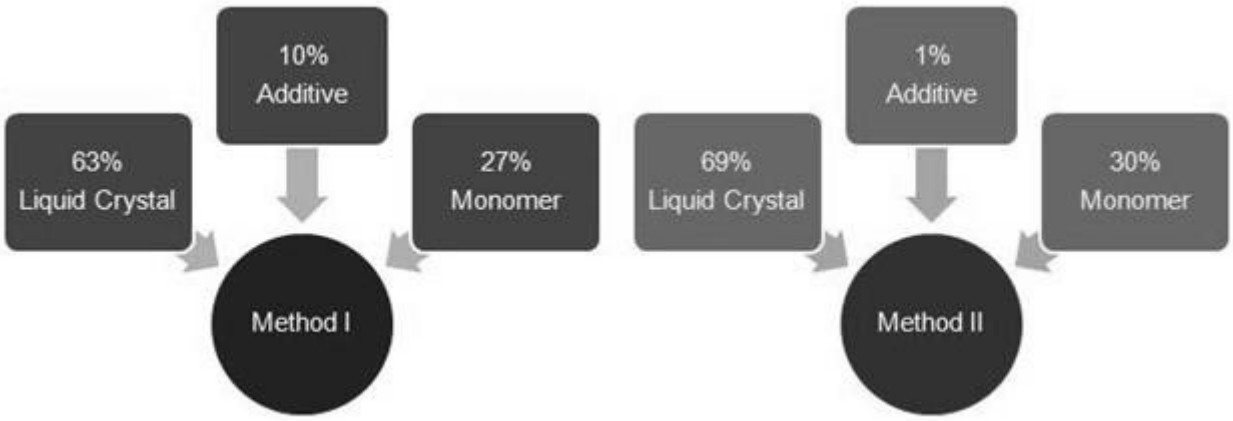


**Figure 3.17 – Schematic illustration of method I and method II for the quantity of additive.**

Finally, a comparison was made with a different surfactant, whose molecule functional group is as equal as octanoic acid, but the chain length is twice longer. Figure 3.18 illustrates the difference between the chain lengths of both compounds.

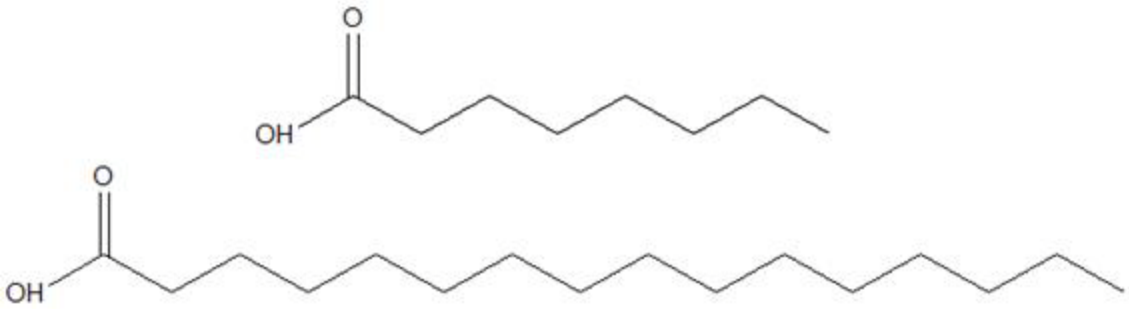


**Figure 3.18 – Schematic illustration of the chain length difference between octanoic and hexadecanoic acids.**

### 3.2.3. Polymerization Induced Phase Separation

There are various methods to prepare a polymer dispersed liquid crystal, but the most common is the polymerization induced phase separation.

This method consists in an initial mixture of monomer and liquid crystal and the phase separation is induced by polymerizing the monomer (Lee, 1999). During the process the liquid crystal becomes less soluble in the polymer and tiny droplets of liquid crystal start to be segregated in the interior of the polymer matrix and at the end of the process, the polymer containing the dispersed liquid crystal droplets forms a solid matrix.

Polymerization induced phase separation is quite complex because phase separation and polymerization occur simultaneously. The degree of polymerization of the

polymerizing component continuously increases as the reaction proceeds and this induces phase separation because the curing point eventually crosses over from the homogeneous region to the two-phase region (Oh & Rey, 2000).

Two types of polymerization induced phase separation are used. One with a photo-initiator with ultraviolet curing and the other with a thermal initiator that reacts when heated.

Initially, the samples with the thermal initiator were prepared in an oven from Memmert. But once the inner temperature was slightly different from the values given by the outer display, a handmade oven was made (Maiau, 2009). This oven operates at $74.0 \pm 0.1$ ℃.

This oven has an auto-tune temperature controller provided by CAL Controls, model $CAL\ 3300$, with a resistance thermometer, $Pt100/RTD - 2$, whose sensor range takes temperature in the interval of $-200 \sim 400$ ℃.

For the photo-polymerization an apparatus was already mounted and ready to operate. This apparatus is composed by several parts that were assembled to form single equipment. Its protocol to operate in safety is very simple. Before starting the device, assure that the lamp is cold, and then the refrigeration system composed by a reflux of water and a cooling fan are started. To guarantee that the system is completely cooled, a hold time of $5$ minutes is taken before starting the light. The device is ready to use after $10$ minutes, so the lamp gets its heat point. To shut down the apparatus, the light interrupter is simply shut down, and then $5 \sim 10$ minutes are taken for the system cool down. The water reflux and the cooling fan are also shut down.

This apparatus is settled on top of an optical breadboard supplied by Thorlabs, as well as the parts that support the filters. The refrigeration system is composed by an inner circuit of water provided from the tap and a cooling fan from Sunon, model $DP209WR$. A shutter was assembled to the machinery with a timer to allow irradiance of the samples at a precise controlled time. The timer is from Omron, model $H5CX$ and it takes time by seconds to a maximum of four digit values. Four filters are being used as wavelength selectors.

One is an infrared filter of water in a stainless steel filter provided by Oriel, model $6127$, a liquid filter for light source, in which a fused silica window is connected at the

end. The other two filters are a $BG3$ band filter, that only permits the passage of light with wavelengths in the range of $250{\sim}500\,nm$, and the final one is an interference filter that only allows the passage of light with wavelengths among the $360{\sim}370\,nm$. This way, the device is customized so the light coming from a low pressure mercury lamp has a wavelength of $366\,nm$. Therefore, only approximately, $20\%$ of the radiation produced by the lamp reaches the samples.

The main device (Newport, 2009) is composed by a PhotoMax™ housing, from Oriel, model $60100$. The PhotoMax™, Figure 3.19, is an efficient and versatile monochromatic illuminator. The interface is also from Oriel, model $60115$. It uses an ellipsoidal reflector, model $60108$ from Oriel, an ellipsoidal reflector assembly of $AlMgF_2$, which surrounds the lamp and collects most of the lamp emission. A lamp socket adapter for $100\,W$ mercury lamps is also included in this apparatus, supplied by Oriel, model $60119$. The output is a very high intensity, full spectrum, focused spot matched to the $1/4\ m$ monochromator. The $100\,W$ mercury lamp is supplied by Osram, being a mercury short-arc $HBO\ 103\ W/2$, which have a typical lifetime of $300$ hours. The power source for this apparatus is from Oriel Instruments, model $68800$. This is an OEM $100\,W$ source wired for $220\,VAC$, connected to the main machinery with an adapted cable, model $68816$.

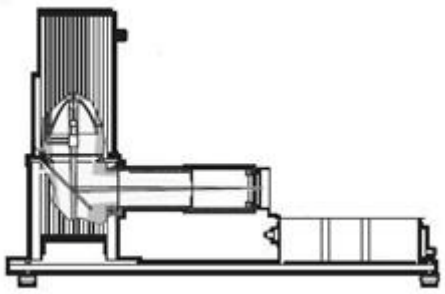

**Figure 3.19 – PhotoMax™ schematic monochromatic illuminator.**

To measure the heating power of radiation, actinometers are used. An actinometer is a chemical system or physical device which determines the number of photons in a beam integrally or per time unit and it is commonly applied to devices used in the ultraviolet and visible wavelength ranges.

In a chemical actinometer, photochemical conversion is directly related to the number of photons absorbed because the chemical action of light means reversible or

irreversible chemical change, like destruction or buildup of molecules and, consequently, of their properties such as spectra (Kuhn et al., 2004).

The actinometry is based on the actinometer of iron (III) oxalate. Four volumetric flasks of $25\ ml$ are used to prepare the solutions irradiated for a time interval of $0{\sim}30\ s$. Cuvettes containing $3\ ml$ of a $0.006\ M$ solution of $[Fe^{III}(C_2O_4)_3^{3-}]$ were irradiated for $0$, $10$, $20$ and $30$ seconds in the monochromatic illuminator. $2\ ml$ of those irradiated cuvettes are added to the volumetric flasks and then, $1\ ml$ of a $1\ M$ solution of acetate buffer along with $2\ ml$ of phenanthroline $0.1\%$ in weight are also added to the respective flask. To reach the $25\ ml$ meniscus, the flask is filled with distilled water.

Equation 5 represents the expression used to calculate the number of photons that cross the samples per unit of time.

$$I_0^{\lambda}\ (Nh\nu.s^{-1}) = F^{\lambda} \times \frac{\Delta A^{510}}{\Delta t\ (s)} \qquad \textbf{(5)}$$

Once the irradiation is made at a wavelength of $366\ nm$, the value of $F^{\lambda}$ is a constant with the value $F^{366} = 2.775 \times 10^{-6}$, previously calculated. $F^{\lambda}$ is a factor that includes quantities such as the volumes used and the quantum yield, $t$ is the irradiation time, in seconds, and $A^{510}$ is the absorbance given by the spectrophotometer at a wavelength of $510\ nm$. The spectrophotometer where the absorbance of the samples was measured is from Shimadzu, model $UV-160A$, an ultraviolet-visible recording spectrophotometer. A graphic of absorbance in order of time is made with the values obtained and a linear regression is estimated onto the graphic giving the value of the slope of that line, representing the parcel $\Delta A^{510}/\Delta t$.

In a physical actinometry, a radiometer is used. This is an easy way to measure the heating power of the radiation, once it is only needed to put the device in front of the beam given by the photo-polymerization apparatus. The radiometer used is from International Light Technologies, model $ILT393-BB$. The peak irradiance is given in $mW.cm^{-2}$ and it can read values in the range of $240{\sim}610\ nm$, as shown in Figure 3.20.

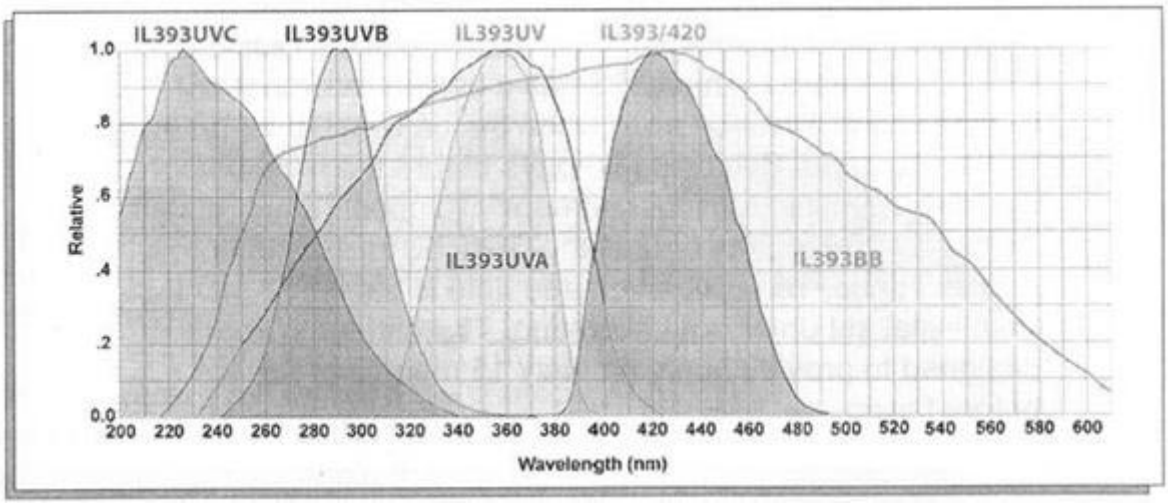


**Figure 3.20 – Spectral ranges according to model.**

### 3.2.4. Indium Tin Oxide Cells

There are two openings on the indium tin oxide cells. A small amount of material is dropped on one of those openings of the empty cell. The capillary force will suck liquid material into the empty cell. It takes a few minutes before the cell is fully filled. Generally the opposite side of the opening where the material is deposited never gets filled, due to air entering in the cell by this other opening.

The filling process can be seen at some angle under light. Once the cell is filled, it is stored at room temperature. For rapid observation of the transparent to opaque transition cool wind is blown against the cell (Instec, 2008).

Instec recommends heating the cell above the isotropic temperature of the liquid crystal used before dropping the material into it. They also suggest that in order to get good alignment, the cell must be cooled down slowly, especially during the phase transition temperature.

### 3.2.5. Polarized Optical Microscopy

A polarizing microscope is a special microscope that uses polarized light for investigating the optical properties of samples in various fields such as the polymer chemistry and liquid crystals (Olympus). Figure 3.21 illustrates one of those types of microscopes.

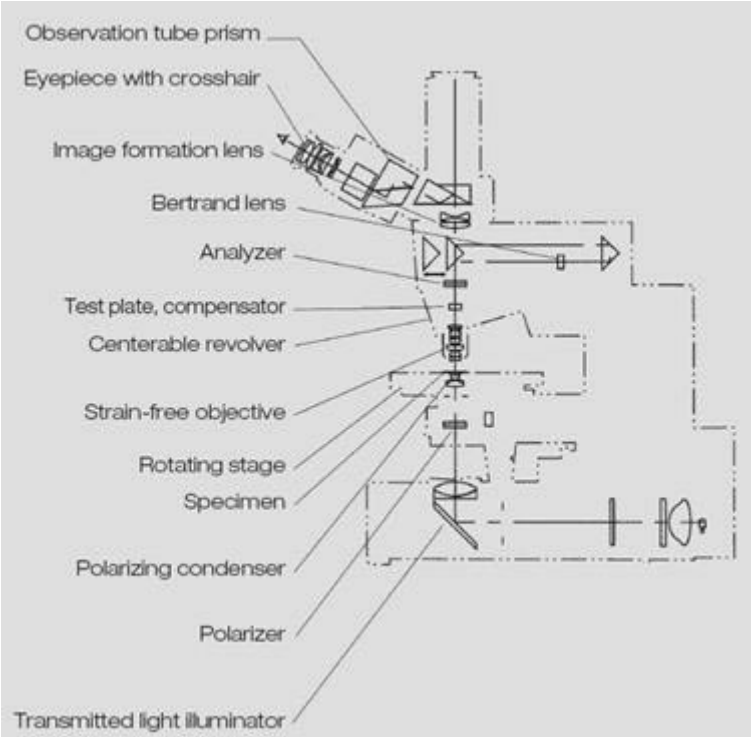


**Figure 3.21 – Construction of a typical transmitted light polarizing microscope.**

A polarizing plate or polarizing prism is often used as the device to change natural light to linearly polarized light. Polarizing devices are the distinctive features of polarizing microscopes. These devices permit passage of light vibrating in only one plane (Stoiber & Morse, 1994).

Configuring the primary and the secondary polarizing devices in the orthogonal directions of each transmitting linearly polarized ray will cut the light. Such state in which the primary light polarizing device is the polarizer and the secondary device is the analyzer is called crossed nicols. Parallel nicols is the state in which the analyzer is rotated to make the direction of the transmitting linearly polarized light match with the polarizer, and the amount of light transmittance is maximized. The next figure (Olympus) illustrates the transmittance of polarized light when nicols are either crossed, Figure 3.22 a), or parallel, Figure 3.22 b).

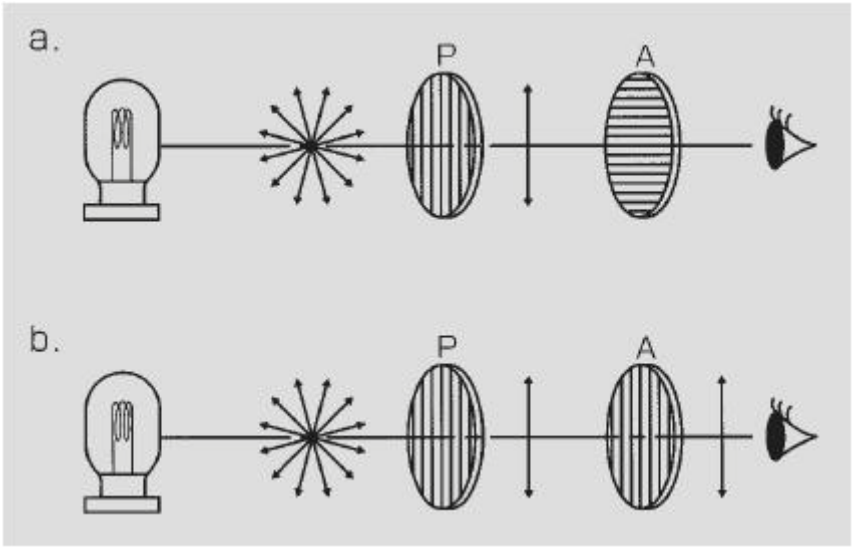


**Figure 3.22 – Schematic illustration of light transmittance according to the nicols alignment.**

The equipment used on this microscopy is from Olympus, model $BH-2$. Several polarizing objectives, strain-free objectives, model series $ACH-P$ from Olympus, were used, which give a magnification of $10\sim50$ times.

Each composite is observed in the interior of an indium tin oxide cell, after tension was applied to the sample, and the guidelines for knowing if polarizers are either crossed or parallel are the spacers inside the indium tin oxide cells. Figure 3.23, adapted (Senyuk, 2006), shows the change in light scattering when rotating the polarizers.

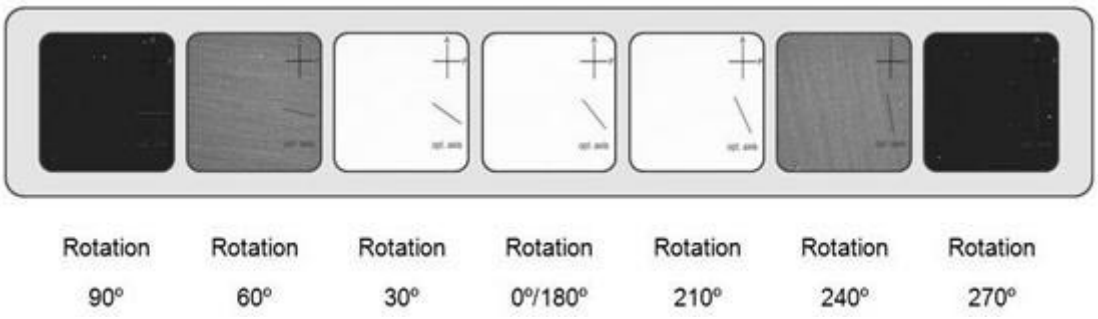


**Figure 3.23 – Image observed under a polarized optical microscope according to the polarizers rotation.**

This allows understanding the orientation of the liquid crystal and its alignment, as well as noticing any permanent memory effects present in the samples. Besides that, it is able to see the texture of the composites and the locations of the liquid crystal domains. The indium tin oxide cell is placed in the rotating stage of the microscope on top of a microscope slide. The sample is observed with the strain-free objectives, starting on the objective of lesser magnifying. All polarized optical microscopy photos were taken with an Olympus $Camedia\ C-5060$ digital camera.

Through polarized optical microscopy it was also made a scanning in temperature that allows the observation of the liquid crystal transitions to the isotropic state and vice-versa. The same microscope was used and the temperature was controlled by a central processor from Mettler, model $FP90$. The cell was placed into a hot stage from Mettler, model $FP28HT$, which was connected to the central processor. The samples were submitted to a sequence of heating and cooling in the temperature range of $25 \sim 100$ ℃ at a speed of 2 ℃$.min^{-1}$.

### 3.2.6. Scanning Electron Microscopy

The scanning electron microscope permits the observation and characterization of heterogeneous organic and inorganic materials on a nanometer to micrometer scale. Figure 3.24 illustrates the two major parts of the scanning electron microscope (Goldstein et al., 2003).

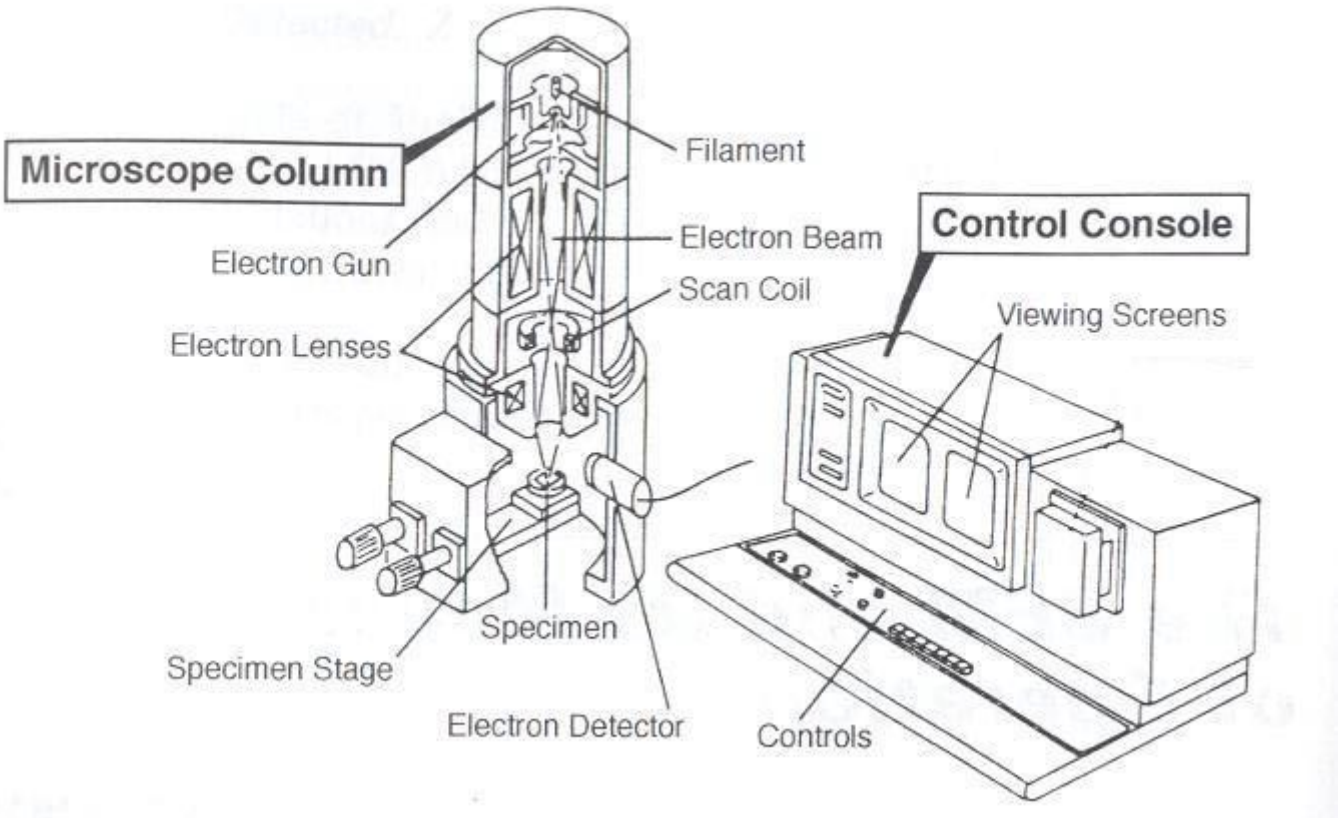


**Figure 3.24 – Construction of a typical scanning electron microscope.**

This microscopy is used to observe the morphology of the composites, once this technique is capable of obtaining three-dimensional-like images of the surfaces of a very wide range of materials.

The equipment used on this microscopy is from Hitachi, model $S-2400$. Its resolution is $4\,nm$, has an acceleration voltage in a range between $0.3{\sim}25\,keV$ and several electron detectors. The diameter of the samples is less than $4\,mm$.

To prepare these films, the procedures are exactly the same as if the composite was inserted into an indium tin oxide cell, but this time, the composite is placed between two chips of potassium bromide, from Riedel-de Haën, which has a molecular weight of $119.01\,g.mol^{-1}$ and a melting point of $729{\sim}731$℃. Product detailed information can be found under CAS number $7758-02-3$. Polymerization induced phase separation methods and equipments are exactly the same as mentioned previously. Potassium bromide is used due to its ease removal when the polymerized composites are dip into distilled water. The potassium bromide is shaped into chips with the assistance of a press.

The press is from Specac and to make the chips of potassium bromide the following procedure was done. First the top bolster must be screwed to work, then the release handle was rotated clockwise and tighten firmly. Finally, until the required load was indicated on gauge, the press was pumped. The press can be pumped until $15$ tonnes, but the red mark on piston starts on $10$ tonnes. Usually, the press is pumped, for $1$ minute, until a middle value between these two, to guarantee that a minimum of, at least, $10$ tonnes were applied to the chip.

After the removal of the potassium bromide, it is visible at naked eye that the film of polymer emerges to the surface of the distilled water. This film is passed to another beaker, this time, containing acetonitrile to dissolve the liquid crystal. This procedure is repeated for three times to assure that no liquid crystal remains in the composite, so it does not appear on the scanning electron microscopy observations.

Acetonitrile is a commercial product from Riedel-de Haën and has a molecular weight of $41.05\,g.mol^{-1}$ and a density of $d_4^{20}=0.782$. Product detailed information can be found under CAS number $75-05-8$.

Polymer materials require a special method of preparation for observation under this microscopy, due to radiation effects that can change and compromises the polymer

during imaging. The preparation is very simple, as the material is chosen carefully from a larger sample and then is placed on sticky tape on a specimen stub. Small amounts of conductive paints are sometimes necessary to connect the specimen to the stub. Very thick coatings of gold are sputter-coated onto samples, with the assistance of a scanning electron microscopy coating system from BioRad Polaron Division.

The coating is used for preventing the charge-up on the specimen surface by covering it with a conductive material and for increasing the second electron emission by covering a specimen of low secondary electron emission with a metal of high secondary electron yield. These coatings appear as shiny mirrors and obliterate some details less than $50\,nm$ in size. Microporous polymers are useful for evaluation of metal coating devices because the granular textures associated with thick coatings of gold by sputter or evaporative coatings are readily observed (Goldstein, et al., 2003).

The software for images treatment is $Multi\ Image\ 2.1$ and $DISS\ 4$.

Because of the large composition of non-reactive component, $E7$, polymerization of the monomer results in the formation of small polymer beads, which are insoluble in the liquid crystal, precipitating and phase separating out, aggregating to form a network structure, seen through scanning electron microscopy.

### 3.2.7. Electro-Optical Studies

The electro-optic characterization of the devices is based on the determination of the voltage dependence of the light transmission coefficient that yields several important parameters including the maximum and minimum transmittance and the applied field. To determine the voltage dependence of the light transmission coefficient, the apparatus, illustrated in Figure 3.25, adapted (Almeida, 2003), was used.

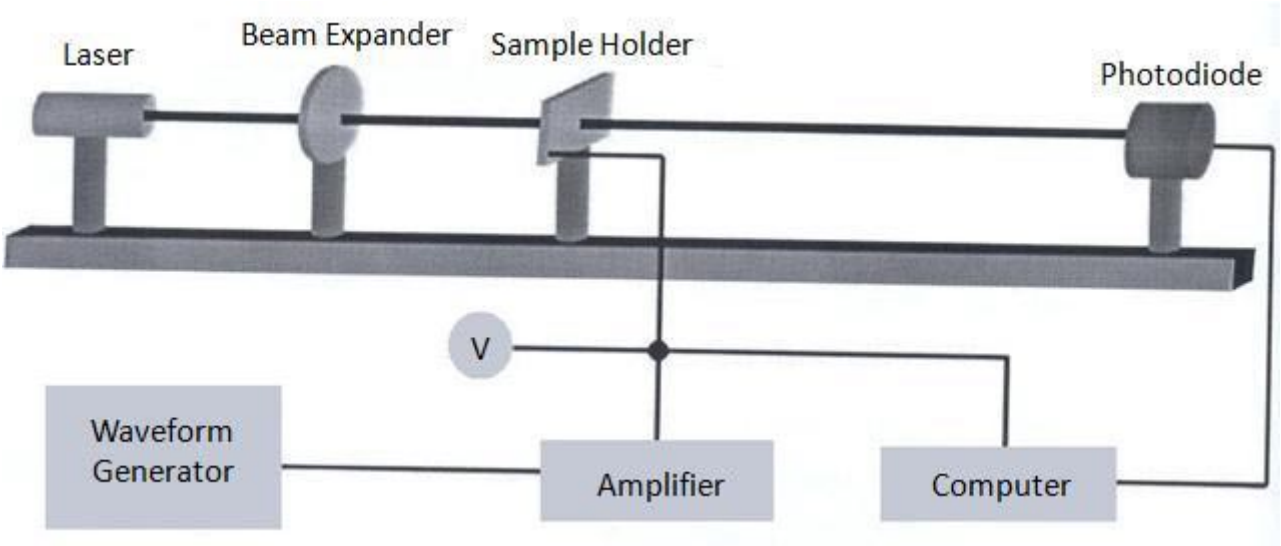


**Figure 3.25 – Schematic illustration of the electro-optic apparatus.**

This apparatus is composed of a Helium-Neon laser head and power supply from JDS Uniphase, model $1137/P$, generating laser light with a wavelength of $632.8\,nm$ used to illuminate the sample. An amplifier from Harman/Kardon, model $HK6850$ is used to increase the strength of the voltage applied to the sample and produced by a waveform generator from Agilent, model $33220A$, that generates a sinusoidal tension with a frequency of $1\,kHz$. The light passing through the sample is detected by a silicon photodiode, whose output, after amplification is fed to a digital oscilloscope from TiePie, model $HS4$, connected to a computer software for data acquisition.

The figures containing the electro-optical studies were carefully treated, so that no more than one curve is presented. Thus, in the graphics the curves are composed by three different assays, transformed into a single one. It is composed with the values obtained for the first run on increasing voltage, then the values obtained for the second run on increasing voltage from the last point were added and, finally, the values obtained for the third run were taken from that point to the end, including both increasing and decreasing voltage values.

### 3.2.8. Differential Scanning Calorimetry

Differential scanning calorimetry is a technique for thermal analysis where the difference of the temperatures, $T_{sample} - T_{reference}$ , is recorded as a function of the temperature of the system, as the sample is heated or cooled at constant speed. It

allows the characterization of materials through fusion, crystallization, glass transition, polymerization and degrees of purity, crystallization and healing.

The calorimeter is from Setaram, model $DSC\ 131$, which can measure temperatures in the range between $-150{\sim}550$ ℃, heating and cooling speeds between $0.01{\sim}99.9$ ℃$.min^{-1}$ and a signal of heat flow between $-100{\sim}100\ mW$, with a resolution of $\pm 0.2\ \mu W$. The samples must contain at least $10\ mg$ of a solid or liquid homogeneous material.

This material is weighted into an aluminium crucible of $100\ \mu l$, which is closed in the case of negative temperatures. The assays were realized under an atmosphere of $N_2$. The samples were submitted to a sequence of a first heating from $-130{\sim}90$ ℃, a cooling from $90{\sim}-130$ ℃ and a second heating from $-130{\sim}90$ ℃, at a speed of $5$ ℃$.min^{-1}$.

### 3.2.9. Dielectric Relaxation Spectroscopy

The dielectric relaxation spectroscopy is a suitable tool to monitor molecular mobility for materials containing permanent dipoles, through the measurement of the complex dielectric constant, when the material is under the influence of an alternating electrical field.

The interaction of electromagnetic waves with matter in the frequency range between $10^{-6}{\sim}10^{12}\ Hz$ is the domain of broadband dielectric spectroscopy. In this extended dynamic range molecular and collective dipolar fluctuations, charge transport and polarization effects at inner and outer boundaries take place and determine the dielectric properties of the material being studied. Dielectric spectroscopy measures the dielectric properties of a medium as a function of frequency (Kremer & Schönhals, 2002). It is based on the interaction of an external field with the electric dipole moment of the sample, often expressed by permittivity.

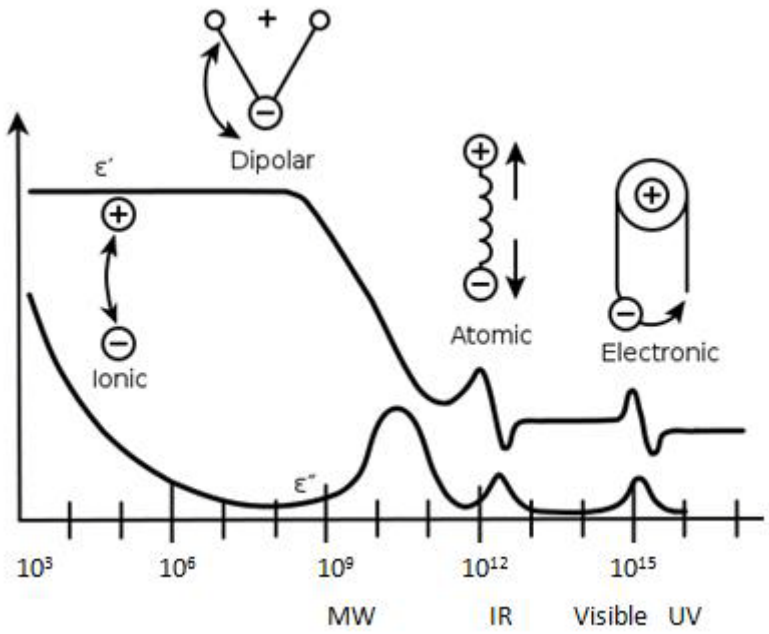


**Figure 3.26 – Dielectric permittivity spectrum over a wide range of frequencies.**

Figure 3.26 illustrates the dielectric permittivity spectrum where the real, $\varepsilon'$, and imaginary, $\varepsilon''$, parts of the permittivity are shown.

This technique is particularly useful in polymer dispersed liquid crystal composites to assess the dynamical changes driven by thermal treatments experienced by the encapsulated material, in particular, when the guest undergoes a liquid to glass transition when supercooled. The comparison of the behavior of impregnated materials with those of bulk systems gives a clear picture of the influence of that entrapment.

In materials where crystallization is avoided, as the case of $E7$, a tremendous increase of viscosity and therefore the characteristic relaxation time occurs and the material enters in a supercooled regime ultimately solidifying in a disordered glass. Thus, both localized and cooperative motions, the later associated with the glass transition, are able to be studied over a large temperature range from the glassy to the liquid state.

The real component of the complex permittivity revealed to be especially useful to monitor phase transitions and transformations that emerge in the spectrum as more or less sharp discontinuities allowing the establishment of a comparison with the differential scanning calorimetry thermograms. In particular, in liquid crystalline materials, the imaginary part of the complex permittivity is sensitive to the

orientations of the nematic director and, consequently, it is possible to infer about the alignment of the liquid crystal.

The dielectric measurements were carried out using an impedance analyzer $ALPHA-N\ Analyzer$ from Novocontrol Technologies, covering a frequency range from $100\ Hz$ to $1\ MHz$ and in different increasing temperature steps from negative temperatures, around $-100$ ℃ to positive ones, around $100$ ℃ and backwards. The dielectric spectra were recorded every $5$℃ and in some vital points the values were recorded every $3$ ℃.

A drop of the compounds and mixtures with three silica spacers with thickness of $50\ \mu m$ was placed between two gold plate electrodes of a parallel plate capacitor. The sample cell, $BDS\ 1200$, also from Novocontrol was mounted on a cryostat, $BDS\ 1100$ and exposed to a heated gas stream being evaporated from a liquid nitrogen dewar. The temperature control of the samples was performed within $\pm 0.5$ ℃, with the $Quatro\ Cryosystem$, supplied by Novocontrol GmbH.

During the assays, the real and imaginary parts of the complex permittivity were measured at the five frequency values described above, with the assistance of a software, $WinDETA\ 4.5$, also from Novocontrol Technologies GmbH.

# *Chapter Four*

# 4. Experimental Results and Analysis

## 4.1. The Octanoic Acid

The octanoic acid is considered a surfactant and is the most common additive that has been tested in polymer dispersed liquid crystal displays. Once this is the most common additive, several studies were made with this single surfactant, such as the addition order, the quantity of additive used and the comparison between octanoic acid and hexadecanoic acid studying the effect of the chain length.

The electro-optical results for the tri(ethylene glycol) dimethacrylate systems with liquid crystal and octanoic acid are presented in Figure 4.1 and Figure 4.4 for different types of initiators.

For the thermal initiator the results obtained are described below and it can be seen that no permanent memory effects occur in this kind of monomer. Transmittance is high and applied voltages are, relatively, low. Comparing this result with the same monomer without the addition of octanoic acid, it is clearly seen that the addition of it optimizes the electro-optic properties of the system, as much in the transmittance obtained as in the applied voltage necessary to its operation.

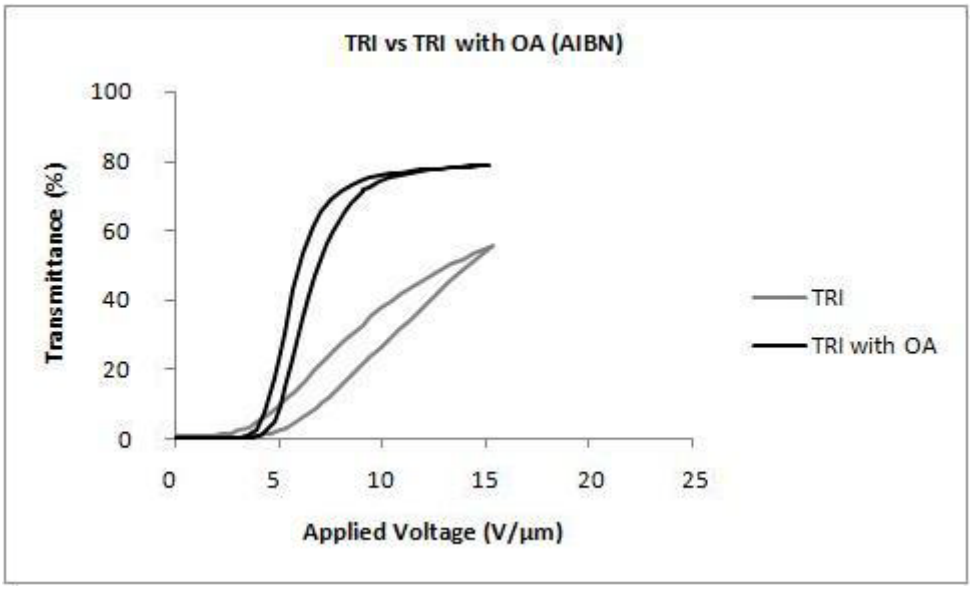


**Figure 4.1 – Electro-optic response of the system (TRI/AIBN/E7) with and without OA.**

The analysis of the textures over polarized light have shown that the sample is homogeneous in its totality, and as can be seen in Figure 4.2, the area where voltage is applied is in a brighter tonality.

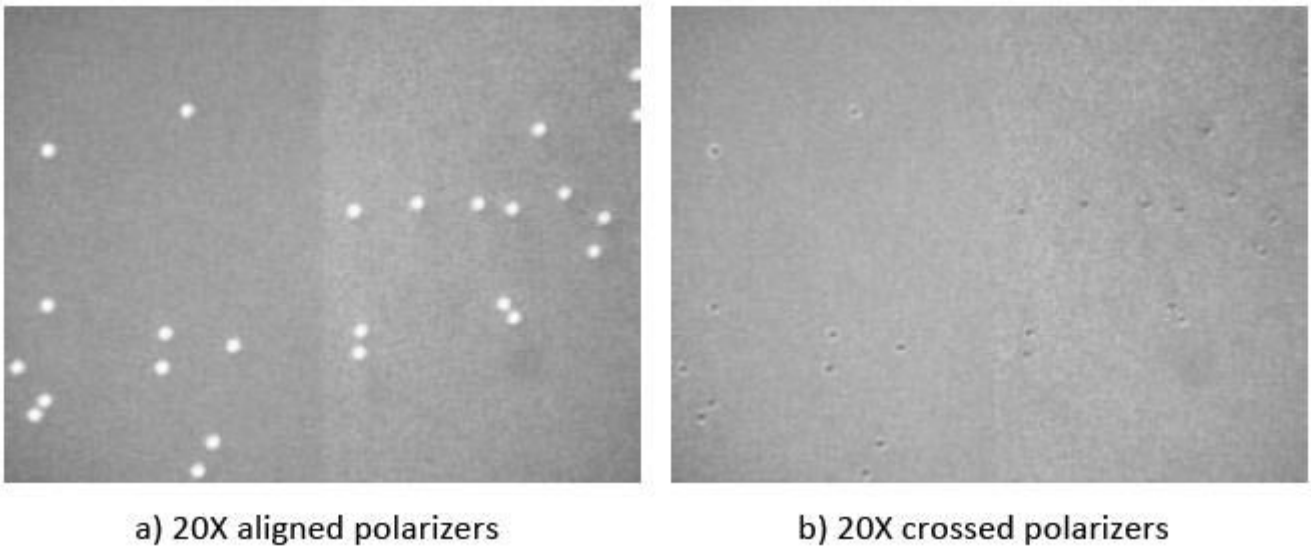


**Figure 4.2 – POM micrograph for (TRI/AIBN/E7/OA)**

In order to relate the transmission-field response to the composite morphology, the system was analyzed by scanning electron microscopy. The respective image is shown in Figure 4.3. Since $E7$ was removed prior to microscope analysis, the dark areas in the micrographs are representative of the original liquid crystal domains. Two phase morphology is observed where the liquid crystal phase seems to become quasi-

continuous among a porous open cell structure formed by the polymerization of the monomer, leading to the tunnel kind holes where the liquid crystal lies.

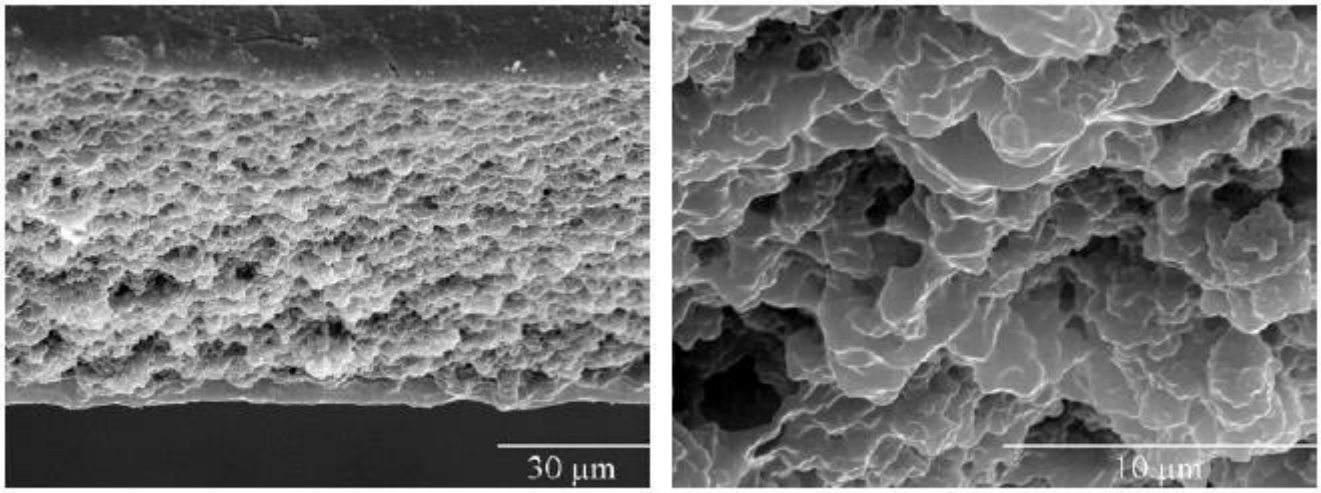


**Figure 4.3 – SEM morphology for (TRI/AIBN/E7/OA).**

The results for the photochemical initiator are described below and, once more, in this kind of monomer no permanent memory effects are obtained. Transmittances are similar, but the applied voltages have also decreased with this type of polymerization initiator. Once again, comparing this result with the ones obtained without the addition of octanoic acid, the same results are visible, this is, lower applied voltages for its operation.

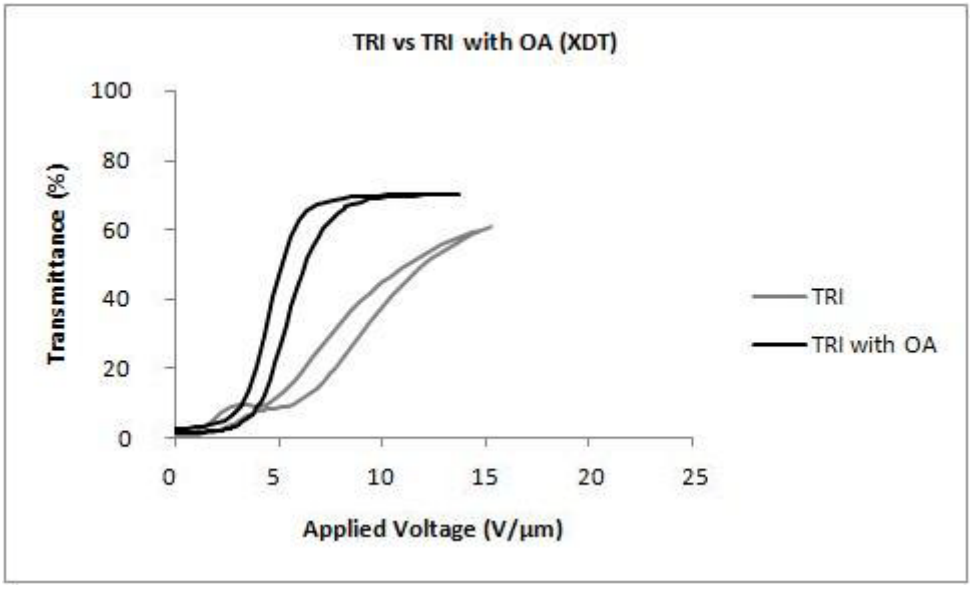


**Figure 4.4 – Electro-optic response of the system (TRI/XDT/E7) with and without OA.**

The analysis of the textures over polarized light have shown that the sample is homogeneous in its totality, and as can be seen in Figure 4.5, the area where voltage is applied is in a brighter tonality, but in this case, not so visible as with the previous sample, obtained with the thermal initiator.

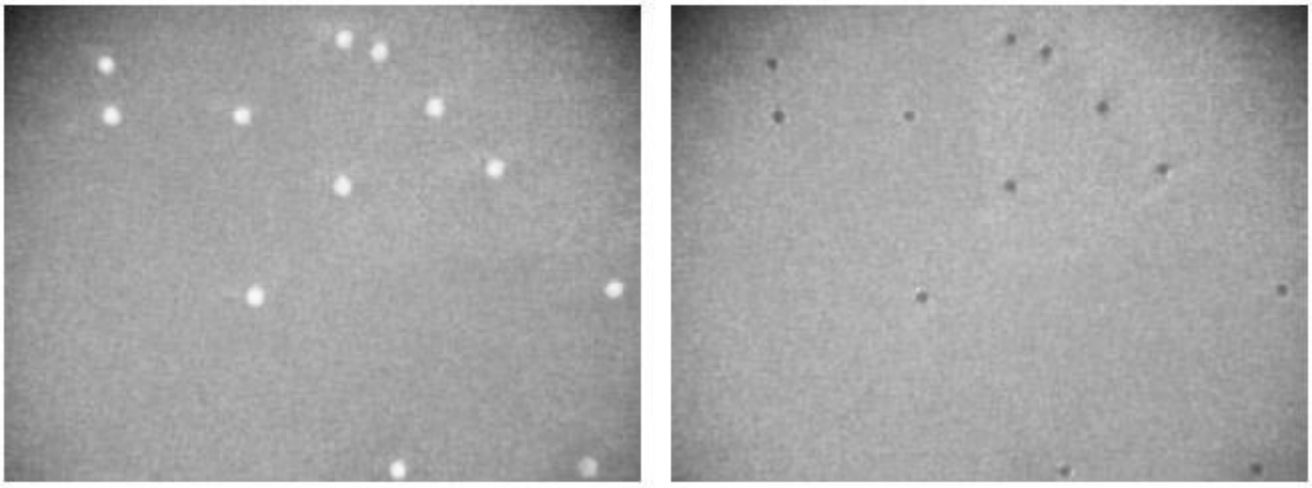


**Figure 4.5 – POM micrograph for (TRI/XDT/E7/OA)**

The electro-optical results for the poly(ethylene glycol) dimethacrylate systems with liquid crystal and octanoic acid are presented in Figure 4.6 and Figure 4.9 for different types of initiators.

For the thermal initiator the results obtained are described below and it can be seen that in this type of monomer, permanent memory effects are present. In this case, two ramps were obtained and this can be due to different regions of the polymer containing different domains of liquid crystal so that the applied voltage to orient these different regions is also different. Transmittances and applied voltages are practically the same when comparing this monomer with and without the addition of octanoic acid.

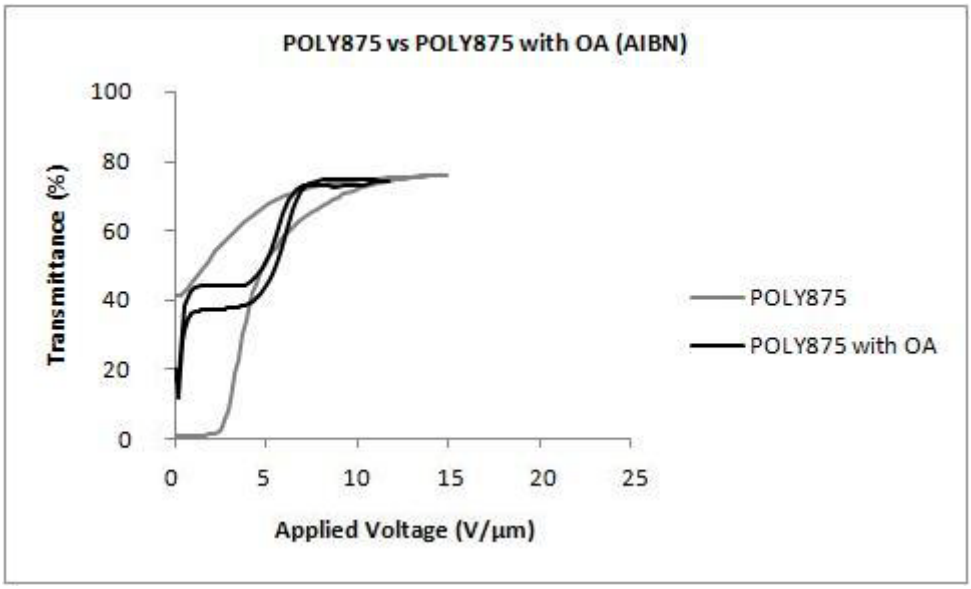


**Figure 4.6 – Electro-optic response of the system (POLY875/AIBN/E7) with and without OA.**

The analysis of the textures over polarized light have shown that the sample has very defects in its totality, and as can be seen in Figure 4.7, the entire sample presents some colors due to the refractive indices of the composite. Conjugating the electro-optic response curve and the polarized light images, this might be happening because the composite orients twice, instead of once like the other samples.

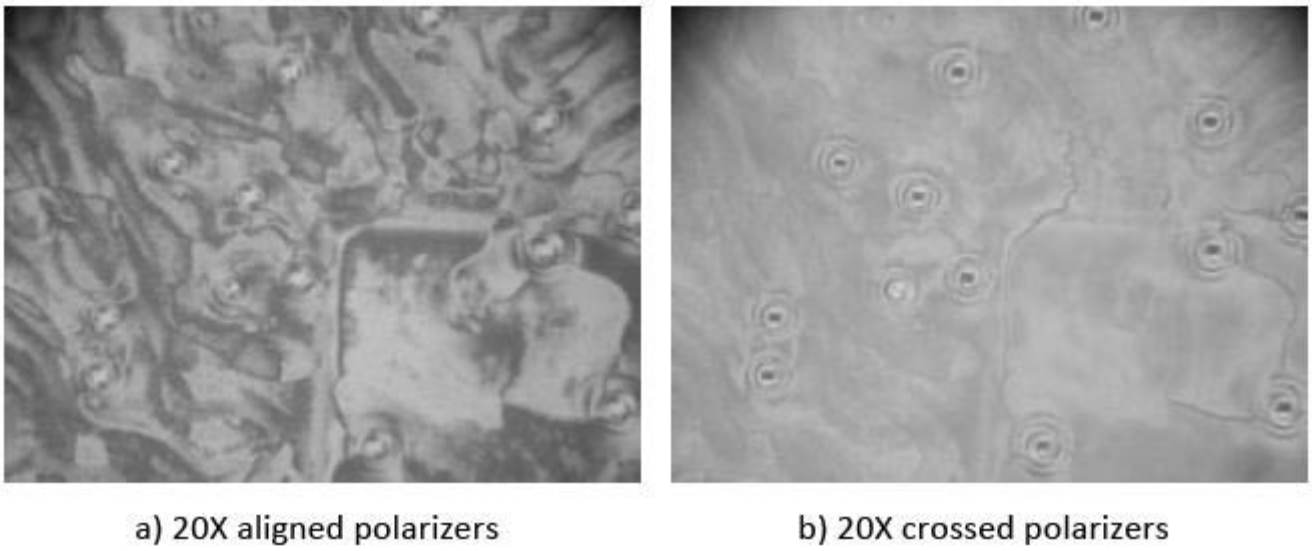


**Figure 4.7 – POM micrograph for (POLY875/AIBN/E7/OA)**

Figure 4.8 shows the scanning electron microscopy micrograph for this system. No polymer beads are observed in contrast with the previous monomer.

This absence can be an indication of higher cross-linking polymerization leading to a higher network density. Once the applied voltages are lower than the ones obtained

with the other monomer, it was expected to observe larger dark areas and polymer beads.

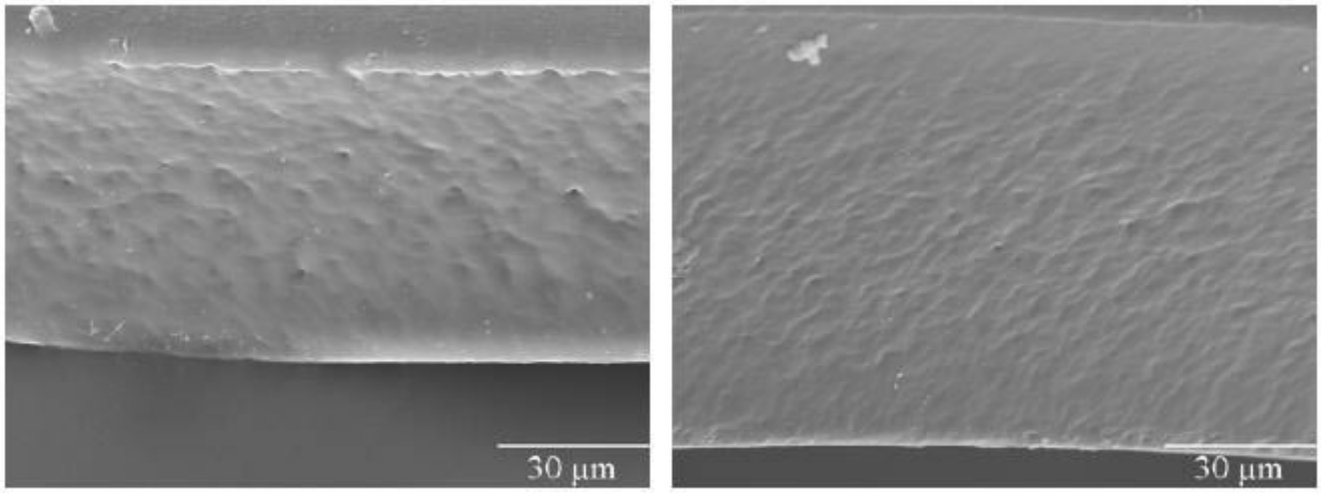


**Figure 4.8 – SEM morphology for (POLY875/AIBN/E7/OA).**

The results for the photochemical initiator are described below and, besides it was thought that permanent memory effects could occur, they do not. This can be explained due to the type of polymerization where polymerization times are lower. Transmittance has decreased comparing with the thermal polymerization initiator and applied voltages have taken the same way, being substantially lower. In this case, comparing the results for this composite with and without octanoic acid, it is visible that the additive decreases the transmittance of the device but reduces for almost a half, the applied voltages necessary for the state transition to occur.

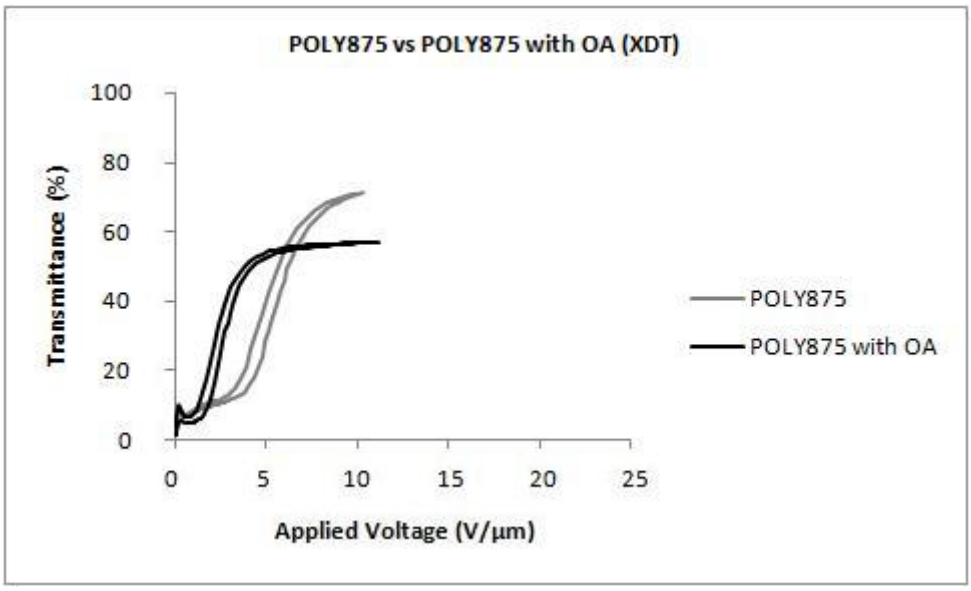


**Figure 4.9 – Electro-optic response of the system (POLY875/XDT/E7) with and without OA.**

The analysis of the textures over polarized light have shown that the sample presents liquid crystal domains in its totality and even in the center where voltage is applied no differences can be noticed, as showed in Figure 4.10. This is a typical micrograph of this kind of monomer with this polymerization initiator, independently of the presence of an additive.

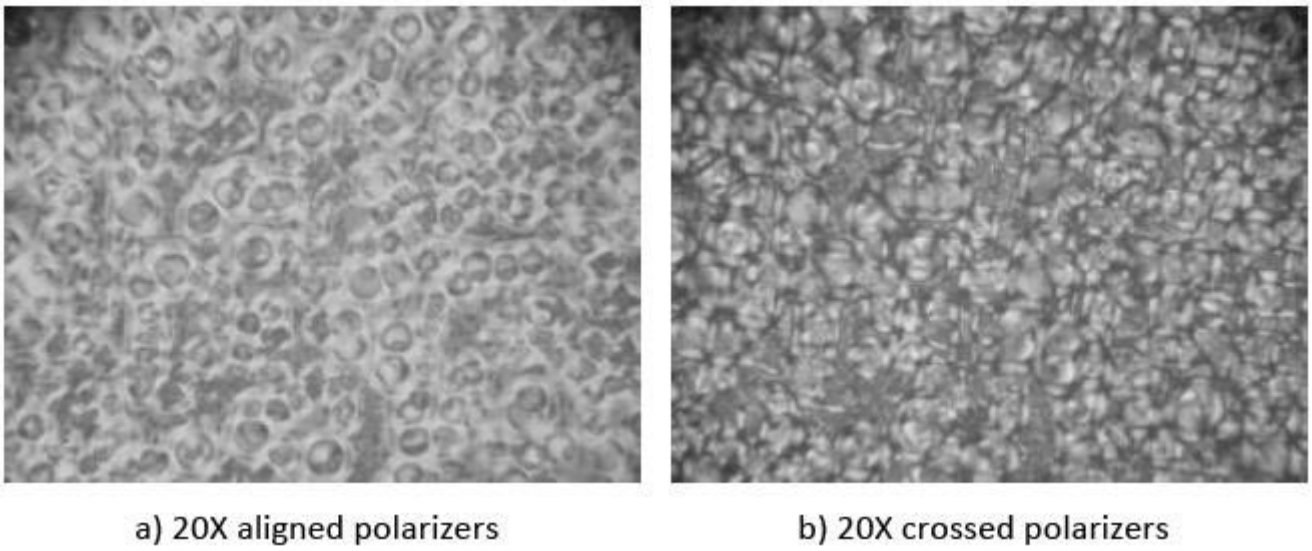


**Figure 4.10 – POM micrograph for (POLY875/XDT/E7/OA)**

This texture is characteristic of the photo polymerized poly(ethylene glycol) dimethacrylate, as is observed in every sample of this kind. Contrary to tri(ethylene glycol) dimethacrylate and the thermally polymerized poly(ethylene glycol) dimethacrylate, whose morphology appears as a continuous phase of composite, in this case, the morphology appears as a two-phase material with several big droplets of liquid crystal, starting to coalesce. This is probably due to the polymerization times that are relatively low and with faster polymerization rates.

### 4.1.1. Addition Order

These assays are also made with octanoic acid, but this time, instead of adding octanoic acid at the end of the mixture preparation, the additive is initially mixed with the liquid crystal and only then, this mixture is added to the monomer.

The electro-optical results for the tri(ethylene glycol) dimethacrylate systems with liquid crystal and octanoic acid with the change in the addition order during the

preparation of the mixture are presented in Figure 4.11 and Figure 4.13 for different types of initiators.

For the thermal initiator the results obtained are described below and it can be seen that no permanent memory effects occur in this kind of monomer. Transmittance is very good, but applied voltages are high. Comparing this result with the same monomer with the addition of octanoic acid, originally prepared, it is clearly seen that the addition order has a reflection on the behavior of the composites, being that the best results are observed with the addition of octanoic acid in the final stage of the preparation of the mixture.

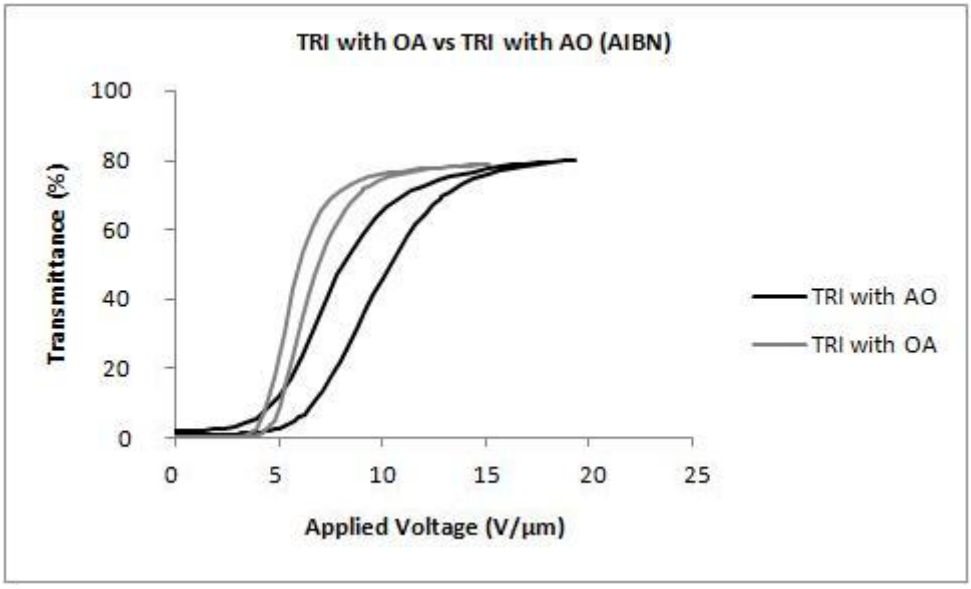


**Figure 4.11 – Electro-optic response of the system (TRI/AIBN/E7) with OA changing the addition order.**

The analysis of the textures over polarized light have shown that the sample is homogeneous in its totality, and as can be seen in Figure 4.12, the area where voltage is applied is in a brighter tonality.

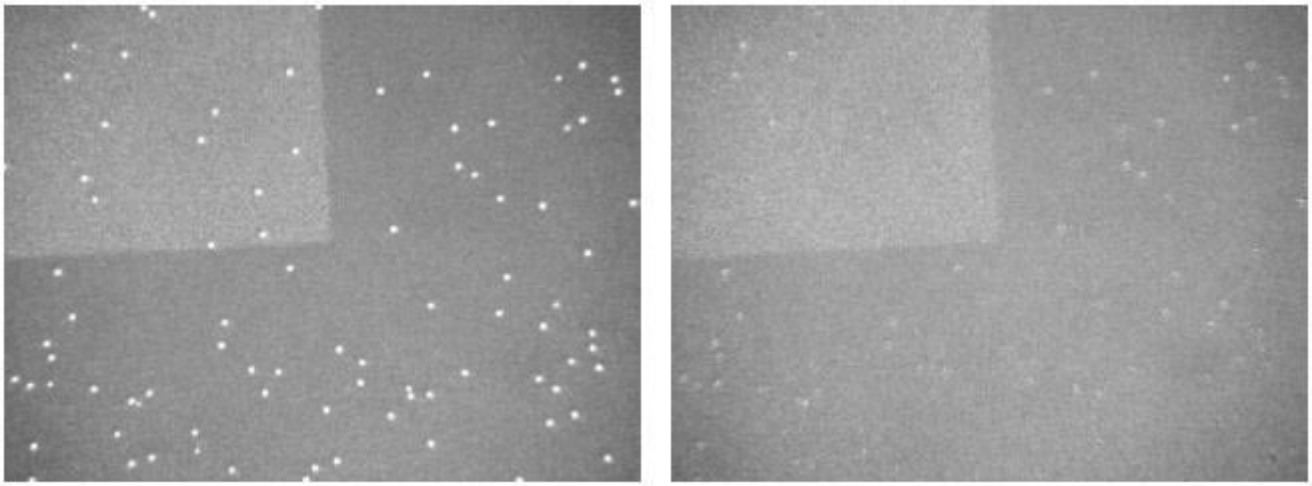


**Figure 4.12 – POM micrograph for (TRI/AIBN/E7/AO)**

The results for the photochemical initiator are described below and it can be seen that with the change on the addition order, still no permanent memory effects occur. Transmittances and applied voltages are practically the same obtained with the thermal initiator. Once again, comparing this result with the ones obtained with the original addition of octanoic acid, the same results are visible, this is, higher applied voltages for its operation and similar transmittances, meaning that the original preparation of the mixtures optimizes the operation of the device.

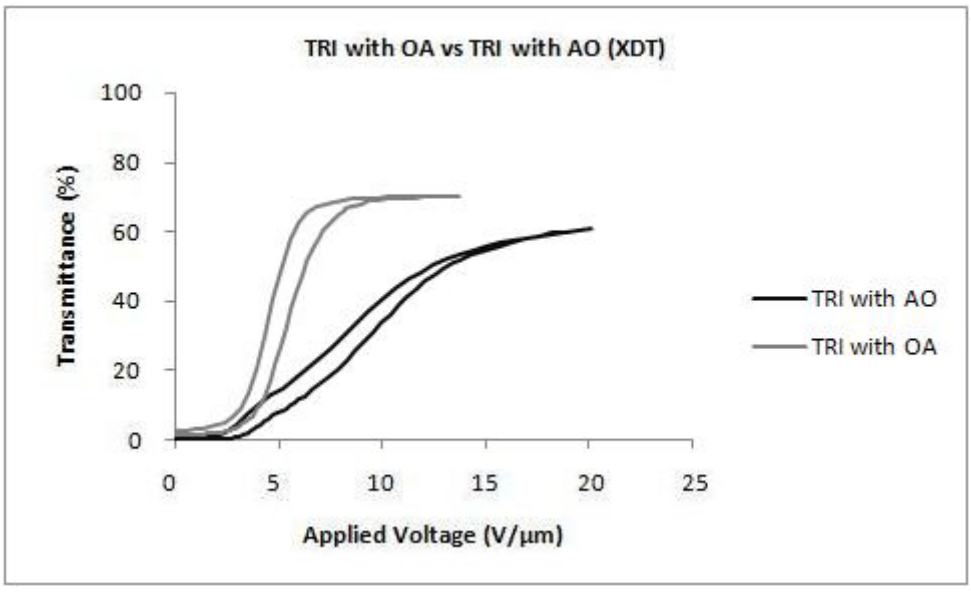


**Figure 4.13 – Electro-optic response of the system (TRI/XDT/E7) with OA changing the addition order.**

The analysis of the textures over polarized light have shown that the sample is homogeneous in its totality, and as can be seen in Figure 4.14, the area where voltage

is applied is in a brighter tonality, but in this case, not so visible as with the previous sample, obtained with the thermal initiator.

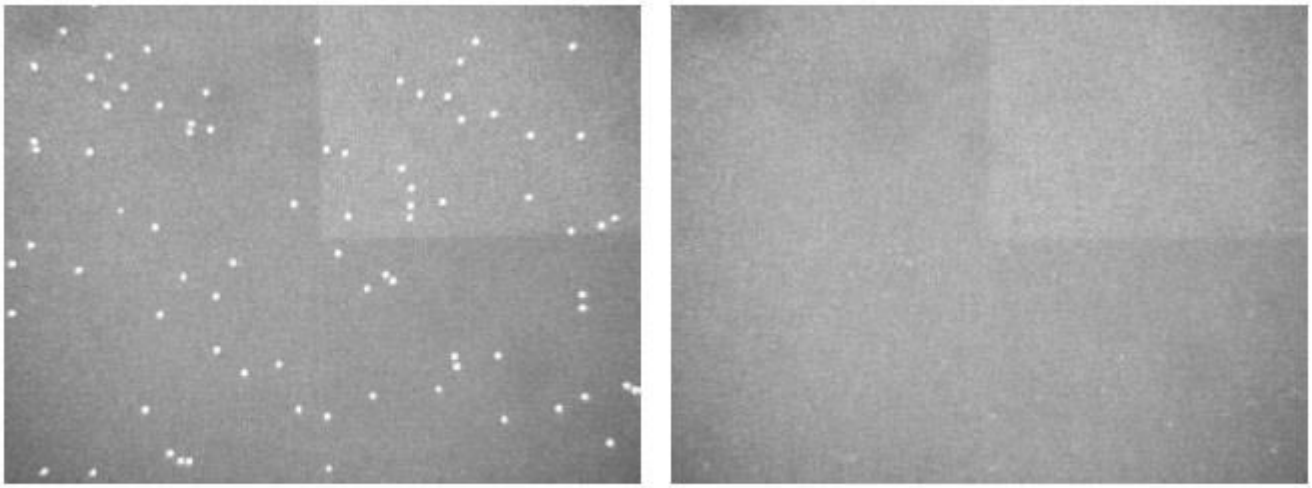

a) 10X aligned polarizers b) 10X crossed polarizers

**Figure 4.14 – POM micrograph for (TRI/XDT/E7/AO)**

The electro-optical results for the poly(ethylene glycol) dimethacrylate systems with liquid crystal and octanoic acid with the change in the addition order during the preparation of the mixtures are presented in Figure 4.15 and Figure 4.17 for different types of initiators.

For the thermal initiator the results obtained are described below and it can be seen that, although permanent memory effects were expected, they are not present. In this case, two ramps were obtained and this can be due to different regions of the polymer containing different domains of liquid crystal so that the applied voltage to orient these different regions is also different. The new method of mixture preparation brought higher transmittances and, practically, the same applied voltage when comparing this monomer with the original addition of octanoic acid.

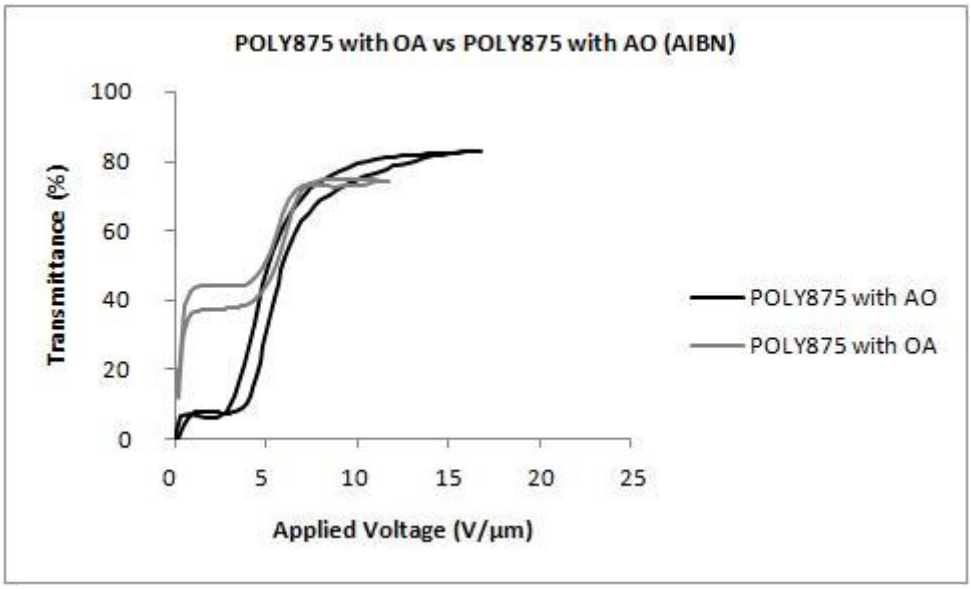


**Figure 4.15 – Electro-optic response of the system (POLY875/AIBN/E7) with OA changing the addition order.**

The analysis of the textures over polarized light have shown that the sample is homogeneous in its totality, and as can be seen in Figure 4.28, the area where voltage is applied is in a brighter tonality.

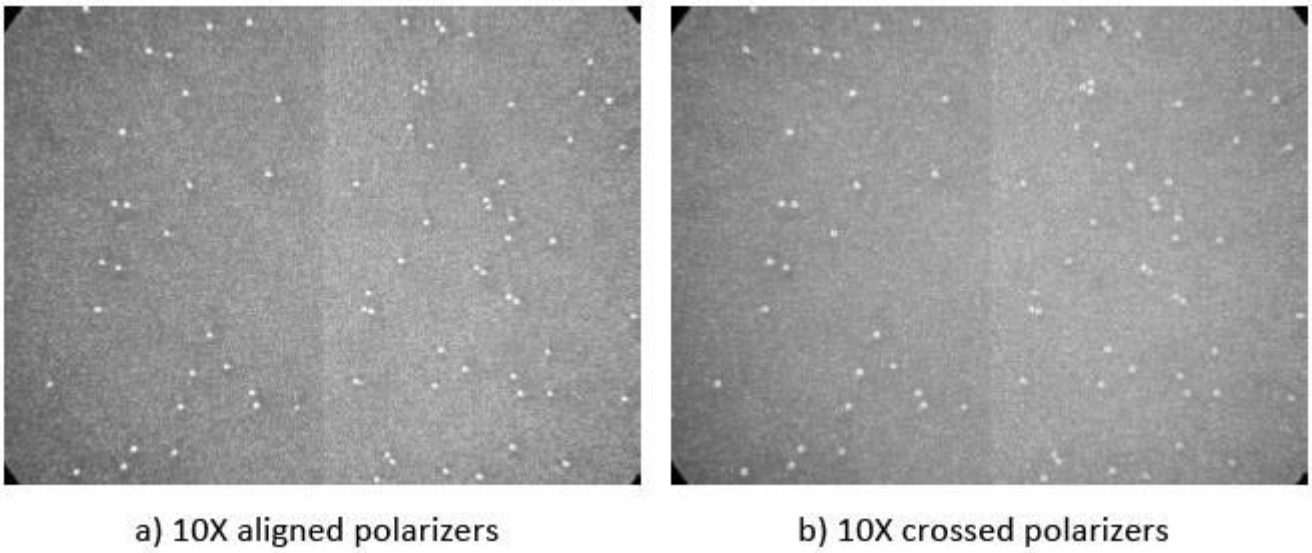


**Figure 4.16 – POM micrograph for (POLY875/AIBN/E7/AO)**

The results for the photochemical initiator are described below and, as can be seen, the transmittance obtained was relatively high and the applied voltages are superior.

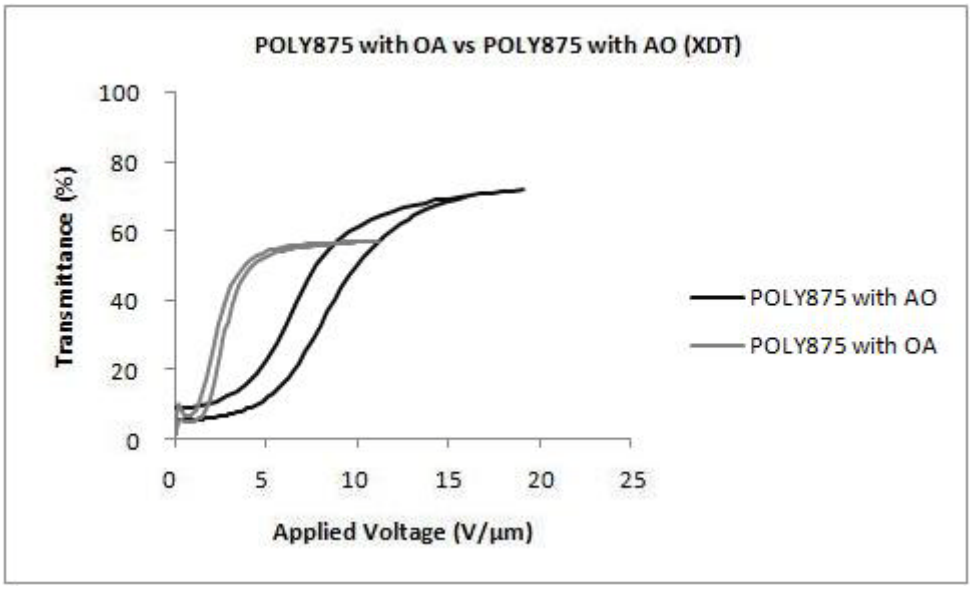


**Figure 4.17 – Electro-optic response of the system (POLY875/XDT/E7) with OA changing the addition order.**

The analysis of the textures over polarized light have shown that the sample presents liquid crystal domains in its totality and even in the center where voltage is applied no differences can be noticed, as showed in Figure 4.18.

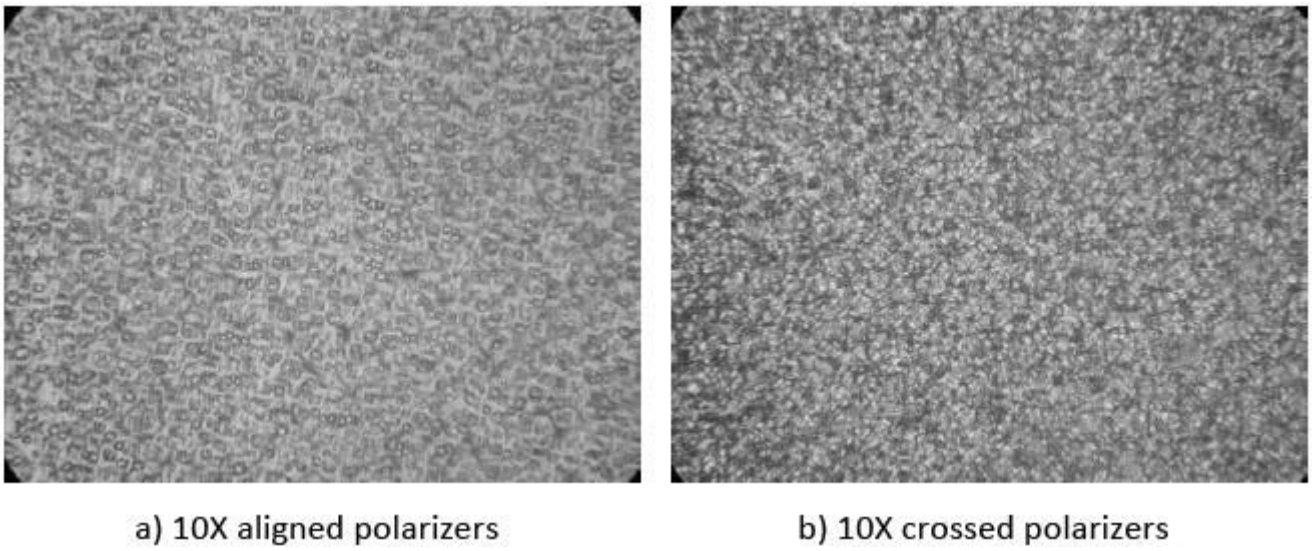


**Figure 4.18 – POM micrograph for (POLY875/XDT/E7/AO)**

### 4.1.2. Quantity of Additive

As in the first scenario, these assays are also made with octanoic acid, but this time, instead of adding 10% of additive, small amounts of additive are used, around 1% in weight.

The electro-optical results for the tri(ethylene glycol) dimethacrylate systems with liquid crystal and octanoic acid in lower quantities are presented in Figure 4.19 and Figure 4.21 for different types of initiators.

For the thermal initiator the results obtained are described below and it can be seen that no permanent memory effects occur in this kind of monomer. Comparing this result with the same monomer with the addition of higher quantities of octanoic acid, it is clearly seen that the higher addition of it optimizes the electro-optic properties of the system, as much in the transmittance obtained as in the applied voltage necessary to its operation.

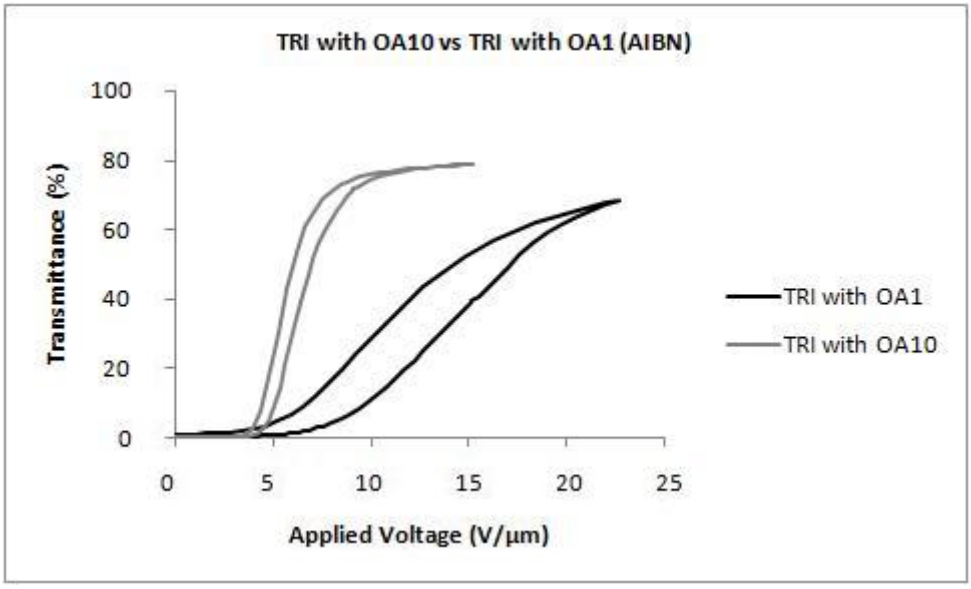


**Figure 4.19 – Electro-optic response of the system (TRI/AIBN/E7) with OA changing the quantity of additive.**

The analysis of the textures over polarized light have shown that the sample is homogeneous in its totality, and as can be seen in Figure 4.20, the area where voltage is applied is in a brighter tonality.

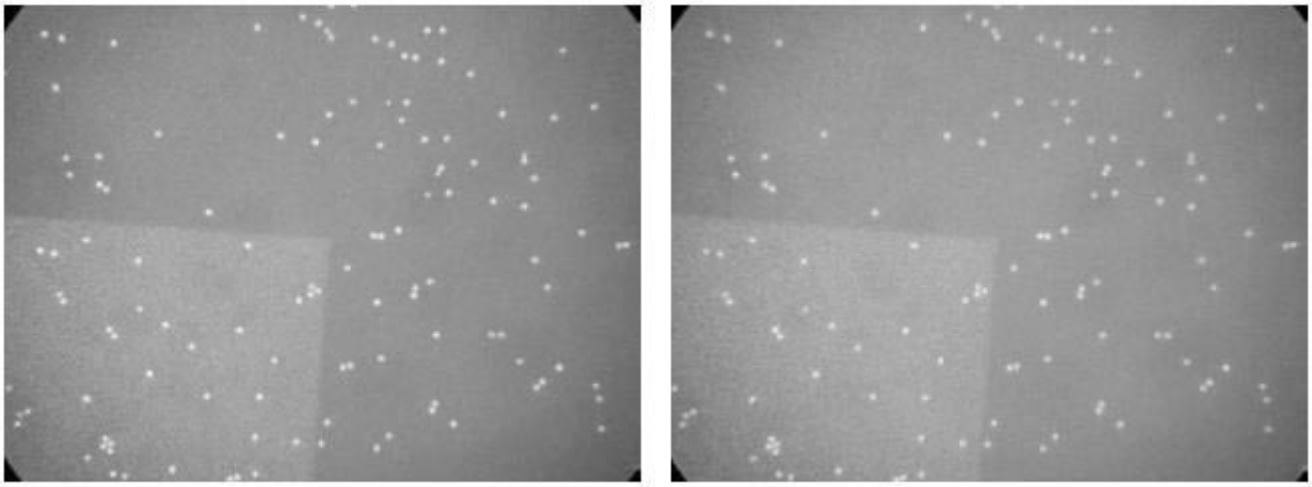


**Figure 4.20 – POM micrograph for (TRI/AIBN/E7/OA1)**

The results for the photochemical initiator are described below and, once more, in this kind of monomer no permanent memory effects are obtained. Transmittances are similar, but the applied voltages are lower with this type of polymerization initiator. Once again, comparing this result with the ones obtained with the addition of higher quantities of octanoic acid, it is seen that the transmittance is very similar but the applied voltages are lower when using more quantity of additive.

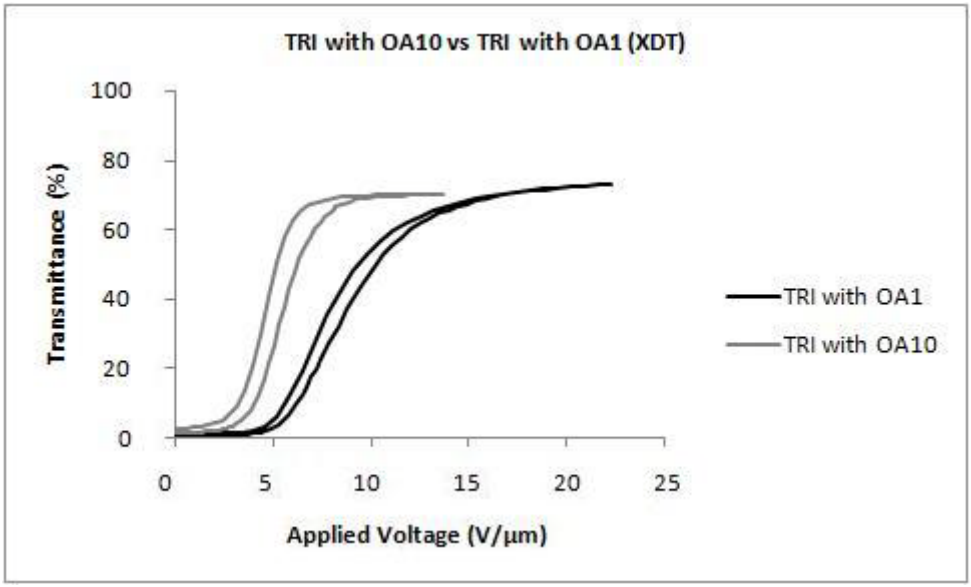


**Figure 4.21 – Electro-optic response of the system (TRI/XDT/E7) with OA changing the quantity of additive.**

The analysis of the textures over polarized light have shown that the sample is homogeneous in its totality, and as can be seen in Figure 4.22, the area where voltage

is applied is in a brighter tonality, but in this case, not so visible as with the previous sample, obtained with the thermal initiator.

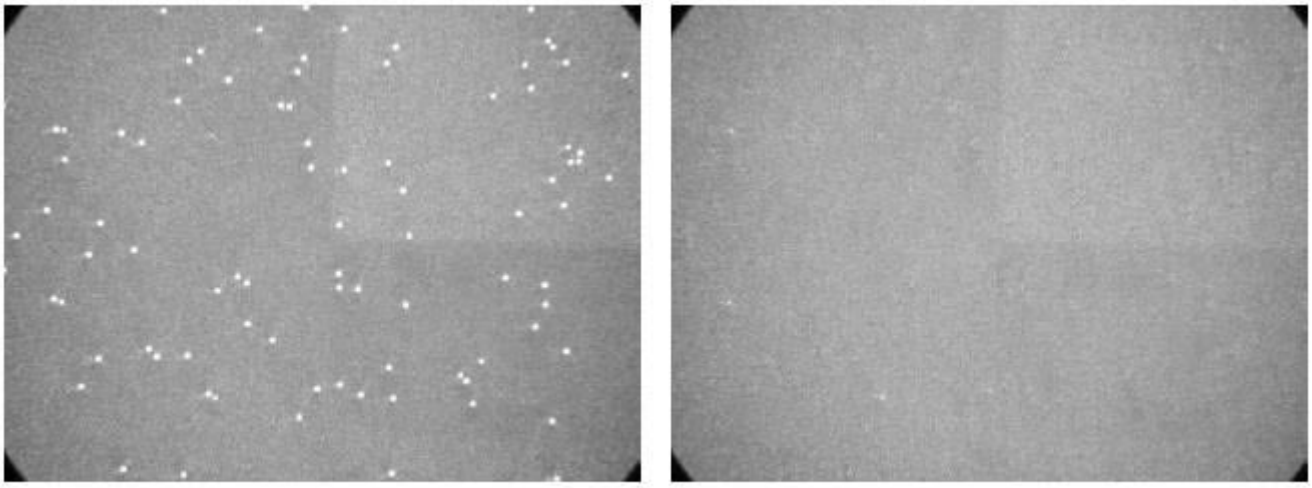

a) 10X aligned polarizers b) 10X crossed polarizers

**Figure 4.22 – POM micrograph for (TRI/XDT/E7/OA1)**

The electro-optical results for the poly(ethylene glycol) dimethacrylate systems with liquid crystal and octanoic acid in lower quantities are presented in Figure 4.23 and Figure 4.25 for different types of initiators.

For the thermal initiator the results obtained are described below and it can be seen that in this type of monomer, permanent memory effects are clearly present. Transmittances are high and applied voltages are low. When comparing this monomer with the addition of higher quantities of octanoic acid, in this case, it performs better when low quantities of additive are mixed in the composite. This might be enhanced due to the ramps observed on the electro-optic results when higher quantities of additive were used.

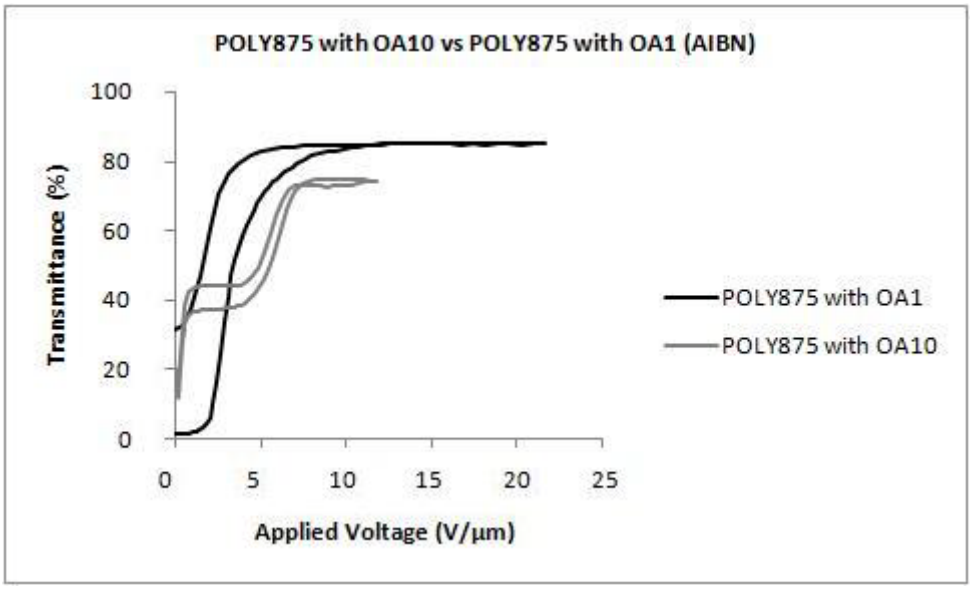


**Figure 4.23 – Electro-optic response of the system (POLY875/AIBN/E7) with OA changing the quantity of additive.**

The analysis of the textures over polarized light have shown that the sample is homogeneous in its totality, and as can be seen in Figure 4.24, the area where voltage is applied is in a total different tonality, representing the permanent memory effects, according to the electro-optical response illustration. Light scatters through the sample, because the orientation of the liquid crystals in that centre is oriented into one direction.

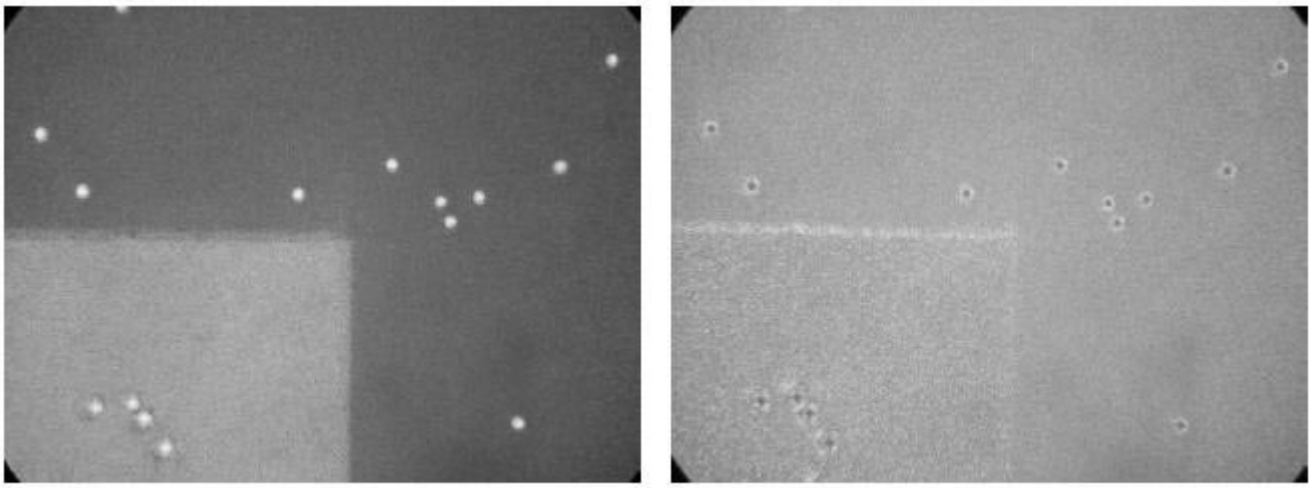


**Figure 4.24 – POM micrograph for (POLY875/AIBN/E7/OA1)**

The results for the photochemical initiator are described below and, besides it was thought that permanent memory effects could occur, they do not. This can be explained due to the type of polymerization where polymerization times are lower.

Transmittance has maintained the same levels of the previous sample, but voltages are higher. In this case, comparing the results for this composite with the addition of higher quantities of octanoic acid, it is visible that with the addition of higher quantities, the applied voltages perform better, while the transmittance obtained is better when using smaller amounts of additive.

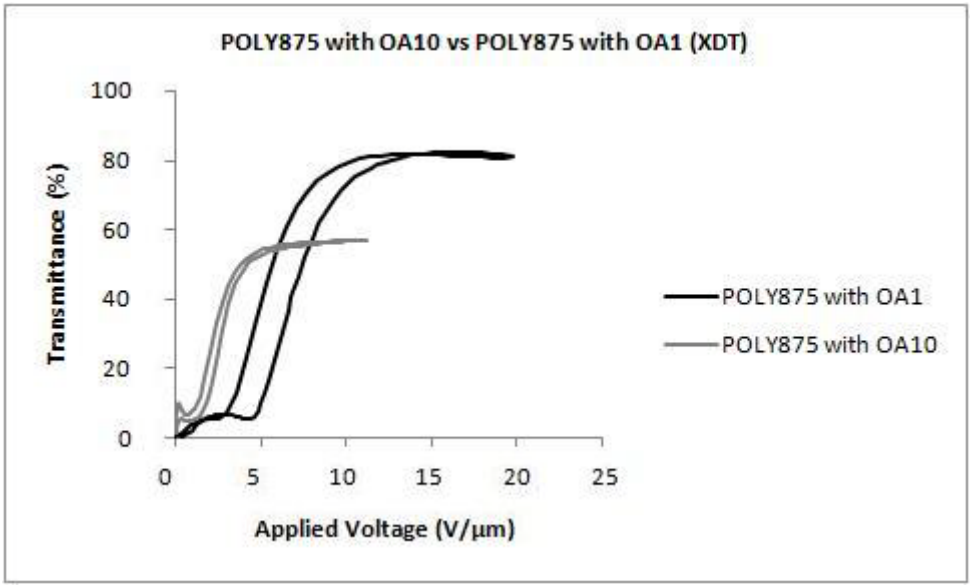


**Figure 4.25 – Electro-optic response of the system (POLY875/XDT/E7) with OA changing the quantity of additive.**

The analysis of the textures over polarized light have shown that the sample presents liquid crystal domains in its totality and even in the center where voltage is applied no differences can be noticed, as showed in Figure 4.26.

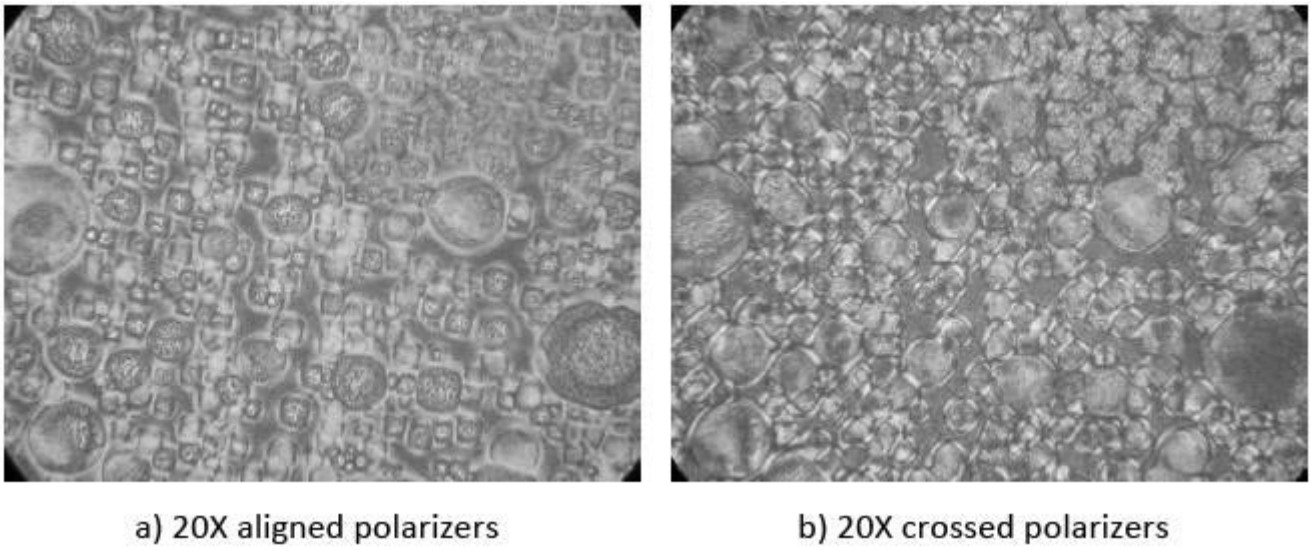


**Figure 4.26 – POM micrograph for (POLY875/XDT/E7/OA1)**

### 4.1.3. Chain Length

Like the other extra tests done, mentioned above, a molecule similar to octanoic acid was used to observe the difference obtained when the chain length of the additive is considerably larger. To do that, hexadecanoic acid was selected once the carbon chain length is twice the carbon chain presented in octanoic acid.

The electro-optical results for the tri(ethylene glycol) dimethacrylate systems with liquid crystal and hexadecanoic acid are presented in Figure 4.27 and Figure 4.30 for different types of initiators.

For the thermal initiator the results obtained are described below and it can be seen that no permanent memory effects occur in this kind of monomer. Comparing this result with the same monomer with a small chain length, it is clearly seen that the additive whose chain is smaller optimizes the electro-optic properties of the system, as much in the transmittance obtained as in the applied voltage necessary to its operation.

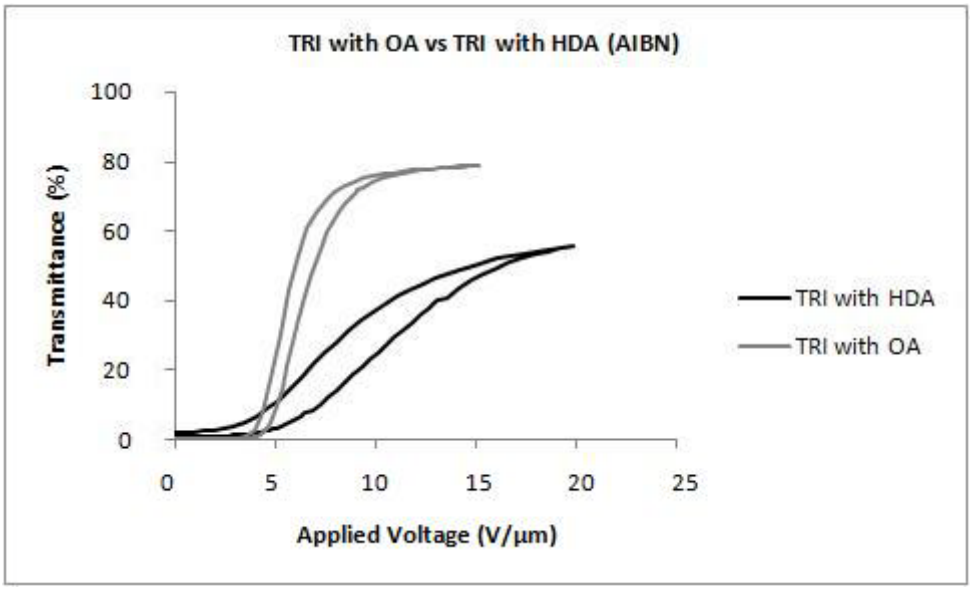


**Figure 4.27 – Electro-optic response of the system (TRI/AIBN/E7) with HDA.**

The analysis of the textures over polarized light have shown that the sample is homogeneous in its totality, and as can be seen in Figure 4.28, the area where voltage is applied is in a brighter tonality.

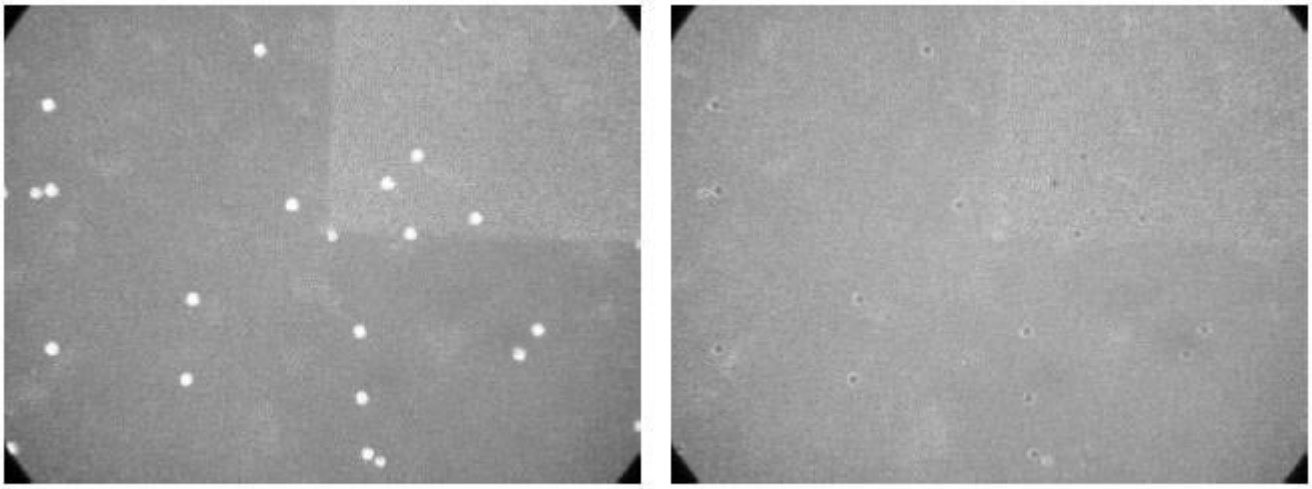


**Figure 4.28 – POM micrograph for (TRI/AIBN/E7/HDA)**

In order to relate the transmission-field response to the composite morphology, the system was analyzed by scanning electron microscopy. The respective image is shown in Figure 4.29. Since $E7$ was removed prior to microscope analysis, the dark areas in the micrographs are representative of the original liquid crystal domains. Two phase morphology is still observed. Although the network density with a higher chain length is visible. The tunnels where the liquid crystal fit are tighter. Therefore, it indicates the reason for a need of higher fields for the device operation.

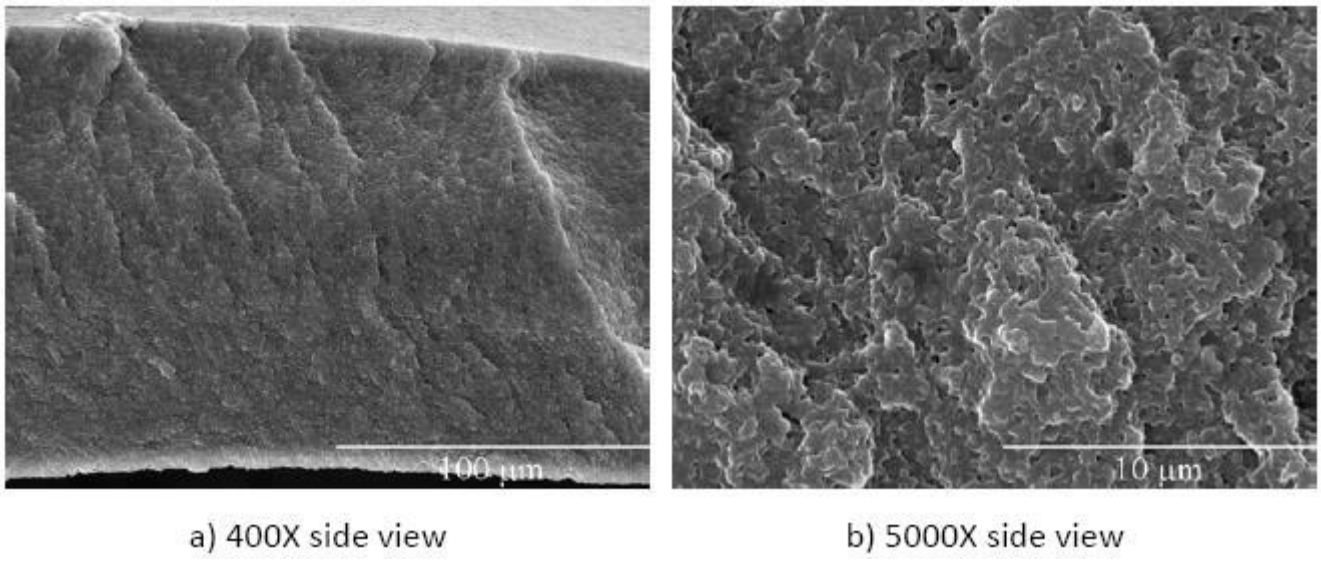


**Figure 4.29 – SEM morphology for (TRI/AIBN/E7/HDA).**

The results for the photochemical initiator are described below and, once more, in this kind of monomer no permanent memory effects are obtained. Transmittances are similar, as well as applied voltages with this type of polymerization initiator. Once

again, comparing this result with the ones obtained with the same monomer with a molecule with the same functional group but with small chain, the same results are visible, this is, lower applied voltages for its operation.

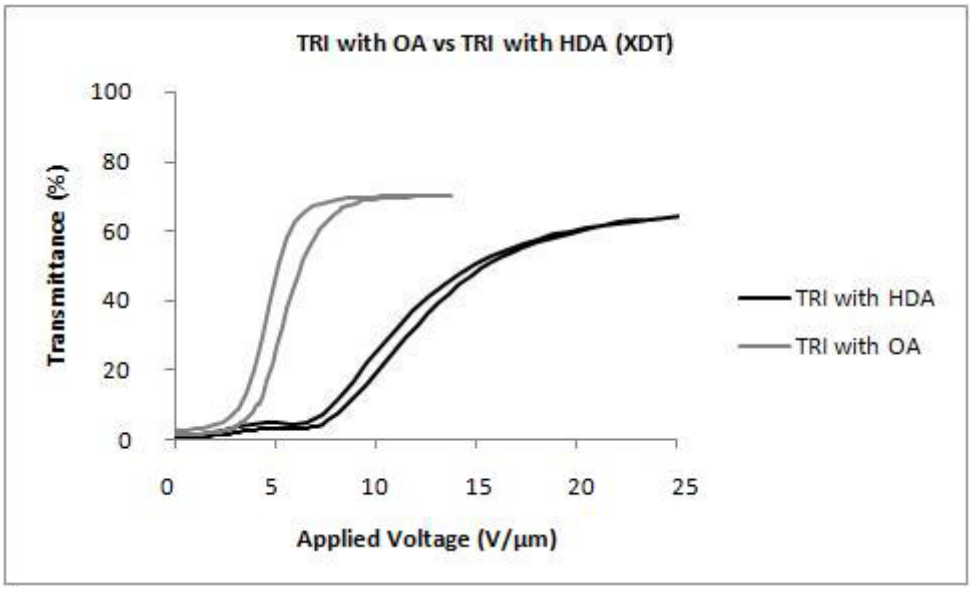


**Figure 4.30 – Electro-optic response of the system (TRI/XDT/E7) with HDA.**

The analysis of the textures over polarized light have shown that the sample is homogeneous in its totality, and as can be seen in Figure 4.31, the area where voltage is applied is in a brighter tonality, but in this case, not so visible as with the previous sample, obtained with the thermal initiator.

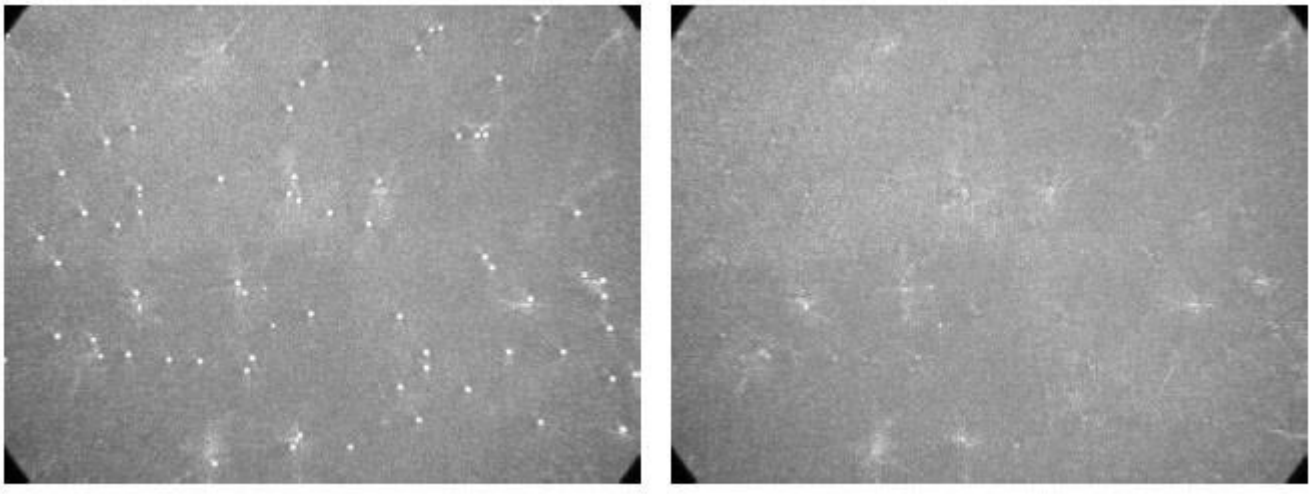


**Figure 4.31 – POM micrograph for (TRI/XDT/E7/HDA)**

The electro-optical results for the poly(ethylene glycol) dimethacrylate systems with liquid crystal and hexadecanoic acid are presented in Figure 4.32 and Figure 4.35 for different types of initiators.

For the thermal initiator the results obtained are described below and it can be seen that in this type of monomer, permanent memory effects are present. Permanent memory effects are substantially visible and more effective with higher chain lengths. Although transmittance is a little lower, applied voltages are practically the same.

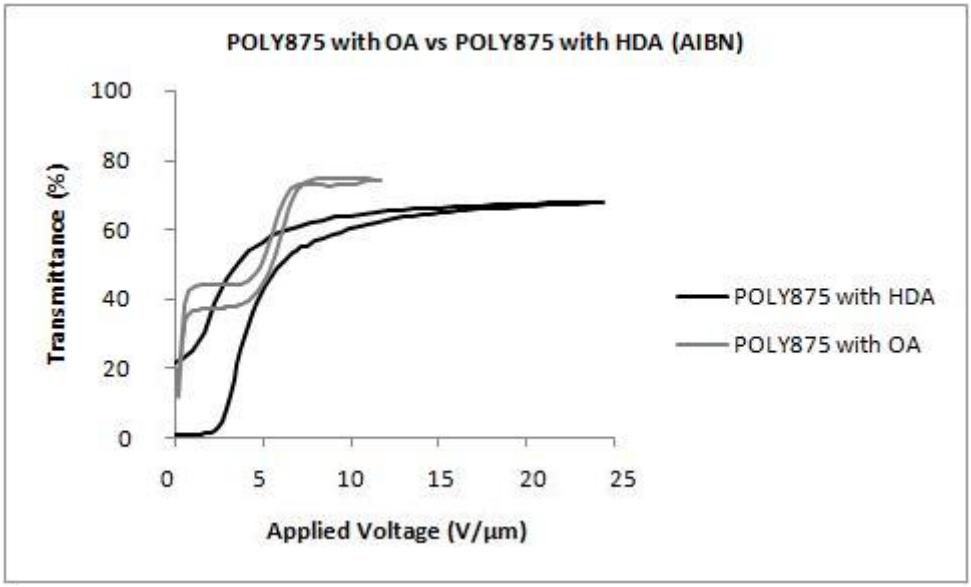


**Figure 4.32 – Electro-optic response of the system (POLY875/AIBN/E7) with HDA.**

The analysis of the textures over polarized light have shown that the sample is homogeneous in its totality, and as can be seen in Figure 4.33, the area where voltage is applied is in a total different tonality, representing the permanent memory effects, according to the electro-optical response illustration. Light scatters through the sample, because the orientation of the liquid crystals in that centre is oriented into one direction.

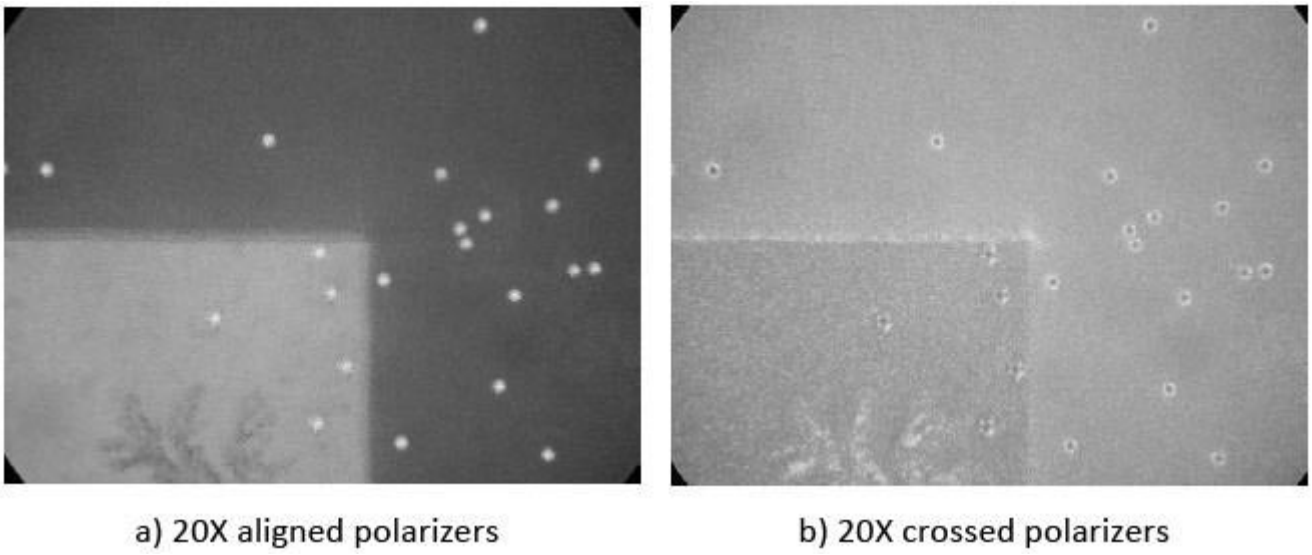


**Figure 4.33 – POM micrograph for (POLY875/AIBN/E7/HDA)**

Figure 4.34 shows the scanning electron microscopy micrograph for this system. No polymer beads are observed in contrast with the previous monomer. This inferior size can be an indication of higher cross-linking polymerization leading to a higher network density. Once the applied voltages are lower than the ones obtained with the other monomer, it was expected to observe larger dark areas and polymer beads.

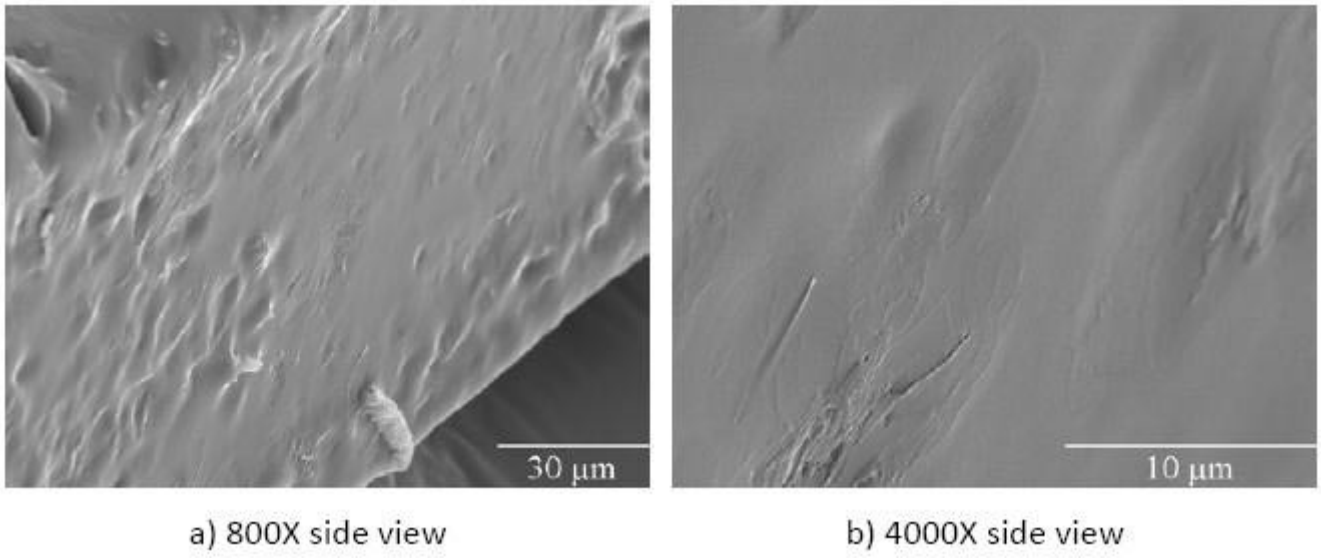


**Figure 4.34 – SEM morphology for (POLY875/AIBN/E7/HDA).**

The results for the photochemical initiator are described below and, besides it was thought that permanent memory effects could occur, they do not. This can be explained due to the type of polymerization where polymerization times are lower. In this case, comparing the results for this composite with a small and larger chain length it is visible that additives containing an extended chain length increase the

transmittance of the device but applied voltages for their operation are relatively higher.

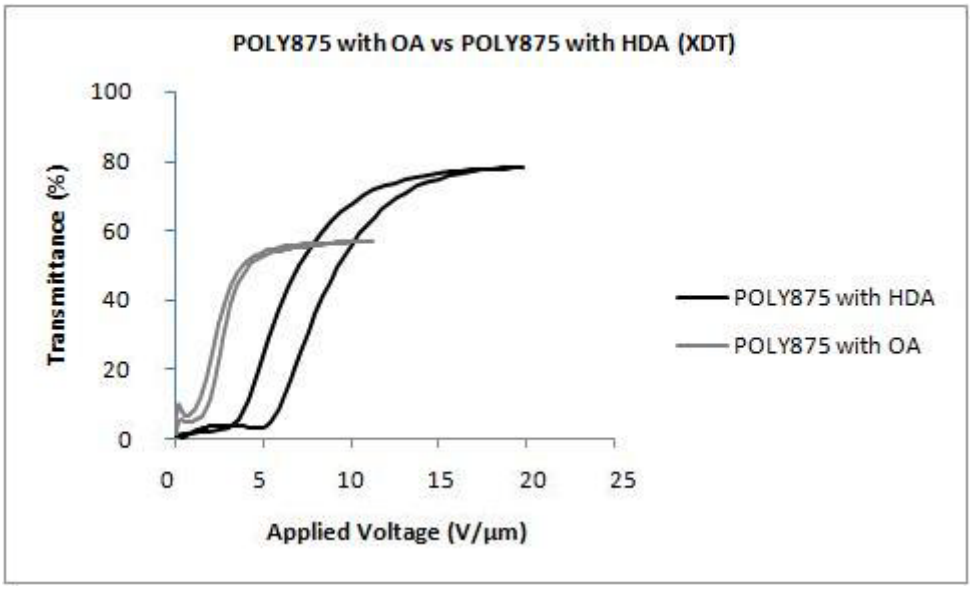


**Figure 4.35 – Electro-optic response of the system (POLY875/XDT/E7) with HDA.**

The analysis of the textures over polarized light have shown that the sample presents liquid crystal domains in its totality and even in the center where voltage is applied no differences can be noticed, as showed in Figure 4.36.

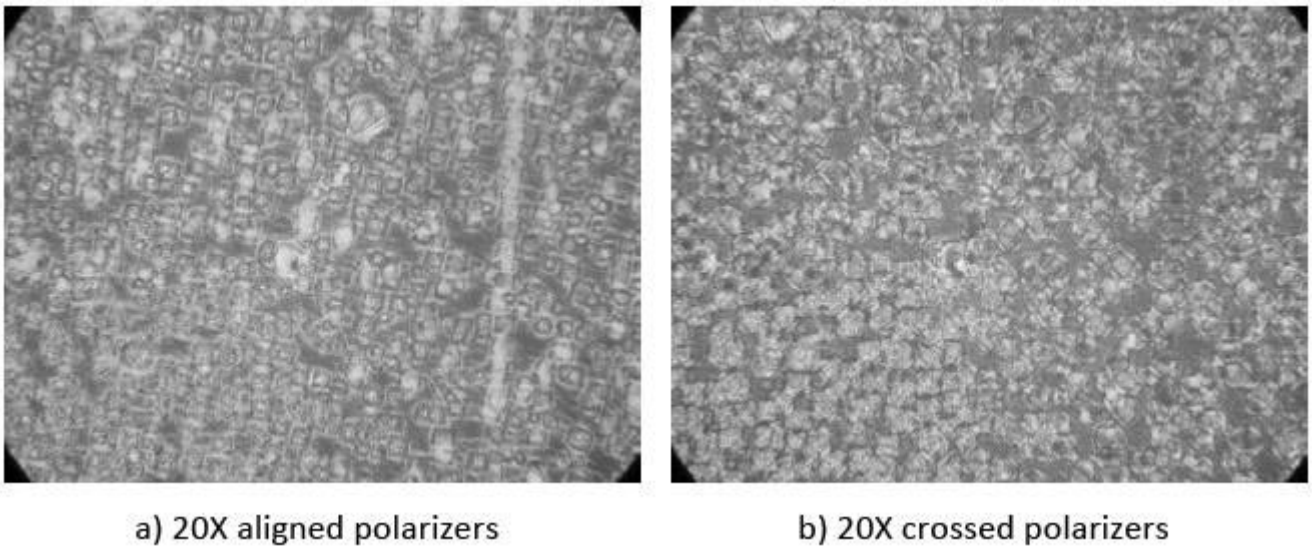


**Figure 4.36 – POM micrograph for (POLY875/XDT/E7/HDA)**

In Table 4.1 are presented the compositions of the samples with the percentages in weight of monomer, weight of liquid crystal and weight of additive for the monomers and their respective polymerization initiator. In the table are presented the composition of the initial samples containing 10% of octanoic acid and the respective

tests made within this additive as well as its comparison about the chain length. The polymerization times for the thermal samples were approximately $24$ hours and for the photochemical samples the times were about $1000{\sim}3000\,s$, because of the values of the calculated actinometry that were obtained between $3.0\times10^{-7}{\sim}1.5\times10^{-6}\,Nhv.min^{-1}$. The lower polymerization times mean that the actinometry values were higher and for higher polymerization times, that means the actinometry values were inferior. For polymerization times of $1000$ seconds, the number of photons that passed through the sample was equivalent to $1.51\times10^{19}$ photons and for the $3000$ seconds irradiation time, the photons traversing the sample were $9.03\times10^{18}$.

**Table 4.1 – Composition of the samples for the extra tests.**

| Monomer and Initiator | Additive | LC | Polymerization Times | Weight Ratio (wt %) | | |
|---|---|---|---|---|---|---|
| | | | | Monomer | LC | Additive |
| TRI AIBN | OA10 | E7 | 20 hours | 27 | 62 | 11 |
| | AO | E7 | 24 hours | 27 | 63 | 10 |
| | OA1 | E7 | 24 hours | 29 | 68 | 3 |
| | HDA | E7 | 24 hours | 27 | 63 | 10 |
| TRI XDT | OA10 | E7 | 1000 seconds | 27 | 62 | 11 |
| | AO | E7 | 1500 seconds | 27 | 63 | 10 |
| | OA1 | E7 | 1500 seconds | 28 | 67 | 5 |
| | HDA | E7 | 3000 seconds | 27 | 63 | 10 |
| POLY875 AIBN | OA10 | E7 | 20 hours | 26 | 61 | 13 |
| | AO | E7 | 24 hours | 27 | 63 | 10 |
| | OA1 | E7 | 24 hours | 29 | 67 | 4 |
| | HDA | E7 | 24 hours | 27 | 62 | 11 |
| POLY875 XDT | OA10 | E7 | 1000 seconds | 27 | 63 | 10 |
| | AO | E7 | 1500 seconds | 27 | 63 | 10 |
| | OA1 | E7 | 1500 seconds | 29 | 67 | 4 |
| | HDA | E7 | 3000 seconds | 27 | 63 | 10 |

The electro-optical properties of the systems described above are resumed in Table 4.2, where the required voltages for their operation and transmittance coefficients are presented.

**Table 4.2 – Electro-optical properties of the composites for the extra tests.**

| Monomer and Initiator | Additive | Transmittance (%) | | | Switching Voltage ($V.\mu m^{-1}$) | Contrast (%) | $T/V$ Ratio |
|---|---|---|---|---|---|---|---|
| | | $T_{max}$ | $T_{min}$ | $T_{half}$ | | | |
| TRI AIBN | OA10 | 79 | 0 | 39 | 6.40 | 79 | 0.305 |
| | AO | 80 | 1 | 40 | 9.50 | 79 | 0.211 |
| | OA1 | 68 | 0 | 34 | 14.30 | 68 | 0.119 |
| | HDA | 55 | 1 | 27 | 10.50 | 54 | 0.129 |
| TRI XDT | OA10 | 70 | 1 | 34 | 5.50 | 69 | 0.309 |
| | AO | 61 | 0 | 30 | 9.45 | 61 | 0.159 |
| | OA1 | 73 | 1 | 36 | 8.70 | 72 | 0.207 |
| | HDA | 64 | 1 | 32 | 11.90 | 63 | 0.134 |
| POLY875 AIBN | OA10 | 75 | 12 | 32 | 4.35 | 63 | 0.368 |
| | AO | 83 | 0 | 41 | 5.45 | 83 | 0.376 |
| | OA1 | 85 | 1 | 42 | 3.15 | 84 | 0.667 |
| | HDA | 68 | 1 | 33 | 4.25 | 67 | 0.388 |
| POLY875 XDT | OA10 | 57 | 1 | 28 | 2.70 | 56 | 0.519 |
| | AO | 72 | 6 | 33 | 8.00 | 66 | 0.206 |
| | OA1 | 82 | 0 | 41 | 6.85 | 82 | 0.299 |
| | HDA | 78 | 0 | 39 | 8.25 | 78 | 0.236 |

The table above summarizes the electro-optical properties of the composites prepared, based on the octanoic acid studies carried out, using Equation 1 for $T_{half}$, Equation 3 for contrast and Equation 4 for the $T/V$ ratio. The values for the switching voltage were obtained through the electro-optic response curves and converted to $V.\mu m^{-1}$.

## 4.2. The Ethylene Glycol

Ethylene glycol was tested to see if there were any improvements in the polymer dispersed liquid crystal systems because this is a molecule similar to the spacers of the monomers. It was also used this compound with the idea that it could turn the monomers that are more compact, more ductile, and therefore, more easy to work with.

The electro-optical results for the tri(ethylene glycol) dimethacrylate systems with liquid crystal and ethylene glycol are presented in Figure 4.37 and Figure 4.40 for different types of initiators.

For the thermal initiator the results obtained are described below and it can be seen that this composite is not appropriate for electro-optic applications, once it requires high voltages and even with high voltages its transmittance is not the most advantageous. It is thought that ethylene glycol might operate as an isolating layer surfacing the liquid crystal.

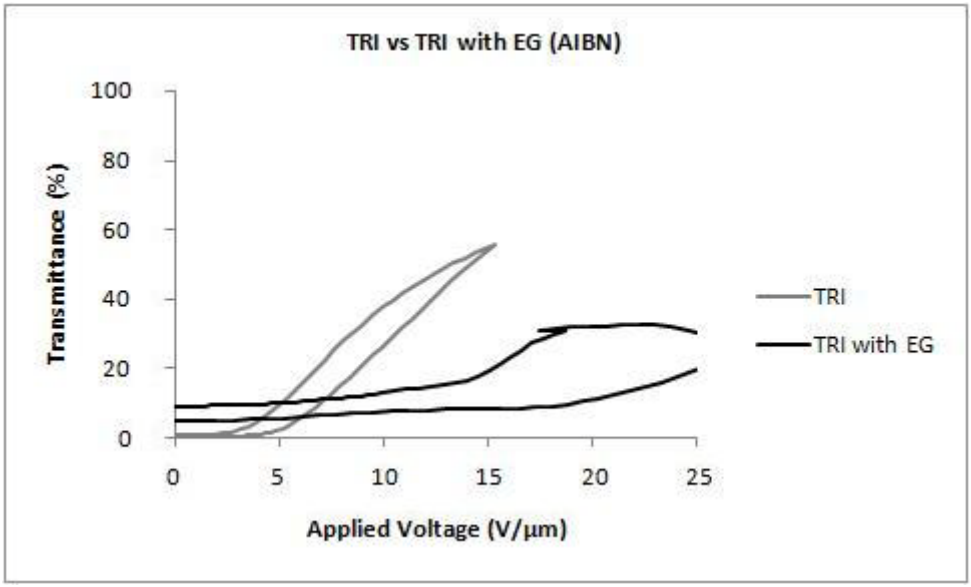


**Figure 4.37 – Electro-optic response of the system (TRI/AIBN/E7) with and without EG.**

The analysis of the textures over polarized light have shown that the sample is homogeneous in its totality, and as can be seen in Figure 4.38, the area where voltage is applied is in a brighter tonality.

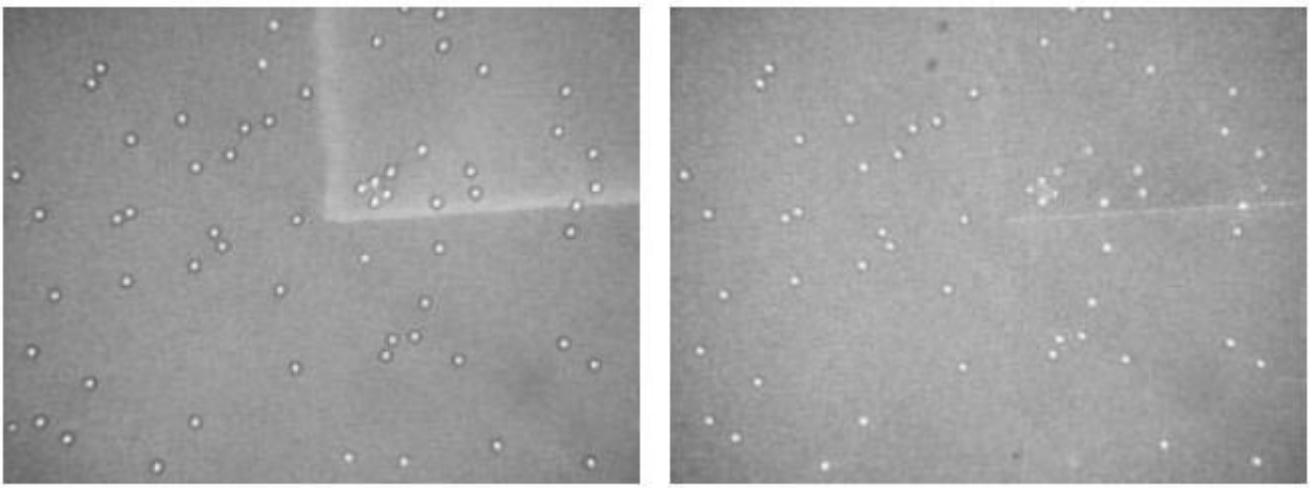

a) 10X aligned polarizers b) 10X crossed polarizers

**Figure 4.38 – POM micrograph for (TRI/AIBN/E7/EG)**

In order to relate the transmission-field response to the composite morphology, the system was analyzed by scanning electron microscopy. The respective image is shown in Figure 4.39. Since $E7$ was removed prior to microscope analysis, the dark areas in the micrographs are representative of the original liquid crystal domains. Two phase morphology is observed where the liquid crystal phase seems to become along the matrix through a porous open cell structure formed by the polymerization of the monomer, leading to the tunnel kind holes where the liquid crystal lies. In this case, besides the enormous amounts of beads, the electro-optic response does not apply. This reveals that, indeed, the ethylene glycol annuls the electro-optic responses of the composite in study.

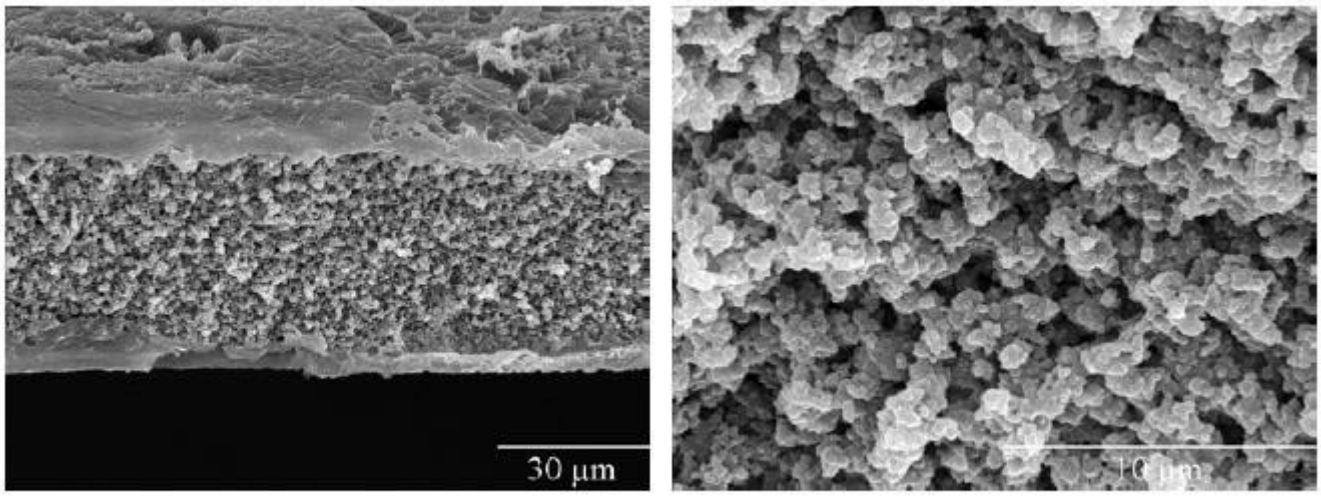


a) 800X side view b) 5000X side view

**Figure 4.39 – SEM morphology for (TRI/AIBN/E7/EG).**

The results for the photochemical initiator are described below and in this specific case, with the photochemical initiator, the additive seems to equal a typical electro-optic response curve for this monomer. Comparing it with the absence of additive, the transmittance is very similar, but the applied voltages are slightly higher.

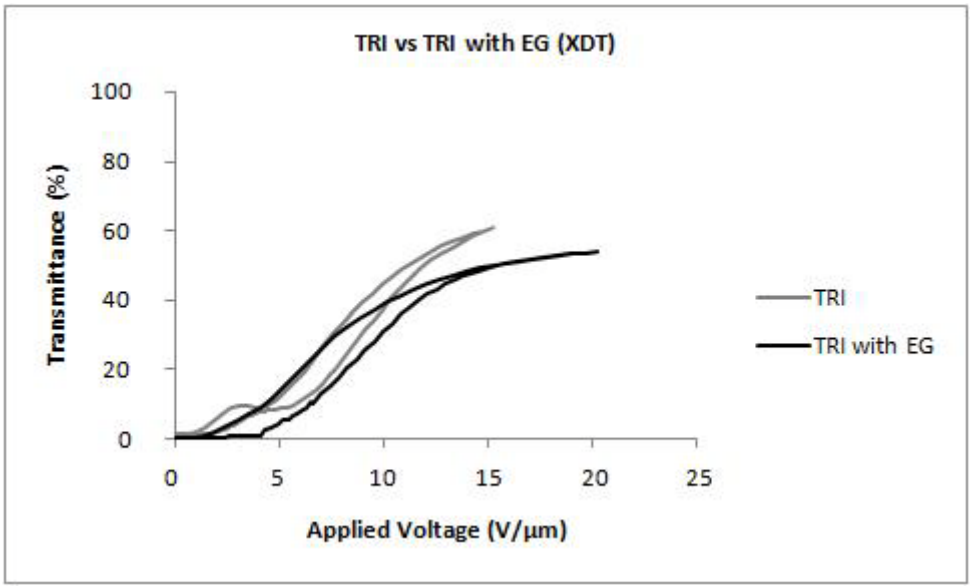


**Figure 4.40 – Electro-optic response of the system (TRI/XDT/E7) with and without EG.**

The analysis of the textures over polarized light have shown that the sample is homogeneous in its totality, and as can be seen in Figure 4.41, the area where voltage is applied is in a brighter tonality, but in this case, not so visible as with the previous sample, obtained with the thermal initiator.

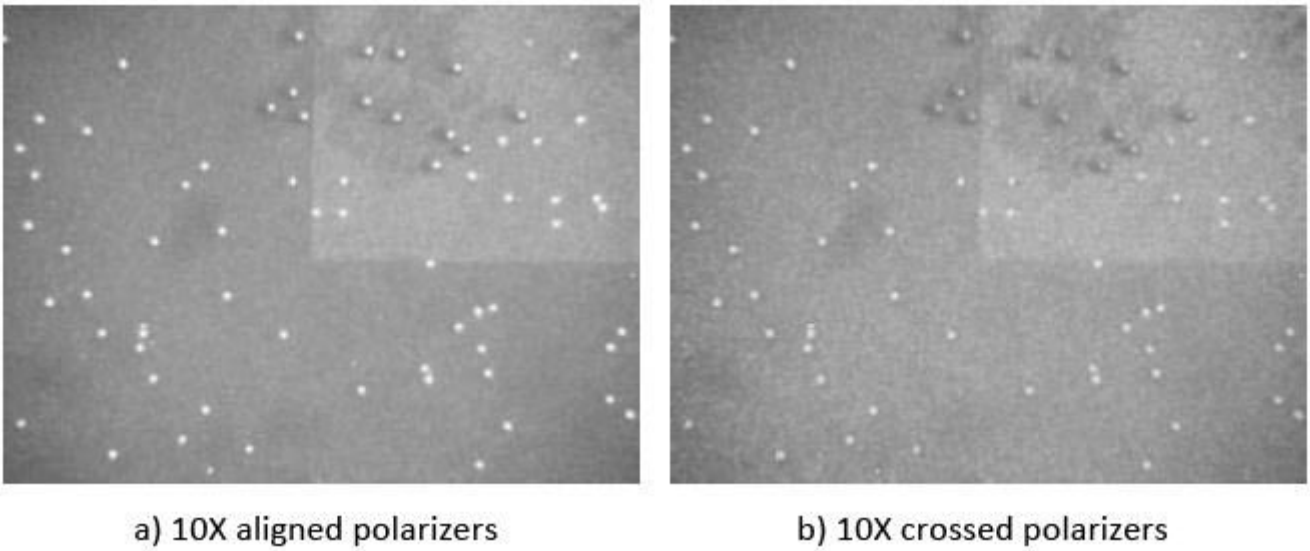


**Figure 4.41 – POM micrograph for (TRI/XDT/E7/EG)**

The electro-optical results for the poly(ethylene glycol) dimethacrylate systems with liquid crystal and ethylene glycol are presented in Figure 4.42 and Figure 4.45 for different types of initiators.

For the thermal initiator the results obtained are described below and it can be seen that in this case, no electro-optic response is obtained, no matter the voltages that are applied to the sample. Comparing this result with the one that does not contain the additive, it is clearly seen that this system does not operate with the presence of ethylene glycol.

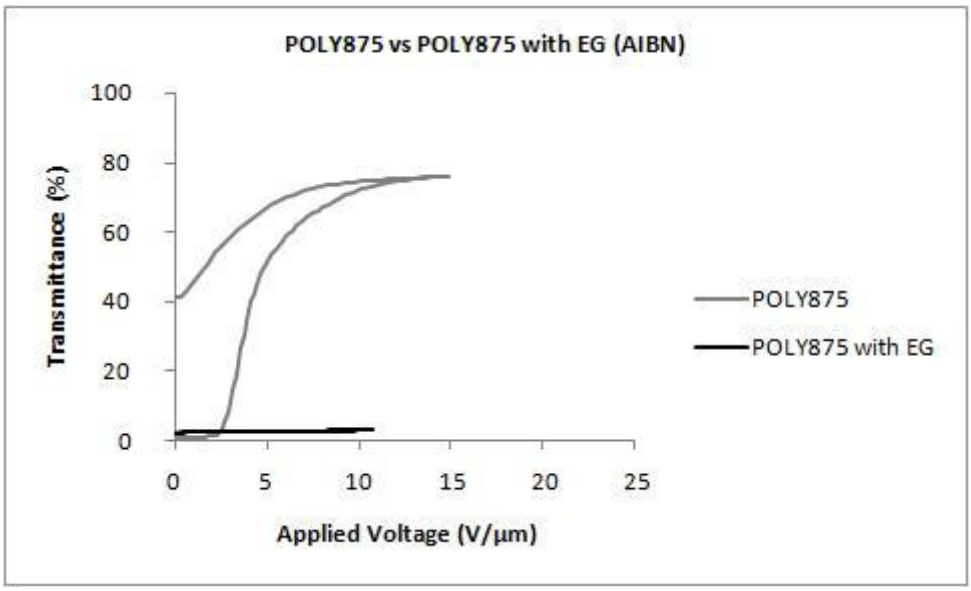


**Figure 4.42 – Electro-optic response of the system (POLY875/AIBN/E7/EG).**

The analysis of the textures over polarized light have shown that the sample has very defects in its totality, and as can be seen in Figure 4.43, the sample is homogeneous in its integrity, but the middle square where voltages are applied is multicolored, due to the refractive indices of the sample. When observing polarized light under aligned polarizers, the square is bright, but when observed with crossed polarizers, the bright zones become multicolored. Conjugating the electro-optic response curve and the polarized light images, this may be the reason for the malfunction of the electro-optic properties of the composite.

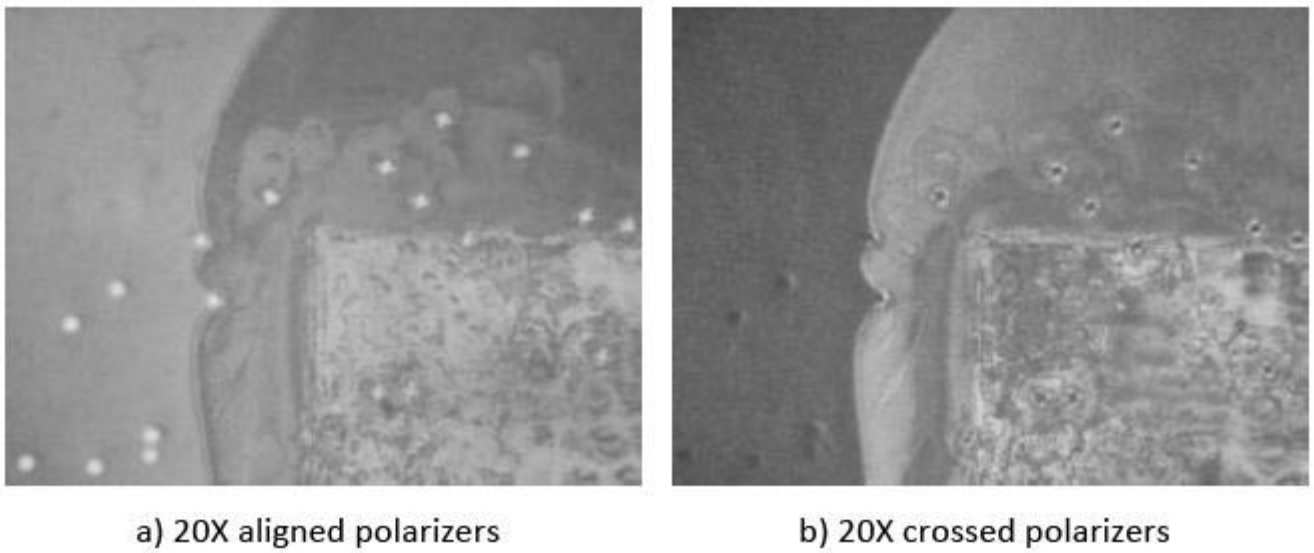


**Figure 4.43 – POM micrograph for (POLY875/AIBN/E7/EG)**

Figure 4.44 shows the scanning electron microscopy micrograph for this system. With this monomer, smaller polymer beads are obtained in comparison with the previous monomer. This inferior size can be an indication of higher cross-linking polymerization leading to a higher network density. The dark areas are of smaller size relatively to the other monomer in study, indicating that liquid crystal domains are of inferior dimensions.

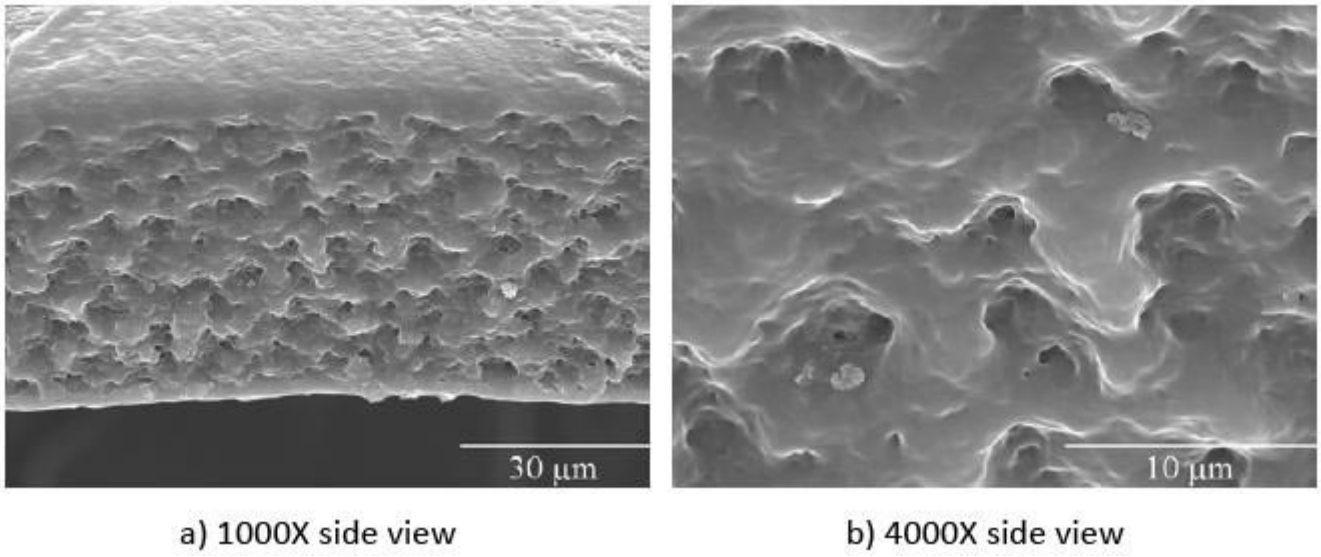


**Figure 4.44 – SEM morphology for (POLY875/AIBN/E7/EG).**

The results for the photochemical initiator are described below. Similarly to the previous sample, this composite does not present any kind of electro-optic response and comparing it with the same monomer but without the presence of the additive, it is obvious that the ethylene glycol does not bring any improvement to these systems.

As in the previous monomer, this additive blocks all the electro-optic properties of the composites.

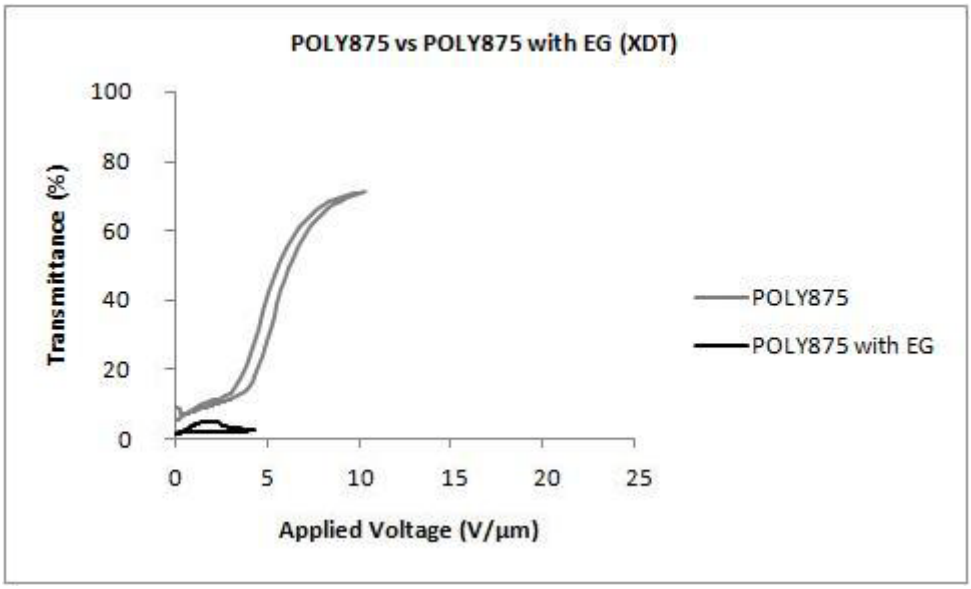


**Figure 4.45 – Electro-optic response of the system (POLY875/XDT/E7) with and without EG.**

The analysis of the textures over polarized light have shown that the sample presents liquid crystal domains in its totality and even in the center where voltage is applied no differences can be noticed, as showed in Figure 4.46. Meanwhile and according to the other samples obtained with ethylene glycol, several spots are also observed among diverse areas of the composite.

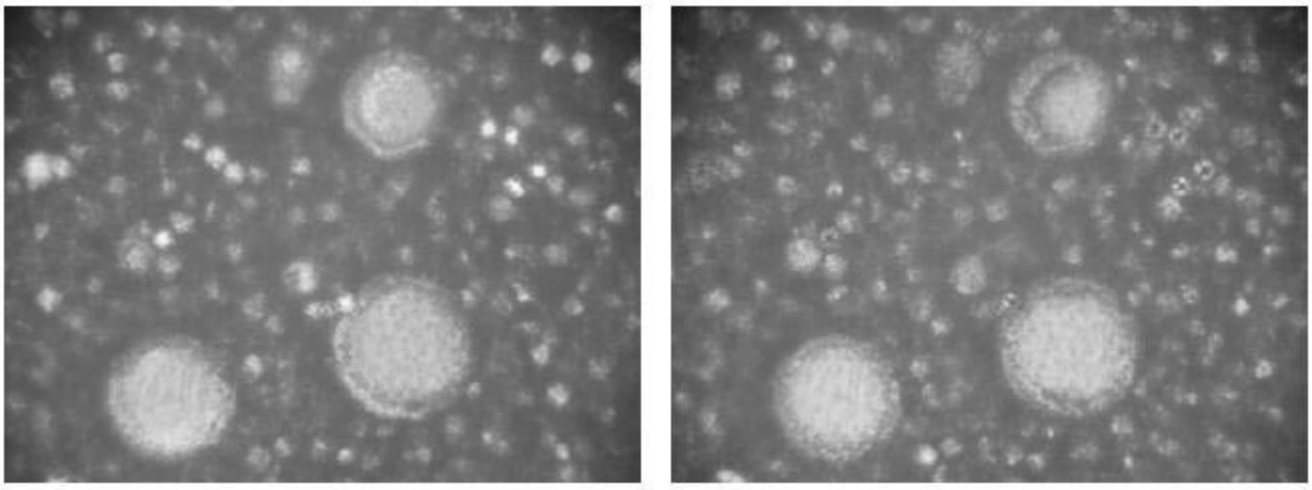


**Figure 4.46 – POM micrograph for (POLY875/XDT/E7/EG)**

A differential scanning calorimetry analysis was made to see if the thermodynamic properties of the liquid crystal were altered in the presence of this additive, so that

could be the reason for the null electro-optic response of these systems. But the analysis revealed that the liquid crystal maintains its properties, that is, the glass transition remains at $T_g = -64$ ℃, the nematic-isotropic temperature remains at $T_{N\rightarrow I} = 57$ ℃ and the same is verified for the opposite effect. This indicates that the main interaction for the addition of ethylene glycol is with the polymer instead of the liquid crystal, as it would be expected, since the spacer of the monomer is constituted by several ethylene glycol molecules.

## 4.3. The Triton X-100

To initiate the test of the surfactants, three surfactants were chosen. The first one is the triton X-100, a nonionic surfactant which has a hydrophilic polyethylene oxide group and a hydrocarbon hydrophobic group, an octylphenyl group. Besides it is very viscous at room temperature, and when stored it is noticed, when mixed, the phase separation between the liquid crystal and the additive, it is soluble in ethylene glycol, the main chain of the monomers in use.

The electro-optical results for the tri(ethylene glycol) dimethacrylate systems with liquid crystal and triton X-100 are presented in Figure 4.47 and Figure 4.50 for different types of initiators.

For the thermal initiator the results obtained are described below and it can be seen that a light permanent memory effect occur in the presence of this additive. Besides transmittance oscillates a bit, the most important is the transmittance at which the system switches from opaque to transparent and in that time, transmittance is very reasonable and at very low applied voltages. Comparing this result with the results done in the analogous work (Maiau, 2009), the effect of triton X-100 at an electro-optic level improve in such a way the performance of the composite, reducing the applied voltages largely.

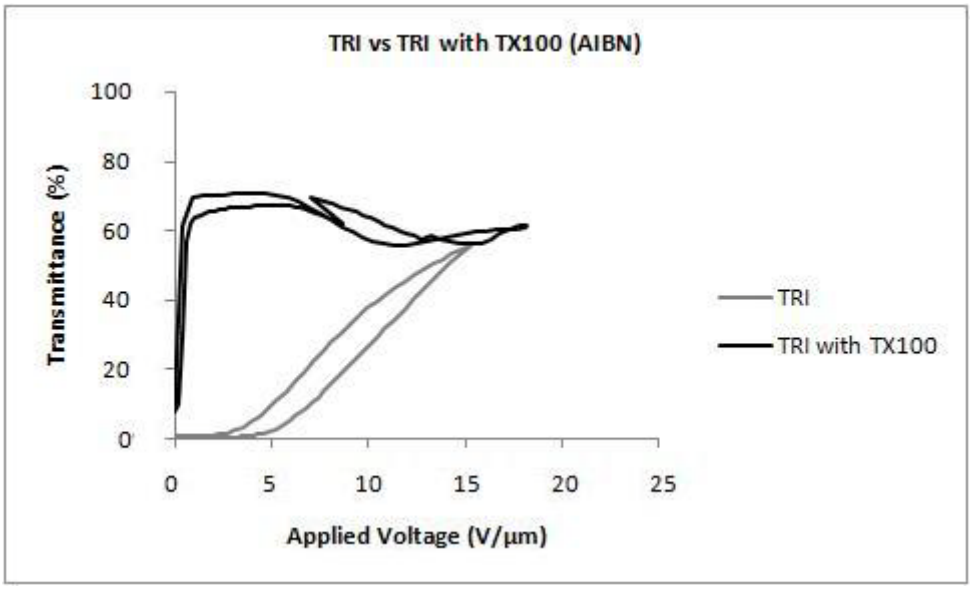


**Figure 4.47 – Electro-optic response of the system (TRI/AIBN/E7) with and without TX100.**

The analysis of the textures over polarized light have shown that the sample is homogeneous in its totality, and as can be seen in Figure 4.48, the area where voltage is applied is in a brighter tonality.

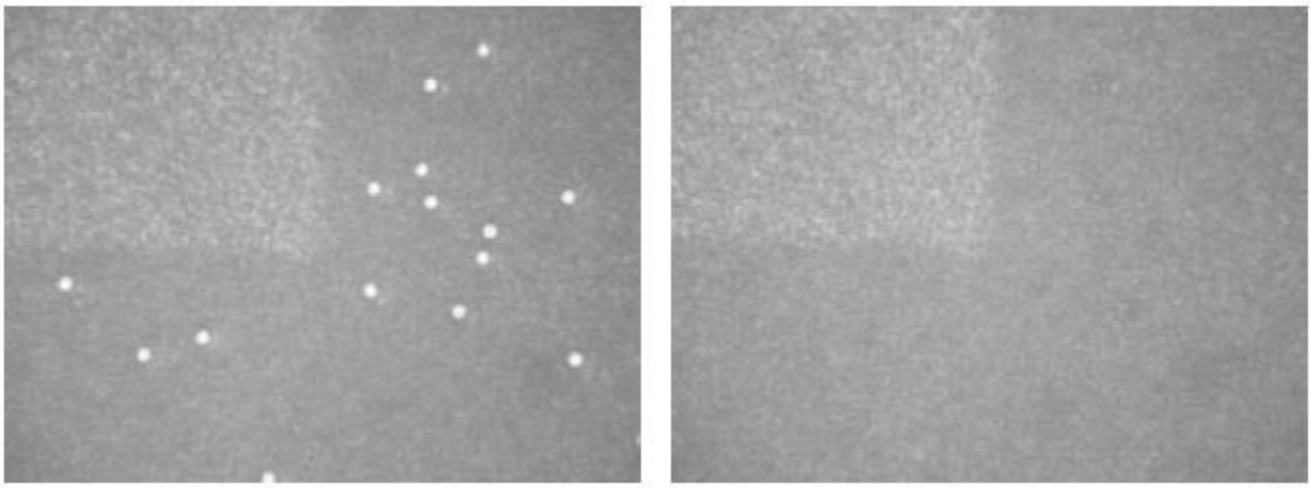


**Figure 4.48 – POM micrograph for (TRI/AIBN/E7/TX100)**

In order to relate the transmission-field response to the composite morphology, the system was analyzed by scanning electron microscopy. The respective image is shown in Figure 4.49. Since $E7$ was removed prior to microscope analysis, the dark areas in the micrographs are representative of the original liquid crystal domains. Two phase morphology is observed where the liquid crystal phase seems to become inside a spongy open cell structure formed by the polymerization of the monomer, leading to

the tunnel kind holes where the liquid crystal is set. The higher magnification shows quite well this tunnels and the raised-relief structure of the composite.

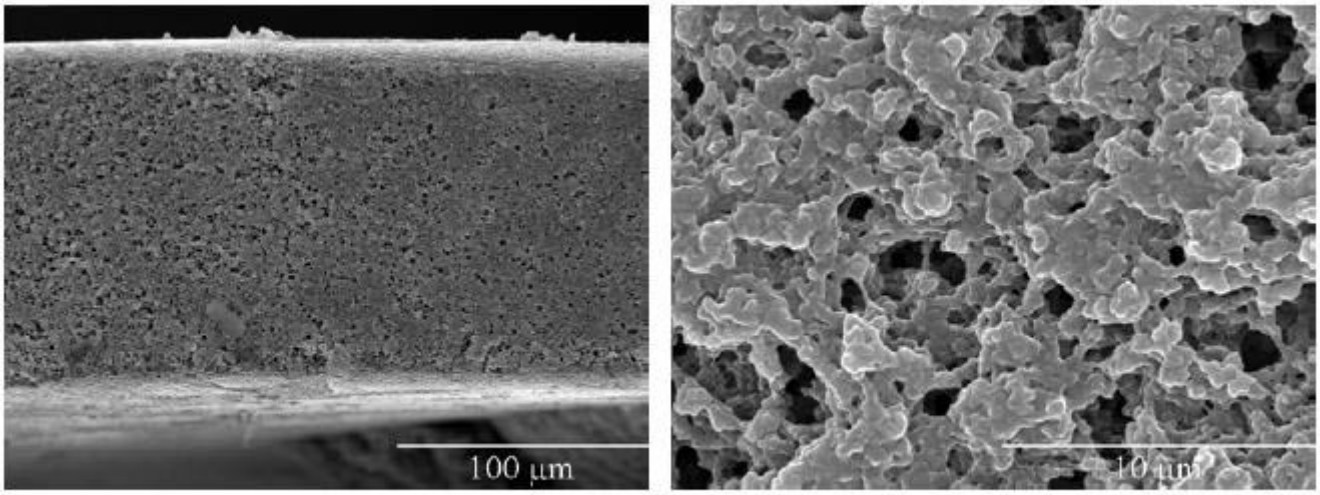


**Figure 4.49 – SEM morphology for (TRI/AIBN/E7/TX100).**

The results for the photochemical initiator are described below and in this case, barely any permanent memory effects are obtained. Transmittance is very similar with the sample prepared thermally and applied voltages are quite the same. When comparing the presence or absence of additive in this composite it can be seen that the applied voltages are highly reduced, but the transmittance maintains its coefficient values.

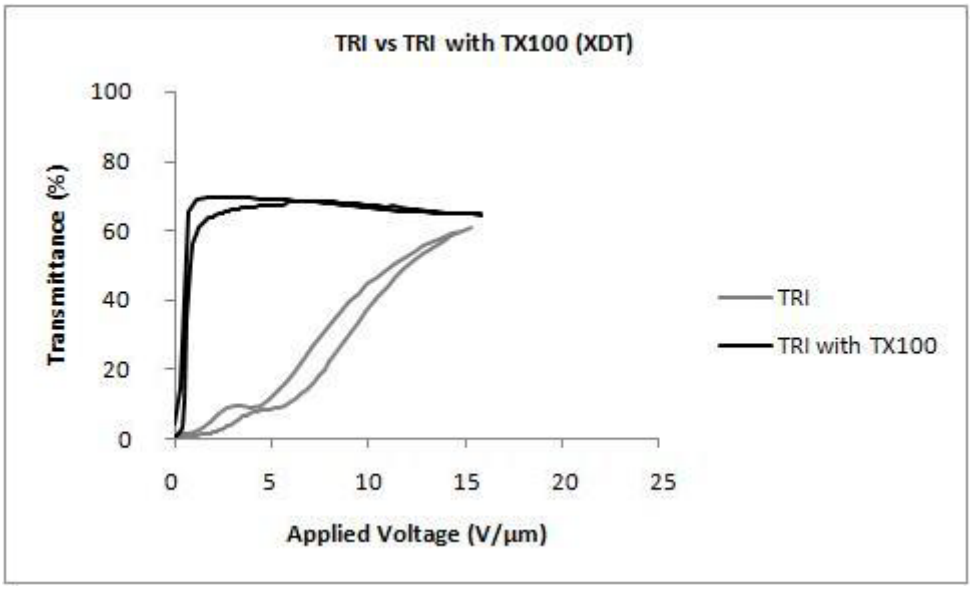


**Figure 4.50 – Electro-optic response of the system (TRI/XDT/E7) with and without TX100.**

The analysis of the textures over polarized light have shown that the sample is homogeneous in its totality, and as can be seen in Figure 4.51, the area where voltage

is applied is in a brighter tonality, but in this case, this time, more visible when compared with the previous sample, obtained with the thermal initiator.

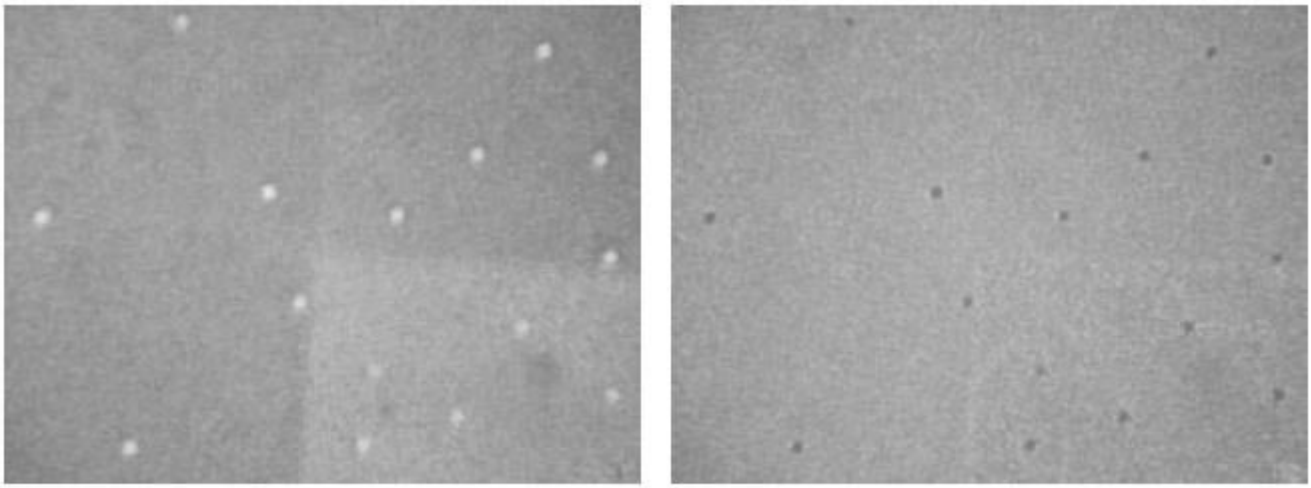

a) 20X aligned polarizers b) 20X crossed polarizers

**Figure 4.51 – POM micrograph for (TRI/XDT/E7/TX100)**

The electro-optical results for the poly(ethylene glycol) dimethacrylate systems with liquid crystal and triton X-100 are presented in Figure 4.52 and Figure 4.55 for different types of initiators.

For the thermal initiator the results obtained are described below and it can be seen that with this additive and with thermal polymerizations, slight permanent memory effects are present. The maximum transmittance is very high and besides applied voltages are slightly higher than the obtained with the other monomer, they still are considerably low. Practically, no permanent memory effects are observed when comparing the sample with the one that does not contain the additive, but transmittances and applied voltages are higher and lower, respectively.

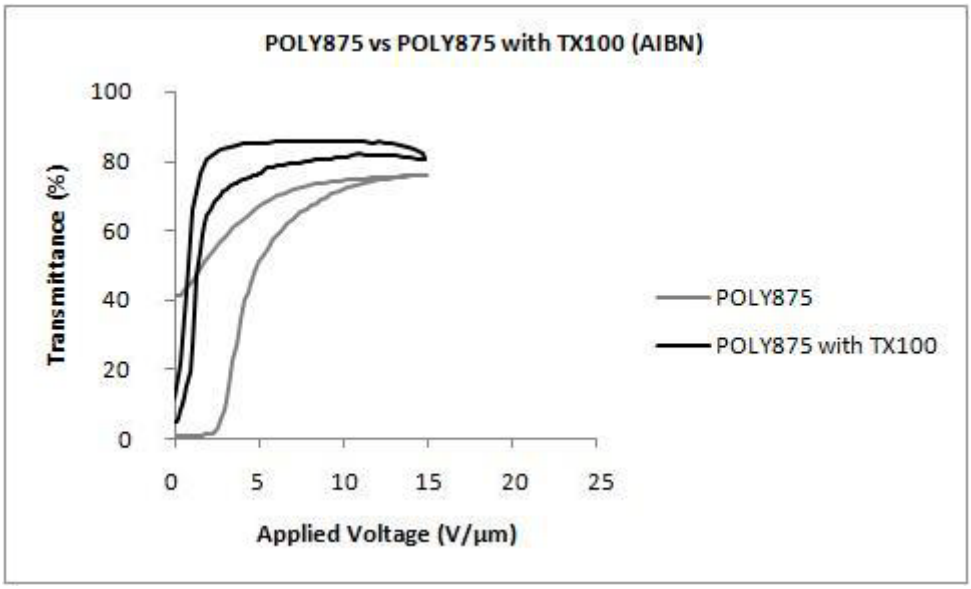


**Figure 4.52 – Electro-optic response of the system (POLY875/AIBN/E7) with and without TX100.**

The analysis of the textures over polarized light have shown that the sample is homogeneous in its totality, and as can be seen in Figure 4.53, the area where voltage is applied is in a brighter tonality.

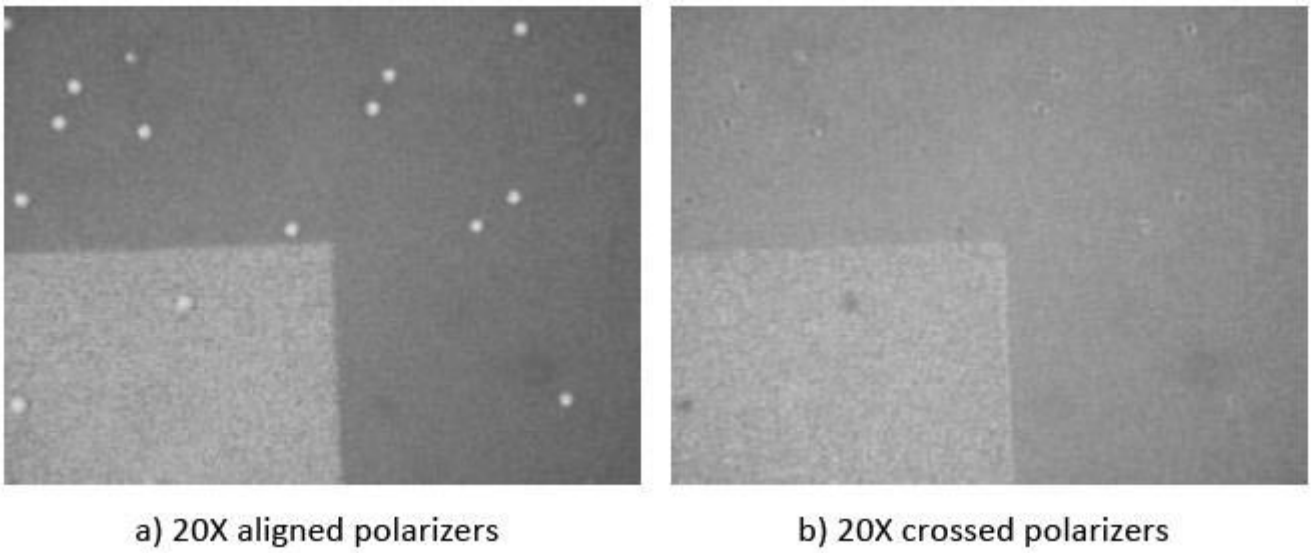


**Figure 4.53 – POM micrograph for (POLY875/AIBN/E7/TX100)**

Figure 4.54 shows the scanning electron microscopy micrograph for this system. No polymer beads are observed in contrast with the previous monomer. This absence can be an indication of higher cross-linking polymerization leading to a higher network density. Once the applied voltages are lower than the ones obtained with the other monomer, it was expected to observe larger dark areas and polymer beads.

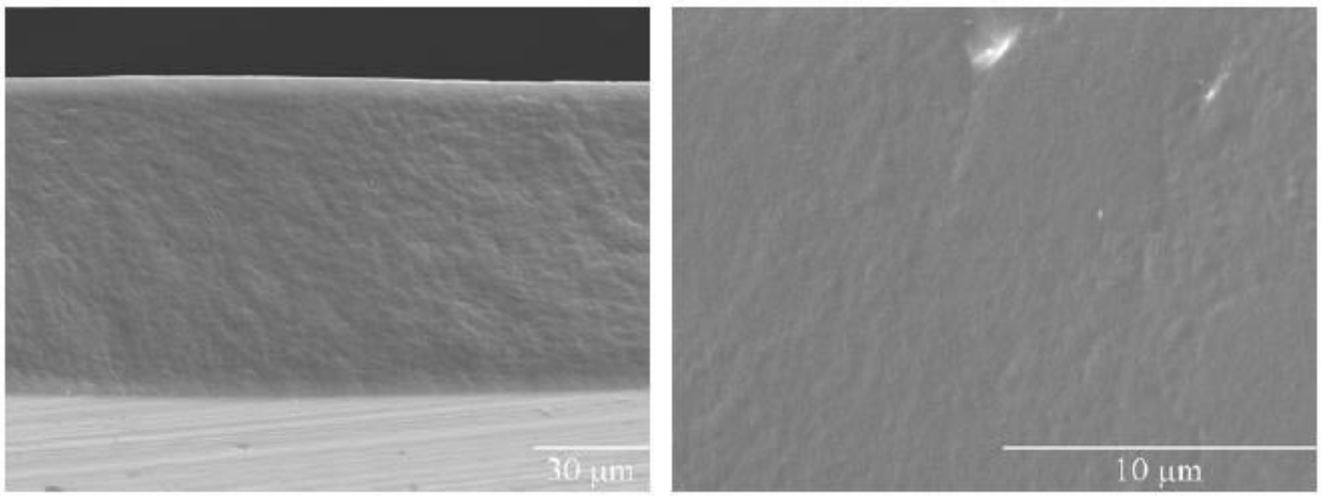


**Figure 4.54 – SEM morphology for (POLY875/AIBN/E7/TX100).**

The results for the photochemical initiator are described below and the response is similar compared with the previous monomer. In this case, the permanent memory effects are practically inexistent. Meanwhile, this composite presents a unique characteristic that is its absence of hysteresis. When voltages are applied the liquid crystals align themselves and when voltages are removed they misalign in the exact same orientation they have taken to align. Once again, the transmittance is very similar and the applied voltages are reduced comparing with the composite without the presence of the surfactant.

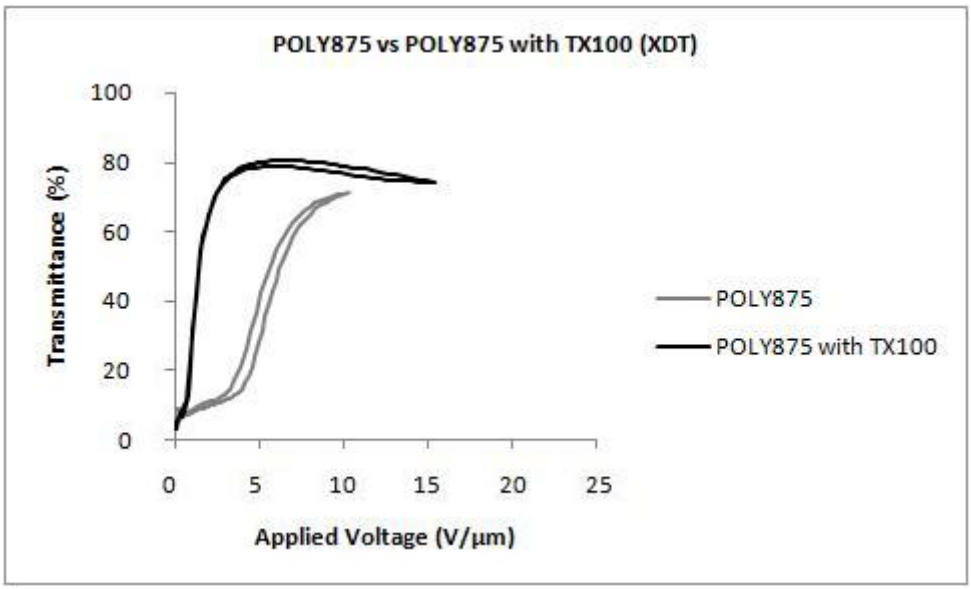


**Figure 4.55 – Electro-optic response of the system (POLY875/XDT/E7) with and without TX100.**

The analysis of the textures over polarized light have shown that the sample presents liquid crystal domains in its totality and even in the center where voltage is applied no differences can be noticed, as showed in Figure 4.56. This is in agreement with what was expected with this monomer, that is, many aligned columns of liquid crystal-holes and a few round domains are displaced all over the sample.

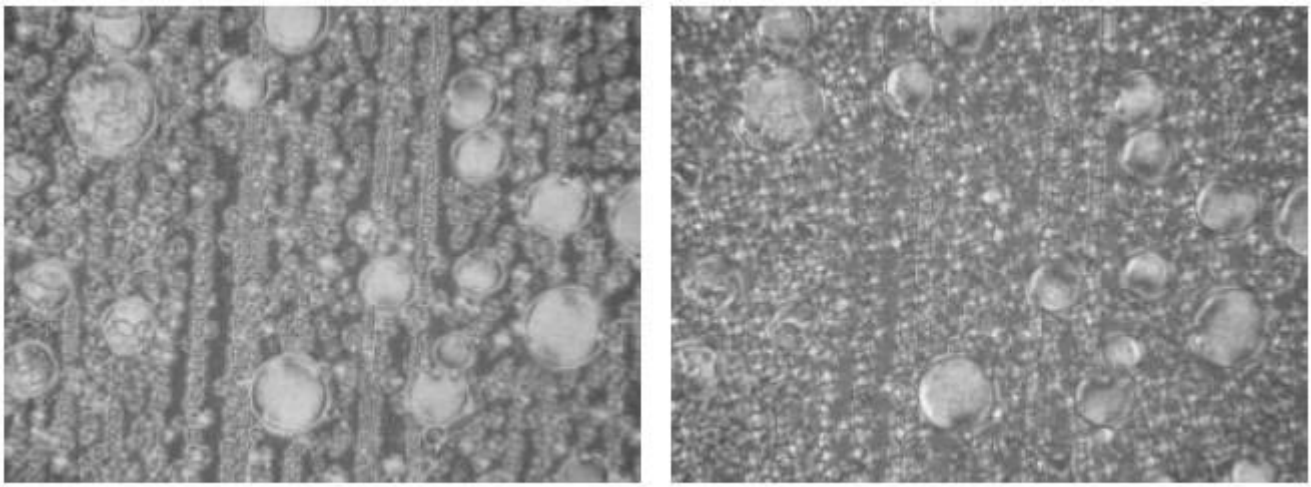


**Figure 4.56 – POM micrograph for (POLY875/XDT/E7/TX100)**

## 4.4. The Cetyl Trimethyl Ammonium Bromide

Another surfactant used was the cetyl trimethyl ammonium bromide, this time, a cationic surfactant. This molecule has a tail of sixteen carbon atoms attached to an ammonia group. As any surfactant, it forms micelles in aqueous solutions.

The electro-optical results for the tri(ethylene glycol) dimethacrylate systems with liquid crystal and cetyl trimethyl ammonium bromide are presented in Figure 4.57 and Figure 4.60 for different types of initiators.

For the thermal initiator the results obtained are described below and it can be seen that no permanent memory effects occur in this kind of monomer with this additive and that the electro-optic response is very similar to the same composite without the presence of the additive. Comparing the electro-optic responses of the systems containing and not containing the additive, they are very similar, but the presence of the additive enhances, a bit, this response.

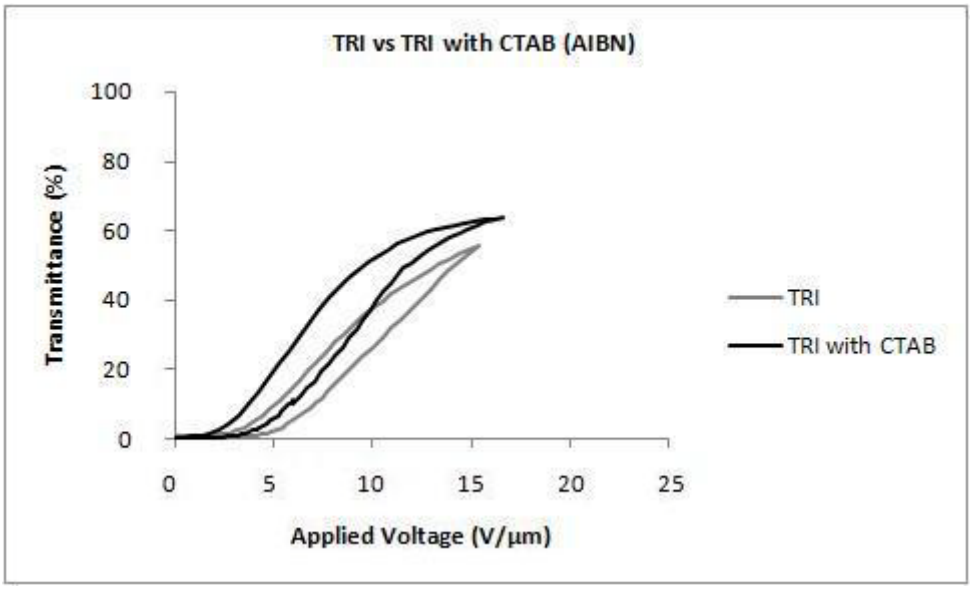


**Figure 4.57 – Electro-optic response of the system (TRI/AIBN/E7) with and without CTAB.**

The analysis of the textures over polarized light have shown that the sample is homogeneous in its totality, and as can be seen in Figure 4.58, the area where voltage is applied is in a brighter tonality.

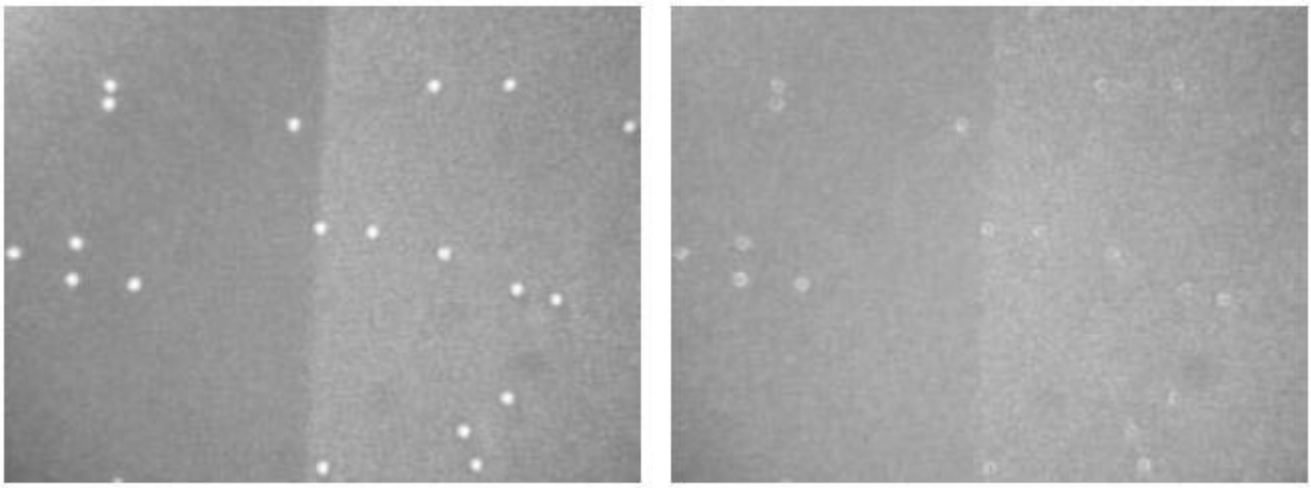


**Figure 4.58 – POM micrograph for (TRI/AIBN/E7/CTAB)**

In order to relate the transmission-field response to the composite morphology, the system was analyzed by scanning electron microscopy. The respective image is shown in Figure 4.59. Since $E7$ was removed prior to microscope analysis, the dark areas in the micrographs are representative of the original liquid crystal domains. In this case, the two phase morphology is barely observed. This might be due to the additive long chain length, in agreement with the hexadecanoic acid results.

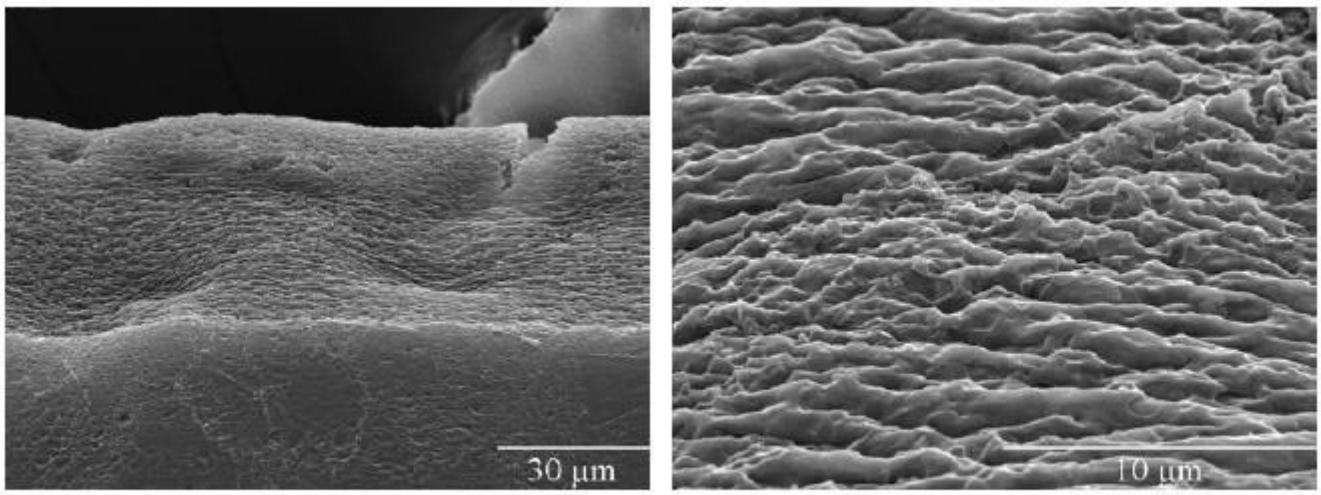


**Figure 4.59 – SEM morphology for (TRI/AIBN/E7/CTAB).**

The results for the photochemical initiator are described below and, once more, in this kind of monomer with this additive, no permanent memory effects are obtained. This time, transmittance has maintained its level, besides the difference in the polymerization type, but applied voltages have decreased. In this case, when comparing both responses, the presence of cetyl trimethyl ammonium bromide affects the applied voltages by decreasing them, as it would be expected in the presence of a surfactant.

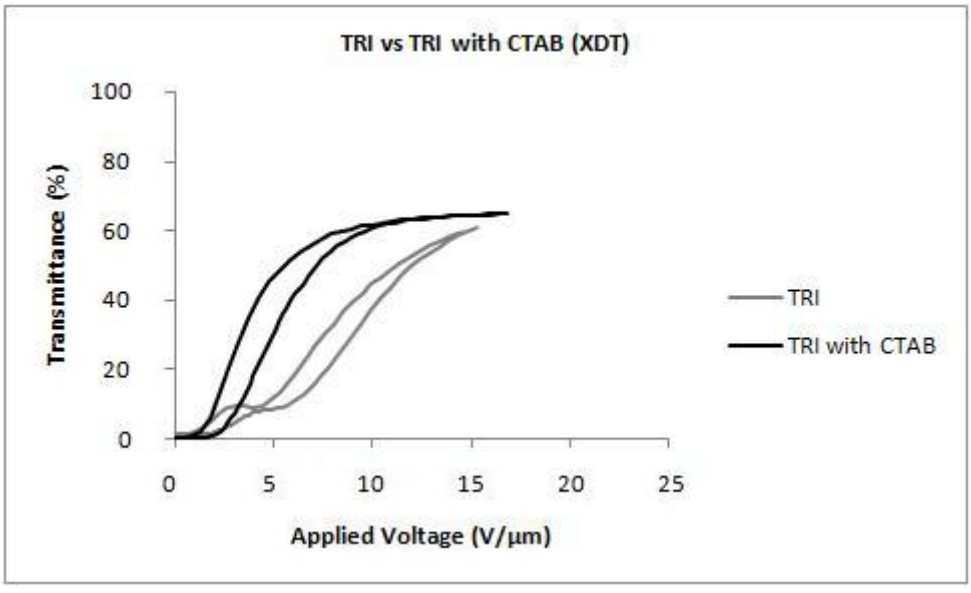


**Figure 4.60 – Electro-optic response of the system (TRI/XDT/E7) with and without CTAB.**

The analysis of the textures over polarized light have shown that the sample is homogeneous in its totality, and as can be seen in Figure 4.61, the area where voltage

is applied is in a brighter tonality, but in this case, not so visible as with the previous sample, obtained with the thermal initiator.

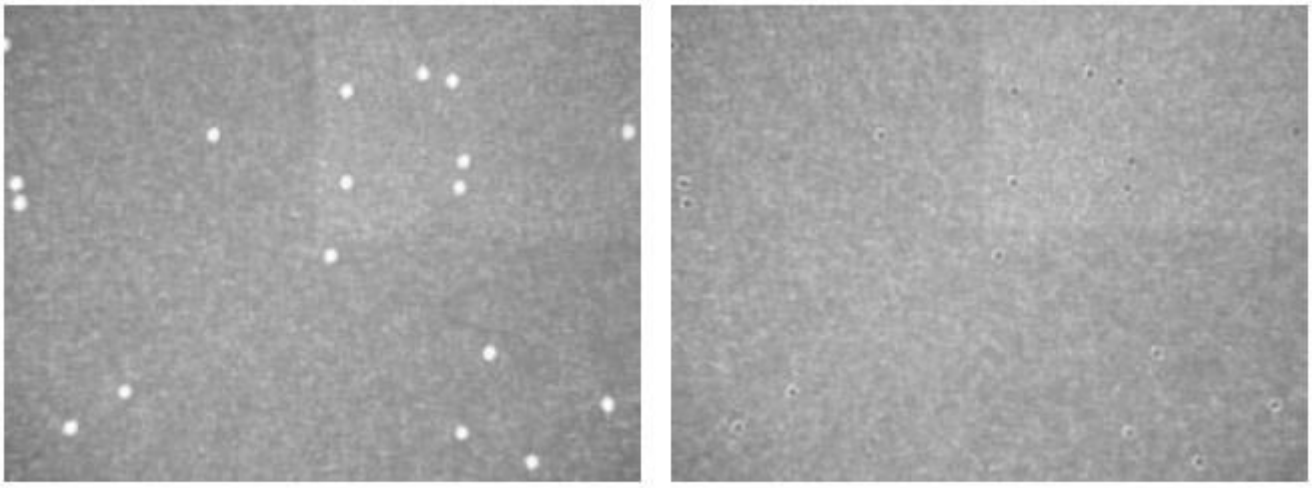

a) 20X aligned polarizers b) 20X crossed polarizers

**Figure 4.61 – POM micrograph for (TRI/XDT/E7/CTAB)**

The electro-optical results for the poly(ethylene glycol) dimethacrylate systems with liquid crystal and cetyl trimethyl ammonium bromide are presented in Figure 4.62 and Figure 4.65 for different types of initiators.

For the thermal initiator the results obtained are described below and it can be seen that in this type of monomer with the referred additive, permanent memory effects are present, although this effect is diminished when compared with the same composite without an additive. With this monomer, the results are very similar when observing the transmittances of the composite containing and not containing the additive, but quite different when looking for applied voltages, which are decreased, taking along with them the decreasing of the permanent memory effect.

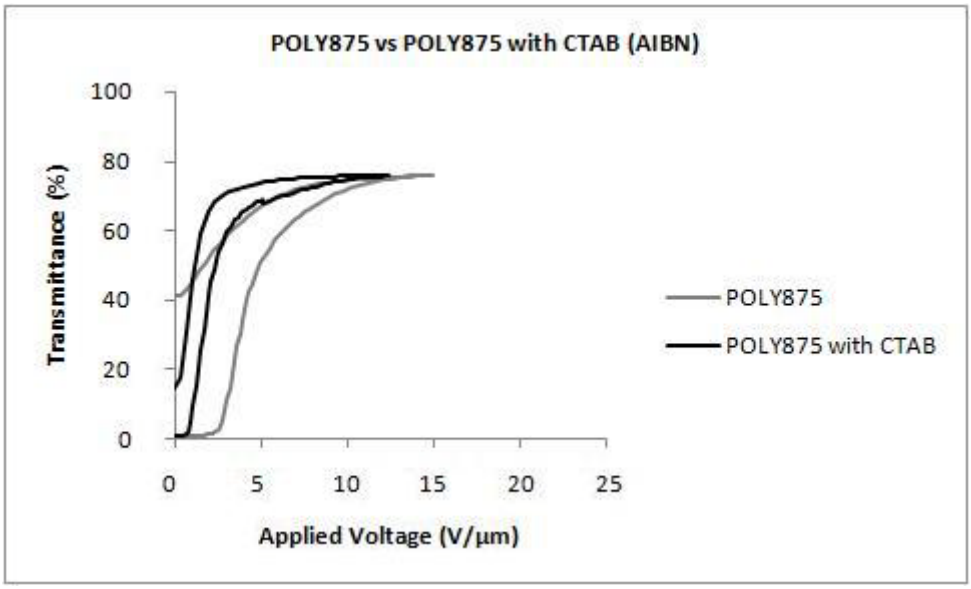


**Figure 4.62 – Electro-optic response of the system (POLY875/AIBN/E7) with and without CTAB.**

The analysis of the textures over polarized light have shown that the sample is homogeneous in its totality, and as can be seen in Figure 4.63, the area where voltage is applied is in a total different tonality, representing the permanent memory effects, according to the electro-optical response illustration. Light scatters through the sample, because the orientation of the liquid crystals in that centre is oriented into one direction.

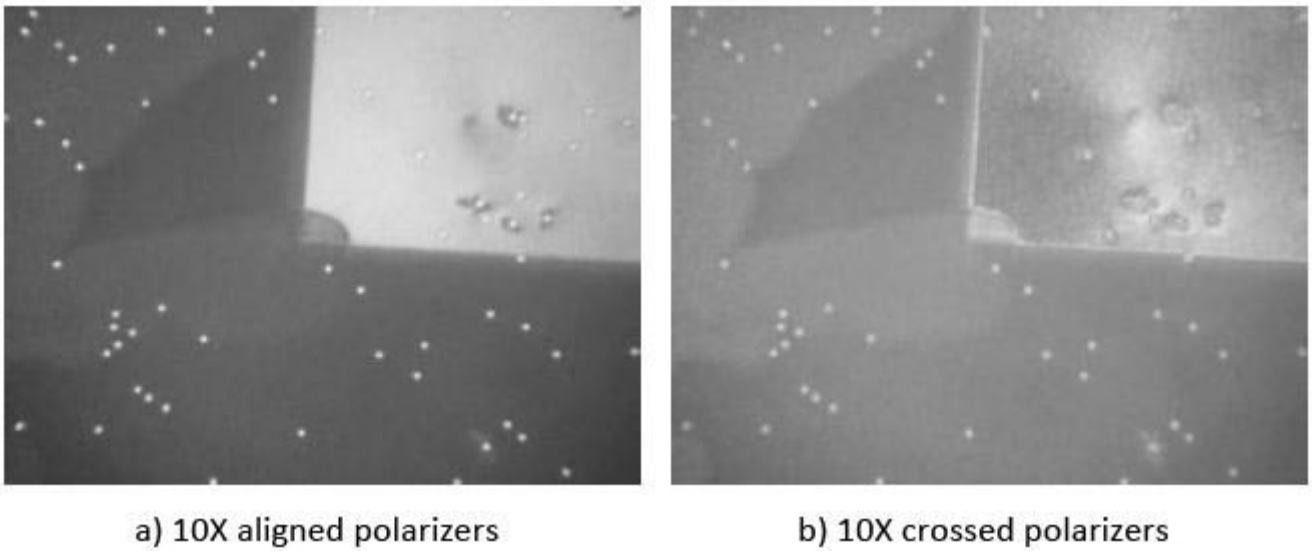


**Figure 4.63 – POM micrograph for (POLY875/AIBN/E7/CTAB)**

Figure 4.64 shows the scanning electron microscopy micrograph for this system. With this monomer, higher polymer beads are obtained in comparison with the previous monomer, besides its amount is very dispersed throughout the sample. These holes of

higher sizes can be linked to the reduced voltages required for the system operation comparing it with the previous result. These holes are of higher size relatively to the other monomer in study, indicating that liquid crystal domains are of superior dimensions and this justifies the need for less applied fields to achieve the transparent state in the composite.

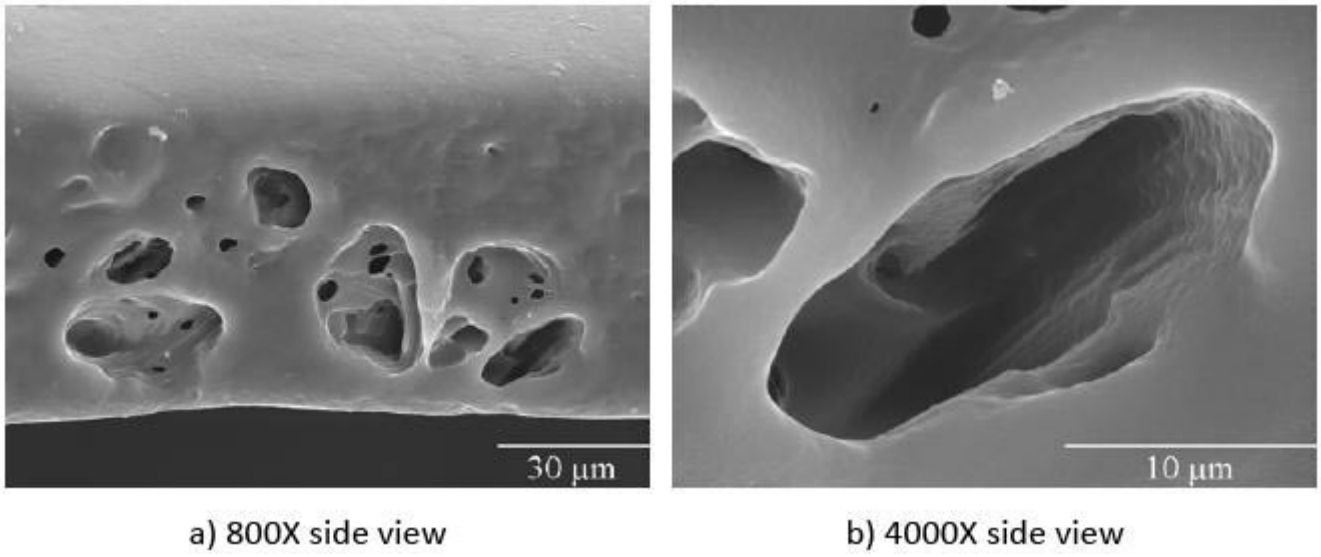


**Figure 4.64 – SEM morphology for (POLY875/AIBN/E7/CTAB).**

The results for the photochemical initiator are described below and, besides it was thought that permanent memory effects could occur, because the monomer is exactly the same, they do not. This can be explained due to the type of polymerization where polymerization times are lower. The comparison between the systems containing and not containing the additive shows that the electro-optic results are similar.

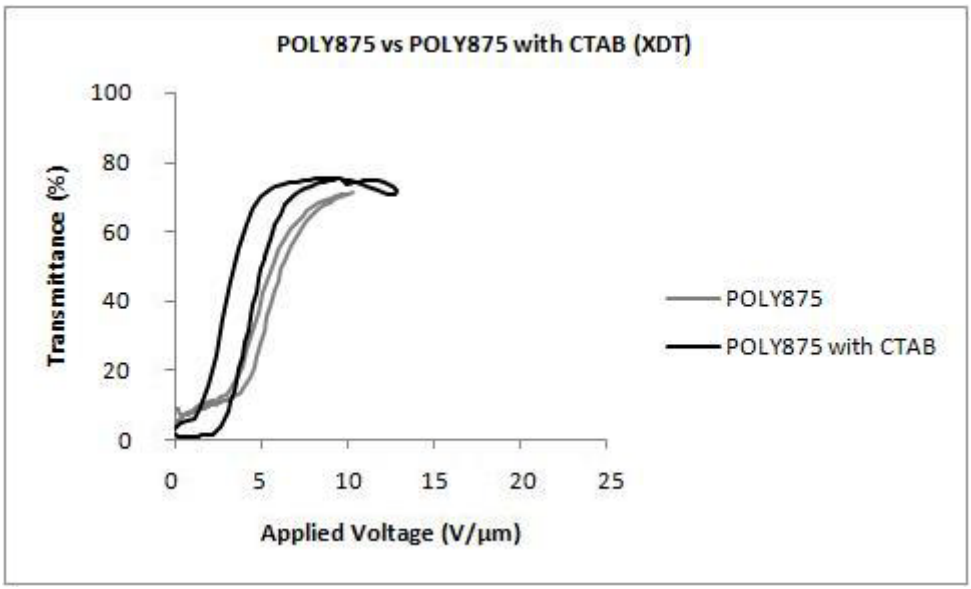


**Figure 4.65 – Electro-optic response of the system (POLY875/XDT/E7) with and without CTAB.**

The analysis of the textures over polarized light have shown that the sample presents liquid crystal domains in its totality and even in the center where voltage is applied, only a slight difference can be noticed, as showed in Figure 4.66.

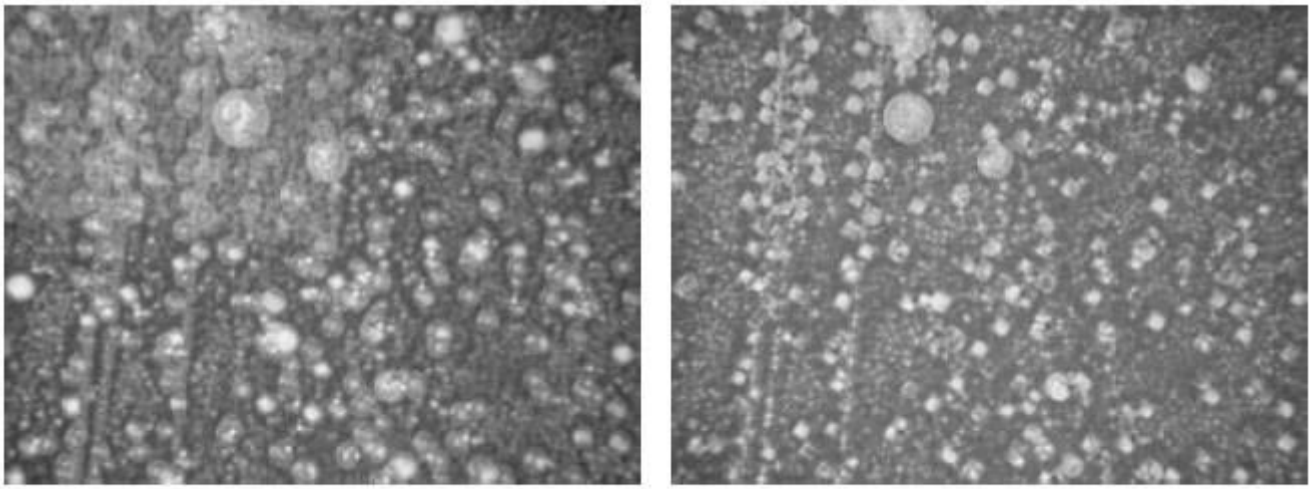


**Figure 4.66 – POM micrograph for (POLY875/XDT/E7/CTAB)**

## 4.5. The Sodium Dodecyl Sulfate

Yet a third surfactant was used, the sodium dodecyl sulfate, an anionic surfactant. This molecule has a tail of twelve carbon atoms attached to a sulfate group, giving the molecule the amphiphilic properties required to form micelles.

The electro-optical results for the tri(ethylene glycol) dimethacrylate systems with liquid crystal and sodium dodecyl sulfate are presented in Figure 4.67 and Figure 4.70 for different types of initiators.

For the thermal initiator the results obtained are described below and it can be seen that a light permanent memory effect is verified, but the transmittance obtained and the applied voltages are not optimal. This is observed in the comparison with and without the addition of sodium dodecyl sulfate, because results obtained without the addition of it are better than the ones obtained with the presence of the additive.

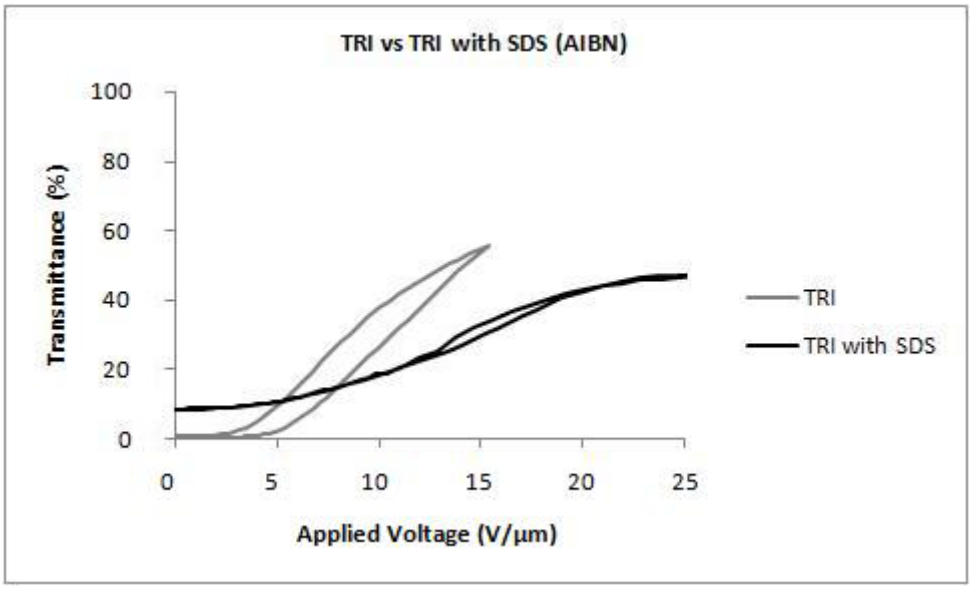


**Figure 4.67 – Electro-optic response of the system (TRI/AIBN/E7) with and without SDS.**

The analysis of the textures over polarized light have shown that the sample is homogeneous in its totality, and as can be seen in Figure 4.68, the area where voltage is applied is in a brighter tonality, besides that difference is not quite noticed.

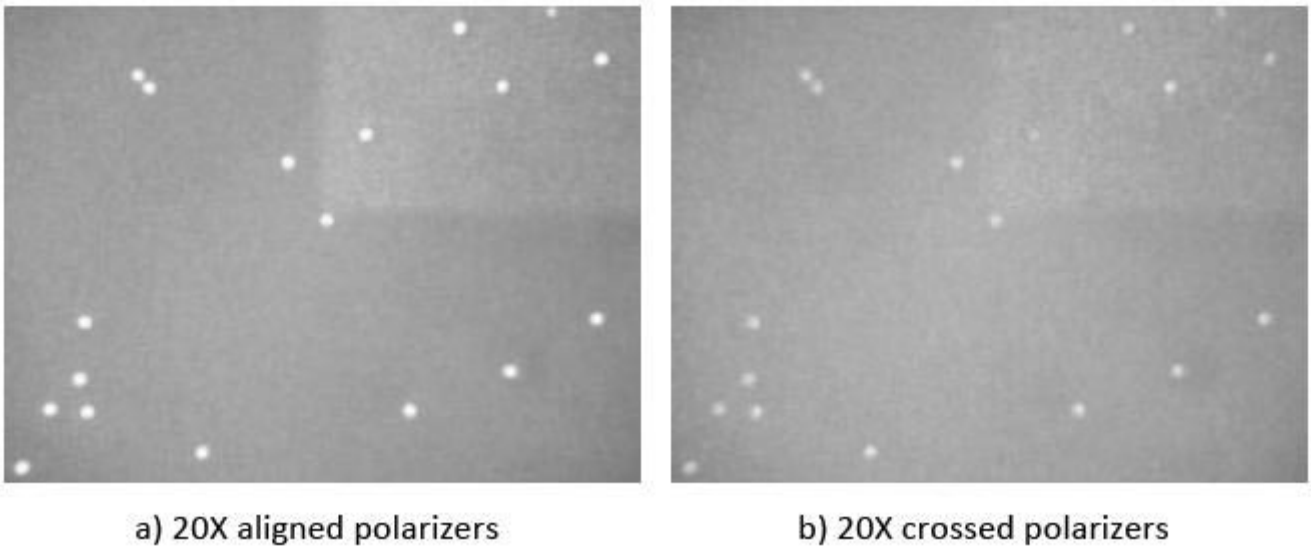


**Figure 4.68 – POM micrograph for (TRI/AIBN/E7/SDS)**

In order to relate the transmission-field response to the composite morphology, the system was analyzed by scanning electron microscopy. The respective image is shown in Figure 4.69. Since $E7$ was removed prior to microscope analysis, the dark areas in the micrographs are representative of the original liquid crystal domains. In this case, the two phase morphology is hard to be observed and the polymer network seems to

be very dense. This might be due to the additive long chain length, in agreement with the hexadecanoic acid results.

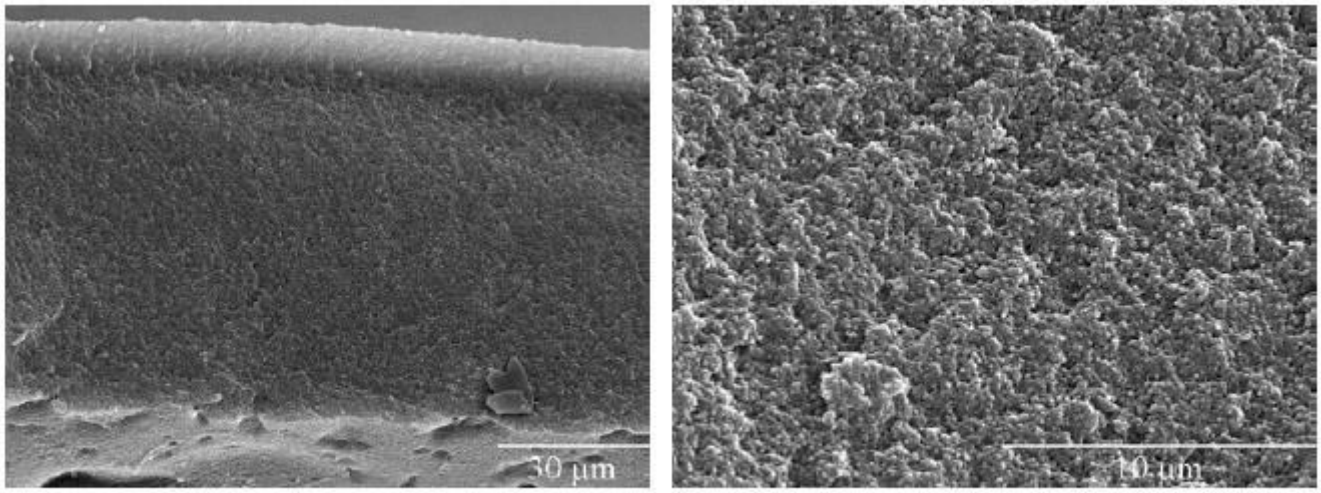


**Figure 4.69 – SEM morphology for (TRI/AIBN/E7/SDS).**

The results for the photochemical initiator are described below and, once more, in this kind of monomer with the respective additive, no permanent memory effects are obtained. With this type of polymerization applied voltages and transmittance are better than the ones observed within the thermal sample. The comparison of the two systems shows that the electro-optic results are very similar.

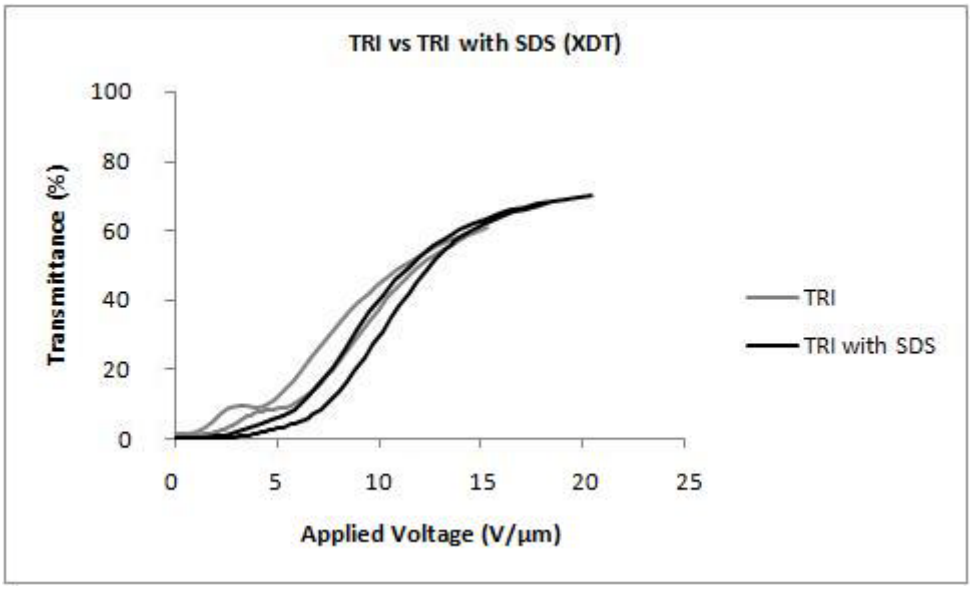


**Figure 4.70 – Electro-optic response of the system (TRI/XDT/E7) with and without SDS.**

The analysis of the textures over polarized light have shown that the sample is homogeneous in its totality, and as can be seen in Figure 4.71, the area where voltage

is applied is in a, barely seen, brighter tonality, but in this case, not so visible as with the previous sample, obtained with the thermal initiator.

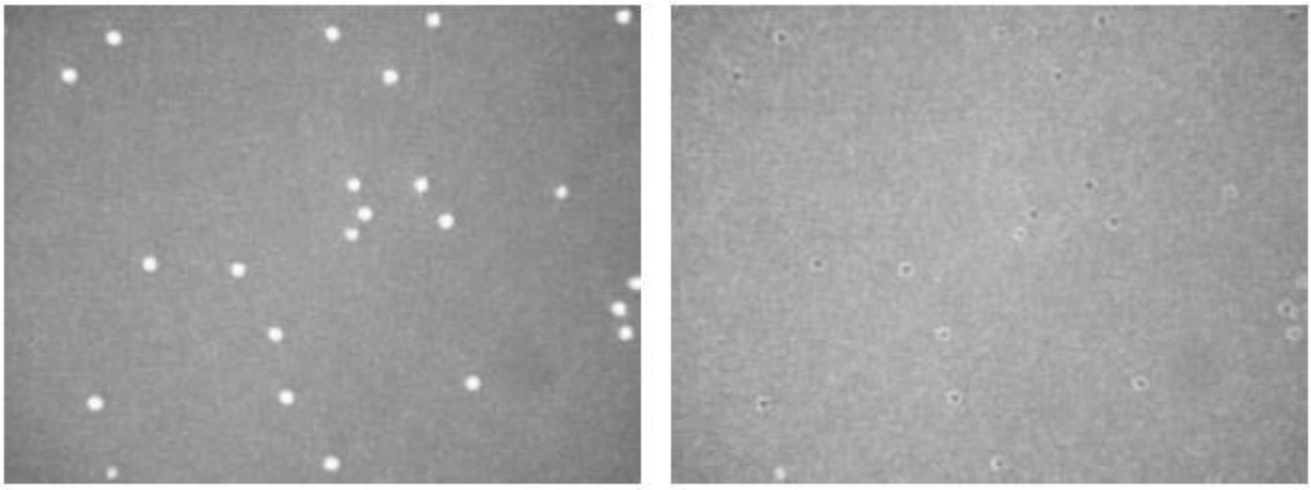

a) 20X aligned polarizers b) 20X crossed polarizers

**Figure 4.71 – POM micrograph for (TRI/XDT/E7/SDS)**

The electro-optical results for the poly(ethylene glycol) dimethacrylate systems with liquid crystal and sodium dodecyl sulfate are presented in Figure 4.72 and Figure 4.75 for different types of initiators.

For the thermal initiator the results obtained are described below and it can be seen that in this type of monomer, permanent memory effects are present, although this effect is diminished when compared with the same composite without an additive. The comparison also shows that applied voltages are lower, as well as the permanent memory effect coefficient, and transmittances are slightly higher

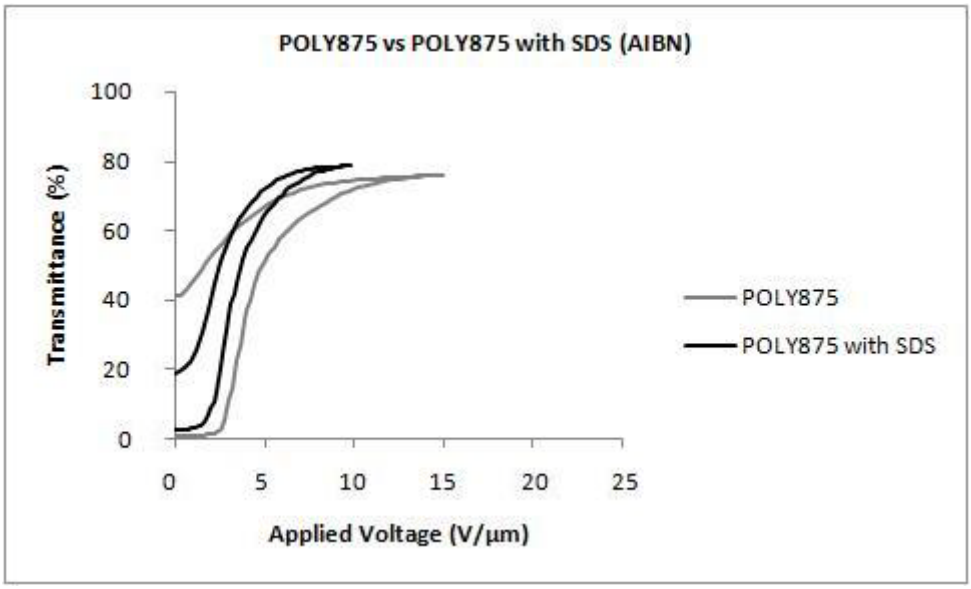


**Figure 4.72 – Electro-optic response of the system (POLY875/AIBN/E7) with and without SDS.**

The analysis of the textures over polarized light have shown that the sample is homogeneous in its totality, and as can be seen in Figure 4.73, the area where voltage is applied is in a total different tonality, representing the permanent memory effects, according to the electro-optical response curve illustration. Light scatters through the sample, because the orientation of the liquid crystals in that centre is oriented into one direction.

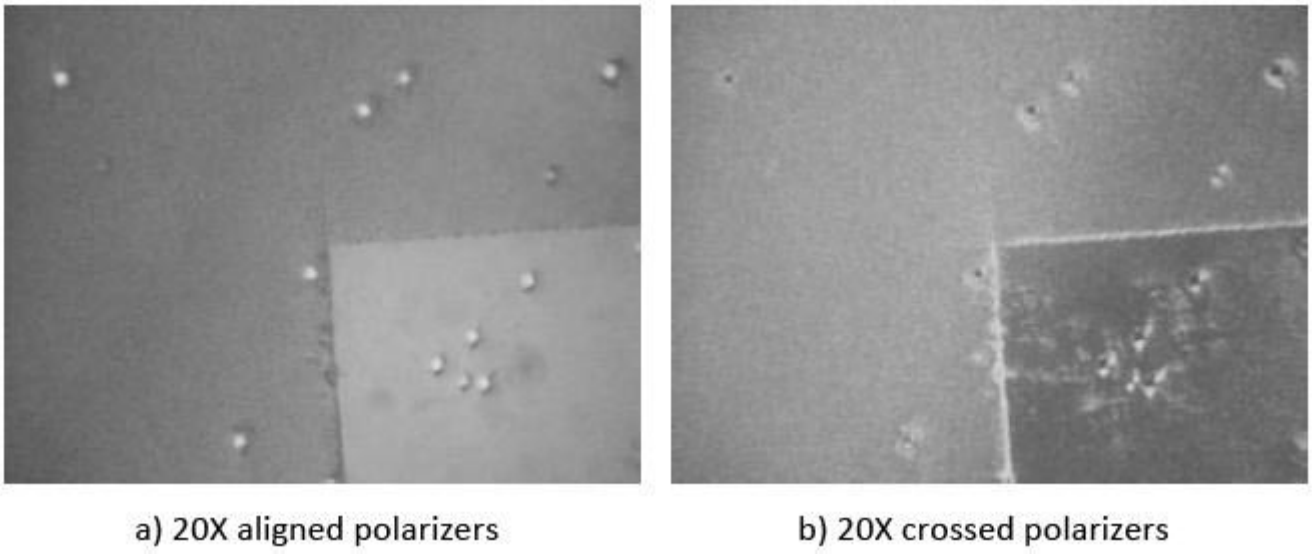


**Figure 4.73 – POM micrograph for (POLY875/AIBN/E7/SDS)**

Figure 4.74 shows the scanning electron microscopy micrograph for this system. In accordance to the previous additive, this one also has a long chain length that, in agreement with the previous long chain results, creates a dense polymer network. In this case, no dark areas are observed due to that density, but it is curious to observe some kind of lamellar leafs that might correspond to the sodium dodecyl sulfate molecules. This proves that this additive has not a great affinity to the liquid crystal and, therefore, the electro-optic results are quite similar to the ones presented in the appendix section for the same monomers without the presence of an additive.

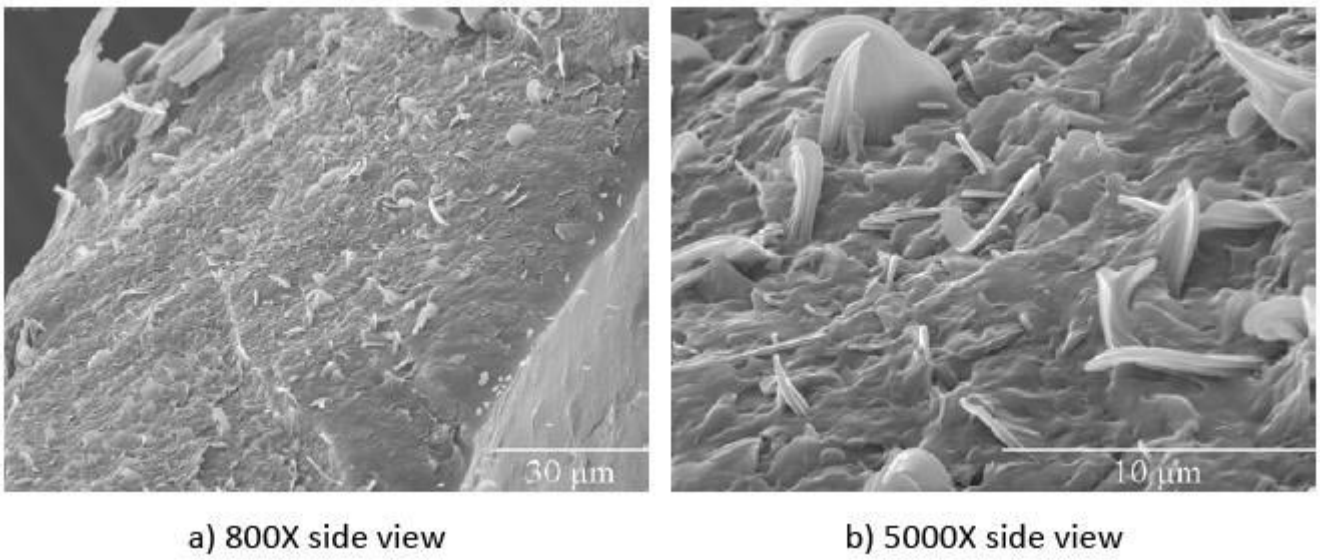


**Figure 4.74 – SEM morphology for (POLY875/AIBN/E7/SDS).**

The results for the photochemical initiator are described below and it can be seen that in this type of monomer, permanent memory effects are barely present. In this case, two ramps were obtained and this can be due to different regions of the polymer containing different domains of liquid crystal so that the applied voltage to orient these different regions is also different. Transmittances and applied voltages are practically the same when comparing this monomer with and without the addition of sodium dodecyl sulfate.

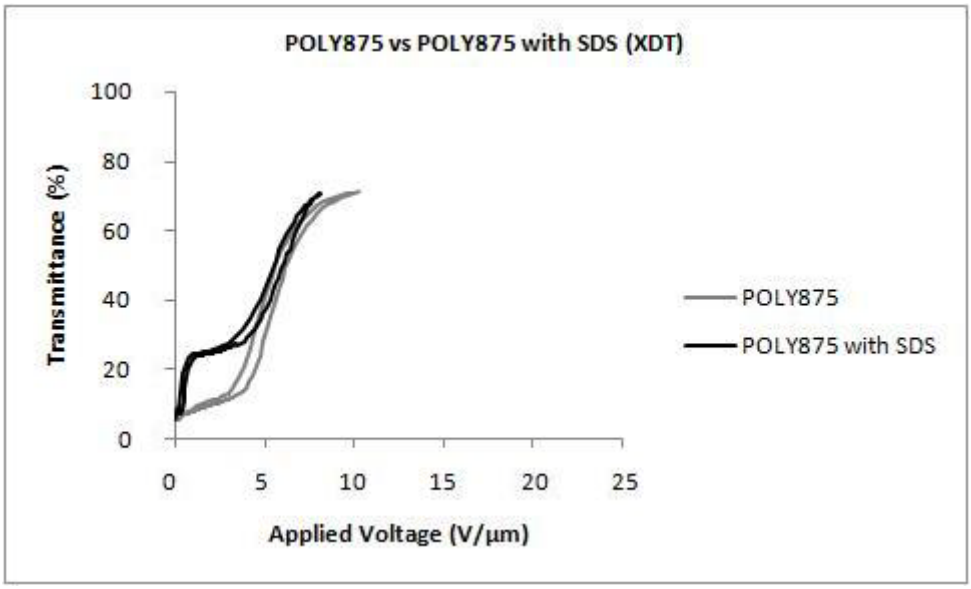


**Figure 4.75 – Electro-optic response of the system (POLY875/XDT/E7) with and without SDS.**

The analysis of the textures over polarized light have shown that the sample presents liquid crystal domains in its totality and even in the center where voltage is applied no

differences can be noticed, as showed in Figure 4.76, and in accordance with all the samples prepared with this monomer and type of polymerization.

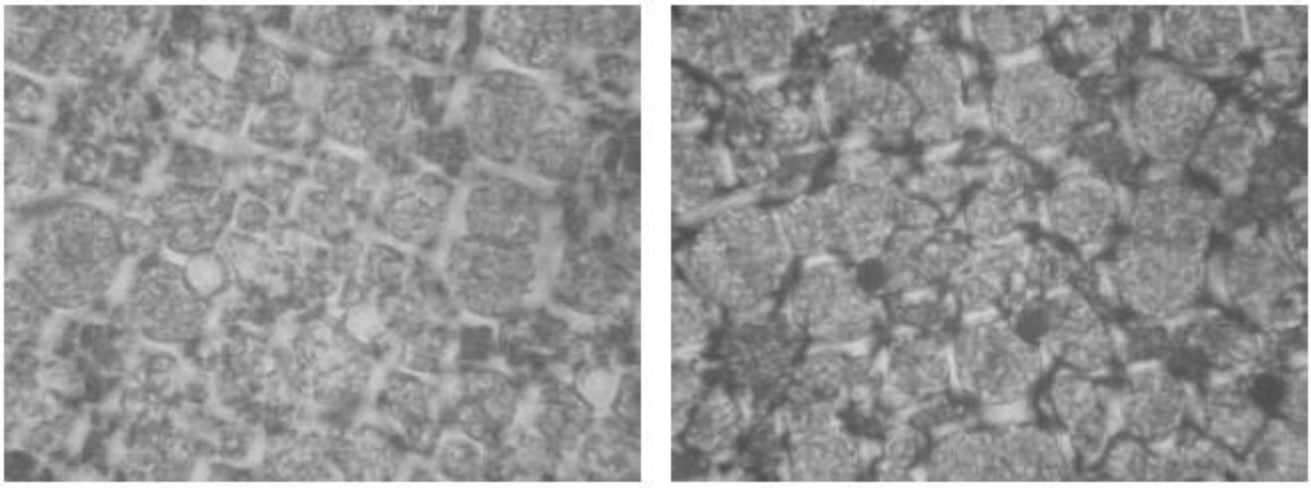

a) 50X aligned polarizers b) 50X crossed polarizers

**Figure 4.76 – POM micrograph for (POLY875/XDT/E7/SDS)**

In Table 4.3 are presented the compositions of the samples with the percentages in weight of monomer, weight of liquid crystal and weight of additive for the monomers and their respective polymerization initiator. Usually, the weight ratios are in the order of $27/63/10$, which means the addition of an exact percentage of $10\%$ of additive. The samples containing different weight ratios mean that the percentage of additive is a little bit higher or lower and this happens, because some additives are denser or more viscous than others. Thus, the preparation of an exact amount of composite becomes a bit difficult when working with samples containing little quantities of material. Once more, the polymerization times for the thermal samples were always approximately $20$ hours and for the photochemical samples the values were in the range of $1000{\sim}4000\ s$, because of the values of the calculated actinometry that were obtained between $3.0 \times 10^{-7}{\sim}1.5 \times 10^{-6}\ Nhv.min^{-1}$. The lower polymerization times mean that the actinometry values were higher and for higher polymerization times, that means the actinometry values were inferior. For polymerization times of $1000$ seconds, the number of photons that passed through the sample was equivalent to $1.51 \times 10^{19}$ photons and for the $4000$ seconds irradiation time, the photons traversing the sample were $1.20 \times 10^{19}$.

**Table 4.3 – Composition of the samples.**

| Monomer and Initiator | Additive | LC | Polymerization Times | Weight Ratio (wt %) | | |
|---|---|---|---|---|---|---|
| | | | | Monomer | LC | Additive |
| TRI AIBN | OA | E7 | 20 hours | 27 | 62 | 11 |
| | EG | E7 | 24 hours | 27 | 62 | 11 |
| | TX100 | E7 | 20 hours | 26 | 61 | 13 |
| | CTAB | E7 | 20 hours | 27 | 63 | 10 |
| | SDS | E7 | 20 hours | 28 | 62 | 10 |
| TRI XDT | OA | E7 | 1000 seconds | 27 | 62 | 11 |
| | EG | E7 | 1500 seconds | 27 | 63 | 10 |
| | TX100 | E7 | 2500 seconds | 26 | 60 | 14 |
| | CTAB | E7 | 2000 seconds | 27 | 63 | 10 |
| | SDS | E7 | 2000 seconds | 27 | 63 | 10 |
| POLY875 AIBN | OA | E7 | 20 hours | 26 | 61 | 13 |
| | EG | E7 | 24 hours | 27 | 62 | 11 |
| | TX100 | E7 | 20 hours | 27 | 63 | 10 |
| | CTAB | E7 | 20 hours | 27 | 63 | 10 |
| | SDS | E7 | 20 hours | 27 | 63 | 10 |
| POLY875 XDT | OA | E7 | 1000 seconds | 27 | 63 | 10 |
| | EG | E7 | 1500 seconds | 27 | 62 | 11 |
| | TX100 | E7 | 2500 seconds | 27 | 64 | 9 |
| | CTAB | E7 | 4000 seconds | 26 | 61 | 13 |
| | SDS | E7 | 4000 seconds | 27 | 63 | 10 |

The electro-optical properties of the systems described above are resumed in Table 4.4, where the required voltages for their operation and transmittance coefficients are presented.

**Table 4.4 – Electro-optical properties of the composites.**

| Monomer and Initiator | Additive | Transmittance (%) | | | Switching Voltage ($V.\mu m^{-1}$) | Contrast (%) | $T/V$ Ratio |
|---|---|---|---|---|---|---|---|
| | | $T_{max}$ | $T_{min}$ | $T_{half}$ | | | |
| TRI AIBN | OA | 79 | 0 | 39 | 6.40 | 79 | 0.305 |
| | EG | 33 | 5 | 14 | 21.95 | 28 | 0.032 |
| | TX100 | 70 | 8 | 31 | 0.40 | 62 | 3.875 |
| | CTAB | 64 | 0 | 32 | 9.05 | 64 | 0.177 |
| | SDS | 47 | 8 | 19 | 10.60 | 39 | 0.090 |
| TRI XDT | OA | 70 | 1 | 34 | 5.50 | 69 | 0.309 |
| | EG | 54 | 0 | 27 | 10.25 | 54 | 0.263 |
| | TX100 | 70 | 1 | 34 | 0.70 | 69 | 2.429 |
| | CTAB | 65 | 0 | 32 | 5.20 | 65 | 0.308 |
| | SDS | 70 | 0 | 35 | 10.65 | 70 | 0.164 |
| POLY875 AIBN | OA | 75 | 12 | 32 | 4.35 | 63 | 0.368 |
| | EG | 3 | 2 | 0 | Undefined | Undefined | Undefined |
| | TX100 | 86 | 5 | 40 | 1.30 | 81 | 1.538 |
| | CTAB | 76 | 1 | 37 | 1.85 | 75 | 1.000 |
| | SDS | 79 | 3 | 38 | 3.15 | 76 | 0.603 |
| POLY875 XDT | OA | 57 | 1 | 28 | 2.70 | 56 | 0.519 |
| | EG | 5 | 1 | 2 | Undefined | Undefined | Undefined |
| | TX100 | 80 | 3 | 39 | 0.95 | 77 | 2.053 |
| | CTAB | 75 | 1 | 37 | 4.45 | 74 | 0.416 |
| | SDS | 70 | 6 | 32 | 4.65 | 64 | 0.344 |

This table is in agreement with the previous table containing the octanoic acid studies, but this time, for the several additives used in this work. This means that the equations related for that table also apply for this one.

This master thesis is complemented with a parallel work entitled “Preparation and Characterization of New Polymer Dispersed Liquid Crystals” (Maiau, 2009). For comparison of the additive effects in the electro-optical properties of the composites, tables were allocated to the appendix section with the results of that parallel work that were kindly consigned and treated in agreement with the ones presented here.

# *Chapter Five*

# 5. Additional Analysis

## 5.1. Differential Scanning Calorimetry

Once the systems containing the triton X-100 were the better results obtained in this work, additional analysis was carried out for further investigation of the composite in cause. Thus, a differential scanning calorimetry analysis was made to the liquid crystal used, the additive used and the respective mixture of both components, being that some similarities were observed.

### 5.1.1. Liquid Crystal

Figure 5.1 and Figure 5.2 illustrate the differential scanning calorimetry analysis of the liquid crystal, $E7$, on its heating and cooling stages, respectively.

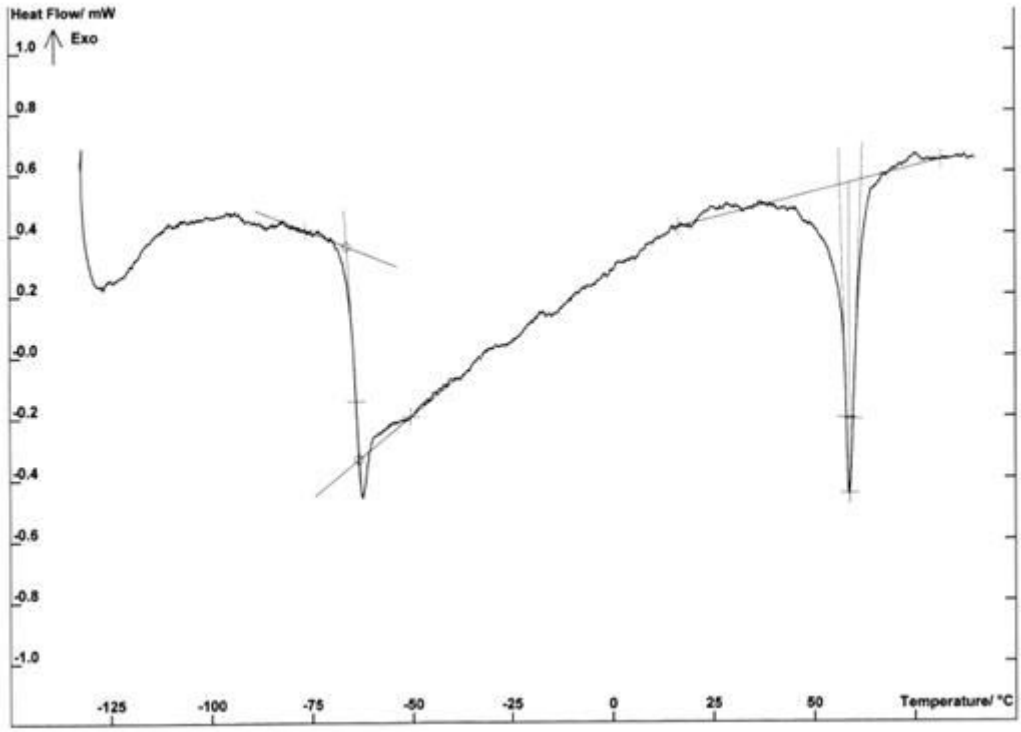


**Figure 5.1 – DSC of E7 on heating stage.**

On heating run two peaks are observed, at a temperature of $-64$ ℃ is the glass transition of the liquid crystal and at a temperature of $57$ ℃ occurs its melting or nematic-isotropic transition, $T_{N\to I}$.

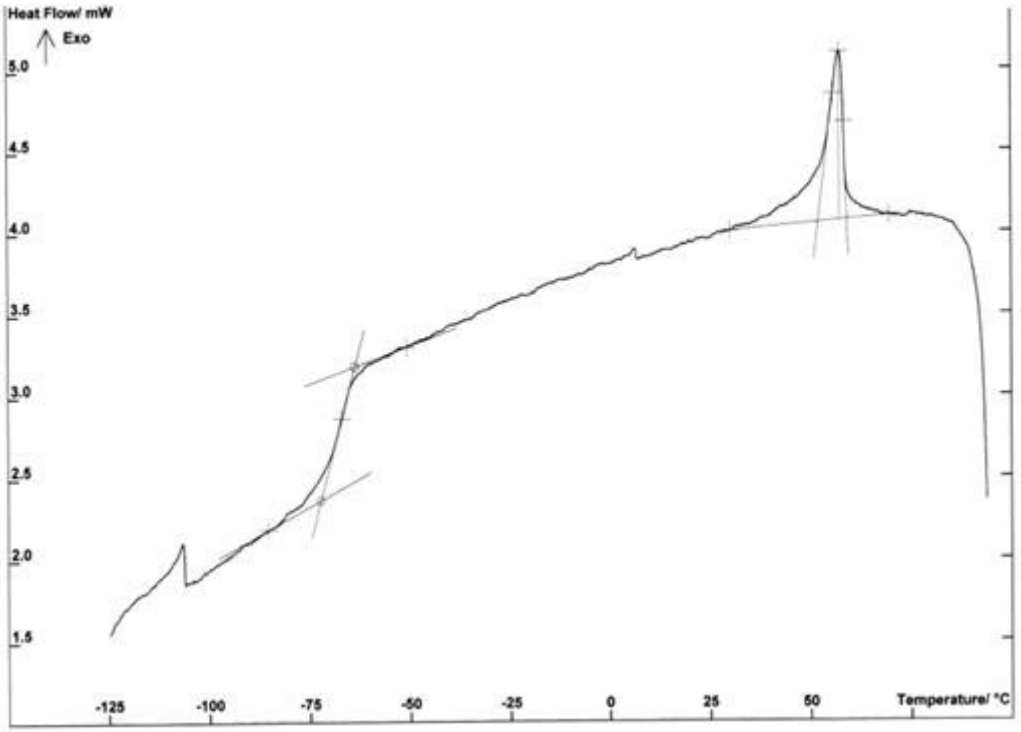


**Figure 5.2 – DSC of E7 on cooling stage.**

On cooling run, also two peaks are observed, as expected, at a temperature of $59$ ℃ is the crystallization or isotropic-nematic transition, $T_{I\to N}$, of the liquid crystal and at a temperature of $-67$ ℃ its glass transition.

### 5.1.2. Surfactant

Figure 5.3 and Figure 5.4 illustrate the differential scanning calorimetry analysis of the surfactant additive, triton X-100, on its heating and cooling stages, respectively.

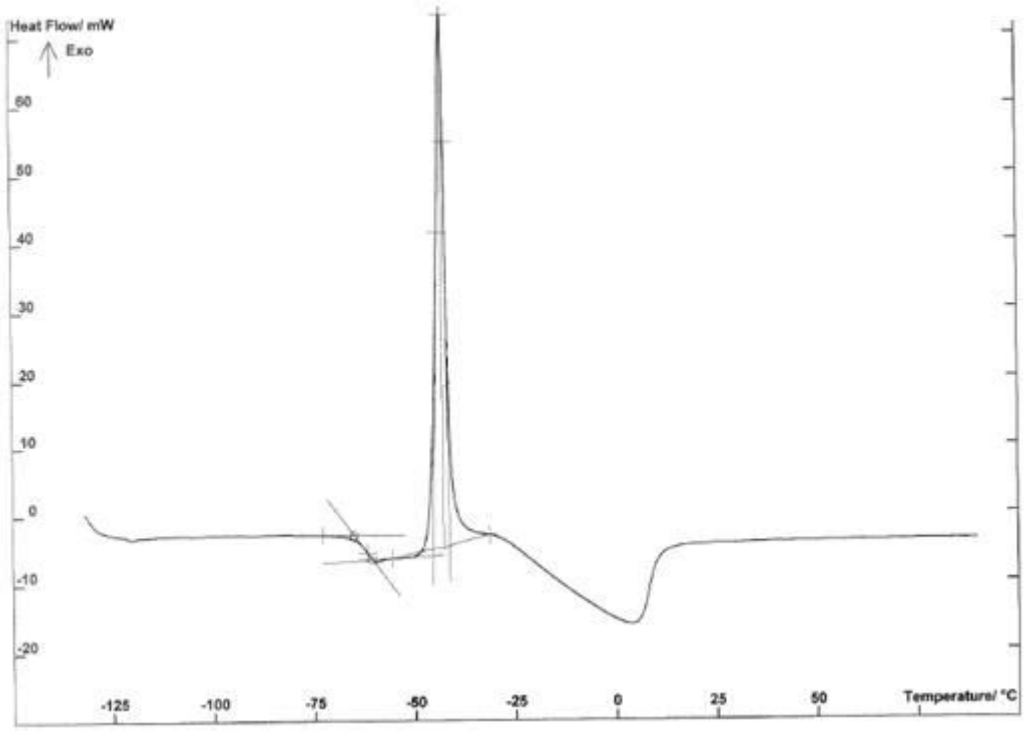


**Figure 5.3 – DSC of TX100 on heating stage.**

On heating run three peaks are observed, at a temperature of $-62$ ℃, a small peak, is the glass transition of the surfactant, at a temperature of $-44$ ℃ occurs a cold crystallization, explicit by the major observed peak, and at a temperature of $5$ ℃ is the melting point of the compound.

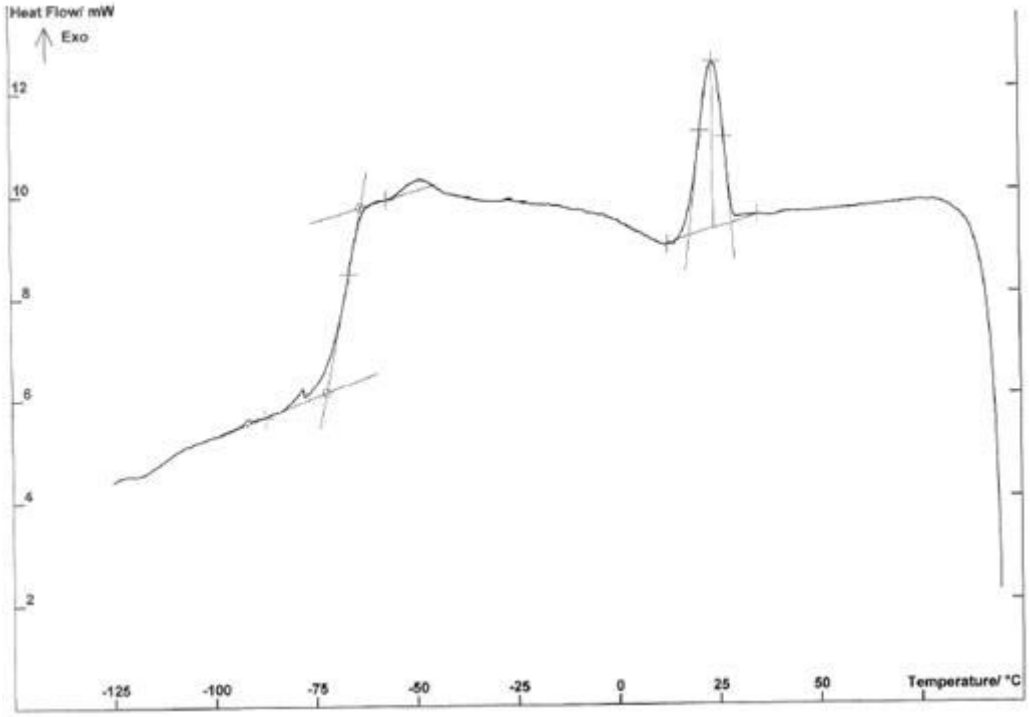


**Figure 5.4 – DSC of TX100 on cooling stage.**

On cooling run, two peaks are observed, at a temperature of 29 ℃ is the crystallization of the surfactant and at a temperature of −66 ℃ its glass transition.

### 5.1.3. Mixture of Liquid Crystal and Surfactant

The liquid crystal and the surfactant present some similarities when observed individually. In Table 5.1 are resumed the physical properties of the two compounds, and it can be observed that both glass transitions, when heating or cooling, are practically the same. The major difference is in the melting and crystallization points of the surfactant, and this might be happening because of the cold crystallization that happens when the sample is submitted to various successive assays of cooling and heating runs.

**Table 5.1 – State transitions of E7 and TX100.**

| State Transitions | Liquid Crystal | Surfactant | Mixture |
|---|---|---|---|
| Glass Transition on heating | $-64$ ℃ | $-62$ ℃ | $-64$ ℃ |
| $T_{N\rightarrow I}$ / Melting | 57 ℃ | 5 ℃ [1] | 49 ℃ |
| $T_{I\rightarrow N}$ / Crystallization | 59 ℃ | 29 ℃ [2] | 47 ℃ |
| Glass transition on cooling | $-67$ ℃ | $-66$ ℃ | $-67$ ℃ |

Figure 5.5 and Figure 5.6 illustrate the differential scanning calorimetry analysis of the mixture, liquid crystal plus surfactant, on its heating and cooling stages, respectively.

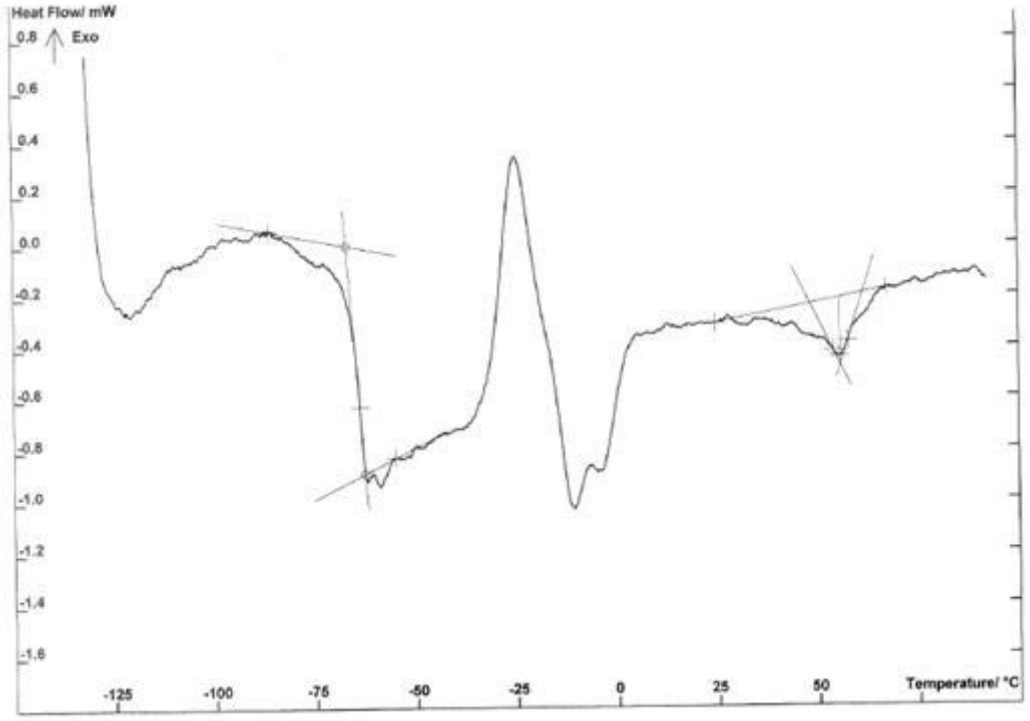


**Figure 5.5 – DSC of the mixture (E7/TX100) on heating stage.**

On heating run four peaks are observed, at a temperature of $-64$ ℃ is the glass transition of the mixture, corresponding to both glass transitions of the single components. The glass transition remained at the same temperature, because the glass transition of the two isolated components is very similar. At a temperature of

[1] In agreement with the specifications of the material safety data sheet, that measures it at $T_m = 6$ ℃.

[2] The temperature where this transition is observed is not completely reproducible, once some impurities might be interfering with the transformation and it has been submitted to several successive cooling and heating runs.

$-25$ ℃ occurs a cold crystallization, explicit by the major observed peak and at a temperature of $-8$ ℃ is the melting point of the compound. Finally, at a temperature of $49$ ℃ is presented the melting or nematic-isotropic transition, $T_{N\to I}$, of the liquid crystal. Comparing this transition with the transition occurred in the single liquid crystal sample, it is observed that it has slightly decreased due to the presence of the surfactant. To analyze the effect of mixing $E7$ with a lower melting temperature compound, assuming that both form a homogeneous mixture, the Fox equation (Fox, 1956) was applied.

$$\frac{1}{T_m + 273.15} = \frac{x}{T_{mA} + 273.15} + \frac{1-x}{T_{mB} + 273.15} \quad \textbf{(6)}$$

Replacing the melting values of $E7$ and triton X-100 obtained on heating runs, presented in Table 5.1, in Equation 6, a value of $46$ ℃ is predicted in reasonable agreement of the mixture melting temperature, which is an indication that both component are miscible in a great extent. Nevertheless, we observe that besides the mixture is fully mixed when stirred, phase separation occurs after a definite period of storage.

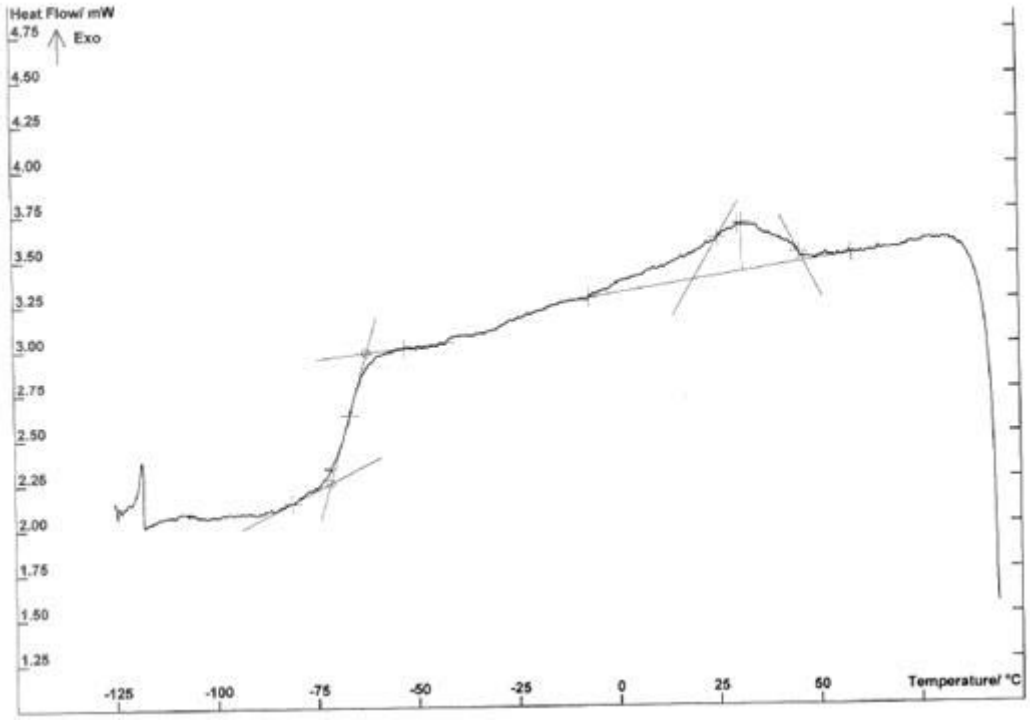


**Figure 5.6 – DSC of the mixture (E7/TX100) on cooling stage.**

On cooling run two peaks are observed, at a temperature of $-67$ ℃ is the glass transition of the mixture, containing both glass transitions of the single components. The glass transition remained at the same temperature, because the glass transition of the two isolated components is very similar to that point. At a temperature of $47$ ℃ occurs the crystallization of the mixture, explicit by the major extensive peak. This peak is extended because it contains the isotropic-nematic transition, $T_{I\rightarrow N}$, of the liquid crystal and the crystallization of the surfactant. This indicates that this transition temperature has also slightly decreased with the presence of the additive.

## 5.2. Dielectric Relaxation Spectroscopy

Yet, another analysis was made to this system, based on dielectric relaxation spectroscopy. The sample analyzed was the sample containing triton X-100, which presents low applied voltages and a high transmittance, meaning that this is the system that combines both, applied voltage and transmittance, electro-optical properties of the composite. While differential scanning calorimetry probes freedom degrees, dielectric relaxation spectroscopy probes dipolar fluctuations but the two techniques can be applied to monitor phase transitions and transformations.

Thermodynamic events monitored by dielectric relaxation spectroscopy are frequency independent, while kinetic transformations are frequency dependent. A parallel can be established with differential scanning calorimetry, where thermodynamic transitions are cooling or heating rate independent but kinetic transformations depend on cooling and heating rates. An appropriate comparison between the two techniques should be made with data obtained by dielectric relaxation spectroscopy collected at the lowest frequencies.

### 5.2.1. Liquid Crystal

Figure 5.7 illustrates the phase transitions of the liquid crystal, $E7$, for a frequency of $10^4\ Hz$, as monitored by dielectric relaxation spectroscopy.

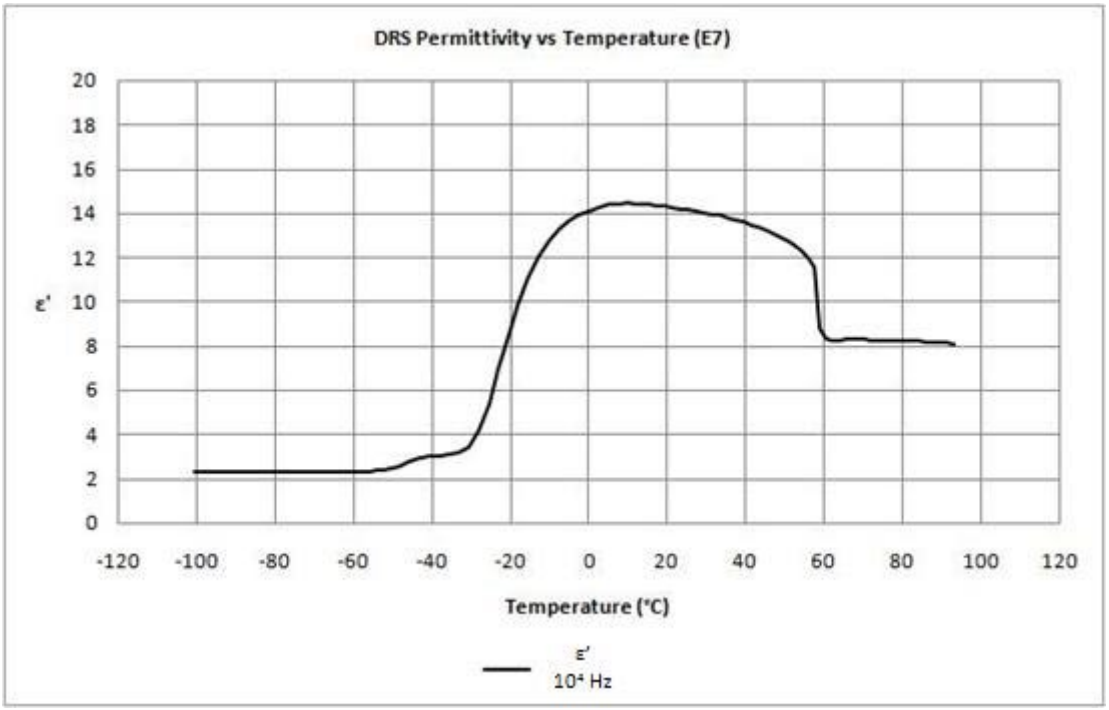


**Figure 5.7 – DRS of E7 for ε'.**

Essentially, two main transitions[3] are revealed from the spectrum. In decreasing temperature order, a first abrupt change occurs at, approximately, $57.6\,℃$, being associated with the nematic-isotropic transition. This was observed at $57.4\,℃$ in differential scanning calorimetry, evidencing the excellent agreement between both techniques. The clearing point is a thermodynamic event being frequency independent, as previously mentioned. This is obvious when observing bulk $E7$ dielectric behavior at different frequencies, where the nematic-isotropic transition is located at the same temperature with no dependence on frequency. This can be seen in the figures presented in the appendix section. By other side, the location of the glass transition is a kinetic phenomenon, thus, frequency dependent.

In the figure above, the step in $\varepsilon'$, located around $-40\,℃$ at a frequency of $10^4\ Hz$, is associated with the glass transition of $E7$. In order to compare it with differential scanning calorimetry, this value should be taken at the lowest frequency, that is $10^2\ Hz$, where the onset of the glass transition occurs and all the curves superimpose in the region preceding the glass transition step. The figures that illustrate this observation are presented in the appendix section. The onset is around $-60\,℃$

[3] Strictly speaking, the super-cooled amorphous glass transition should be designated as transformation, since the glass is not a true phase, as thermodynamically defined.

revealing, once again, a very good agreement between dielectric relaxation spectroscopy and differential scanning calorimetry.

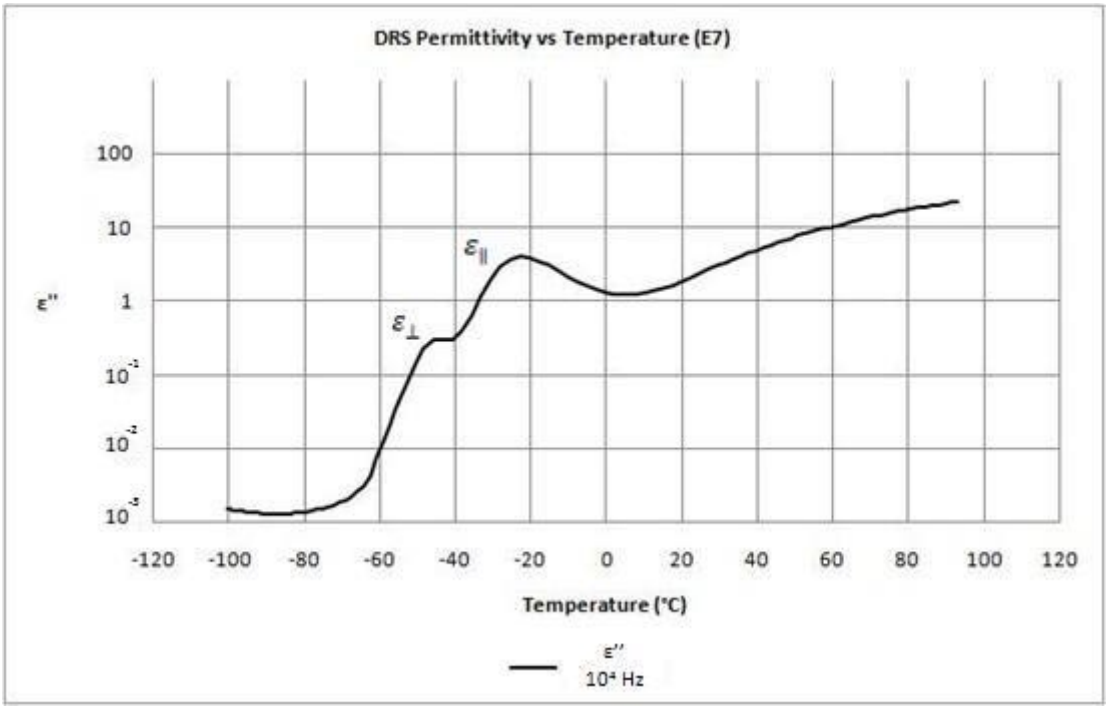


**Figure 5.8 – DRS of E7 for ε''.**

The dielectric relaxation response of bulk $E7$ at a frequency of $10^4\ Hz$, Figure 5.8, analyzed through the imaginary part of the complex permittivity, shows essentially two main relaxation processes designated by $\varepsilon_{\parallel}$ and $\varepsilon_{\perp}$. The parallel component is associated mainly with orientations of dipole parallel to the applied electric field, while the perpendicular one is associated mainly with orientations of dipole perpendicular to the applied electric field. In the figure, the two ramps correspond to the perpendicular and parallel parts, respectively.

From the spectrum it can be concluded that bulk $E7$ on a gold substrate assumes a main orientation parallel to the electric field. To note that $\varepsilon''$ is plotted in logarithmic scale, otherwise it was not possible to visualize the lower intense $\varepsilon_{\perp}$ process. This behavior is in agreement with the findings of Brás et al.. A main orientation of the liquid crystal director parallel to the electric field means that molecules arrange on the gold substrate with their long axis perpendicular to the electrode surface. In the indium-tin oxide cells the orientation is the opposite, being mainly perpendicular to the electric field, this is, parallel to the indium-tin oxide glass surface (Brás et al., 2008).

### 5.2.2. Surfactant

Figure 5.9 illustrates the phase transitions of the surfactant additive, triton X-100, for a frequency of $10^4\ Hz$, as measured by dielectric relaxation spectroscopy, upon cooling and on further heating.

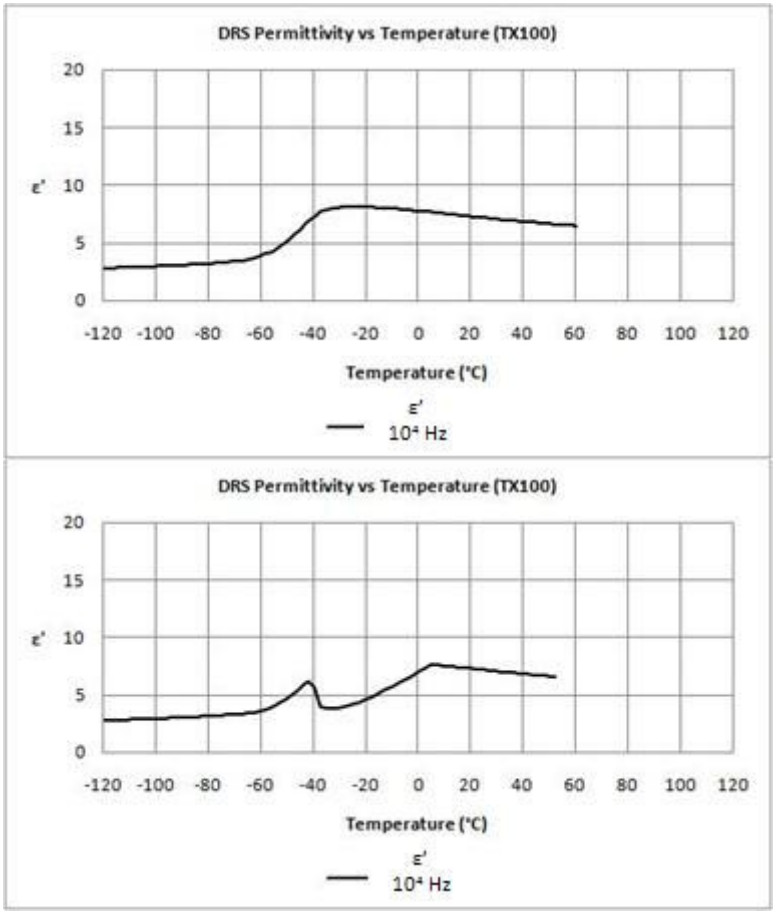


**Figure 5.9 – DRS of TX100 on cooling and heating runs for ε'.**

In the differential scanning calorimetry scan an exothermal peak is observed at around $29\,℃$ due to crystallization, followed by a step in heat flow at $-66\,℃$ due to vitrification, so this is a good estimation of the glass temperature.

The temperature dependent behavior of $\varepsilon'$ seen by dielectric relaxation spectroscopy on cooling does not exhibit the usual drop due to crystallization and only the glass transition is observed, so crystallization was avoided due to a relatively high cooling rate. This is frequently found in vitrifying liquids allowing triton X-100 to be classified as a glass former. To our best knowledge, the observation of this effect is not already published in literature.

On further heating, differential scanning calorimetry exhibits the signature of the glass transition followed by crystallization as described above. The crystallization observed on heating coming from the glass is designated as cold crystallization (Diogo & Ramos, 2006) being observed for triton X-100 at around $-44\,℃$ followed by a broad endothermic peak due to the melting.

Dielectric relaxation spectroscopy is coherent with this behavior since the process associated with the glass transition is detected on heating with an onset around $-70\,℃$ followed by a sudden decrease due to cold crystallization at around $-40\,℃$. A subsequent increase due to melting is observed above $-30\,℃$. Interesting is the fact that both compounds, triton X-100 and $E7$, exhibit very similar glass transitions, as confirmed by both techniques.

### 5.2.3. Mixture of Liquid Crystal and Surfactant

Figure 5.10 illustrates the phase transition analysis of the mixture containing the liquid crystal with the presence of the additive, for a frequency of $10^4\ Hz$, as monitored by dielectric relaxation spectroscopy, as well as the respective comparison with neat liquid crystal, in grey.

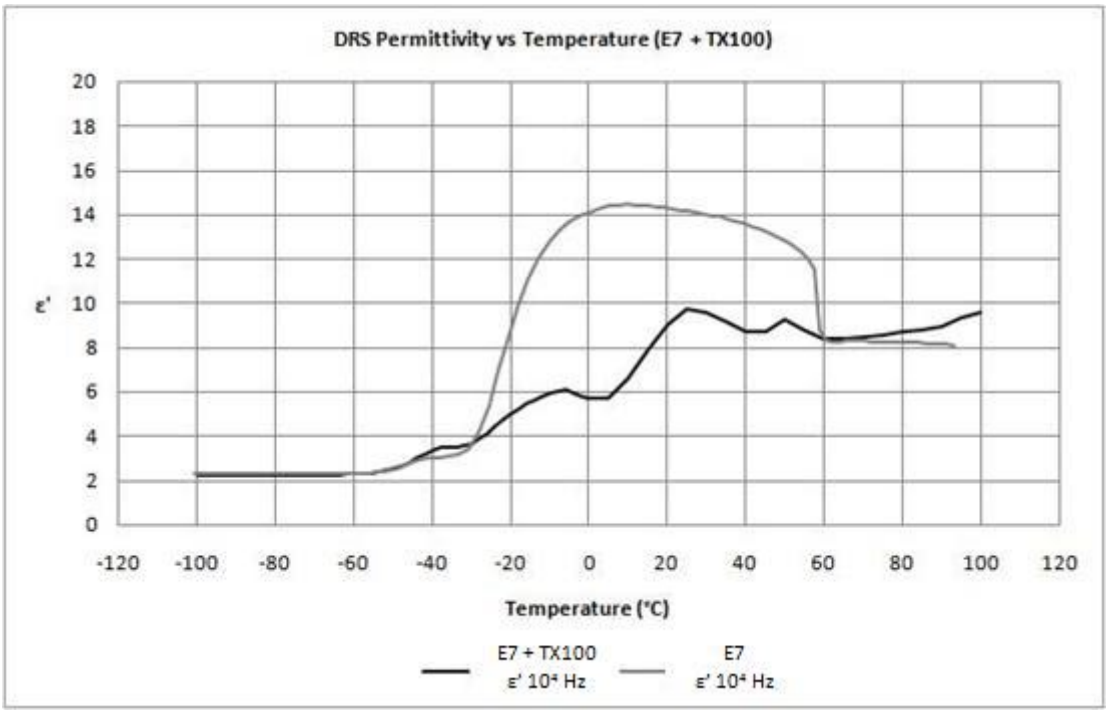


**Figure 5.10 – DRS of the mixture (E7/TX100) for ε'.**

The differential scanning calorimetry shows the heat capacity jump at $-64$ ℃ due to a single glass transition which is indistinguishable from the individual components. At around $-25$ ℃ the exothermal peak due to cold crystallization is detected immediately followed by melting, characterized by the endothermic peak. At high temperatures, above $48$ ℃, a broad endothermic peak is observed due to the nematic-isotropic transition of $E7$ that emerges at a lower temperature relatively to bulk liquid crystal. It should be pointed out that this transition is not as sharp as seen in neat liquid crystal, rather an extended endothermic signature appear, that could have a contribution of a further melting of triton X-100.

Analyzing the dielectric relaxation spectroscopy data, it is observed that, on heating, after a first step on $\varepsilon'$ due to glass transition, above $-60$ ℃, seen in both bulk liquid crystal and mixture of liquid crystal with additive, a drop is observed due to cold crystallization at $-8$ ℃, followed by an increase due to melting. At high temperatures a discontinuity around $60$ ℃ is observed. Whether this is the nematic-isotropic transition of $E7$ is not straight forward due to the lack of sharpness that characterizes this type of material transformation. To clarify this behavior, a polarized optical microscopy analysis was carried out. The small peak that anticipates this transformation is probably crystallization and melting of triton X-100 occurring in a low extent. In subsequent cooling there is no evidence of either isotropic-nematic transition or crystallization of triton X-100 at least down to $20$ ℃. Below this temperature, triton X-100 seems to crystallize due to the nematic-isotropic transition, that is not so abrupt as in neat liquid crystal, probably anticipated by crystallization and melting of triton X-100, evidenced by the small peak that precedes the nematic-isotropic transition. Dielectric relaxation spectroscopy could bring, in the end, a more detailed information relative to differential scanning calorimetry due to the slowness of the spectra collection that was taken each $5$ ℃.

In Figure 5.11 is presented the dielectric relaxation spectroscopy analysis of the mixture containing the liquid crystal with the presence of the additive, for a frequency of $10^4\ Hz$, as well as the respective comparison with bulk liquid crystal, in grey.

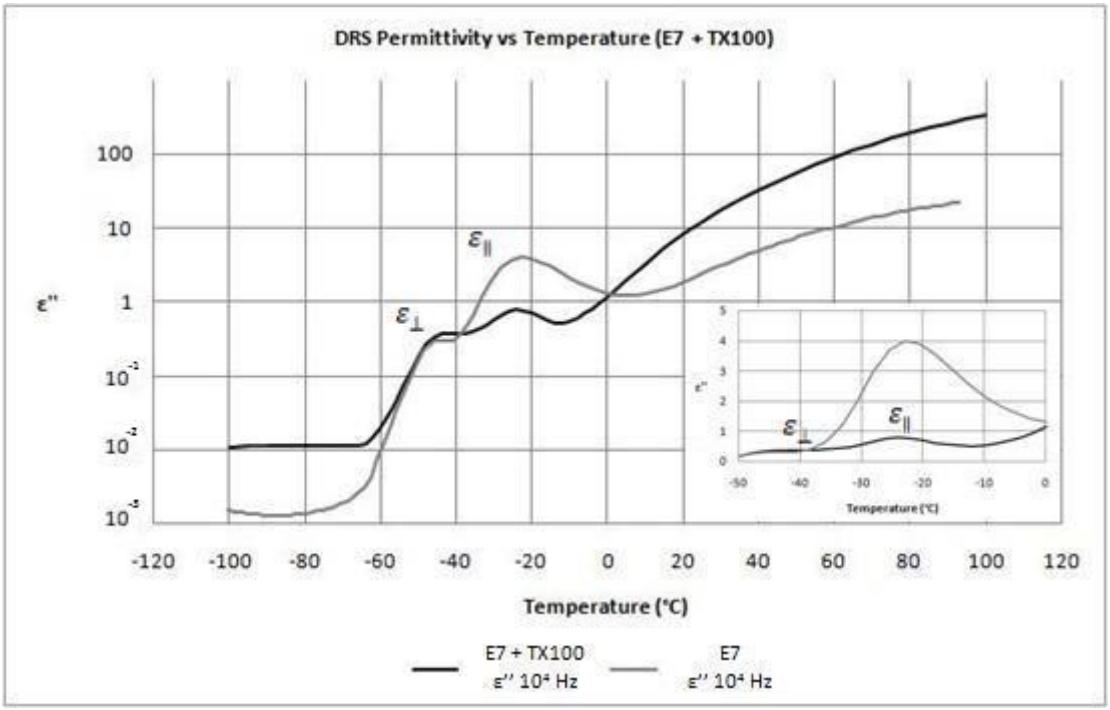


**Figure 5.11 – DRS of the mixture (E7/TX100) for ε''.**

Basically, no temperature shift is observed in the location of the two $E7$ relaxational processes, which is not surprising due to the similarities of the respective glass transitions, but an orientation effect occurs. While in neat $E7$ the liquid crystal molecules lie mainly parallel to the applied electric filed, perpendicular to the gold substrate, as seen by the main contribution of the $\varepsilon_{\parallel}$ in the mixture both parallel and perpendicular components became more similar, revealing a higher disorder of the molecular arrangement in the mixture. Generally, when the fraction of molecules with parallel arrangement is very similar to the fraction with perpendicular alignment, the magnitude of $\varepsilon_{\parallel}$ is twice larger than $\varepsilon_{\perp}$. Thus, to determine the overall orientation, the perpendicular contribution should be multiplied by a factor of two. If we do so in the mixture response, an almost equal intensity of the two alignments is observed in the inset figure, with linear plots.

### 5.2.4. Liquid Crystal Composite

Figure 5.12 illustrates the phase transition analysis of the liquid crystal, $E7$, in a polymer matrix, given by dielectric relaxation spectroscopy, for a frequency of $10^4\ Hz$.

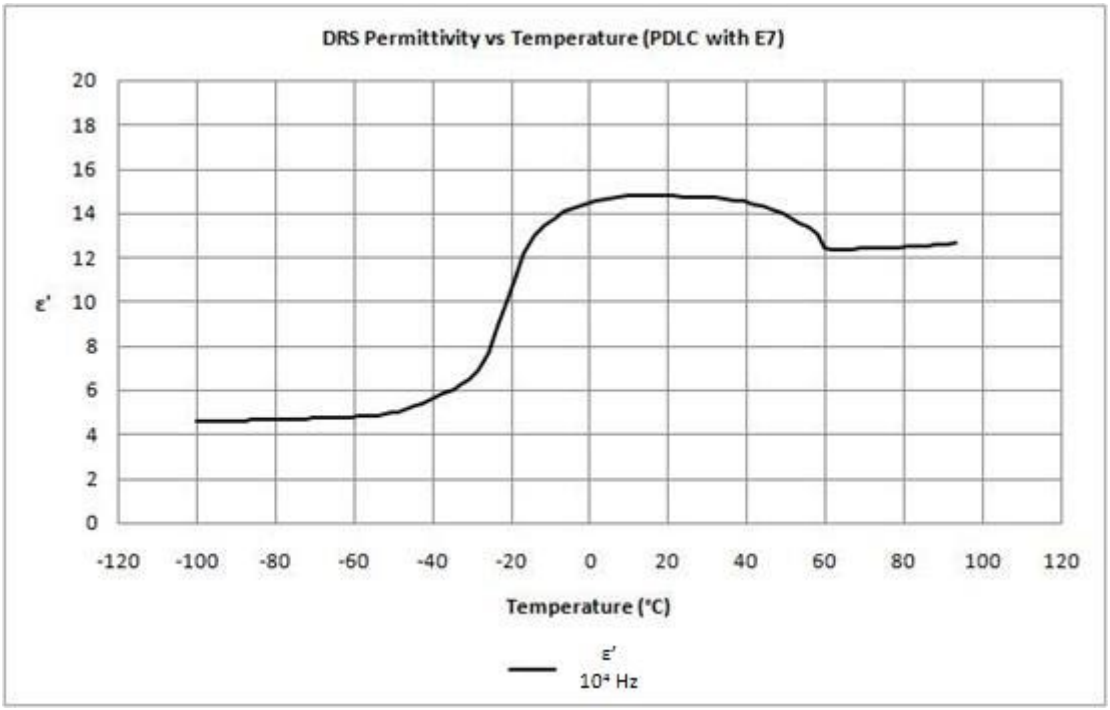


**Figure 5.12 – DRS of E7 in a polymer matrix for ε'.**

The nematic to isotropic transition keeps the neat liquid crystal location, $T_{N\to I} = 60$ ℃. Also the glass transition is observed in the same temperature range although less abrupt when compared with neat liquid crystal.

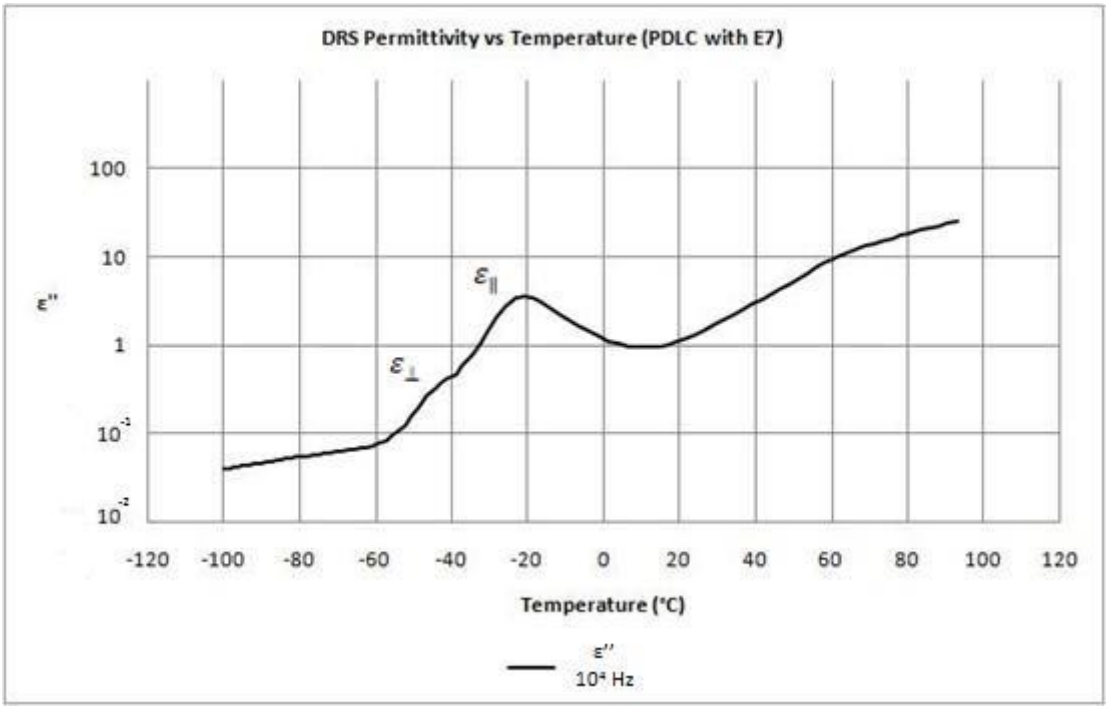


**Figure 5.13 – DRS of E7 in a polymer matrix for ε''.**

Figure 5.13 illustrates the two components of the imaginary part of the complex permittivity. In the composite, the response is similar to $E7$ lying in a gold surface with

the parallel component being the main contribution to the spectrum. This can be interpreted as the liquid crystal being encapsulated inside the polymer matrix without contacting directly the indium-tin oxide surface, since when $E7$ lies in an indium-tin oxide surface, the orientation is mainly perpendicular.

### 5.2.5. Mixture Composite

Figure 5.14 illustrates the analysis of the phase transitions of the mixture containing the liquid crystal with the presence of the additive, in a polymer matrix, for a frequency of $10^4\,Hz$, according to the dielectric relaxation spectroscopy measurements, as well as a comparison with the composite without the presence of the additive, in grey.

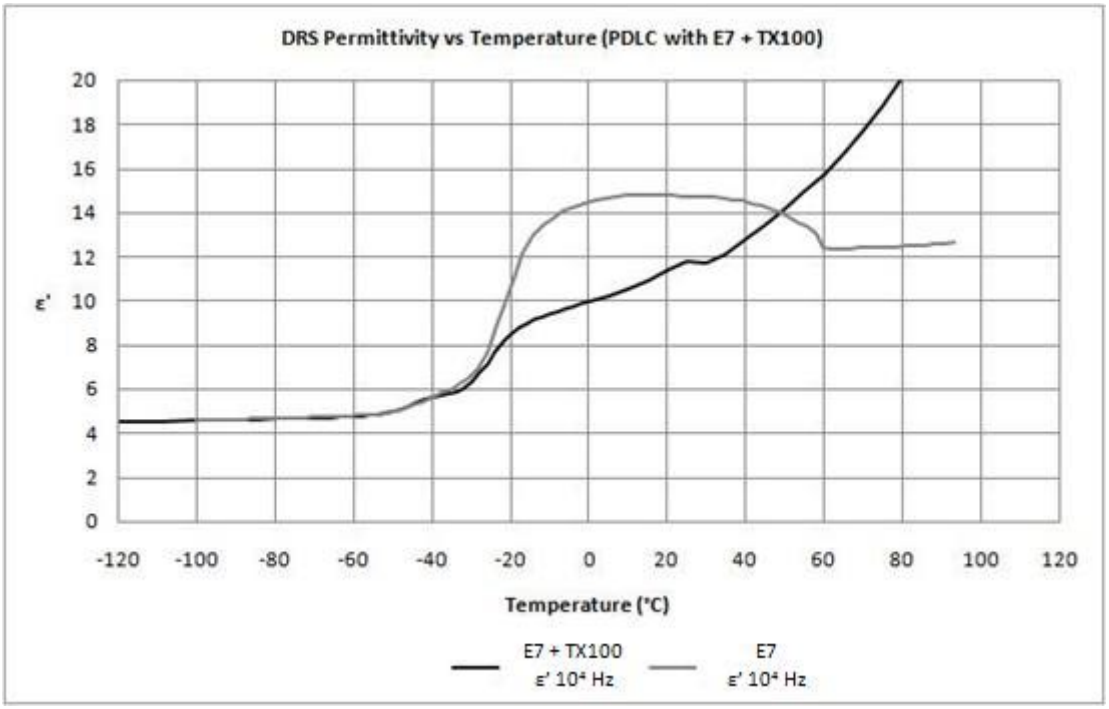


**Figure 5.14 – DRS of the mixture (E7/TX100) in a polymer matrix for ε'.**

In this composite no crystallization interferes with the measurements. Interesting is the absence of a clear nematic to isotropic transition of bulk $E7$, however, the discontinuity in both real, figure above, and imaginary, figure below, parts of the complex permittivity seems to indicate that the clearing point is shifted to a temperature close to $30\ ℃$. Once again, a polarized optical microscopy analysis helped

to clarify this. In the remaining temperature range only the signature of the liquid crystal is observed.

In Figure 5.15 is presented the dielectric relaxation spectroscopy analysis of the mixture containing the liquid crystal with the presence of the additive in a polymer matrix, for a frequency of $10^4\ Hz$, as well as the respective comparison with the polymer matrix containing only the liquid crystal, in grey.

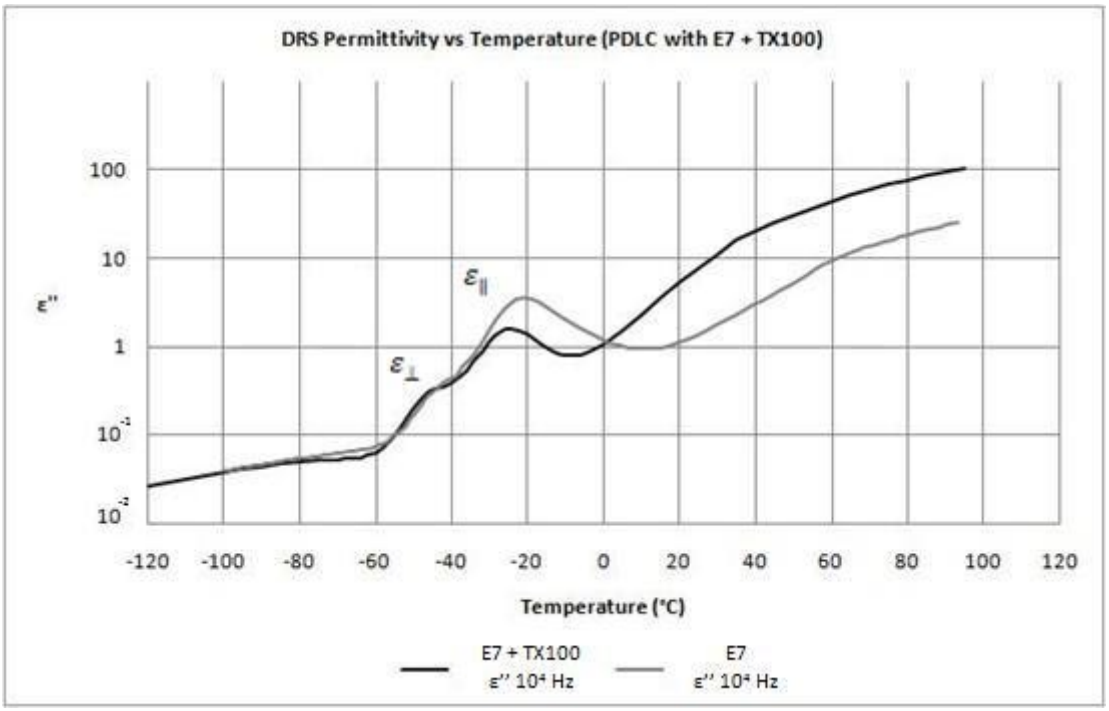


**Figure 5.15 – DRS of the mixture (E7/TX100) in a polymer matrix for ε''.**

Mainly, the observed behavior corresponds to bulk $E7$, although a small shift to lower temperatures of the maximum location of the peak occurs. This was confirmed in the isotherm analysis, where a deviation of the peak maximum was observed towards high frequencies, revealing an enhanced mobility of the liquid crystal in the polymer.

All the data collected for the composites in a polymer matrix was made with the poly(ethylene glycol) dimethacrylate for the assays containing polymer with liquid crystal only and tri(ethylene glycol) dimethacrylate for the assays containing polymer with the mixture of liquid crystal and surfactant.

## 5.3. Scanning Temperature in Polarized Optical Microscopy

A scanning temperature was made in polarized optical microscopy to verify the state transitions of the composite with triton X-100 as an additive and to understand what effect it has on the state transitions of $E7$ when mixed with it. Table 5.2 shows the state transitions observed for this mixture. These results were obtained under the circumstance of crossed polarizers.

**Table 5.2 – Nematic-isotropic and isotropic-nematic transitions of (E7/TX100).**

| State Transitions | LC + Surfactant[4] | LC + Surfactant[5] | PDLC |
|---|---|---|---|
| $T_{N\rightarrow I}$ | 52.3 ℃ | 59.5 ℃ | 36.9 ℃ |
| $T_{I\rightarrow N}$ | 38.9 ℃ | 45.5 ℃ | 32.3 ℃ |

These results confirm the previous differential scanning calorimetry and dielectric relaxation spectroscopy predictions for this system, that is, the transition properties of $E7$ have decreased when mixed with the surfactant, triton X-100.

The results obtained inside an indium tin oxide cell shows that the two components were already separated, once the state transition values are characteristic of the bulk $E7$. Therefore, the results that prove the additive effect in the state transitions of the liquid crystal are the ones obtained with a microscope slide and a cover slip right after stirred, to guarantee that both components were mixed when the scanning temperature was run.

Figure 5.16 illustrates the micrographs taken through polarized light with crossed polarizers, evidencing the moments before, during and after the nematic-isotropic transition, for the composite that contains, besides the liquid crystal and the surfactant, the use of tri(ethylene glycol) dimethacrylate photo polymerized.

[4] This measure was made with the mixture placed between a microscope slide and a cover slip, right after stirred.

[5] This measure was made with the mixture placed into an indium tin oxide cell, some time before stirring it.

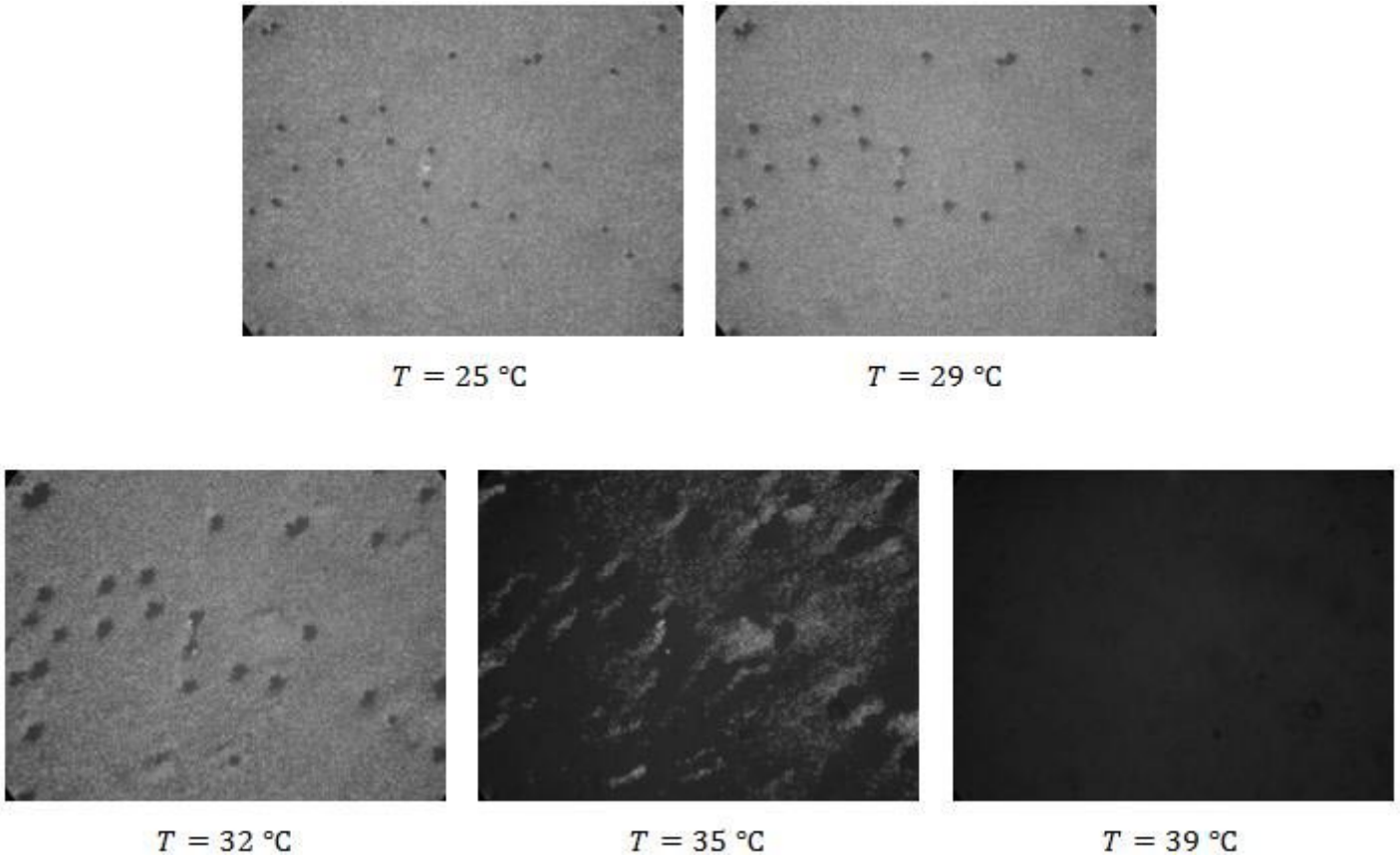


**Figure 5.16 – POM scanning temperature micrograph for (TRI/XDT/E7/TX100) on heating run.**

Meanwhile, after the clearing point, a cooling run was initiated for the observation of the opposite transition. Figure 5.17 illustrates the isotropic-nematic transition of the polymer dispersed liquid crystal.

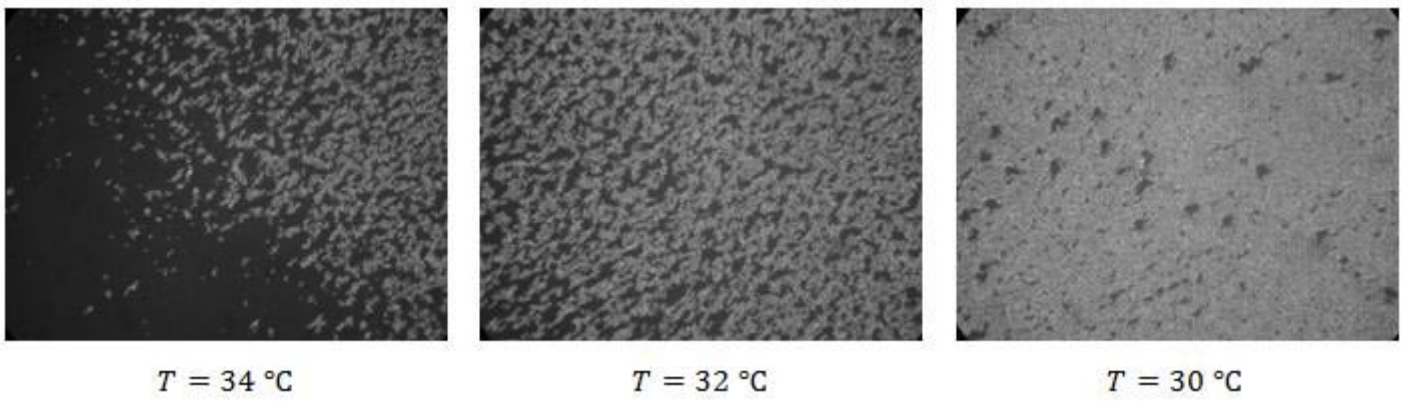


**Figure 5.17 – POM scanning temperature micrograph for (TRI/XDT/E7/TX100) on cooling run.**

# *Chapter Six*

## 6. Conclusion

From the results obtained in this study, it can be concluded that the best results were obtained with the system containing the triton X-100 as an additive.

For the results obtained with the different octanoic acid studies, addition order, quantity of additive used and chain length, respectively, for both monomers and polymerization initiators, a parameter selection can be made to choose which parameters best suit the device.

Therefore, with the information gathered with the analysis of the electro-optic results, the parameters that best fit in the polymer dispersed liquid crystal device are, generally, the addition of the surfactant to the mixture of polymer and liquid crystal, higher quantities of additive used and shorter chain lengths. An exception occurs with the thermal poly(ethylene glycol) dimethacrylate composite, where larger chain lengths and small amounts of additive proved to be more efficient.

For the results obtained in order of the monomer used, it is clearly seen that the suitable monomer is the poly(ethylene glycol) dimethacrylate. Some exceptions occur with the ethylene glycol and with the triton X-100. For the first case, the suitable monomer is the tri(ethylene glycol) dimethacrylate and for the second case, both the monomers fit very well with the respective additive. But in a general way, the poly(ethylene glycol) dimethacrylate seems better for the desired applications. Figures are placed in the appendix section for better observation of this comparison.

The fact that this monomer is better is related with its length, once it is larger than the other monomer used. This induces larger inner spaces in the surface of the polymer,

where more liquid crystal droplets can fit. Besides that, this monomer can achieve results where permanent memory effects are present, a peculiarity of it when compared with the other monomer used.

For the results obtained in order of the polymerization initiator used, it is clearly seen that both the polymerization initiators, the p-xylene N,N-diethyldithiocarbamate and the α,α'-azoisobutyronitrile are very similar, once for determined monomer the thermal initiator is better while for other monomer the photochemical initiator works better. Some exceptions also occur, in the cases of the octanoic acid and the triton X-100, because for both monomers, both polymerization initiators are quite similar and very effective. But in a general way, the p-xylene N,N-diethyldithiocarbamate seems better for the desired applications. Figures are placed in the appendix section for better observation of this comparison.

The fact that this polymerization initiator fits better to the polymer dispersed liquid crystal systems is related with its polymerization time and rate, which are considerably lower and faster, respectively, that if the thermal initiator was used.

Finally, for the results among all the additives used, it is explicit that the systems containing the addition of triton X-100 to the composites are the most effective and the ones that present a better performance, because low voltages and high transmittances are obtained. The worst scenario occurs with the addition of ethylene glycol, especially with the poly(ethylene glycol) dimethacylate photo and thermally polymerized. Figures are placed in the appendix section for better observation of this comparison.

Triton X-100 is the additive that has the best interaction with the composites, in particular, with the liquid crystal. The anisotropic components of the liquid crystal are altered when mixed with this surfactant, being that they are decreased for almost a half, as well as the state transitions of it that are slightly decreased, especially when mixed in the polymer matrix.

# *Chapter Seven*

## 7. Future Work

Many are the perspectives of future work in this field of investigation, which may contribute for a better comprehension of these systems and possible improvements in the operation and properties of the same.

No other liquid crystal, than $E7$, was used in this experimental work, so for future works, the use of other liquid crystals with electric and optic properties different from the one used in this work, could lead to the achievement of devices with different electro-optic properties, which could assure its use in other applications.

The same works for the monomers used, once no other than monomers based on ethylene glycol were used in this work. Thus, and knowing that the poly(ethylene glycol) dimethacrylate is a monomer that reproduced good results, for future works it would be recommended to use monomers similar to this one. Several new monomers were synthesized in a partnership of the project, also based on acrylate, but not tested yet. Others, as benzyl, phenyl and glycidyl methacrylate, were bought, once they are commercially available, but not tested yet.

The results obtained with the cetyl trimethyl ammonium bromide and the sodium dodecyl sulfate might be quite dubious, once those are solid compounds and it is a little hard to work with solid compounds to make the mixtures, once in the preparation of the indium tin oxide cells, some white material, probably corresponding to the powder of the additive do not fit in the cell, although most of the material does. Therefore, aqueous solutions of these surfactants, with subsequent solvent evaporation would help mixing them with the monomer and liquid crystal, so they

become more miscible. Triton X-100 is a possibility, once it is compatible with other ionic and non-ionic surfactants.

Another possible improvement would be the recurrent use of triton X-100, as part of the composite mixtures, because this was the most advantageous additive and the one that produced the most favorable results. For instance, its addition with the 4-phenylbenzonitrile might enhance the electro-optical properties of the devices. The triton X series includes several types of compounds, which could be tested to see if their performance equals the triton X-100.

# *Chapter Eight*

## 8. References


- Ahn, W., & Ha, K. (1999). Temperature Effects on LC Droplets Formation of PDLC Films with Thermoplastic Matrix. *Korea Polymer Journal 7* , 130-135.
- Aldrich. (1999). *Inhibitor removers and prepacked columns.* Technical Bulletin Al-154.
- Almeida, P. (2003). Estudo e optimização de um novo dispositivo electro-óptico tipo PDLC. *Dissertação de Doutoramento* .
- Almeida, P., Tavares, S., Martins, A., Godinho, M., Cidade, M., & Figueirinhas, J. (2002). Cross-linked hydroxypropylcellulose films: mechanical behaviour and electro-optical properties of PDLC type cells. *Optical Materials 20* , 97-100.
- Atkins, R., & West, J. *Effect of Thickness on PDLC Electro-Optics.* Ohio: Kent State University.
- Bedjaoui, L., Gogibus, N., Ewen, B., Pakula, T., Coqueret, X., Benmouna, M., et al. (2004). Preferential solvation of the eutectic mixture of liquid crystals E7 in a polysiloxane. *Polymer 45* , 6555-6560.
- Brás, A., Casimiro, T., Caldeira, J., & Aguiar-Ricardo, A. (2005). Solubility of the Nematic Liquid Crystal E7 in Supercritical Carbon Dioxide. *Journal of Chemical & Engineering Data 50* , 1857-1860.
- Brás, A., García, O., Viciosa, M., Martins, S., Sastre, R., Dias, C., et al. (2008). Dielectric relaxation studies and electro-optical measurements in poly(triethylene glycol dimethacrylate)/nematic E7 composites exhibiting an anchoring breaking transition. *Liquid Crystals 35* , 429-441.

- Choi, S., Park, N., & Suh, K. (1998). Electro-optical properties of Polymer Dispersed Liquid Crystal (PDLC) with ionic contents in matrix polymers. *Applied Chemistry 2* , 543-546.
- Chung, D., Tsuda, H., Chida, H., & Mochizuki, A. (1997). Effects and structural model of surfactants on the hysteresis behavior of polymer dispersed liquid crystals. *Molecular Crystals and Liquid Crystals 304* , 81-87.
- Collings, P. (2002). *Liquid Crystals - nature's delicate phase of matter.* New Jersey: Princeton University Press.
- Collings, P., & Hird, M. (2004). *Introduction to Liquid Crystals - Chemistry and Physics.* London: Taylor & Francis.
- Cook, W., Forsythe, J., Irawati, N., Scott, T., & Xia, W. (2003). Cure Kinetics and Thermomechanical Properties of Thermally Stable Photopolymerized Dimethacrylates. *Journal of Applied Polymer Science 90* , 3753-3766.
- Cupelli, D., Nicoletta, F., de Filpo, G., Chidichimo, G., Fazio, A., Gabriele, B., et al. (2004). Fine adjustment of conductivity in polymer-dispersed liquid crystals. *Applied Physics Letters 85* , 3292-3294.
- Deshmukh, R., & Malik, M. (2008). Effect of Temperature on the Optical and Electro-Optical Properties of Poly(methyl methacrylate)/E7 Polymer-Dispersed Liquid Crystal Composites. *Journal of Applied Polymer Science 109* , 627-637.
- Diogo, H., & Ramos, J. (2006). Are Crystallization and Melting the Reverse Transformation of Each Other? *Journal of Chemical Education 83* , 1389-1392.
- Doane, J. (2006). PDLC shutters: where has this technology gone? *Liquid Crystals 33* , 1313-1314.
- Fox, T. (1956). Factors Influencing Glass Formation and Crystallization in Polymers. *Bulletin of the American Physical Society 1* , 123.
- Goldstein, J., Newbury, D., Joy, D., Lyman, C., Echlin, P., Lifshin, E., et al. (2003). *Scanning Electron Microscopy and X-Ray Microanalysis.* New York: Kluwer Academic/Plenum Publishers.
- Gordon, W. (1997, May). *Virtual Textbook*. Retrieved from Polymers & Liquid Crystals Introduction: http://plc.cwru.edu/tutorial/enhanced/files/textbook.htm
- Han, J. (2006). Study of Memory Effects in polymer Dispersed Liquid Crystal Films. *Journal of the Korean Physical Society 49* , 1482-1487.

† Higgins, D., Hall, J., & Xie, A. (2005). Optical Microscopy Studies of Dynamics within Individual Polymer-Dispersed Liquid Crystal Droplets. *Accounts of Chemical Research 38* , 137-145.

† Huang, Z., Chidichimo, G., & Golemme, A. *The electrical field in a nematic droplet dispersed in polymer matrix.* Shandong: Valiant Fine Chemicals.

† Instec. (2008). *Liquid Crystal Cells and Cell Holder.* Colorado.

† Justice, R., Schaefer, D., Vaia, R., Tomlin, D., & Bunning, T. (2005). Interface morphology and phase separation in polymer-dispersed liquid crystal composites. *Polymer 46* , 4465-4473.

† Kalkar, A., Kunte, V., & Deshpande, A. (1999). *Electro-optic Studies on Polymer-Dispersed Liquid Crystal Composite Films. I. Composites of PVB-E7.* Mumbai: University of Mumbai.

† Karapinar, R. (1998). Electro-Optic Response of a Polymer Dispersed Liquid Crystal Film. *Journal of Physics 22* , 227-235.

† Kato, T., & Mizoshita, N. (2002). Self-assembly and phase segregation in functional liquid crystals. *Current Opinion in Solid State and Materials Science 6* , 579-587.

† Kim, B., & Woo, J. (2007). Surfactant Effects on Morphology and Switching of Holographic PDLCs Based on Polyurethane Acrylates. *ChemPhysChem 8* , 175-180.

† Kim, J., Kim, H., Lee, M., & Magda, J. (2004). Interfacial Tension of a Nematic Liquid Crystal/Water Interface with Homeotropic Surface Alignment. *Langmuir 20* , 8110-8113.

† Klosterman, J., Natarajan, L., Tondiglia, V., Sutherland, R., & White, T. (2004). The influence of surfactant in reflective HPDLC gratings. *Polymer 45* , 7213-7218.

† Koo, J., No, Y., Jeon, C., & Kim, J. (2008). Improvement of Electro-Optic Properties in PDLC Device by Using New Cross-Linker for the Control of the Contrast Ratio, Response Time and Driving Voltage. *Molecular Crystals and Liquid Crystals 491* , 58-66.

† Kremer, F., & Schönhals, A. (2002). *Broadband Dielectric Spectroscopy.* Verlag: Springer.

† Kuhn, H., Braslavsky, S., & Schmidt, R. (2004). Chemical Actinometry. *Pure and Applied Chemistry 76* , 2105-2146.

† Lee, J. (1999). Polymerization-induced phase separation. *Physical Review E 60* , 1930-1935.

† Levy, D., del Monte, F., Quintana, X., & Otón, J. (1997). Color Displays with Gel-Glass Dispersed Liquid Crystals. *Journal of Sol-Gel Science and Technology 8* , 1063-1066.

† Levy, O. (2000). Electro-optical phase shift in polymer dispersed liquid crystals. *The European Physical Journal E 3* , 11-20.

† Li, W., Cao, Y., Cao, H., Kashima, M., Kong, L., & Yang, H. (2008). Effects of the Structures of Polymerizable Monomers on the Electro-optical Properties of UV Cured polymer Dispersed Liquid Crystal Films. *Journal of Polymer Science 46* , 1369-1375.

† Liu, J., & Wu, F. (2005). Synthesis of Photoisometric Azobenzene Monomers and Model Compound Effect on Electric-Optical Properties in PDLC films. *Journal of Applied Polymer Science 97* , 721-732.

† Liu, Y., Sun, X., Dai, H., Liu, J., & Xu, K. (2004). Effect of surfactant on the electro-optical properties of holographic polymer dispersed liquid crystal Bragg gratings. *Optical Materials 27* , 1451-1455.

† Maiau, A. (2009). Preparation and Characterization of New PDLCs. *Unpublished* .

† Malik, P., & Raina, K. (2004). Droplet orientation and optical properties of polymer dispersed liquid crystal composite films. *Optical Materials 27* , 613-617.

† Martins, A. (2004). Cristais Líquidos - janelas inteligentes, mostradores flexíveis, papel digital... *JORTEC 2004* .

† Maschke, U., Coqueret, X., & Benmouna, M. (2002). Electro-Optical Properties of Polymer-Dispersed Liquid Crystals. *Macromolecular Rapid Communications 23* , 159-170.

† Merck, & KGaA. (2008). *Technical data sheet: E7.* Darmstadt: Licristal - Liquid Crystal Division.

† Mucha, M. (2002). Polymer as an important component of blends and composites with liquid crystals. *Progress in Polymer Science 28* , 837-873.

† Newport. (2009). *Light Sources*. Retrieved from Newport - Oriel sales: http://www.newport.com/Light-Sources/368011/1033/catalog.aspx

† Nicoletta, F., de Filpo, G., Iemma, F., & Chidichimo, G. (2000). OFF State Alignment in PDLCs by Polymerization of Monomer Additives. *Molecular Crystals and Liquid Crystals 339* , 159-166.

† Oh, J., & Rey, A. (2000). Theory and simulation of polymerization-induced phase separation in polymeric media. *Macromolecular Theory and Simulations 9* , 641-660.

† Olympus. *Basics of Polarizing Microscopy.*

† Otsu, T., & Kuriyama, A. (1984). Living mono and biradical polymerizations in homogeneous system synthesis of AB and ABA type block copolymers. *Polymer Bulletin 11* , 135-142.

† Park, N., Cho, S., Kim, J., & Suh, K. (2000). Preparation of Polymer-Dispersed Liquid Crystal Films Containing a Small Amount of Liquid Crystalline Polymer and Their Properties. *Journal of Applied Polymer Science 77* , 3178-3188.

† Patnaik, S., & Pachter, R. (1998). Anchoring characteristics and interfacial interactions in a polymer dispersed liquid crystal: a molecular dynamics study. *Polymer 40* , 6507-6519.

† Pogue, R., Natarajan, L., Siwecki, S., Tondiglia, V., Sutherland, R., & Bunning, T. (2000). Monomer functionality effects in the anisotropic phase separation of liquid crystals. *Polymer 41* , 733-741.

† Senyuk, B. (2006, Summer). *Liquid Crystals: a Simple View on a Complex Matter*. Retrieved from Kent State University SPIE Student Chapter: http://dept.kent.edu/spie/liquidcrystals/

† Shim, S., Woo, J., Kim, H., & Kim, B. (2008). Effects of surfactant and molecular weight of polyol on grating formation and switching of holographic PDLC. *Polymers for Advanced Tecnhologies 19* , 1550-1557.

† Stoenescu, D., Martinot-Lagarde, P., & Dozov, I. (1999). Anchoring Transition Dominated by Surface Memory Effect. *Molecular Crystals and Liquid Crystals 329* , 339-348.

† Stoiber, R., & Morse, S. (1994). *Crystal Identification with the Polarizing Microscope.* London: Chapman & Hall.

† Torgova, S., Dorozhkina, G., Novoseletskii, N., & Umanskii, B. (2004). Investigation of memory effect in dichroic dyes based PDLC films. *Molecular Crystals and Liquid Crystals 412* , 513-517.

† Tsvetkov, V., Tsvetkov, O., & Balandin, V. (1999). Anisotropic Properties of the LC Surface Tension. *Molecular Crystals and Liquid Crystals 329* , 305-312.

† Wang, P., & MacDiarmid, A. (2007). Integration of polymer-dispersed liquid crystal composites with conducting polymer thin film toward the fabrication of flexible display devices. *Displays 28* , 101-104.

† White, T., Natarajan, L., Bunnings, T., & Guymon, C. (2007). Contribution of monomer functionality and additives to polymerization kinetics and liquid crystal phase separation in acrylate-based polymer-dispersed liquid crystals (PDLCs). *Liquid Crystals 34* , 1377-1385.

† Xinology. (2008). *PDLC Film/PDLC Glass - Polymer Dispersed Liquid Crystal Film/Glass*. Retrieved from Xinology: http://www.xinology.com/en/eg_cpml_laminat_pdlc.htm

† Zhang, W., Lin, J., Yu, T., Lin, S., & Yang, D. (2003). Effect of electric field on phase separation of polymer dispersed liquid crystal. *European Polymer Journal 39* , 1635-1640.

# Appendix Section

## A.1. Comparison between Monomers

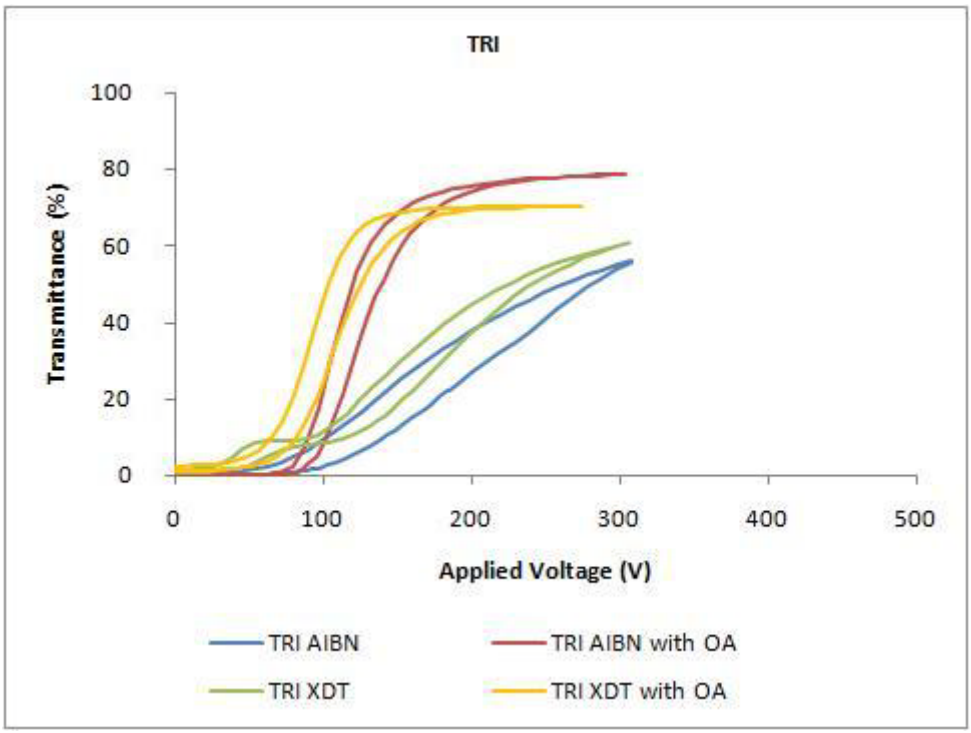


**Figure A.1 - Electro-optic response of the systems based on (TRI/E7) with and without OA for a 20 µm cell gap.**

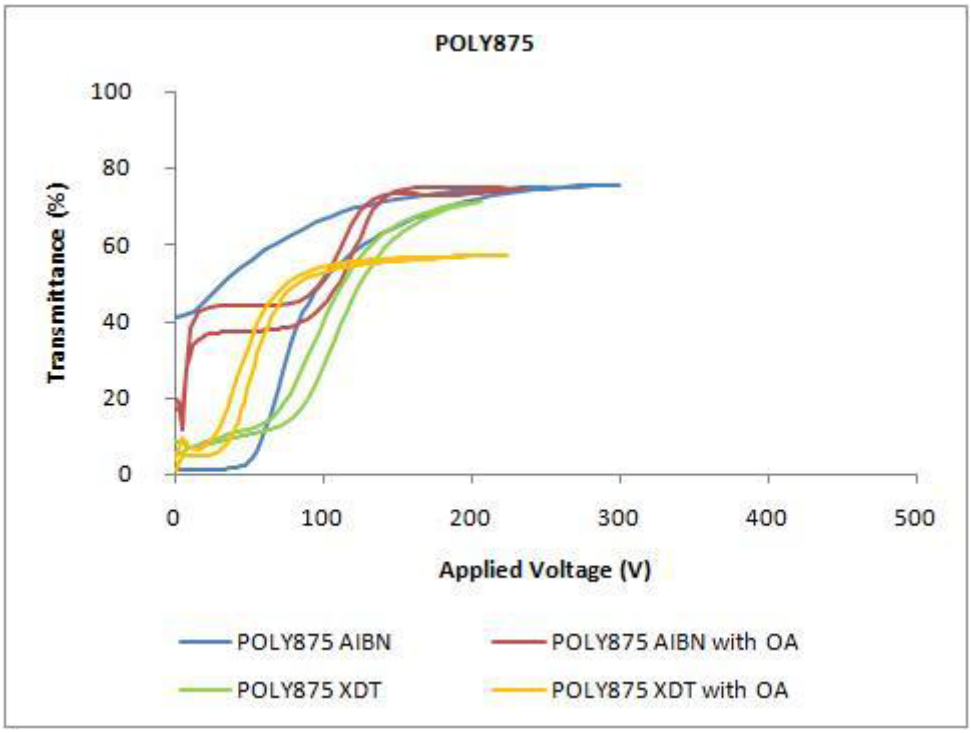


**Figure A.2 – Electro-optic response of the systems based on (POLY875/E7) with and without OA for a 20 µm cell gap.**

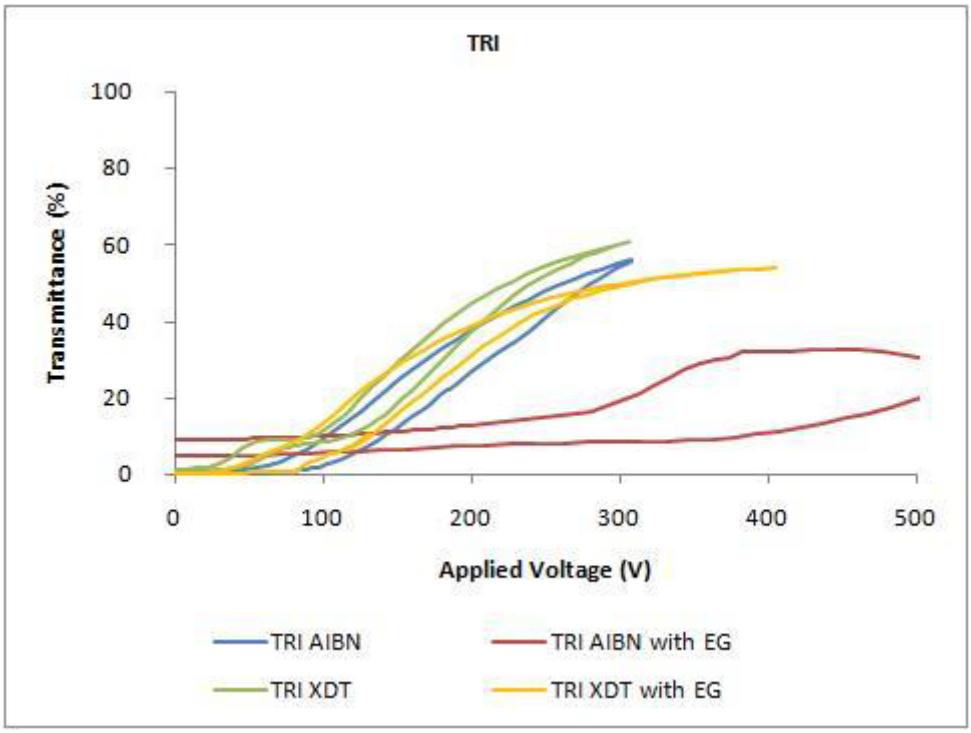


**Figure A.3 – Electro-optic response of the systems based on (TRI/E7) with and without EG for a 20 µm cell gap.**

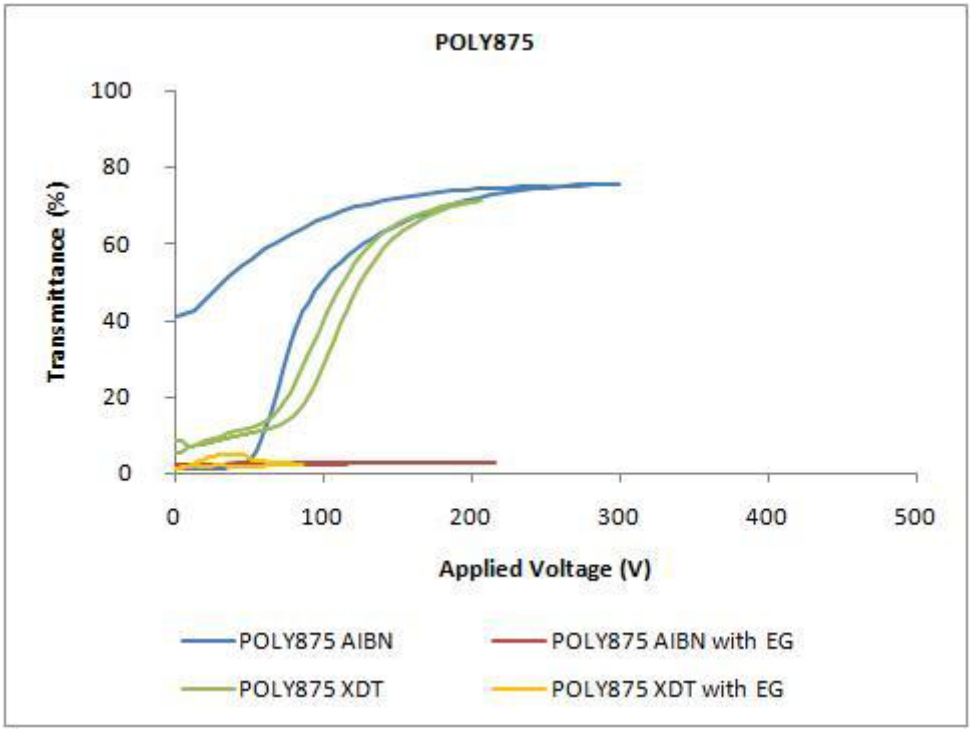


**Figure A.4 – Electro-optic response of the systems based on (POLY875/E7) with and without EG for a 20 µm cell gap.**

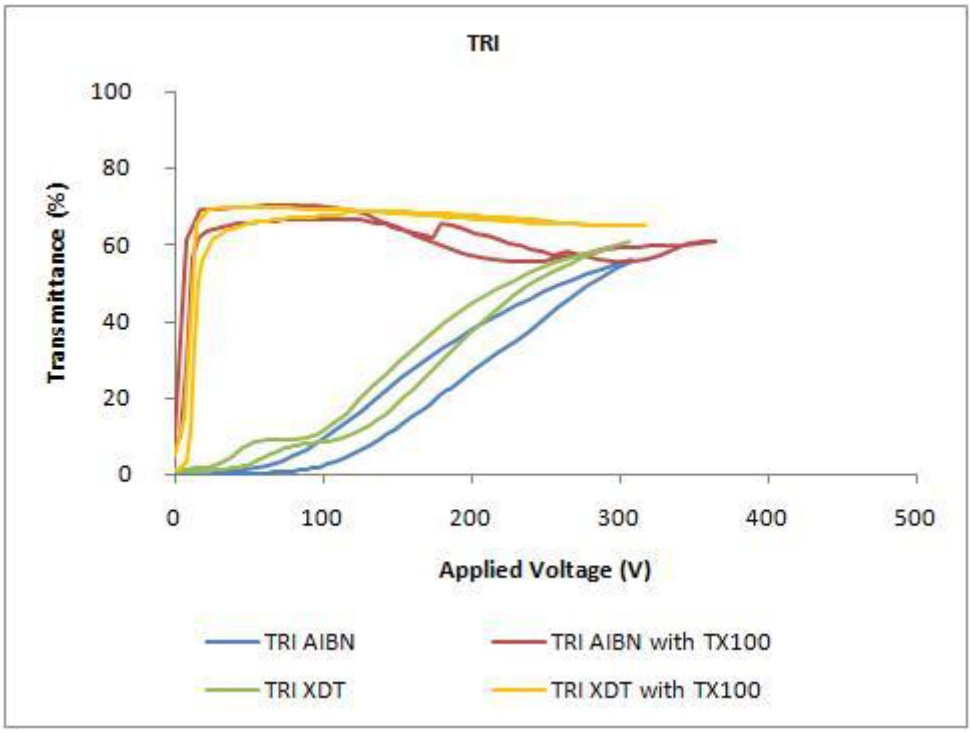


**Figure A.5 – Electro-optic response of the systems based on (TRI/E7) with and without TX100 for a 20 µm cell gap.**

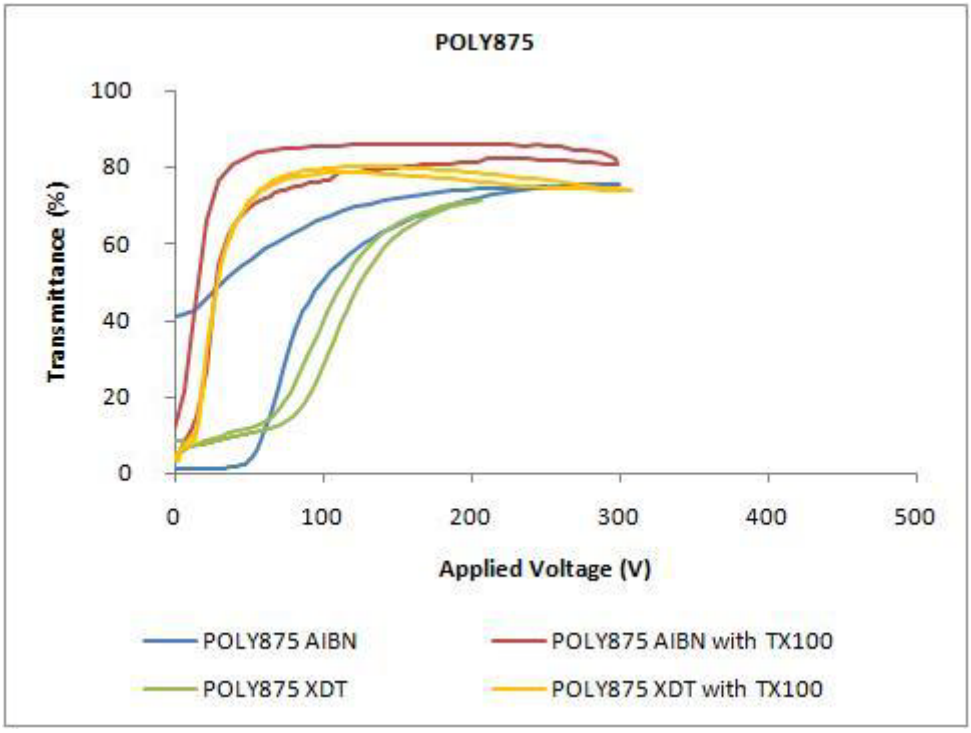


**Figure A.6 – Electro-optic response of the systems based on (POLY875/E7) with and without TX100 for a 20 µm cell gap.**

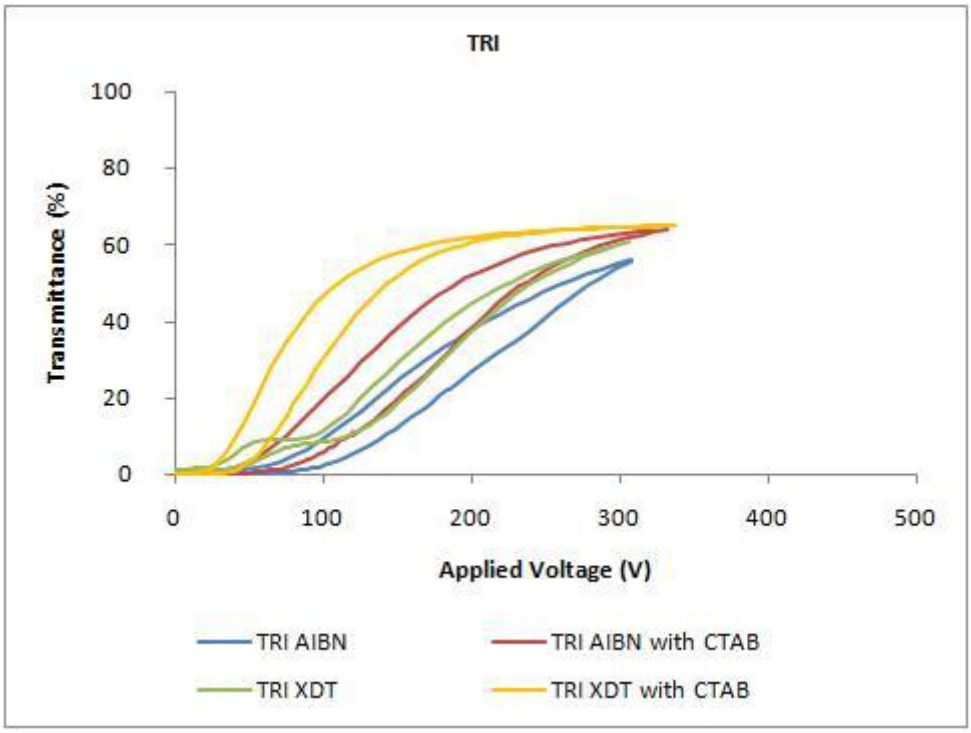


**Figure A.7 – Electro-optic response of the systems based on (TRI/E7) with and without CTAB for a 20 µm cell gap.**

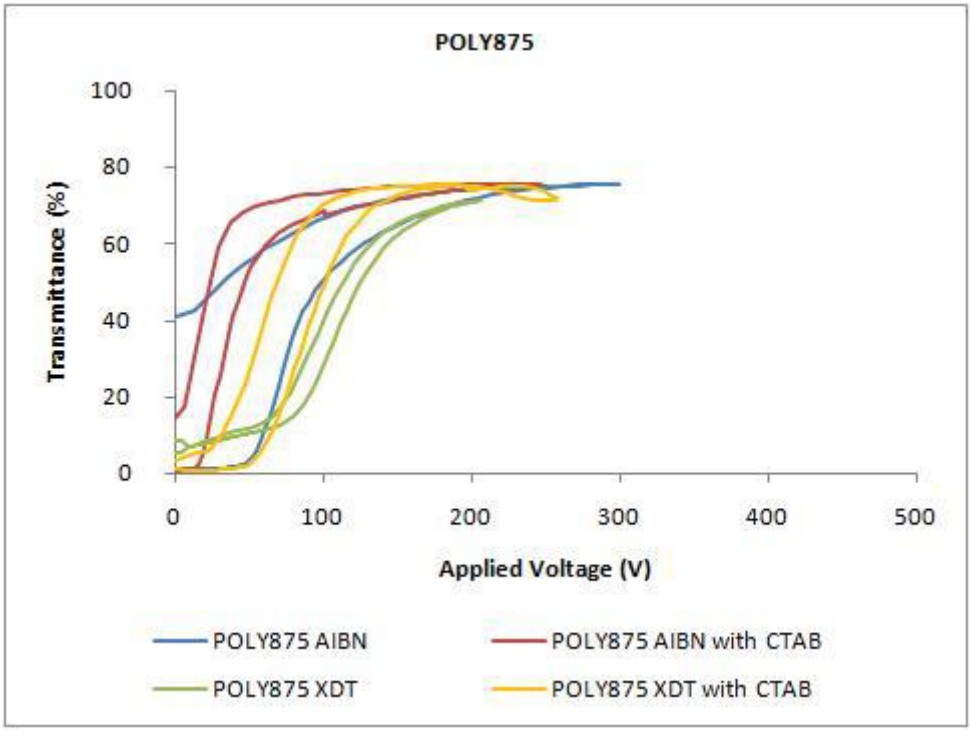


**Figure A.8 – Electro-optic response of the systems based on (POLY875/E7) with and without CTAB for a 20 µm cell gap.**

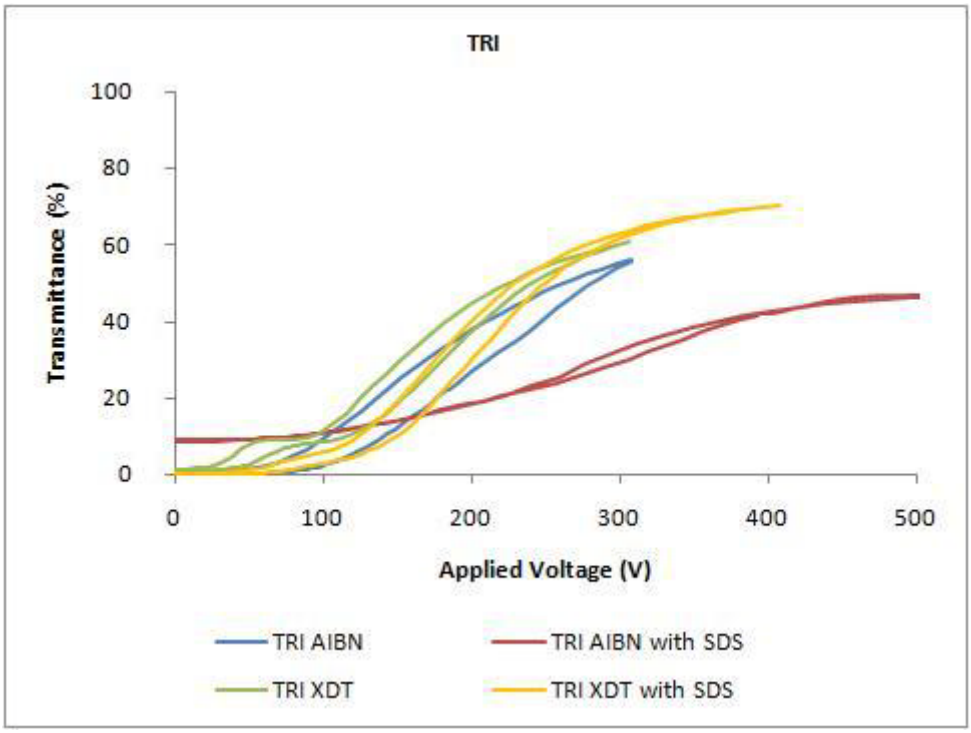


**Figure A.9 – Electro-optic response of the systems based on (TRI/E7) with and without SDS for a 20 µm cell gap.**

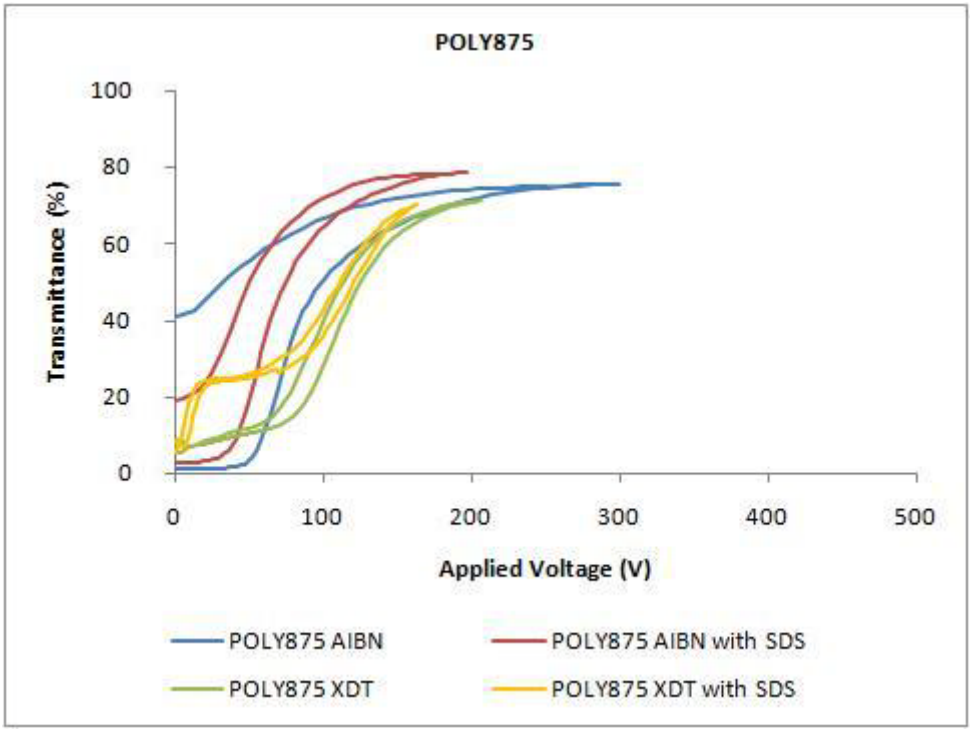


**Figure A.10 – Electro-optic response of the systems based on (POLY875/E7) with and without SDS for a 20 µm cell gap.**

## A.2. Comparison between Polymerization Initiators

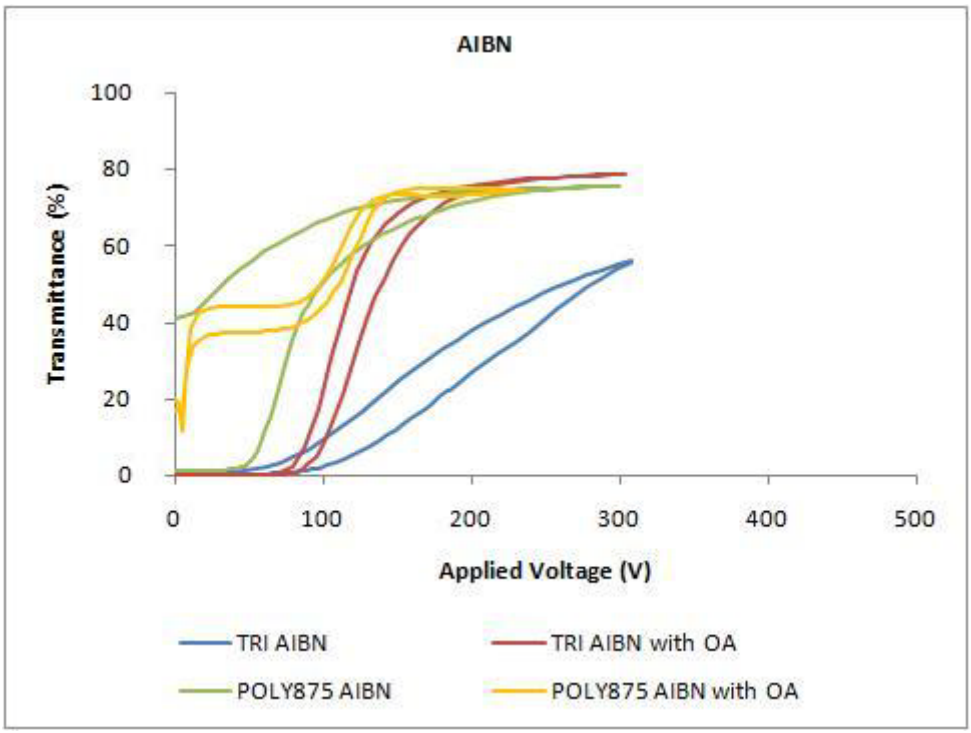


**Figure A.11 - Electro-optic response of the systems based on (AIBN/E7) with and without OA for a 20 µm cell gap.**

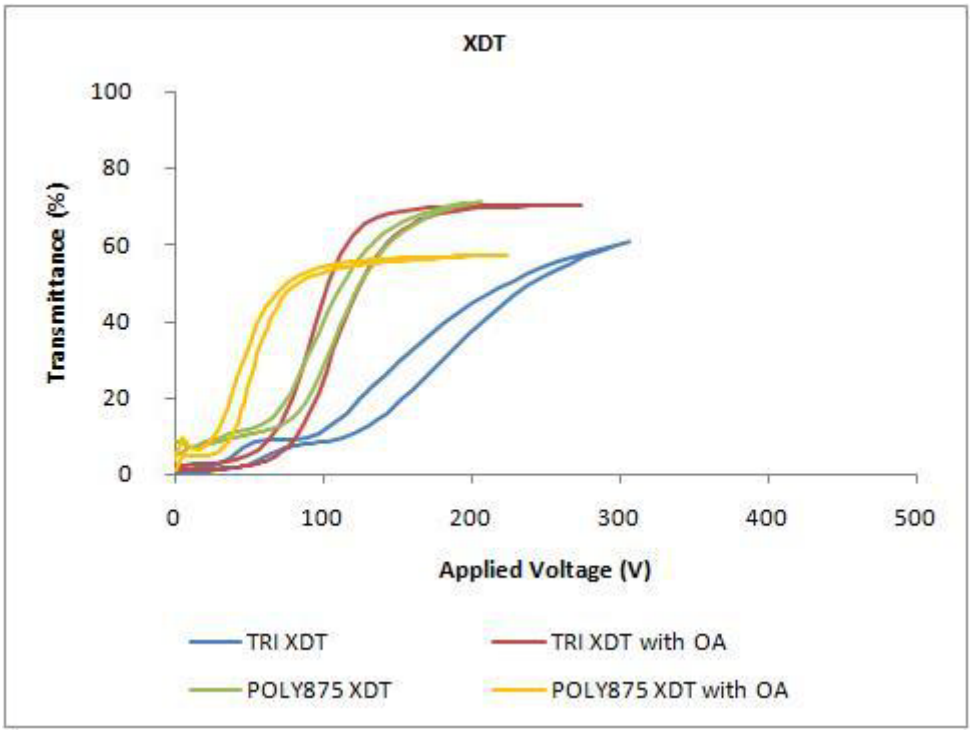


**Figure A.12 – Electro-optic response of the systems based on (XDT/E7) with and without OA for a 20 µm cell gap.**

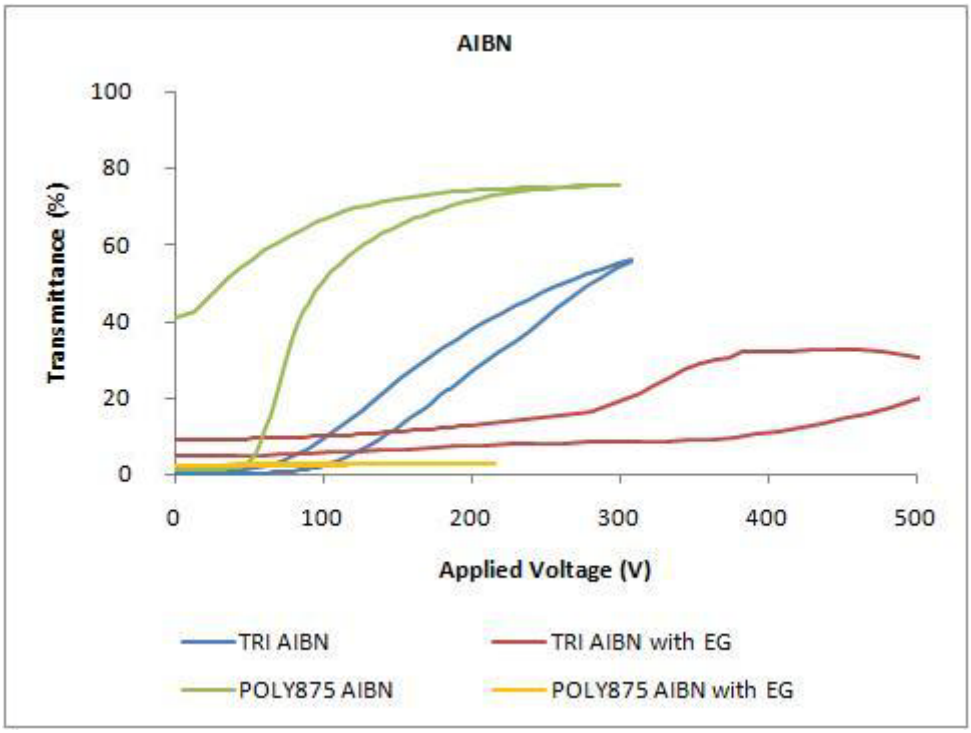


**Figure A.13 – Electro-optic response of the systems based on (AIBN/E7) with and without EG for a 20 µm cell gap.**

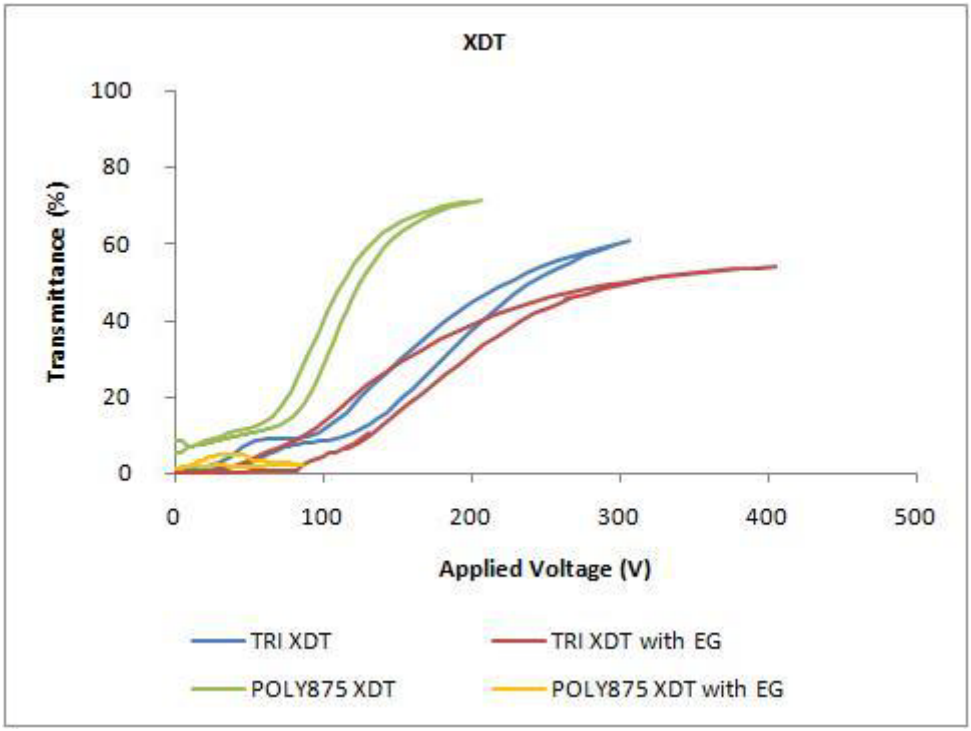


**Figure A.14 – Electro-optic response of the systems based on (XDT/E7) with and without EG for a 20 µm cell gap.**

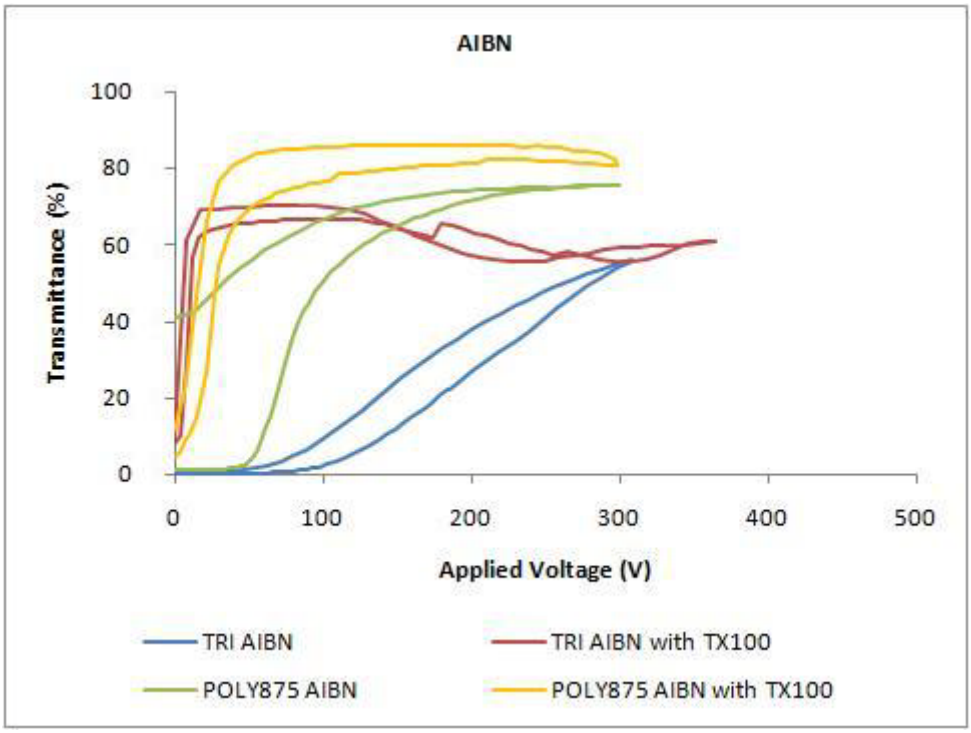


**Figure A.15 – Electro-optic response of the systems based on (AIBN/E7) with and without TX100 for a 20 µm cell gap.**

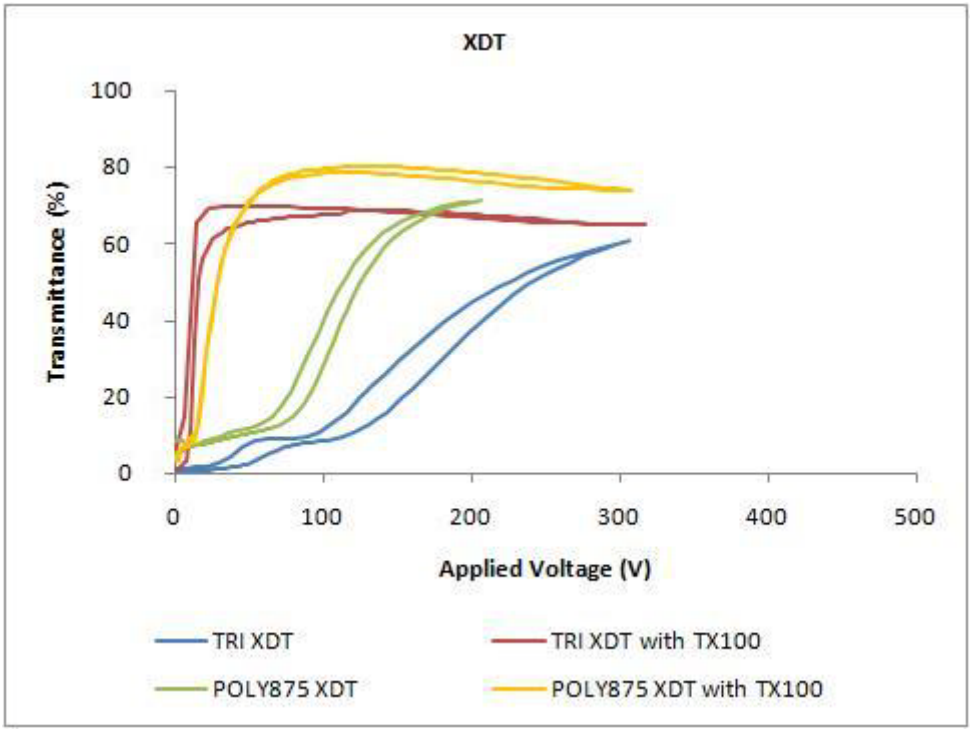


**Figure A.16 – Electro-optic response of the systems based on (XDT/E7) with and without TX100 for a 20 µm cell gap.**

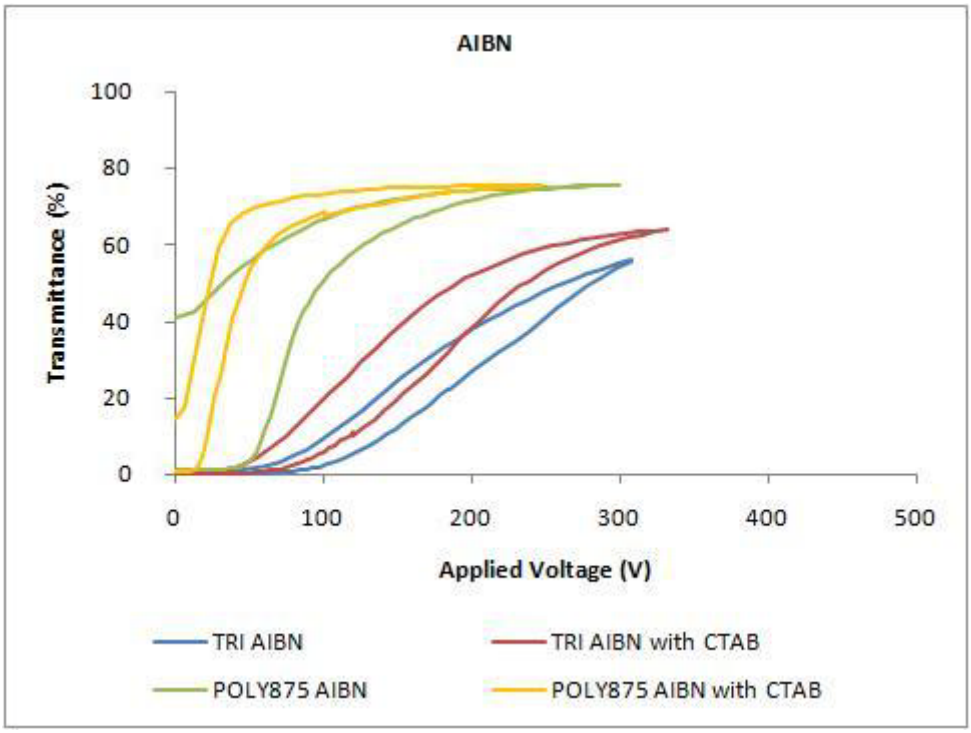


**Figure A.17 – Electro-optic response of the systems based on (AIBN/E7) with and without CTAB for a 20 µm cell gap.**

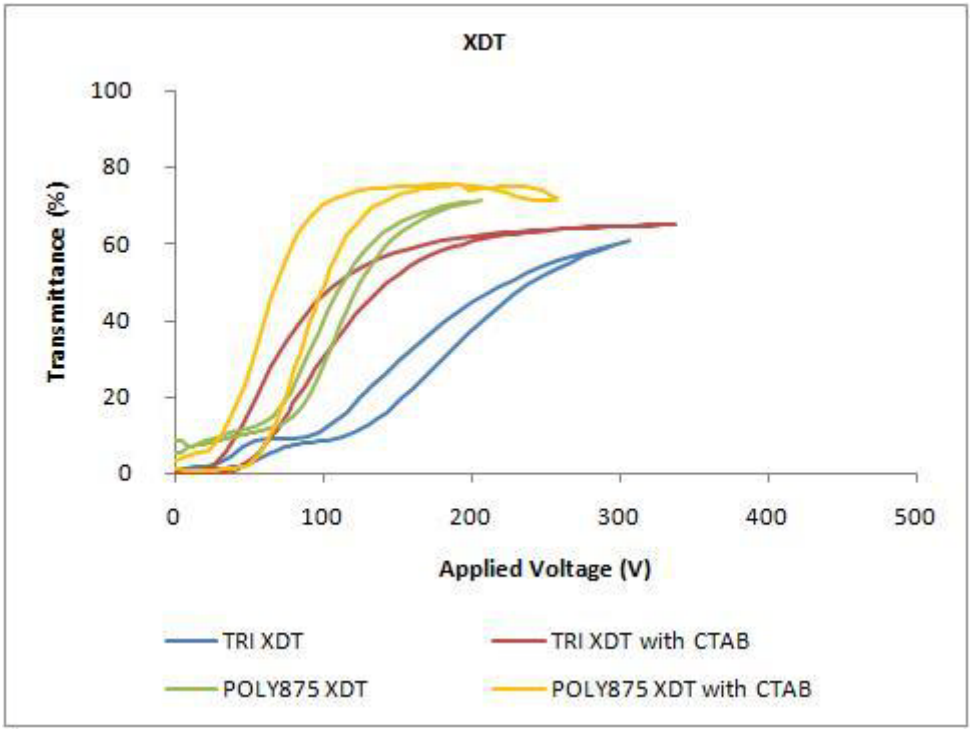


**Figure A.18 – Electro-optic response of the systems based on (XDT/E7) with and without CTAB for a 20 µm cell gap.**

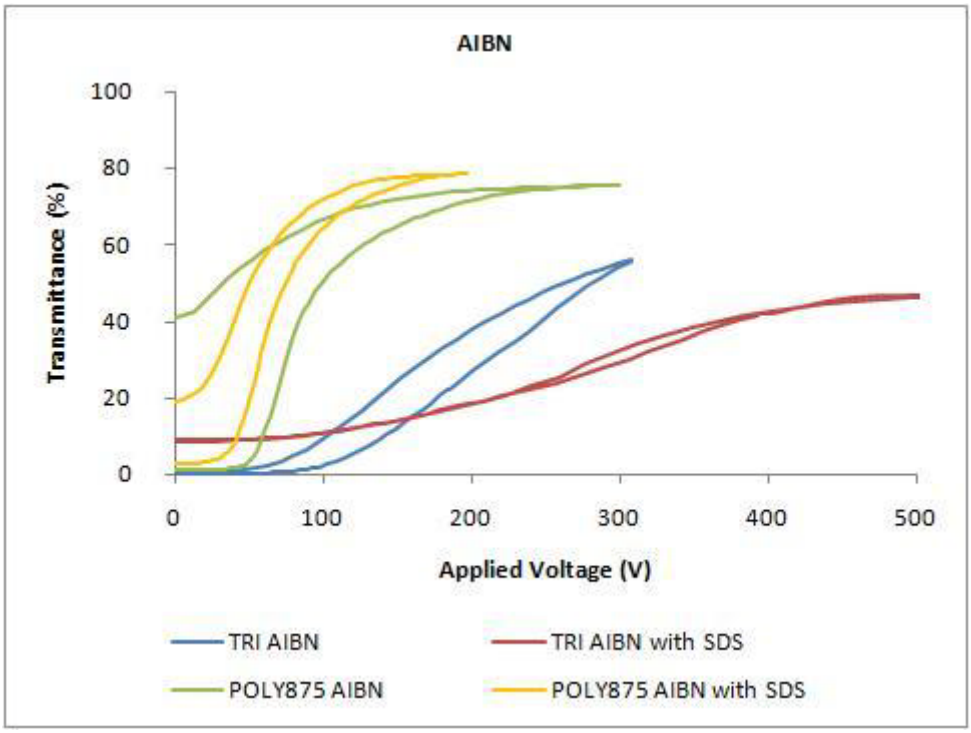


**Figure A.19 – Electro-optic response of the systems based on (AIBN/E7) with and without SDS for a 20 µm cell gap.**

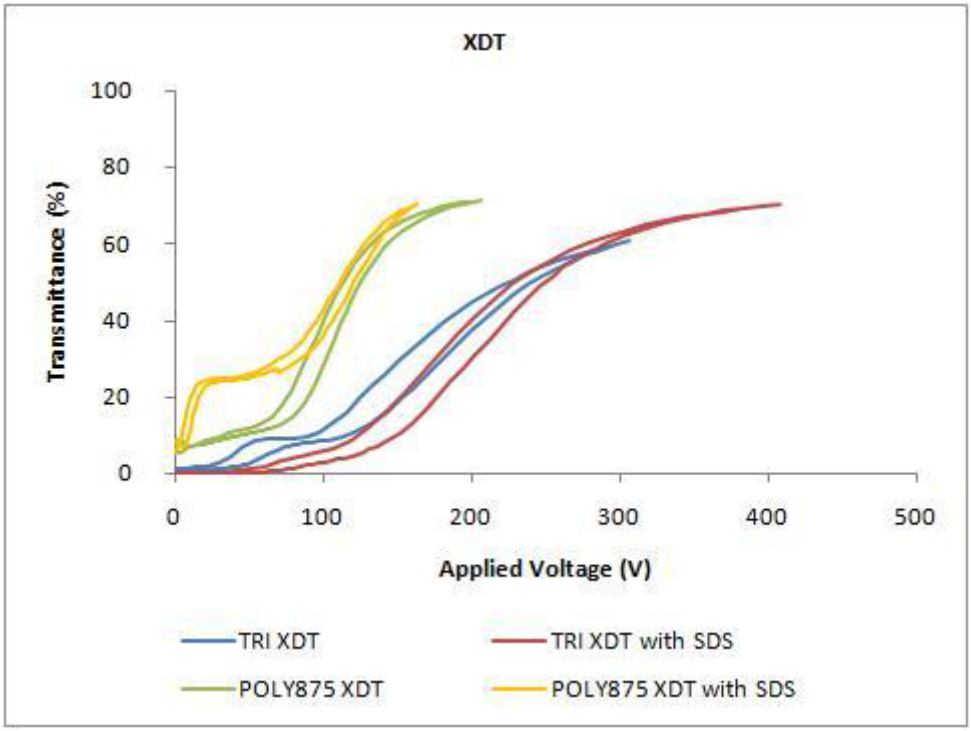


**Figure A.20 – Electro-optic response of the systems based on (XDT/E7) with and without SDS for a 20 µm cell gap.**

## A.3. Comparison between Additives

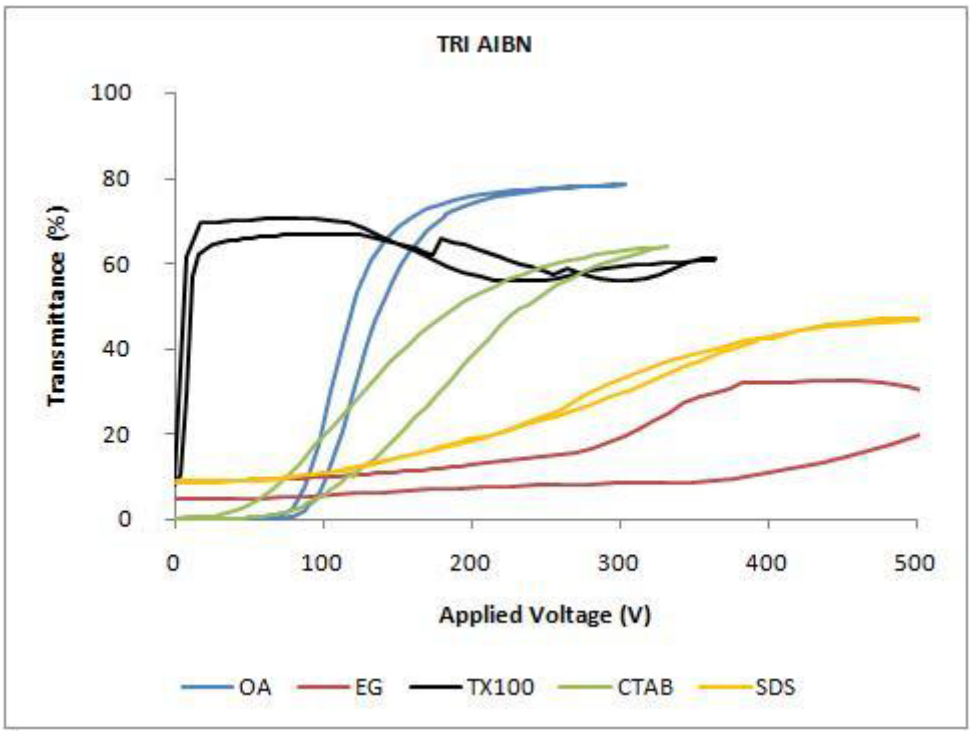


**Figure A.21 – Electro-optic response of the systems based on (TRI/AIBN/E7) for a 20 µm cell gap.**

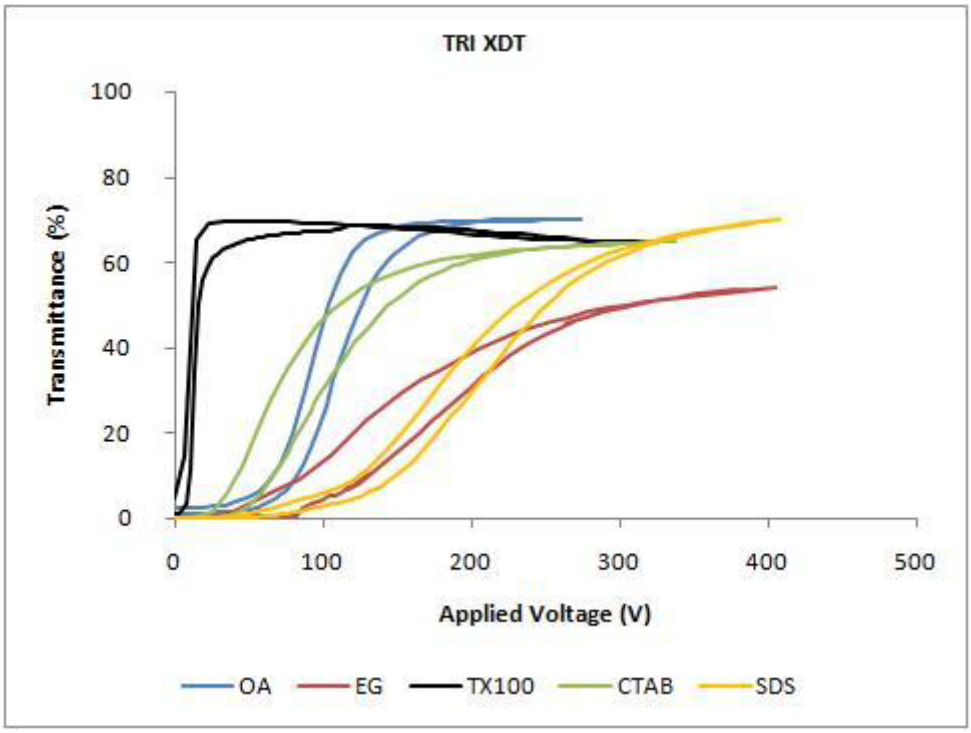


**Figure A.22 – Electro-optic response of the systems based on (TRI/XDT/E7) for a 20 µm cell gap.**

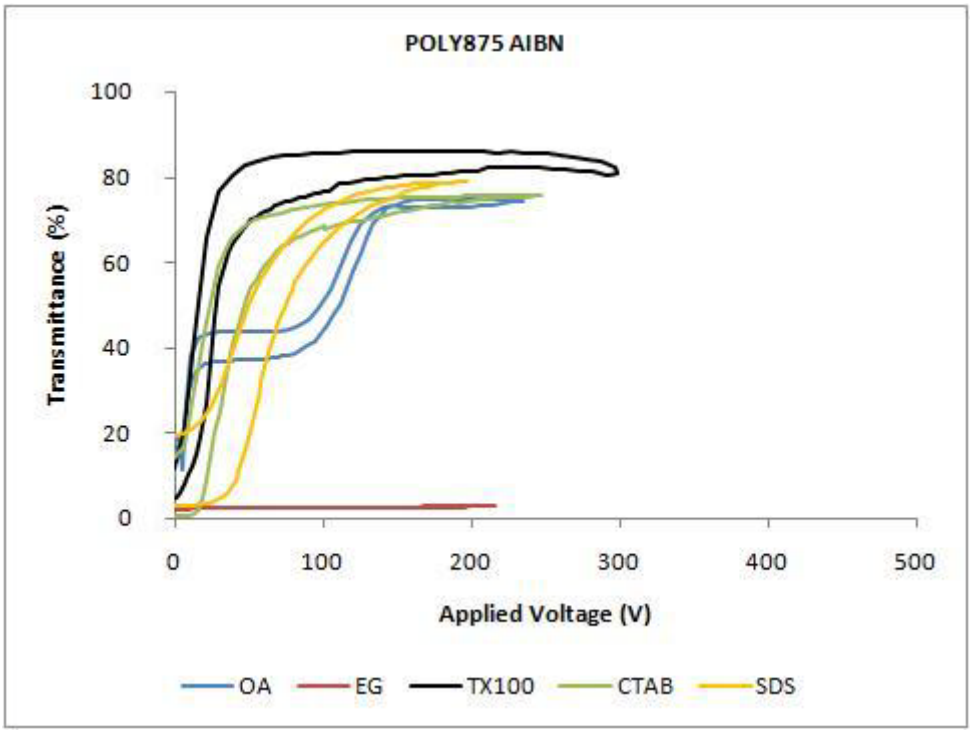


**Figure A.23 – Electro-optic response of the systems based on (POLY875/AIBN/E7) for a 20 µm cell gap.**

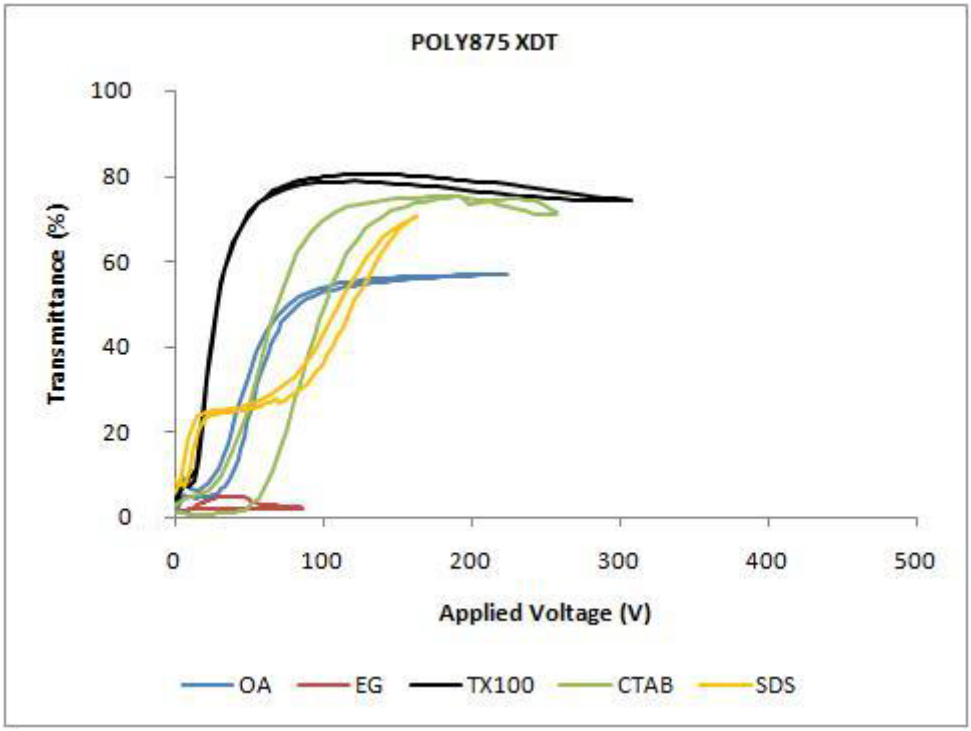


**Figure A.24 – Electro-optic response of the systems based on (POLY875/XDT/E7) for a 20 µm cell gap.**

## A.4. Dielectric Relaxation Spectroscopy of the Liquid Crystal

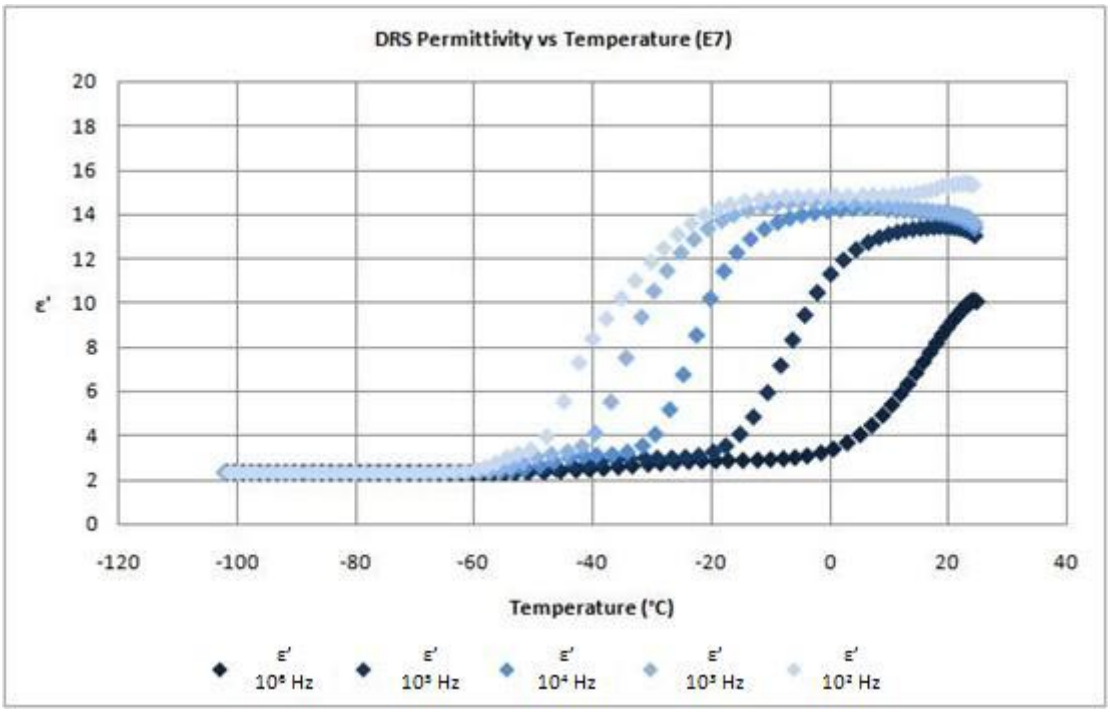


**Figure A.25 – DRS of E7 on cooling illustrating several frequencies for ε'.**

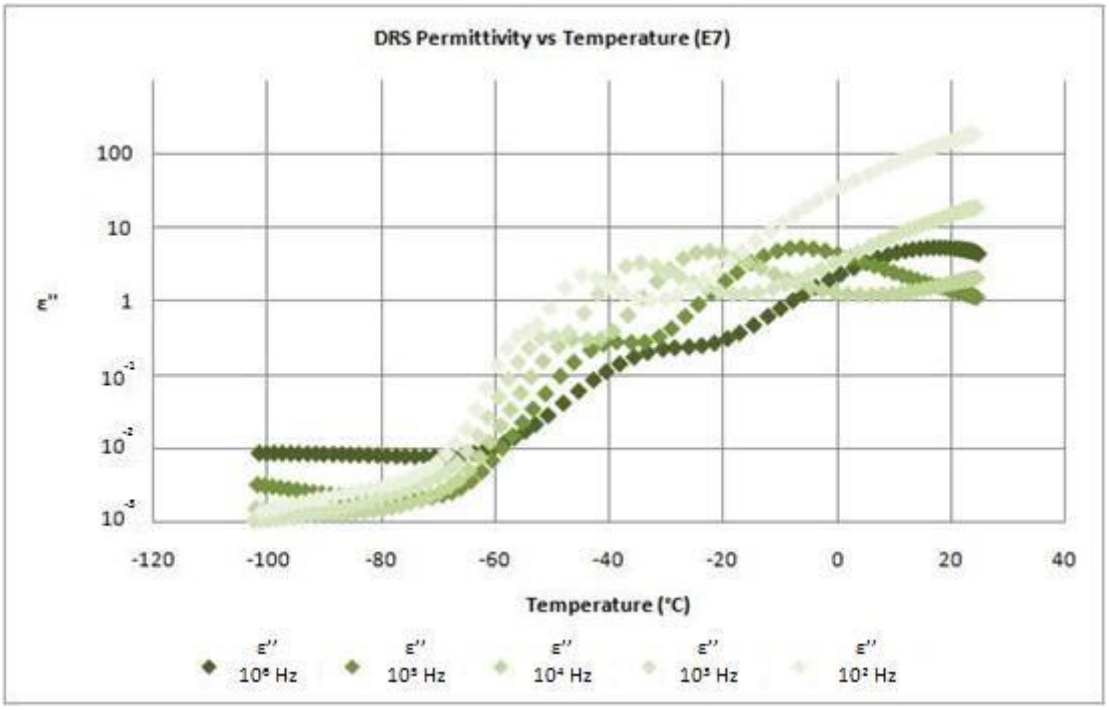


**Figure A.26 – DRS of E7 on cooling illustrating several frequencies for ε''.**

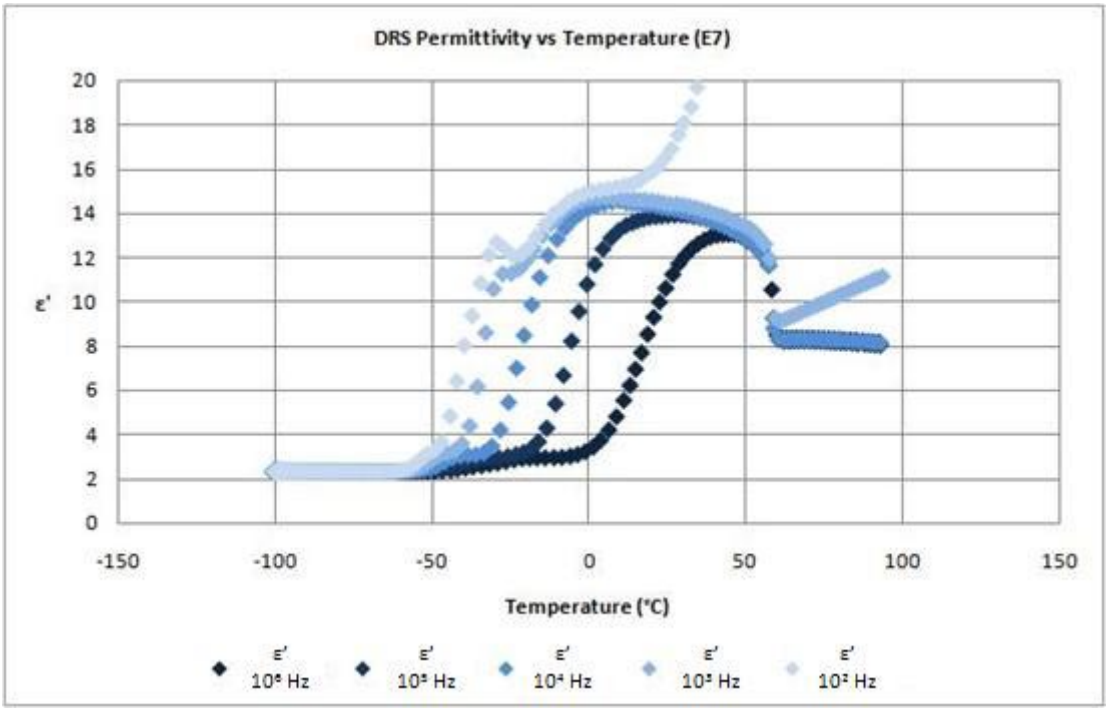


**Figure A.27 – DRS of E7 on heating illustrating several frequencies for ε'.**

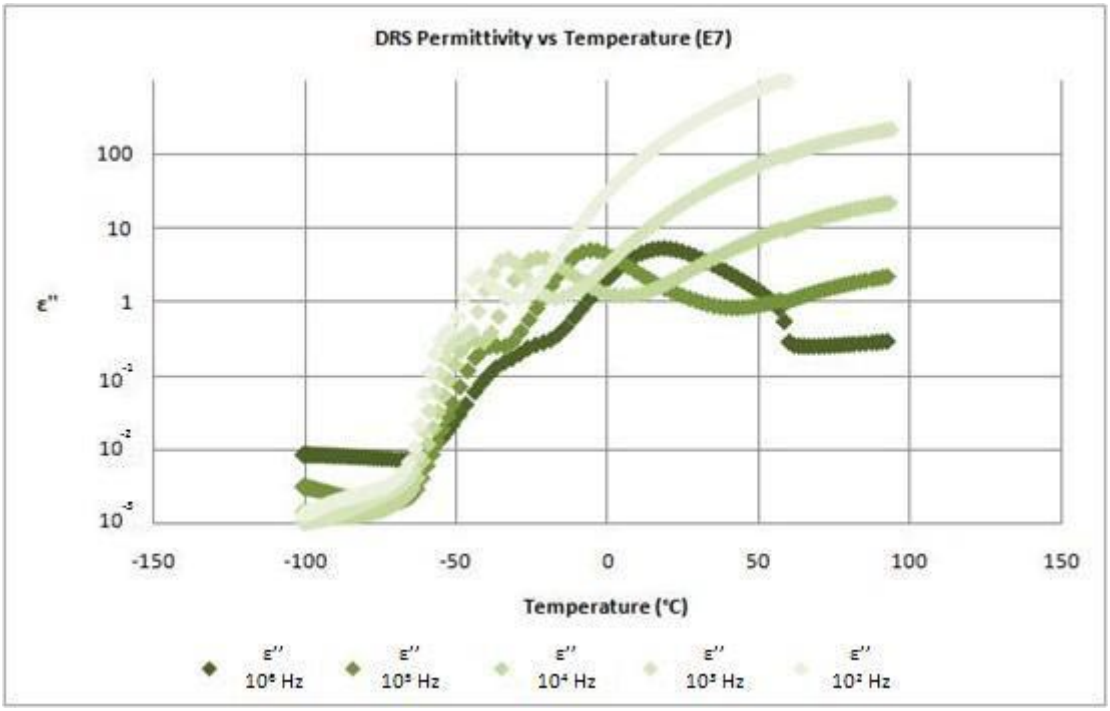


**Figure A.28 – DRS of E7 on heating illustrating several frequencies for ε''.**

## A.5. Dielectric Relaxation Spectroscopy of the Surfactant

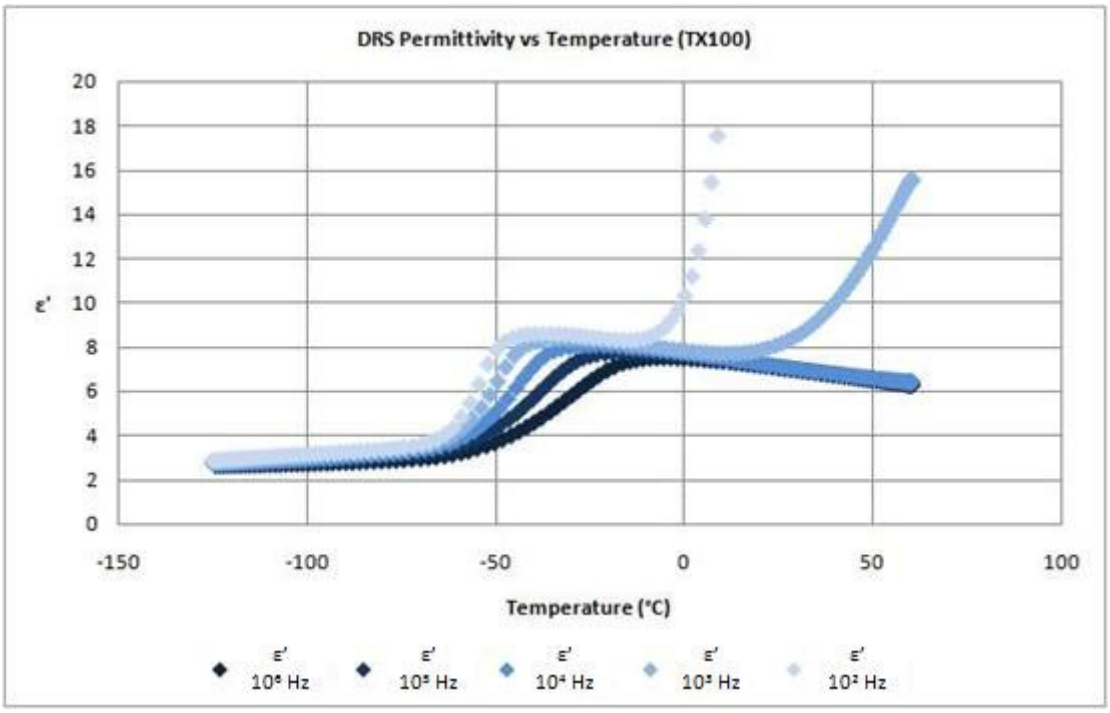


**Figure A.29 – DRS of TX100 on cooling illustrating several frequencies for ε'.**

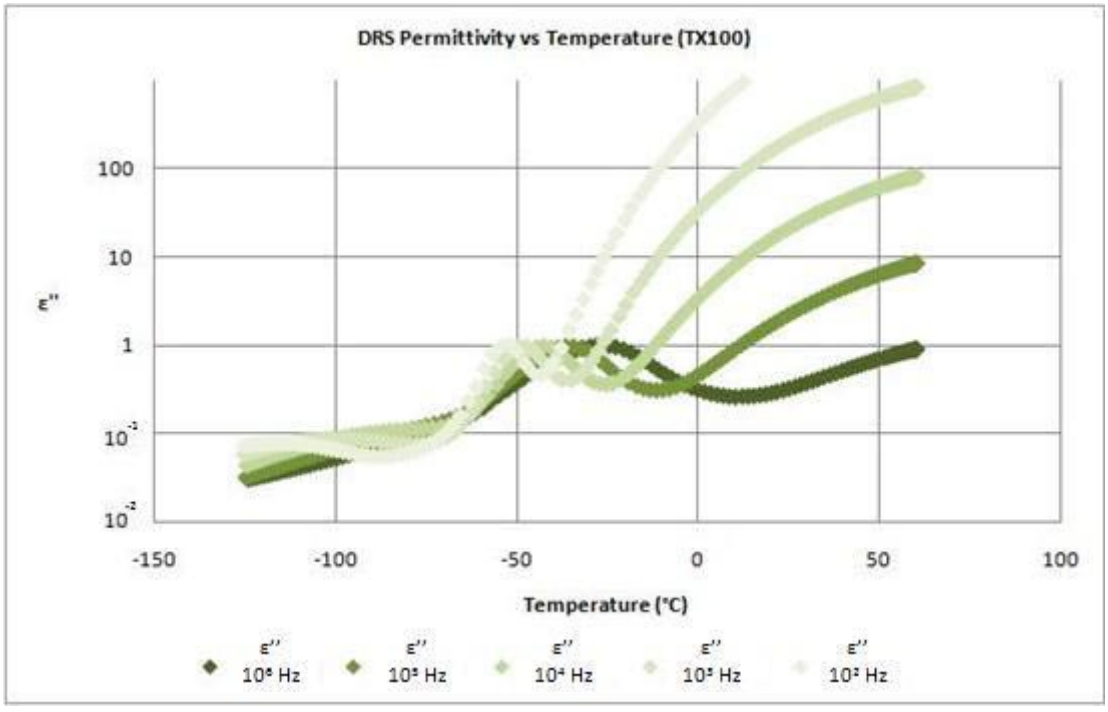


**Figure A.30 – DRS of TX100 on cooling illustrating several frequencies for ε''.**

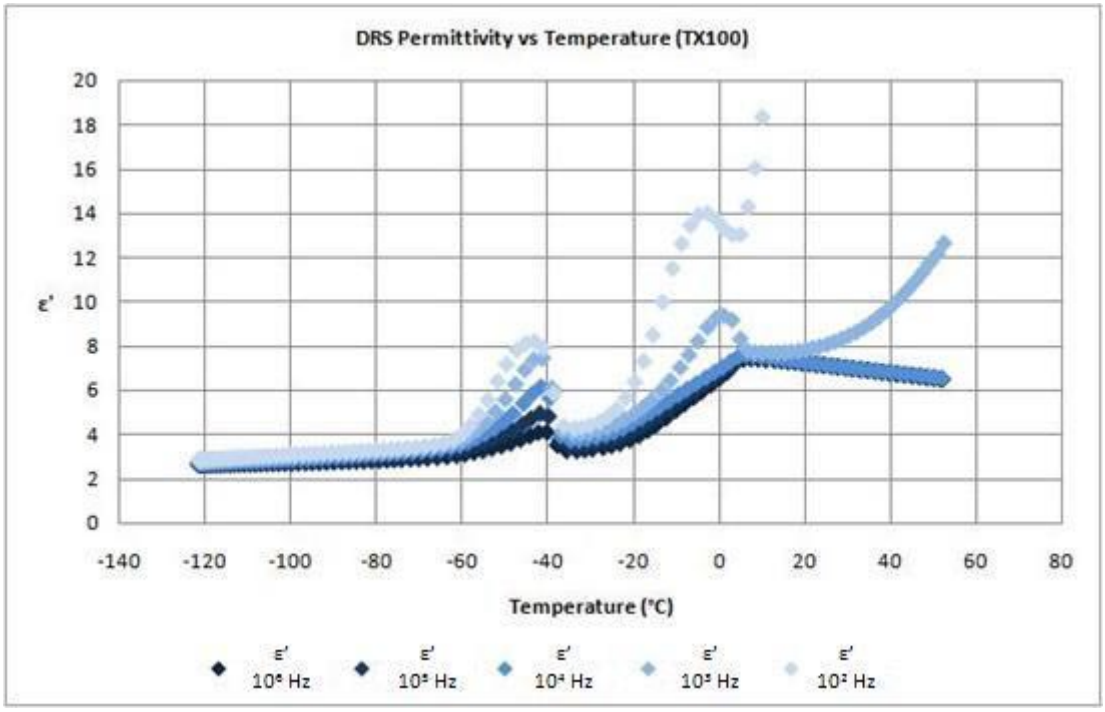


**Figure A.31 – DRS of TX100 on heating illustrating several frequencies for ε'.**

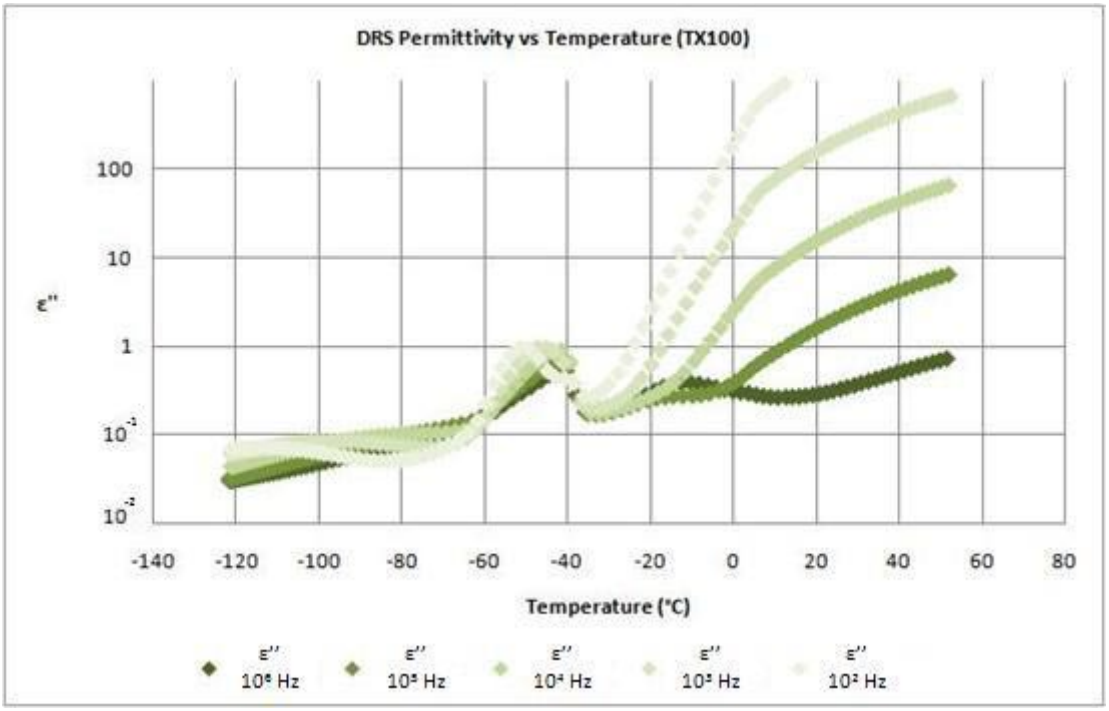


**Figure A.32 – DRS of TX100 on heating illustrating several frequencies for ε''.**

## A.6. Dielectric Relaxation Spectroscopy of the Mixture

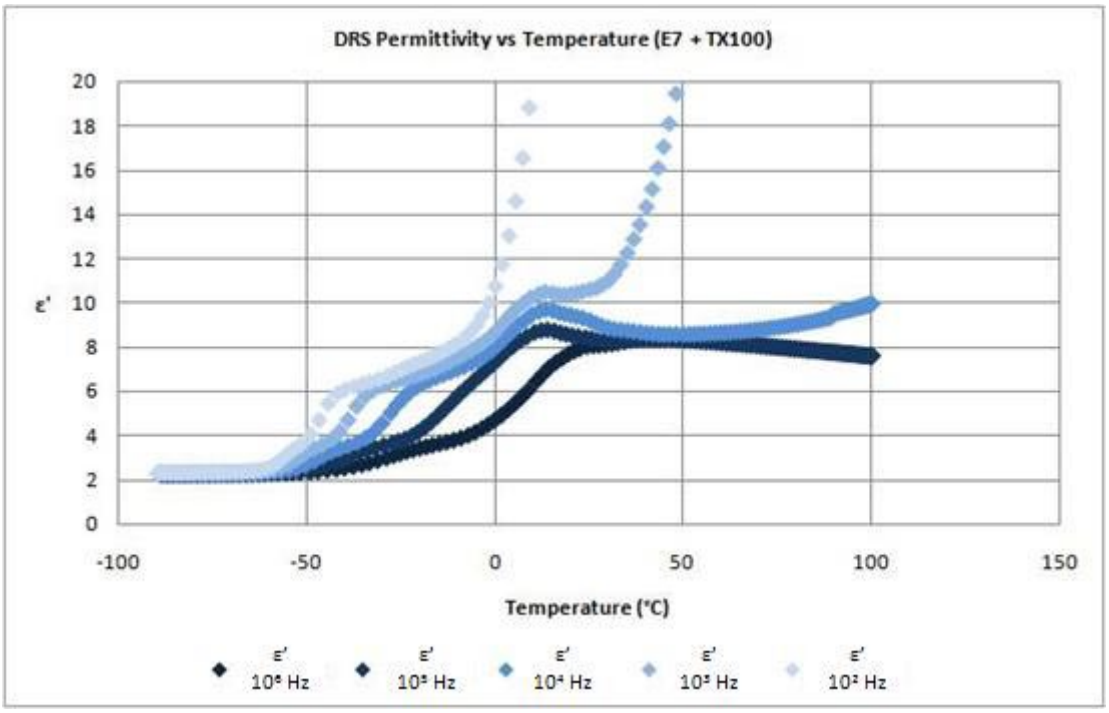


**Figure A.33 – DRS of the mixture on cooling illustrating several frequencies for ε'.**

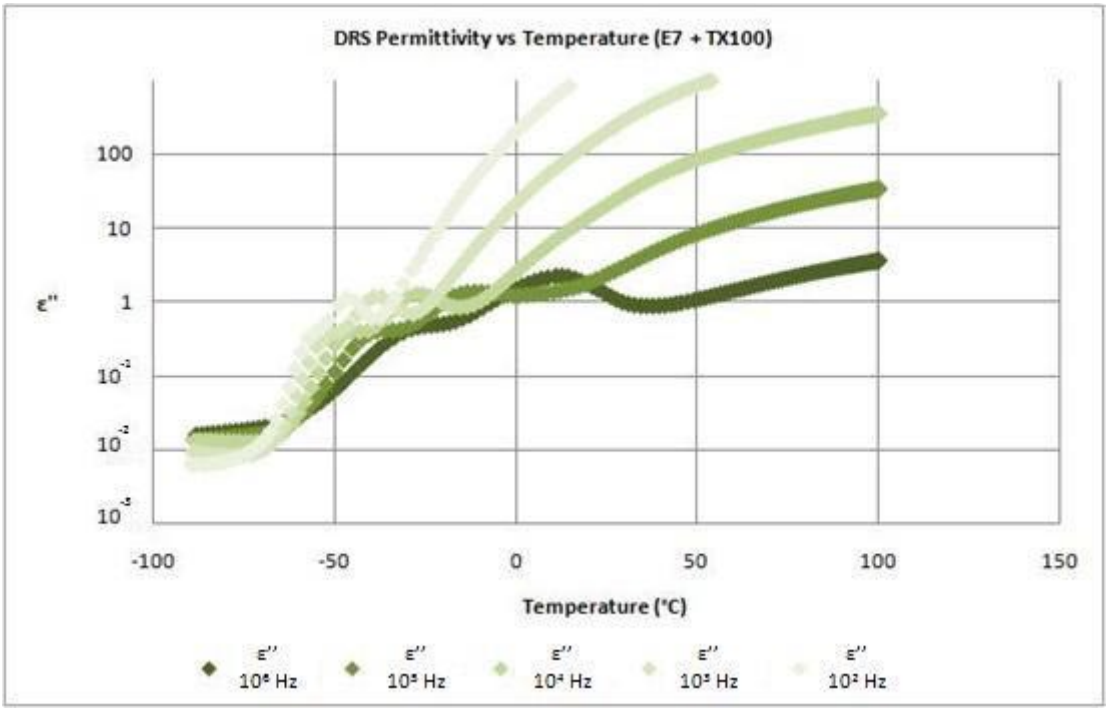


**Figure A.34 – DRS of the mixture on cooling illustrating several frequencies for ε''.**

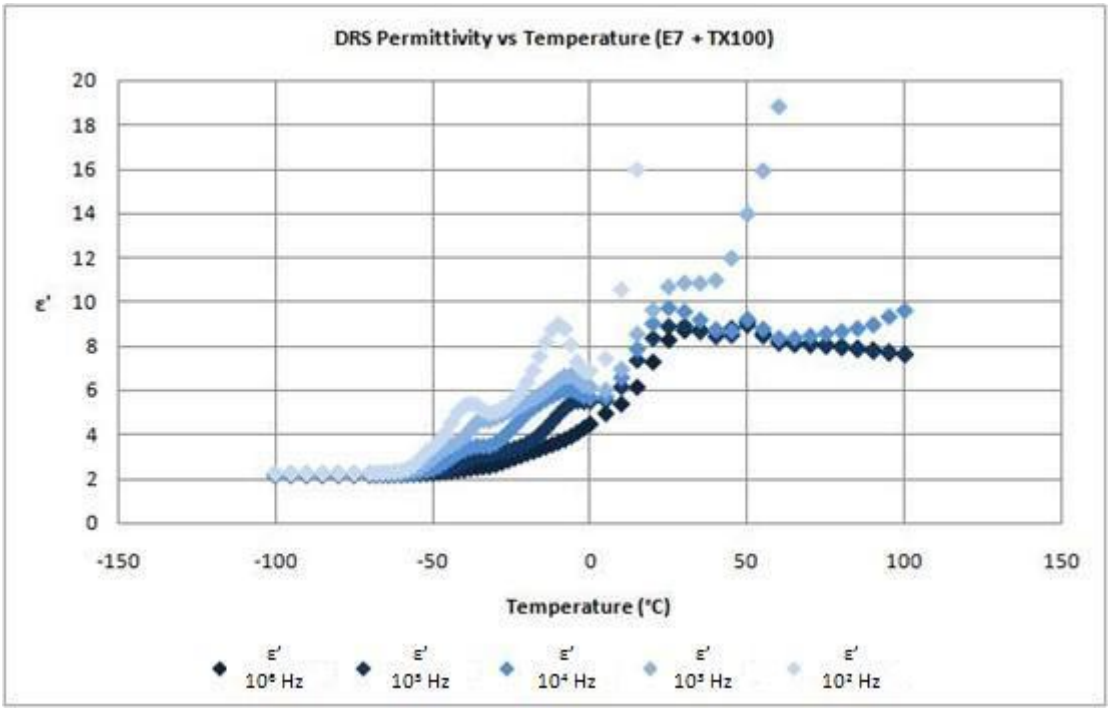


**Figure A.35 – DRS of the mixture on heating illustrating several frequencies for ε'.**

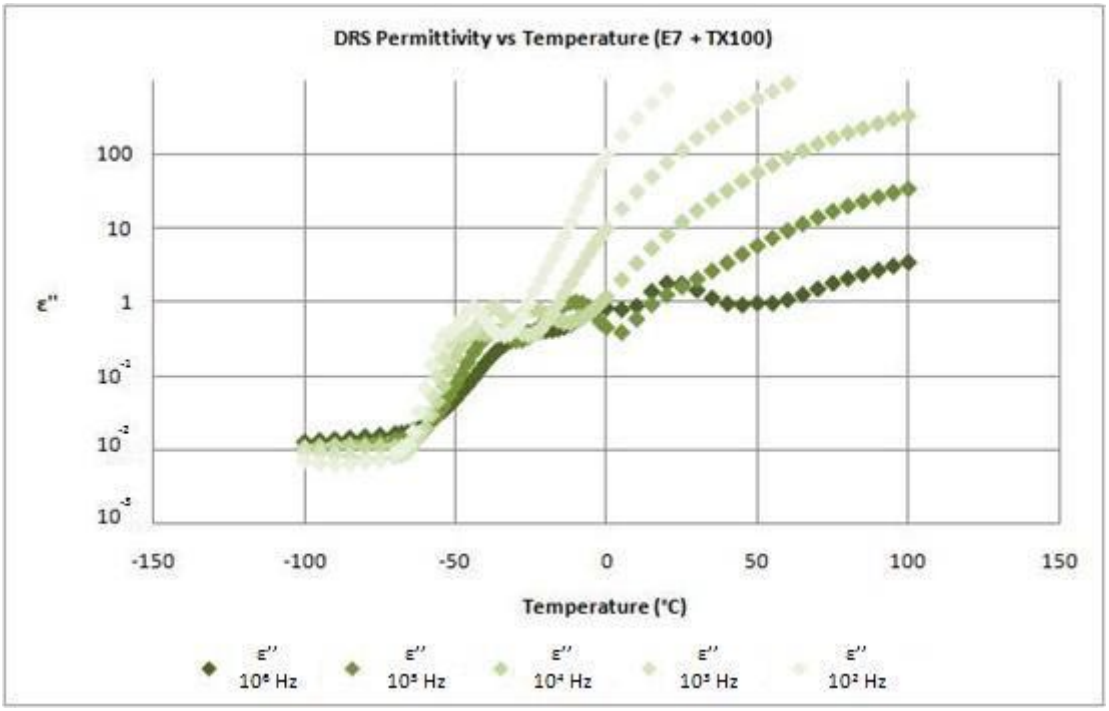


**Figure A.36 – DRS of the mixture on heating illustrating several frequencies for ε''.**

## A.7. Electro-optical Properties of Composites without Additive

**Table A.1 – Composition of the samples without additive.**

| Monomer | Initiator | LC | Polymerization Times | Weight Ratio (wt %) | |
|---|---|---|---|---|---|
| | | | | Monomer | LC |
| TRI | AIBN | E7 | 14 hours | 30 | 70 |
| | XDT | E7 | 1500 seconds | 30 | 70 |
| POLY875 | AIBN | E7 | 14 hours | 30 | 70 |
| | XDT | E7 | 1500 seconds | 30 | 70 |

**Table A.2 – Electro-optical properties of the composites without additive.**

| Monomer | Initiator | Transmittance (%) | | | Switching Voltage ($V.\mu m^{-1}$) | Contrast (%) | $T/V$ Ratio |
|---|---|---|---|---|---|---|---|
| | | $T_{max}$ | $T_{min}$ | $T_{half}$ | | | |
| TRI | AIBN | 56 | 0 | 28 | 10.25 | 56 | 0.137 |
| | XDT | 61 | 1 | 30 | 9.05 | 60 | 0.166 |
| POLY875 | AIBN | 76 | 1 | 37 | 4.10 | 75 | 0.451 |
| | XDT | 71 | 5 | 33 | 5.25 | 66 | 0.314 |